

# Amine— and Phosphine—Borane Adducts: New Interest in Old Molecules

Anne Staubitz, Alasdair P. M. Robertson, Matthew E. Sloan, and Ian Manners\*

School of Chemistry, University of Bristol, Bristol, U.K., BS8 1TS

Received April 5, 2010

## Contents

1. Introduction and Scope	4023	5.1.3. Mechanistic Proposals Concerned with the Role of the Metal Center	4045
2. History and Synthesis of Amine— and Phosphine—Borane Adducts	4025	5.2. Solvolysis of Amine—Borane Adducts	4050
2.1. Amine—Borane Adducts	4025	5.3. Electroless Plating	4051
2.1.1. History of Amine—Borane Adducts	4025	5.4. Anti-Reflection Films	4052
2.1.2. Synthesis of Amine—Borane Adducts	4025	6. Synthesis of Main-Group Metal—Amidoboranes, Phosphidoboranes, and Related Species	4052
2.2. Phosphine—Borane Adducts	4026	6.1. Main-Group Metal Amidoboranes	4052
2.2.1. History of Phosphine—Borane Adducts	4026	6.2. Main-Group Metal—Phosphidoboranes and Related Species	4053
2.2.2. Synthesis of Phosphine—Borane Adducts	4027	7. Coordination Chemistry of Amine— and Phosphine—Borane Adducts with Transition Metals	4055
3. Structure, Bonding, and Physical Properties of Amine— and Phosphine—Borane Adducts	4027	7.1. Metal Complexes of Phosphine— and Amine—Borane Adducts of Type <b>Ia</b> and <b>Ib</b>	4055
3.1. Bonding and Properties of Amine— and Phosphine—Borane Adducts: Influence and Strength of Lewis Acidity of the Borane and Lewis Basicity of the Group 15 Element	4027	7.1.1. Monodentate Complexes	4055
3.2. Analogy Between C—C and B—N Bonds	4030	7.1.2. Chelating Phosphine—Borane Ligands of Type <b>Ia</b> and <b>Ib</b>	4057
3.3. Classical Adducts and Frustrated Lewis Pairs	4030	7.2. Transition Metal Amidoborane Complexes of Type <b>Ila</b>	4058
4. Reactivity and Functionalization of Amine— and Phosphine—Borane Adducts	4031	7.3. Lewis-Acid-Stabilized Metal Phosphidoborane Complexes of Type <b>Ilb</b>	4059
4.1. Key Reactivity of Amine— and Phosphine—Borane Adducts	4031	7.4. Metal Boryl Complexes of Type <b>Ilc</b>	4060
4.1.1. Amine— and Phosphine—Borane Adducts As Reducing Agents	4031	7.5. Lewis-Acid/Base-Stabilized Phosphinoborane, Complexes of Type <b>Ill</b>	4061
4.1.2. Synthetic Applications of Amidoborane Adducts ( $[\text{NR}_2 \cdot \text{BR}_3]^-$ )	4035	8. Polyaminoboranes and Polyphosphinoboranes	4062
4.1.3. Hydroboration with Amine—Borane Adducts	4035	8.1. Polyaminoboranes	4062
4.1.4. Hydrophosphination	4037	8.1.1. Cyclic Oligomers	4062
4.1.5. Radical Reactions	4038	8.1.2. Synthesis of Polyaminoboranes	4063
4.1.6. Applications of Amine—Boranes Based on the Polarity of the Bond	4039	8.1.3. Computational Analysis of Polyaminoboranes	4064
4.1.7. The Borane Moiety as a Protecting Group for Amines	4039	8.2. Polyphosphinoboranes	4066
4.1.8. The Borane Moiety as a Protecting Group of Phosphines	4039	8.2.1. Synthesis of Polyphosphinoboranes	4066
4.2. Functionalization of Amine— and Phosphine—Borane Adducts	4040	8.2.2. Toward Applications for Polyphosphinoboranes and Alternative Synthetic Approaches	4066
4.2.1. Functionalization at Nitrogen and Phosphorus	4040	8.2.3. Computational Structure Analysis and Predictions of Polyphosphinoboranes	4068
4.2.2. Functionalization at Boron	4041	8.3. Polyphosphinoborane/Polyaminoborane Copolymers (PPB/PAB)	4069
5. Dehydrogenation Reactions	4042	8.3.1. Linear Oligomers	4069
5.1. Catalytic Dehydrocoupling of Amine— and Phosphine—Boranes	4042	8.3.2. Computational Analysis of PBNB Polymers	4069
5.1.1. Experimental Studies	4042	9. Outlook	4070
5.1.2. Mechanistic Proposals Concerned with Product Formation	4044	10. Abbreviations and Definitions	4070
		11. Acknowledgments	4070
		12. Appendix	4071
		13. References	4073

## 1. Introduction and Scope

Amine— and phosphine—borane adducts are well-known as classic examples of compounds arising from the reactions between Lewis bases and Lewis acids and their preparation

\* To whom correspondence should be addressed. E-mail: ian.manners@bristol.ac.uk.



Anne Staubitz studied biochemistry at the University of Tübingen, Germany, but decided to pursue chemistry after working in Paul Knochel's group (LMU Munich) on novel Grignard reagents for her diploma thesis. She obtained her PhD in the group of Varinder Aggarwal from the University of Bristol, U.K., before working as a postdoc with Ian Manners, University of Bristol, U.K., in the field of catalytic dehydrocoupling of amine–boranes. After seven enjoyable years in the U.K., she accepted a position as a Juniorprofessorin (Assistant Professor) at the University of Kiel in 2010, where she is working in the field of conducting polymers and switchable polymeric systems.



Matthew E. Sloan studied chemistry at the University of Swansea, where he completed his MChem in 2006 with a project supervised by Christopher Morley investigating the synthesis of chalcogen linked ferrocene dimers. In 2010, he completed his PhD investigating the transition-metal-catalyzed dehydrocoupling of amine–borane adducts with Ian Manners at the University of Bristol. He is currently working as a postdoc for Warren Piers at the University of Calgary.



Alasdair P. M. Robertson studied chemistry at the University of St Andrews, Scotland, with an integrated year in industry working for a University spin-out company developing a novel geometry solid-oxide fuel cell. He completed his MChem in 2008, with a final year project under Derek Woollins investigating novel complexes of the  $S_2N_2^{2-}$  ligand, and was awarded the Irvine Jubilee Medal as most distinguished student of that year. He then moved south to the University of Bristol to pursue a PhD under Ian Manners in the field of catalytic dehydrocoupling of group 13/15 adducts, where he is currently in his second year of studies.

dates from the 19th century. Since 2000, these species have attracted increasing attention as reagents, hydrogen storage materials, polymer precursors, and also with respect to their coordination chemistry. There are numerous reviews in the literature concerning the various aspects of the formation and derivatization of amine–boranes<sup>1</sup> and phosphine–boranes,<sup>1i,2</sup> and their use in organic synthesis and medicinal applications.<sup>1c–e</sup> This review aims to focus on recent developments, and in the case of their use as reagents, we will give a detailed discussion only if the group 13–group 15 bond is preserved in the reaction. The review will also focus exclusively on the borane adducts of nitrogen and phosphorus-donors. The chemistry of the heavier group 13–15 adducts will therefore not be discussed in detail, although some relevant data on their characteristics will be included for comparative purposes. The properties of these heavier adducts have been comprehensively reviewed elsewhere.<sup>3</sup>



Ian Manners was born in London, England, and after receiving his Ph.D. from the University of Bristol in 1985 in the area of transition metal chemistry (with N. G. Connelly), he conducted postdoctoral work in Germany in main-group chemistry (RWTH Aachen, with P. Paetzold) and in the U.S.A. on polymeric materials (Penn State, with H.R. Allcock). He joined the University of Toronto, Canada, as an Assistant Professor in 1990 and was promoted to Professor in 1995. He was awarded a Canada Research Chair in 2001. In 2006, he returned to his Alma Mater to take up a Chair in Inorganic, Macromolecular, and Materials Chemistry, supported by the award of a Marie Curie Chair from the European Union and a Wolfson Research Merit Award from the Royal Society. His research interests focus on the development of new synthetic reactions in inorganic chemistry and their applications in molecular synthesis, polymer and materials science, supramolecular chemistry, and nanoscience and are documented in over 500 career publications.

In the first part of the review, we provide a brief history of the development of amine– and phosphine–borane chemistry (section 2) and set the scene for the remainder of the review with a short discussion of their most important structural and chemical properties (sections 3 and 4), as they form the fundamental basis for any applications. Primary and secondary amine– and phosphine–boranes can undergo dehydrogenation or dehydrocoupling reactions,<sup>4</sup> which will be discussed in detail in section 5, with a particular focus on the proposed mechanisms for these transformations. Sections 6 and 7 cover main-group metal amidoboranes and transition metal complexes of amine– and phosphine–boranes, respectively. In section 8, the formation and structure of polyaminoboranes and polyphosphinoboranes are described

alongside potential applications. We conclude the review with a brief outlook section.

One species, ammonia–borane, has received disproportionately more attention than any other amine– or phosphine–borane adduct, mainly due to its potential as a hydrogen storage material.<sup>5</sup> To provide a balanced view covering all aspects of amine– and phosphine–borane adducts, the most prudent solution was to write a separate, comprehensive review focusing solely on ammonia–borane and closely related materials,<sup>6</sup> thereby allowing us to describe key aspects of the broad class of compounds in the current review. We therefore explicitly exclude a detailed discussion of hydrogen storage aspects or dehydrogenation methods such as addition of additives, which have exclusively been described for ammonia–borane.

## 2. History and Synthesis of Amine– and Phosphine–Borane Adducts

### 2.1. Amine–Borane Adducts

#### 2.1.1. History of Amine–Borane Adducts

Compounds containing dative bonds between boron and nitrogen have been known since the early 19th century. The first compound of this type, ammonia-trifluoroborane,  $\text{H}_3\text{N}\cdot\text{BF}_3$ , was prepared in 1809 by Gay-Lussac<sup>7</sup> and also represented the first coordination compound of any type. Since this initial report, research on this adduct<sup>8</sup> and a plethora of analogs has been reported with important pioneering contributions by Wiberg and Stock.<sup>9</sup>

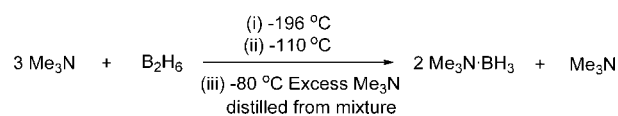
After the discovery of ammonia-trifluoroborane in 1809, surprisingly, it was not until 1937 that the first amine–borane containing only hydride substituents on boron was reported by Burg and Schlesinger, *N,N,N*-trimethylamine–borane,  $\text{Me}_3\text{N}\cdot\text{BH}_3$ .<sup>10</sup> This species was formed by direct reaction of trimethylamine and diborane (see section 2.1.2), which proved to be a useful general synthetic method for amine–borane synthesis, and its advent initiated a rapid growth in the number of reported primary, secondary, and tertiary amine–borane adducts. Various other routes have since been established, the most general being the convenient reaction between amines and the labile borane Lewis base adducts  $\text{BH}_3\cdot\text{THF}$  and  $\text{BH}_3\cdot\text{SMe}_2$ , (see section 2.1.2).<sup>1k</sup> This process cannot be used, however, where either the Lewis acid or Lewis base is particularly sterically hindered, in which case classical adduct formation can be impaired. In 2006, these systems were shown to exhibit unexpected reactivity, including the heterolytic cleavage of various bonds, most notably that of dihydrogen.<sup>11</sup> Bond activation of this type was termed “activation by frustrated Lewis pairs, (FLP)”. This area has recently been reviewed in depth and will therefore not be discussed in detail.<sup>11b</sup> There are a number of technical applications of amine–borane adducts as stabilizers in polymer formulations, the bleaching of wood pulp, photographic applications, and as fuel additives. These uses are described mainly in the patent literature and will not be discussed in detail this review.<sup>1m</sup> Historically and to the present day, their most widespread applications are based on their reducing ability, either for uses in organic reactions or in electroless plating processes, or as easy to handle borane reagents for hydroborations. On the other hand, the use of amine–boranes as precursors to inorganic polymers and as interesting ligands with novel bonding modes is a very recent development and will be a major focus of this review. The

use of ammonia–borane as a potential portable hydrogen storage material has attracted a surge of interest as a result of the high hydrogen content (19.6 wt %) and is covered in detail in our other review.<sup>6</sup>

#### 2.1.2. Synthesis of Amine–Borane Adducts

A variety of common routes to amine–borane adducts are known. For  $\text{BH}_3$  as the Lewis acidic component, the oldest is the direct reaction of the required amine with diborane,  $\text{B}_2\text{H}_6$ . Diborane, first systematically investigated by Stock in 1912,<sup>12</sup> is a pyrophoric, highly reactive gas, which forms from the electron deficient borane in order to gain the energetically more favored electron octet. In solution and in the gas phase, diborane can react with amines to give simple monomeric adducts of the form  $\text{R}_x\text{H}_{3-x}\text{N}\cdot\text{BH}_3$ . Because of the highly reactive nature of diborane however, and the resulting difficulties in its handling, the use of this route is fairly uncommon on a laboratory scale. This method is nonetheless effective and was employed in the first synthesis of *N,N,N*-trimethylamine–borane,  $\text{Me}_3\text{N}\cdot\text{BH}_3$ , in 1937 (Scheme 2.1.),<sup>10</sup> and a number of other adducts, for example adducts of pyridines,<sup>13</sup> or an aza-ferrocene,<sup>14</sup> and a number of secondary<sup>15</sup> and tertiary amines.<sup>15a,16</sup>

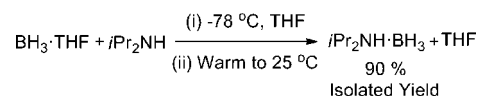
#### Scheme 2.1. Reaction of Trimethylamine and Diborane, Condensed Phase



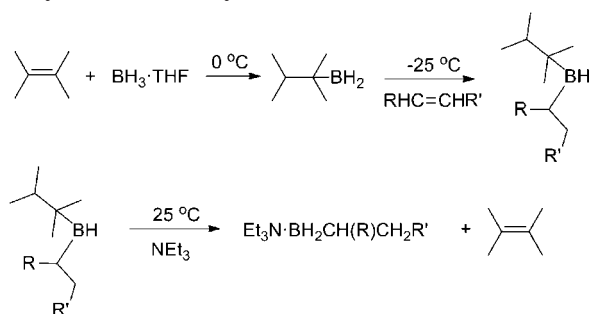
It should be noted that in the case of ammonia–borane,  $\text{NH}_3\cdot\text{BH}_3$ , direct reaction of ammonia with diborane is low yielding in the desired adduct (5% at  $-83 \text{ }^\circ\text{C}$ , 22% at  $-44 \text{ }^\circ\text{C}$ ).<sup>17a</sup> The major reaction product in this case results from unsymmetrical cleavage of diborane to produce an ionic species, the diammoniate of diborane,  $[\text{H}_2\text{B}(\text{NH}_3)_2][\text{BH}_4]$ , (DADB).<sup>17</sup>

Alternative and more commonly used reagents to provide the  $\text{BH}_3$  moiety are borane-tetrahydrofuran ( $\text{BH}_3\cdot\text{THF}$ ) and borane-dimethylsulfide ( $\text{BH}_3\cdot\text{SMe}_2$ ) (see for example Scheme 2.2). These species react directly with free amine, commonly in THF or DCM solution to produce the desired amine–borane complex. The displaced THF or  $\text{SMe}_2$  can subsequently be easily removed from the reaction by distillation.<sup>1g</sup> These precursors tend to be less favored for use in larger scale preparations of amine–borane adducts because of relatively low long-term stability in the case of  $\text{BH}_3\cdot\text{THF}$ <sup>18</sup> and also the issue of liberation of large quantities of flammable, toxic, and highly malodorous dimethyl sulfide in the case of  $\text{BH}_3\cdot\text{SMe}_2$ .<sup>1g</sup>

#### Scheme 2.2. Synthesis of Diisopropylamine–Borane via the Borane-THF Precursor



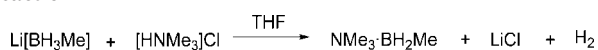
Just as it is possible to use the unsubstituted borane complexes  $\text{BH}_3\cdot\text{THF}$  and  $\text{BH}_3\cdot\text{SMe}_2$ , substituted boranes (in the form of diboranes, THF complexes, or  $\text{Me}_2\text{S}$ ) may also be used for the preparation of amine–borane adducts, despite the often somewhat reduced Lewis acidity compared to  $\text{BH}_3$ . As this is an important route, we will briefly describe possible syntheses of alkyl boranes to provide some background information without attempting to cite the literature

**Scheme 2.3. Synthesis of an Alkylborane Complex of Triethylamine via Thexylborane**


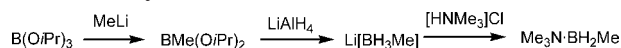
comprehensively. Alkyl boranes could be synthesized via routes based on hydroboration of olefins, although the process is often uncontrolled, with multiple substitutions prevailing.<sup>19</sup> However, the development of bulky protecting groups on the borane allowed facile monosubstitution. The most well-known protecting group of this type is thexyl, which could be introduced by the hydroboration of 2,3-dimethyl-2-butene.<sup>19</sup> Upon reaction with disubstituted terminal or internal olefins the thexyl group effectively prevented polysubstitution at boron, enabling a clean monoalkylation to produce thexylmonoalkylboranes.<sup>20</sup> The thexyl group could then be easily removed in a dehydroboration reaction via reaction with free amine, thus producing amine adducts of alkylboranes (Scheme 2.3).

This procedure was less effective with regard to mono-substituted terminal olefins that tended to react with thexyl borane to produce dihydroborated species,  $\text{BR}_2\text{thex}$ , because of the reduced steric interactions with the bulky thexyl group.<sup>20</sup> Other substituted boranes used to form amine–borane adducts<sup>21</sup> were thiolated boranes,<sup>21b–d,22</sup> although tri-thiolated boranes did not form stable adducts.<sup>23</sup> While thiolated amine–boranes used to be of merely academic interest, there has been a resurgence in terms of their importance because thiolation of amine–boranes or polyaminoboranes may play a pivotal role in the regeneration of spent fuel from dehydrogenated ammonia–borane.<sup>24</sup> The use of thiols for digestion of spent fuel is reviewed in detail in our other review on ammonia–borane.<sup>6</sup>

A third route, common for the synthesis of boron-functionalized amine–boranes, produces the amine–borane adduct via reaction of an alkali metal borohydride with the hydrochloride salt of the required amine (Scheme 2.4).<sup>25</sup> This route has recently been reported to be particularly suited to the preparation of ammonia–borane from  $\text{NaBH}_4$  and  $\text{NH}_4\text{Cl}$ .<sup>25c</sup> Using this route, various alkyl substituted amine–boranes have been prepared along with cyano-functionalized adducts of the form  $\text{R}_3\text{N}\cdot\text{BH}_2\text{CN}$ .<sup>26</sup>

**Scheme 2.4. Synthesis of *N,N,N*-Trimethylamine–*B*-methylborane via Borohydride/Amine Hydrochloride Reaction**


Usually, substituted alkali metal borohydrides are synthesized from borate esters, whereby these are reacted with an alkyl lithium base to introduce the alkyl groups (mono-, di-, or trialkylation depending on the stoichiometric ratio), followed by reduction with  $\text{LiAlH}_4$  to nucleophilically introduce the desired hydridic substituents (Scheme 2.5). The amine–borane adduct can then be formed by reaction of the lithium alkylborohydride with

**Scheme 2.5. Synthesis of  $\text{Me}_3\text{N}\cdot\text{BH}_2\text{Me}$  from  $\text{B}(\text{O}i\text{Pr})_3$** 

**Scheme 2.6. Amine-Exchange Reaction of Methylamine–Borane with Excess Trimethylamine**


the desired amine hydrochloride.<sup>27</sup> This method could also be used to produce cyanoboranes, isocyanoboranes, and subsequently, amine– or phosphine–(iso)cyanoborane adducts via a similar methodology.<sup>28</sup>

A further common route to amine–boranes is via amine-exchange from an existing adduct.<sup>29</sup> The method exploits the dissociative equilibrium that occurs for all adducts in solution (Scheme 2.6). The position of the equilibrium is defined by the strength of the two potential adducts, that is, the amine forming the stronger complex with the borane moiety will be energetically favored. However, the equilibrium can be shifted by employing the desired amine in large excess. This process is particularly favorable if the amine being displaced is more volatile, ideally being evolved as a gas from the reaction mixture.

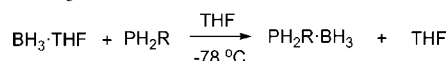
In addition to the electronic factors, steric contributions to adduct stability must be considered. For example, it has been demonstrated that pyridine can displace trimethylamine from  $\text{Me}_3\text{N}\cdot\text{BMe}_3$  despite the lower  $\text{p}K_a$  of the pyridine conjugate acid ( $\text{p}K_a$  of pyridine- $\text{H}^+$  = 3.5 (in DMSO) or 12.3 (in MeCN) compared to  $\text{p}K_a$  for trimethylamine- $\text{H}^+$  = 9.0 (in DMSO) or 18.4 (in MeCN)).<sup>30</sup> This is an inversion of the situation for the nonmethylated borane wherein trimethylamine can quantitatively displace pyridine in pyridine–borane,  $\text{pyr}\cdot\text{BH}_3$ . It is postulated that on addition of alkyl groups at boron, steric repulsion favors the less encumbered pyridine adduct over the trimethylamine analog.<sup>29b</sup>

## 2.2. Phosphine–Borane Adducts

### 2.2.1. History of Phosphine–Borane Adducts

As with the case of amine adducts of borane, phosphine–boranes have been known for over one hundred years: the first example, phosphine trichloroborane,  $\text{H}_3\text{P}\cdot\text{BCl}_3$ , was reported by Besson in 1890.<sup>31</sup> Detailed investigations of these adducts were only fully instigated in the mid-20th century with Gamble and Gilmont successfully synthesizing “diborane diphosphine”, at low temperature. The product was postulated to be  $\text{B}_2\text{H}_6\cdot 2\text{PH}_3$ ,<sup>32</sup> on the basis of Stock’s work on the amine analog 20 years beforehand,<sup>33</sup> which was later demonstrated to be the diammoniate of diborane. Unlike Stock’s ammonia derivative which was stable to dissociation, diborane diphosphine was reported to dissociate above  $-30\text{ }^\circ\text{C}$  into diborane and phosphine. Later analysis of the same material suggested a misinterpretation of the initial data. The diborane diphosphine was in fact monomeric in nature, and the true formulation was  $\text{PH}_3\cdot\text{BH}_3$ , the simplest phosphine–borane adduct, which existed as a white solid with a melting point of  $32\text{--}33\text{ }^\circ\text{C}$  without apparent decomposition.<sup>34</sup>

Further research in the area extended the methodology to secondary and tertiary alkyl functionalized phosphine–boranes of the general form  $\text{R}_2\text{PH}\cdot\text{BH}_3$  and  $\text{R}_3\text{P}\cdot\text{BH}_3$ , respectively.<sup>35</sup> These species, synthesized by direct reaction of diborane and di- or trialkylphosphines at low temperature were found to

**Scheme 2.7. Synthesis of a Primary Phosphine–Borane Adduct via  $\text{BH}_3 \cdot \text{THF}$  Precursor**

be significantly more stable (at ambient temperature) than primary *P*-alkylphosphine–borane adducts, which tend to dissociate easily.<sup>36</sup> This increased stability was postulated to arise from the greater basicity of the phosphorus center in alkylated species resulting from increased electron density donated from the alkyl groups. As a consequence, a stronger phosphorus–boron bond is formed, producing a more robust series of complexes. Historically the best known application of phosphine–boranes is probably in the synthesis of phosphines, where the borane merely serves as a protecting group. Since this application is well established, we will discuss it only very briefly (section 4.1.8). Apart from this, the main interest today is their use as ligands in transition metal complexes, which led to the discovery of fascinating new bonding motifs, as monomers for the formation of polyphosphinoboranes, and in the case of sterically encumbered examples, as FLPs.

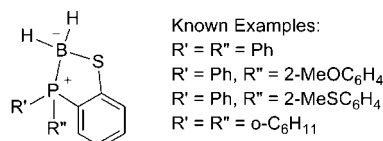
**2.2.2. Synthesis of Phosphine–Borane Adducts**

Aside from the inherently hazardous direct reaction of diborane and the required phosphine, which is now rarely used,<sup>34</sup> phosphine–borane syntheses on a laboratory scale tend to involve direct addition of primary, secondary, or tertiary phosphines to  $\text{BH}_3 \cdot \text{THF}$  or  $\text{BH}_3 \cdot \text{SMe}_2$ , upon which the more strongly donating phosphine rapidly displaces the weaker Lewis base (Scheme 2.7).<sup>37,38</sup>

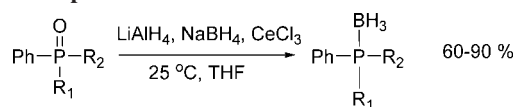
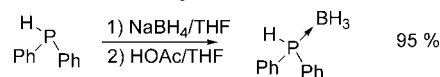
Generally the product can then be isolated and purified by distillation, crystallization or sublimation. As for amine–borane synthesis, these reagents tend to be less favored for use on larger scale preparation of phosphine–borane adducts because of issues of long-term stability ( $\text{BH}_3 \cdot \text{THF}$ ) and elimination of malodorous gases ( $\text{BH}_3 \cdot \text{SMe}_2$ ).<sup>1g</sup>

There are also examples of *B*-thiolated phosphine–boranes, many (but not all)<sup>21a</sup> of which are cyclic species (Figure 2.1).<sup>39</sup> Such a species could be prepared by synthesizing a phosphine with an appropriately spaced thiol in the molecule. When the thiol was deprotonated and reacted with  $\text{H}_2\text{BCl} \cdot \text{SMe}_2$ , the B–S bond formed by nucleophilic substitution, with concomitant formation of the P–B dative bond. Oxidants such as *m*CPBA (*m*-chloroperoxybenzoic acid) were able to oxidize the thiol group to the sulfoxide, in both open<sup>40</sup> and cyclic<sup>39a</sup> systems in quantitative yield without oxidation of the phosphorus atom, which was protected by the borane.

Where larger quantities of phosphine–boranes are required, including in industry, alternative syntheses have been developed focusing on sodium borohydride,  $\text{NaBH}_4$ , with a hydride acceptor. This can be the phosphine oxide or a phosphonium cation, where at least one substituent is hydrogen. This concept was initially developed for the synthesis of amine–boranes but has been expanded successfully into the field of phosphine–boranes.<sup>41</sup> It was first



**Figure 2.1.** Cyclic phosphine–boranes with a B–S bond.

**Scheme 2.8. Example of a Phosphine–Borane Synthesis from a Phosphine Oxide****Scheme 2.9. Example Synthesis of a Phosphine–Borane Adduct via Sodium Borohydride with Acetic Acid<sup>41</sup>**

reported, for example, that a phosphine oxide precursor could be reduced in a single pot reaction with a mixture of  $\text{LiAlH}_4$ ,  $\text{NaBH}_4$ , and  $\text{CeCl}_3$  at ambient temperature to give the adduct directly (Scheme 2.8).<sup>42</sup>

The cerium(III) chloride proved to be key to this reaction, with no reaction in its absence. It was postulated that its role is to activate species for the phosphine oxide via co-ordination (presumably via the oxygen atom), thereby rendering the phosphine oxide a better electrophile and facilitating deoxygenation via  $\text{LiAlH}_4$ , as well as activating  $\text{NaBH}_4$ . Furthermore, it has also been demonstrated that mono- and dichlorophosphines can be utilized in reactions with borohydride reagents to produce primary and secondary phosphine–borane adducts, respectively. Various reports exist regarding this method, with the fundamental advantage of this procedure being that primary and secondary phosphines do not need to be handled directly, avoiding the associated inherent associated safety hazards.<sup>2c,43</sup>

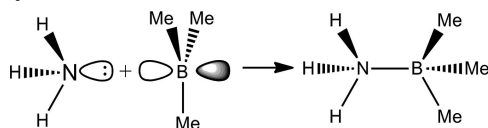
More recently a novel and facile synthetic route to phosphine–borane adducts from  $\text{NaBH}_4$  has been developed, wherein the latter was reacted with secondary or tertiary phosphines along with a proton source generating  $\text{BH}_3$  *in situ*, which could then form the phosphine–borane adduct in high yield (Scheme 2.9).<sup>41</sup>

Phosphine-/amine-exchange reactions are also a well-established route to phosphine–borane adducts. As discussed previously with regard to amine–amine exchange, amine–borane adducts can be treated with excess phosphine to yield the phosphine–borane adduct and free amine via an equilibration process. The position of the equilibrium in these processes depends on the difference in donor ability between the amine and phosphine respectively, itself defined by the substituents present in terms of electronic and steric effects. Indeed several studies have used displacement of trimethylamine from trimethylamine–borane as a means of the quantification of donor ability of substituted phosphines.<sup>44</sup>

While it is more common to prepare amine–boranes from phosphine–boranes via exchange equilibria (see also section 4.1.8 on the deprotection of phosphine–boranes), the reverse reaction has also been reported.<sup>29b</sup>

**3. Structure, Bonding, and Physical Properties of Amine– and Phosphine–Borane Adducts****3.1. Bonding and Properties of Amine– and Phosphine–Borane Adducts: Influence and Strength of Lewis Acidity of the Borane and Lewis Basicity of the Group 15 Element**

The adducts of group 13 and group 15 elements effectively comprise two distinct units, a group 13 center and a group

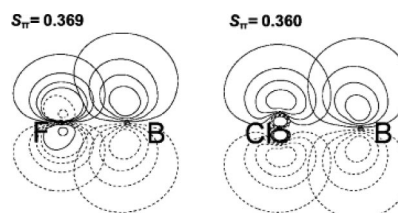
**Scheme 3.1. Simplified  $sp^3\sigma$ – $p\sigma$  Overlap in Ammonia and Trimethylborane to Produce  $\text{NH}_3\cdot\text{BMe}_3$** 


15 center, connected by a dative bond. In this Lewis acid/Lewis base adduct, the group 15 species can be considered to provide both electrons for the bond from a lone pair, acting as a two electron donor. Conversely, the group 13 center is electron deficient and accepts both electrons into a vacant  $p$ -orbital. The adduct, which results from the combination of the two fragments, is formally uncharged, although electronegativity values suggest a partial negative charge at the group 15 center remains and, therefore, a partial positive charge at boron. This interpretation is also confirmed by the dipole moment determined for these simple adducts, calculated from measurements obtained by gas phase microwave analysis,<sup>45</sup> which confirms that the bonding pair is more closely associated with the donor atom.<sup>46</sup>

The formation of the adduct bond leads to pyramidalization of the borane moiety to produce an approximately tetrahedral geometry, with a change in hybridization at boron from approximately  $sp^2$  to  $sp^3$  (Scheme 3.1).

Amine- and phosphine-borane adducts can be considered textbook examples of Lewis acid-Lewis base adducts. Because of this, the most accessible approach to discuss the factors contributing to the stability of the central dative bond is to first describe the factors contributing to the strength of boron Lewis acids and amine- and phosphine-Lewis bases themselves. However, while this may give a generalized estimate of the strength of the dative bond, it is now accepted that the dative bond dissociation energy is *not* directly related to Lewis acid or Lewis base strength.<sup>47</sup> It has to be borne in mind that both absolute and relative Lewis acidity are influenced by the Lewis base.<sup>48</sup> Thus,  $\text{BF}_3$  forms a weaker bond with  $\text{NH}_3$  than  $\text{BCl}_3$ , but a stronger bond to the weakly basic  $\text{CO}$ .<sup>49</sup> Furthermore,  $\text{BH}_3$  forms more stable adducts with thioethers than  $\text{BF}_3$ , whereas for others the reverse is true.<sup>50</sup>

A very important example that can be found in many textbooks and is still often taught is the relative Lewis acidity of the halogenated boranes,  $\text{BF}_3$ ,  $\text{BCl}_3$ ,  $\text{BBR}_3$ . Here, the order of stability of the complexes with  $\text{NH}_3$  decreases in the order  $\text{BBR}_3 > \text{BCl}_3 > \text{BF}_3$ ,<sup>51</sup> which is initially counterintuitive as one would expect the highly electronegative F substituents to remove electron density from the boron center more efficiently than Cl or Br, which should lead to increased Lewis acidity. A very simple explanation for this trend is that the halogen lone pairs may interact with the empty  $p$ -orbital on boron which would lead to a delocalized  $\pi$ -bond, and thereby reducing the effective Lewis acidity. This hypothesis, which has been suggested in many modified forms,<sup>49a,52</sup> claims that because of the similar energies and shapes of the orbitals on B and F, this interaction is strongest for these first row atoms, thus accounting for the unexpected trend. However, the more modern literature highlights various flaws associated with this basic explanation. The differences in bonding of  $\text{BH}_3$  in comparison with  $\text{BF}_3$  or  $\text{BCl}_3$  with different Lewis bases<sup>50,51c</sup> cannot be explained simply by a  $p(\pi)$ – $p(\pi)$ -hyperconjugation. Furthermore, if this explanation were true, it should be expected that the energy of pyramidalization of boron from trigonal planar to tetrahedral would



**Figure 3.1.** Natural hybrid orbital overlap yielding coordinate covalent  $\pi$ -bonds between boron and fluorine/chlorine within  $\text{BH}_2\text{X}$ .  $S_\pi$  represents the overlap integral corresponding to the natural hybrid orbitals involved. Reprinted with permission from ref 47b. Copyright 2009 American Chemical Society.

be higher in the case of F than Cl as a substituent, because in the former case, a stronger  $\pi$ -system would be disturbed. However, it was shown computationally that the opposite is true: the enthalpy of pyramidalization from the trigonal planar geometry was in fact found to be higher for  $\text{BCl}_3$  than  $\text{BF}_3$ , assuming the same initial geometries.<sup>52a</sup> A contribution to this field in 2009 described the “impact of halogen lone pairs upon understanding Lewis acidity as dubious”<sup>47b</sup> and that Lewis acidity should be gauged based upon valence deficiency<sup>53</sup> or the ability of boron to accept an electron pair.<sup>47b,51d</sup> It was found<sup>47b</sup> that the natural bond orbital (NBO) ( $\pi$ ) overlap integrals between F and B in  $\text{BF}_3$  and Cl and B in  $\text{BCl}_3$  were virtually identical with only slightly better overlap found between F and B (Figure 3.1), which was in accordance with previous reports,<sup>52b,d</sup> but contradicted others.<sup>51d</sup>

From studies of Lewis acidity by *ab initio*, DFT, and NBO methods, it was found that boron Lewis acidity depended mainly upon substituent size and electronegativity. It was suggested that the major contributant to effective boron Lewis acidity in the case of the trihalides is the  $\sigma$ -bond orbital overlap between boron and the various halogens.<sup>47b</sup> Plumley and Evanseck demonstrated that increased  $\sigma$ -bond overlap led to increased electron density at boron and hence reduced acidity. On moving down group 17 from  $\text{BF}_3$  to  $\text{BCl}_3$ , they proposed that the  $\sigma$ -overlap between a boron  $sp^2$  hybrid and a  $sp^n$  orbital on the halide increases due to improved matching of the orbital dimensions, which was a general periodic trend, but particularly pronounced for halides (Figure 3.2).<sup>47b</sup>

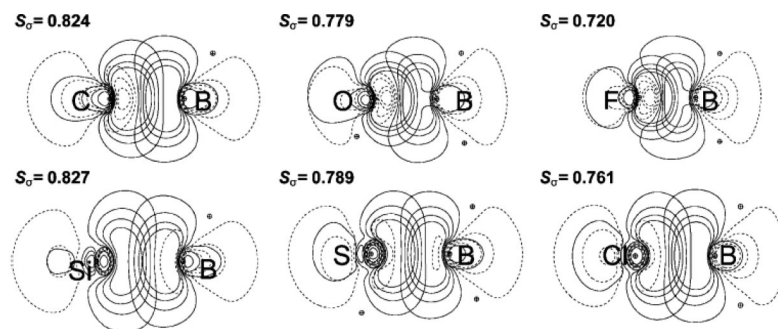
Bessac and Frenking approached the problem by analyzing the cumulative effect of these factors via computational means, where the various factors influencing adduct formation were separated and individually quantified.<sup>47a</sup> Initially the bond dissociation energy,  $\Delta E$  (or De), was separated into two components,  $\Delta E_{\text{prep}}$  and  $\Delta E_{\text{int}}$  (eq 3.1). The former refers to the energy required to distort the two components of the adduct from their initial equilibrium geometries and electronic ground states to their final geometries and electronic states within the compound.  $\Delta E_{\text{int}}$  represents the instantaneous interaction energy between the two fragments of the molecule. This contribution was further divided into three components:  $\Delta E_{\text{elstat}}$ ,  $\Delta E_{\text{Pauli}}$ , and  $\Delta E_{\text{orb}}$  as indicated in eq 3.2.

$$\Delta E(= -\text{De}) = \Delta E_{\text{prep}} + \Delta E_{\text{int}} \quad (3.1)$$

where

$$\Delta E_{\text{int}} = \Delta E_{\text{elstat}} + \Delta E_{\text{Pauli}} + \Delta E_{\text{orb}} \quad (3.2)$$

The various subfactors with  $\Delta E_{\text{int}}$  were defined as follows:  $\Delta E_{\text{elstat}}$  gives the electrostatic interaction energy between the



**Figure 3.2.** Natural hybrid orbital overlap yielding the  $\sigma$ -bond between boron and X (X = CH<sub>3</sub>, OH, F, SiH<sub>3</sub>, SH, and Cl) within BH<sub>2</sub>X.  $S_0$  represents the overlap integral corresponding to the natural hybrid orbitals involved. Reprinted with permission from ref 47b. Copyright 2009 American Chemical Society.

respective fragments;  $\Delta E_{\text{Pauli}}$  the repulsive interactions between the fragments resulting from two electrons with the same spin being forced to share the same region of space, and  $\Delta E_{\text{orb}}$  relating to the relaxation of the Kohn–Sham orbitals relaxing to their optimal form. It was concluded that to understand the trends in Lewis acidity/basicity within borane adducts, *all* of the above energetic factors must be considered, with the bond dissociation energy itself a poor measure of intrinsic Lewis acidity or basicity.

Lewis acidity has also been claimed to be correlated to the LUMO level of the Lewis acid,<sup>54</sup> which is indeed higher for BF<sub>3</sub> than BCl<sub>3</sub>.<sup>52b,54</sup> However, in a more detailed study, taking into account the partially and mixed *B*-halogenated ammonia–boranes, NH<sub>3</sub>·BH<sub>*m*</sub>F<sub>*n*</sub>Cl<sub>*p*</sub> (with  $m + n + p = 3$ ) this explanation was contradicted, as such a trend was no longer apparent.<sup>47b</sup>

For phosphine–boranes, a *d*-orbital contribution has been discussed, producing a bonding interaction with the hydrogens at boron for BH<sub>3</sub> as a Lewis acid in a  $d\pi$ – $p\pi$  manner, similar to the concept of hyperconjugation.<sup>44b</sup> However, further studies in this area drew this concept of boron–phosphorus backbonding into question, suggesting, based on studies of F<sub>3</sub>P·BH<sub>3</sub>, that the only bonding may be that of the central  $\sigma$ -dative bond.<sup>55</sup> It was argued that although the bonding in this adduct was strong, the bond length and heat of dissociation neither confirmed nor denied the presence of additional back-bonding. Calculations by Nakagawa and co-workers contradicted the earlier suggestion that  $d\pi$ – $p\pi$  backdonation increased the strength of the phosphine–borane adduct bond, suggesting that the stabilization resulting from this interaction is effectively negligible.<sup>56</sup> Their calculations did however indicate that the *d*-orbitals are involved in stabilization, their interaction, reinforcing the existing dative  $\sigma$  bond, reducing the polarization energy (the polarization term describes the energy arising from the deformation of the electron clouds of two molecular fragments brought into proximity of each other)<sup>49b</sup> in H<sub>3</sub>P·BH<sub>3</sub> by 7.5 kcal/mol.

Whatever the exact factors that influence Lewis acidity and basicity, some general trends can be observed. Generally, the addition of electron donating groups, such as alkyl chains at the group 15 center increases the strength of the dative bond, with an inverse effect if the same substituent is placed at boron.<sup>57</sup> This effect is exemplified in the correlation between BH<sub>3</sub> and BMe<sub>3</sub> complexes of mono-, di-, and trialkylamine, as demonstrated by Haaland (Table 3.1).<sup>46</sup>

Comparing the gas-phase dissociation energies of alkylamine–alkylborane complexes indicates a reduction in stability with increasing alkyl substitution at boron. The possibility that a reduced dissociation energy could be the result of steric interactions in this case was ruled out as

**Table 3.1.** Gas-Phase Dissociation Enthalpies,  $\Delta H_{\text{dis}}$  (kcal/mol), of Complexes of Borane and Trimethylborane

	BH <sub>3</sub>	BMe <sub>3</sub>
H <sub>3</sub> N	31.1 ± 1.0 <sup>a</sup>	13.8 ± 0.3
MeH <sub>2</sub> N	35.0 ± 0.8 <sup>b</sup>	17.6 ± 0.2
Me <sub>2</sub> HN	36.4 ± 1.0 <sup>b</sup>	19.3 ± 0.2
Me <sub>3</sub> N	34.8 ± 0.5 <sup>b</sup>	17.6 ± 0.2

<sup>a</sup> Estimated based on other entries in table.<sup>46</sup> <sup>b</sup> Calculated from standard enthalpies of the reactions  $2 \text{Me}_n\text{H}_{3-n}\text{N} \cdot \text{BH}_3(\text{g}) \rightarrow \text{B}_2\text{H}_6(\text{g}) + 2\text{Me}_n\text{H}_{3-n}\text{N}(\text{g})$ <sup>58</sup> and the dissociation enthalpy of diborane.<sup>59</sup>

alkylation at nitrogen did not show the same effect but in fact led to increased stability because of increased electron density at nitrogen, enhancing its Lewis basicity.<sup>46</sup>

Another illustrative example are group 15 adducts of boronic esters. While tri(alkoxy)boranes tended to form poorly stable adducts, triarylborates, B(OAr)<sub>3</sub> formed simple 1:1 amine–borane adducts relatively easily.<sup>60</sup> This difference in stability was postulated to arise from a reduction in basicity at the oxygen centers through resonance interaction between the oxygen and the aromatic ring, resulting in a more electron deficient boron center.<sup>60</sup> However, the only reports of mono- and disubstituted alkoxyboranes are of transient species, isolated in low temperature matrices. Since these disproportionate to the trisubstituted derivatives and unsubstituted amine–boranes at ambient temperature,<sup>61</sup> this experimental result again casts doubt on the explanation of substituent lone pair involvement.

It has been demonstrated that at the most fundamental level, increasing the steric bulk at either or both group 13/15 center decreases the complex stability.<sup>57,62</sup> This is exemplified in the series of molar enthalpies of reactions for various amines with BH<sub>3</sub>·THF at 25 °C:  $n\text{BuNH}_2 \cdot \text{BH}_3 > n\text{Bu}_2\text{NH} \cdot \text{BH}_3 > n\text{Bu}_3\text{N} \cdot \text{BH}_3$  and  $\text{Et}_2\text{NH} \cdot \text{BH}_3 > n\text{Pr}_2\text{NH} \cdot \text{BH}_3 > n\text{Bu}_2\text{NH} \cdot \text{BH}_3$ .<sup>62</sup> This can be attributed simply to poorer overlap of orbitals because of the additional steric constraints. However, it has also been suggested that with regard to the group 15 center, the addition of increasingly bulky alkyl groups has the effect of increasing the C–E–X (E = N or P, X = C or H) bond angle which may in turn also affect the Lewis basicity of the group 15 center.<sup>3</sup> The reduction in basicity results from a decrease in the *p*-character of the lone-pair and an increase in *s*-character. Computational screening of a variety of group 13/15 donor–acceptor complexes bearing fluorinated substituents with respect to their donor–acceptor dissociation energies and approximate Lewis acidities of the group 13 moieties was contributed by Gille and Gilbert.<sup>63</sup>

While the energy contribution of pyramidalization on Lewis acid strength purely based on electronic factors has

been contradicted as an explanation,<sup>47b</sup> steric arguments dictate that this reduction in bond angle between the borane substituents must be to some extent energetically unfavorable and, hence, makes an unfavorable contribution to the overall enthalpy of adduct formation.<sup>47a</sup> This effect is particularly pronounced in the formation of adducts in which the borane unit is functionalized with particularly bulky groups. In addition, it has been noted that the enthalpy of bond dissociation of alane complexes of amine and phosphines is often higher than that of the boron analogs purportedly because of more facile pyramidalization at the larger aluminum center.<sup>47a</sup>

It should be noted that the computational studies discussed above are all based on gas phase calculations. They must therefore be treated with some care because the adduct geometry and the central dative bond in particular are highly dependent on its environment, with dissociation enthalpies potentially influenced by electrostatic interactions with the medium. A more detailed discussion of these factors is presented in our other review on ammonia–borane, for which these contributions have been studied both computationally and experimentally.<sup>6</sup>

### 3.2. Analogy Between C–C and B–N Bonds

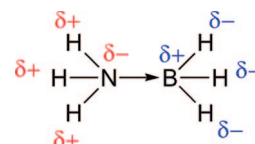
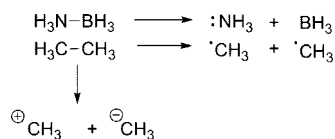
Historically, many comparisons have been drawn regarding the similarity between boron–nitrogen (B–N) bonds and carbon–carbon bonds (C–C). The two bonds are isoelectronic, although the source of the bonding electron pair differs between the two species. Indeed in many aspects, carbon can be considered to possess properties perfectly intermediate to boron and nitrogen, including atomic size and electronegativity (Table 3.2).

Clearly in the case of C–C bonds, the bonding is covalent in nature, with a single electron being contributed to the bonding pair by each carbon center. In the case of B–N bonds, where nitrogen provides both bonding electrons, two different elements are involved, with strongly differing electronegativity values, which leads to a significantly polarized bond.<sup>65</sup> The simplest example of this analogy is found in ammonia–borane,  $\text{H}_3\text{N}\cdot\text{BH}_3$ , and ethane,  $\text{H}_3\text{C}-\text{CH}_3$  as discussed by Haaland.<sup>46</sup> Breaking the central B–N bond in ammonia–borane produces two uncharged species, namely  $\text{BH}_3$  and  $\text{NH}_3$ . In the case of ethane, breaking the central carbon–carbon bond occurs in either of two distinct ways (Scheme 3.2). Cleavage can occur homolytically to yield two uncharged radical species or, alternatively, via a heterolytic mechanism producing a carbanion,  $\text{CH}_3^-$ , and carbocation,  $\text{CH}_3^+$  respectively, wherein both electrons from the bonding pair are lost to a single  $\text{CH}_3$  unit.<sup>46</sup> The

**Table 3.2. Comparison of Fundamental Properties of Boron, Carbon, and Nitrogen<sup>64</sup>**

	Boron	Carbon	Nitrogen
Valence electrons	3	4	5
Covalent radius (pm)	88	77	70
Pauling electronegativity	2.0	2.5	3.0

### Scheme 3.2. Thermal Fragmentation of Ammonia–Borane and Ethane



**Figure 3.3.** N–H and B–H bond polarizations in ammonia–borane. (Polarization resulting from central bond not included.)

relative strengths of the central bond differ significantly between ammonia–borane and ethane. In ammonia–borane, the central dative bond has a measured dissociation enthalpy of 27.2 kcal/mol at 25 °C, whereas the central covalent bond in ethane is more than three times stronger under the same conditions, 90.1 kcal/mol.<sup>66</sup> It should be noted that these bond breaking mechanisms are fundamentally different but are compared here because they represent the lowest-energy bond breaking process for each class of compound in the gas phase.

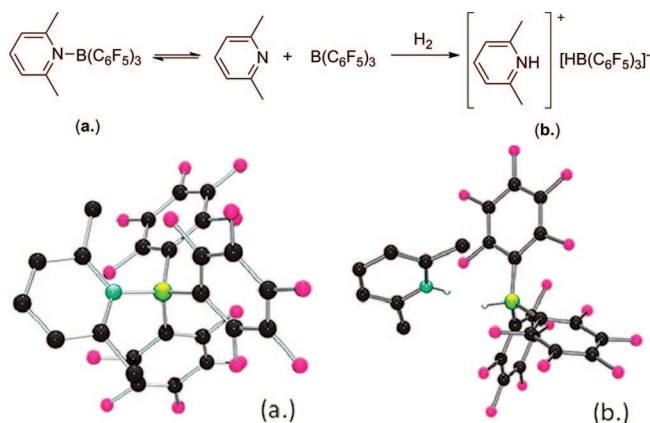
The different bonding characteristics in simple B–N and C–C systems are highlighted in the physical properties of ammonia–borane and ethane, respectively, which are dominated by polarity. In ethane, the central C–C bond is nonpolar, and all hydrogen atoms are identical and weakly acidic in nature because of the slightly greater electronegativity of carbon relative to hydrogen.<sup>67</sup> Intermolecular interactions are therefore limited to weak van der Waals forces, hence the gaseous state of this hydrocarbon at room temperature. In comparison, ammonia–borane is a solid at room temperature with a melting point of 114 °C,<sup>68</sup> with bonding significantly more polar in nature (for a detailed discussion of the melting point of ammonia–borane see our other review).<sup>6</sup> Further to this electrostatic argument considering the whole adduct, the respective polarities of the N–H and B–H hydrogen atoms may also have a significant effect. The hydrogens at nitrogen are acidic in character because of the increased electronegativity of nitrogen, 3.04,<sup>67</sup> relative to hydrogen, 2.20.<sup>67</sup> Inversely, the hydrogens at boron are hydridic in nature because of the reduced electronegativity of boron, 2.04,<sup>67</sup> which leads to polarization of the bond toward hydrogen. This results in a highly polar structure (Figure 3.3) and leads to intermolecular dihydrogen bonds, thereby also accounting for the high melting point.<sup>6</sup>

### 3.3. Classical Adducts and Frustrated Lewis Pairs

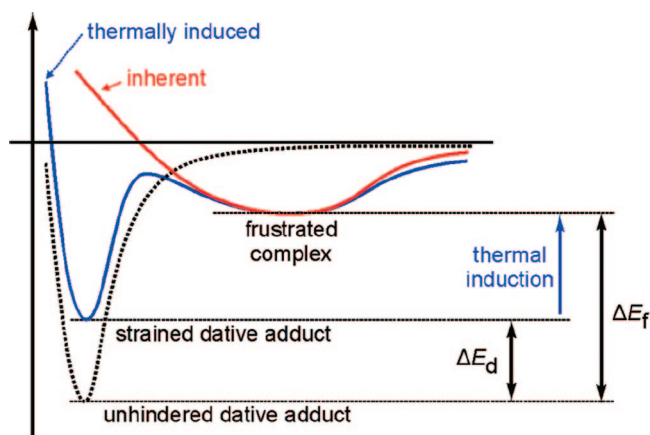
In addition to the classical adducts of amines or phosphines with boranes, it is also possible to combine Lewis acids and Lewis bases, which are too sterically hindered to form a classical adduct. These have received considerable recent interest since Stephan and co-workers discovered the ability of such mixtures to activate small molecules (for reviews, see refs 11b and 69). We will not attempt to cover this rapidly moving field comprehensively but merely point out the fundamental reactivity patterns. Initially, it was believed that a necessary requirement for dihydrogen activation by sterically hindered Lewis acid/Lewis base pairs was that the formation of an adduct was completely prevented. However, it has been shown that this is not necessarily the case.<sup>70</sup> The combination of lutidine and  $\text{B}(\text{C}_6\text{F}_5)_3$  as Lewis base and Lewis acid, respectively, did appear to produce an adduct, which was confirmed by X-ray crystallography (Scheme 3.3). Crucially however, this complex was shown by solution NMR spectroscopy to be in equilibrium with the dissociated state. When this 1:1 mixture was exposed to a hydrogen



**Scheme 3.3. Activation of Hydrogen by a Classical Lewis Acid/Lewis Base Complex with Single Crystal X-ray Structures of the Adduct and Borohydride Salt<sup>a</sup>**



<sup>a</sup> Reprinted with permission from ref 70. Copyright 2009 American Chemical Society.



**Figure 3.4.** Comparison of the potential energy profiles of classical dative complexes, frustrated Lewis pairs and thermally induced frustrated Lewis pairs. Reprinted with permission from ref 71. Copyright 2009 American Chemical Society.

atmosphere, lutidinium borohydride  $[2,6\text{-Me}_2\text{C}_5\text{H}_3\text{NH}]^+[(\text{C}_6\text{F}_5)_3\text{BH}]^-$  formed (Scheme 3.3).

Pápai has formulated a generalized description of the frustrated Lewis pair.<sup>71</sup> This concept differentiates between unhindered dative adducts, whose potential curve along the Lewis acid–Lewis base coordinate follows a standard anharmonic potential with a minimum where the bond is formed (Figure 3.4, dotted line). Conversely, in frustrated complexes this minimum is inaccessible for steric reasons (Figure 3.4, red line). Instead a shallow minimum at much larger distances exists, which represents the frustrated complex, held only together by dispersion forces and, in some cases peripheral hydrogen bonds. In between these extremes, there is the thermally induced frustrated Lewis pair, where the dative adduct exists, but is strained and reactive (Figure 3.4, blue line). The frustrated complex, still somewhat higher in energy than the strained dative adduct, is accessible in such systems if thermal induction is provided.

Further insight into the unusual reactivity of FLPs has been provided through calculations by Grimme and Erker.<sup>72</sup> They suggest that the ability of the frustrated Lewis pair to activate small molecules such as  $\text{H}_2$  results from the

polarization occurring as a result of the electric field derived from the presence of donor and acceptor atoms.

## 4. Reactivity and Functionalization of Amine– and Phosphine–Borane Adducts

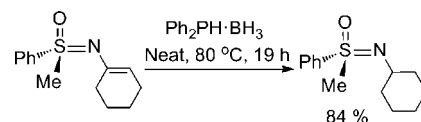
### 4.1. Key Reactivity of Amine– and Phosphine–Borane Adducts

Although it is not possible within the context of this review to provide a comprehensive section on reactivity and functionalization without adding inordinate length to the article, we aim to outline the main classes of reactions for amine– and phosphine–borane adducts. Following the development of facile synthetic routes to a range of amine–boranes, many have become useful reagents in a number of synthetic procedures. The fundamental reactions of amine– and phosphine–boranes with hydrogen substituents are dominated by attack of basic reagents at the protic hydrogens at nitrogen or phosphorus, leading to deprotonation (see section 4.2.1) whereas acids tend to attack the hydridic substituents at boron (see section 4.2.2).

#### 4.1.1. Amine– and Phosphine–Borane Adducts As Reducing Agents

Apart from a single reference,<sup>73</sup> phosphine–boranes have not found use as reducing reagents in synthesis at the time of writing. However, we suspect that such reagents may have some useful potential, because the reduction of a chiral *N*-vinyl sulfoximine was achieved in very high yield (Scheme 4.1).<sup>73</sup> Phosphine–boranes have, however, been used for reduction processes under physiological conditions,<sup>74</sup> but a detailed discussion of biochemical processes is beyond the scope of this review.

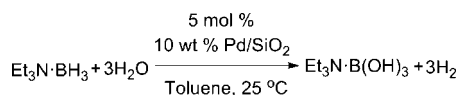
#### Scheme 4.1. Reduction of *N*-Vinylsulfoximines by a Phosphine–Borane



In contrast to this, there is a substantial body of work concerning the use of amine–borane adducts as reducing agents, which has recently been reviewed.<sup>1k,m,75</sup> Here, we will only discuss some of the most recent publications in detail, specifically from 2000 onward.

In principle, three different modes of reaction are known. First, amine–boranes with hydridic substituents at boron, can react with protic solvents via reductive solvolysis. These processes are likely to be very similar to dihydrogen generating reactions which are briefly discussed in section 5.2 or electroless plating processes discussed in section 5.3 and in our other review.<sup>6</sup> Second, in nonprotic solvents, free dihydrogen may be released using thermal or catalytic dehydrogenation reactions, the latter of which will be discussed in section 5.1 and are mentioned here only in terms of synthetic usefulness. A third pathway is represented by true transfer hydrogenations, which are either catalyzed by a metal, or can even proceed without a metal if the substrate is sufficiently polar and thereby activated, such as in the case of imines.

**4.1.1.1. Reductive Solvolysis Procedures with Synthetic Applications.** A protic solvent, potentially under catalytic

**Scheme 4.2. Example of a Catalytic Hydrolysis of Triethylamine–Borane<sup>76b</sup>**


conditions, may react with the hydridic hydrogens at the borane center and liberate hydrogen gas exothermically (and exergonically), producing the corresponding amine–borate complex (Scheme 4.2).<sup>76</sup> However, the hydrogen need not always be released. In the presence of an appropriate acceptor, it is possible that hydrogenations can be effected in open systems with quantitative up-take of dihydrogen (see below).

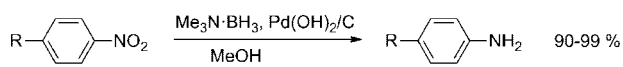
Reacting similarly to metal borohydrides, MBH<sub>4</sub>, amine–boranes are capable of reducing various functional groups, for example, ketones and aldehydes to the corresponding alcohols. Amine–boranes can be advantageous to borohydride reagents because of their high solubility in organic solvents and comparatively reduced sensitivity to acids.<sup>11</sup> However, despite this, the activity of amine–boranes adducts as reducing agents is often enhanced by the use of acidic conditions, which allows for fine-tuning of the reductive strength of the reagent.<sup>77</sup> The reduction of cyclohexanone to the corresponding alcohol for example with *N,N,N*-trimethylamine–borane at ambient temperature could be increased from a negligible rate under neutral conditions with no conversion occurring over 38 h, to 80% conversion within 8 min on acidification with aqueous hydrochloric acid.<sup>78</sup> The reducing ability of amine–borane adducts was found to be highly dependent upon the amine present within the complex. In the case of aliphatic-substituted amine–boranes, reducing ability generally decreased with increasing alkyl substitution: H<sub>3</sub>N·BH<sub>3</sub> > RNH<sub>2</sub>·BH<sub>3</sub> > R<sub>2</sub>NH·BH<sub>3</sub> > R<sub>3</sub>N·BH<sub>3</sub>.<sup>1k</sup> In the analogous systems containing *N*-aryl functional groups, the reducing effect correlated more strongly with the basicity of the amine, with lower amine p*K*<sub>a</sub> producing improved reducing ability.

Another possibility for the use of amine–boranes as reductants was to employ such adducts for the metal-catalyzed methanolysis of amine–boranes in a transfer hydrogenation. The system was tolerant of various functional groups and gave generally good yields (Scheme 4.3).<sup>79</sup>

The reaction proved to be relatively generally applicable and not restricted to tertiary amine–boranes. For example, the reducing system *t*BuNH<sub>2</sub>·BH<sub>3</sub>/10% Pd–C/methanol proved to be highly efficient for a range of functional groups (Table 4.1).<sup>79a</sup>

A practical application for such a reduction process was an amine–borane deprotection where a *N*-benzyl protecting group, a substituent on the amine moiety, was reduced with concomitant cleavage of the N–B bond in the adduct (tandem methanolysis/hydrogenolysis) (Scheme 4.4).<sup>79a,c</sup> However, in some instances, the protecting group could be preserved.<sup>80</sup>

For hydrogenation of a range of olefins, it could be shown that the reaction with a catalyst and a reducing agent was

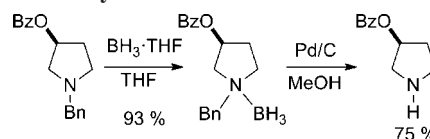
**Scheme 4.3. Palladium-Catalyzed Reduction of Nitroaromatics Using *N,N,N*-Trimethylamine–Borane in Methanol<sup>79b</sup>**


R = H, Me, CO<sub>2</sub>Me, CN, CH<sub>2</sub>OH, OH, OMe, NHAc, F

**Table 4.1. Efficient Reduction by Pd-Catalyzed Methanolysis of *t*BuNH<sub>2</sub>·BH<sub>3</sub><sup>a</sup>**

Entry	Substrate	Product	Time (h)	Yield %
1			4	93
2			8	94
3			4	92 <sup>b</sup>
4			15	81 <sup>c</sup>
5			9	97 <sup>b</sup>
6			120	82
7			11	83 <sup>d</sup>
8			1	90

<sup>a</sup> Reactions were conducted in a sealed vessel at room temperature on 50 mmol of substrate in 30 mL of methanol with 20 mmol of *t*BuNH<sub>2</sub>·BH<sub>3</sub> and 174 mg of 10% Pd–C, unless otherwise noted. <sup>b</sup> As in footnote a, except on 25 mmol of substrate. <sup>c</sup> Regioselectivity was 24:1 in favor of the secondary alcohol, as determined by <sup>1</sup>H NMR. <sup>d</sup> Reaction performed in ethanol to avoid transesterification.

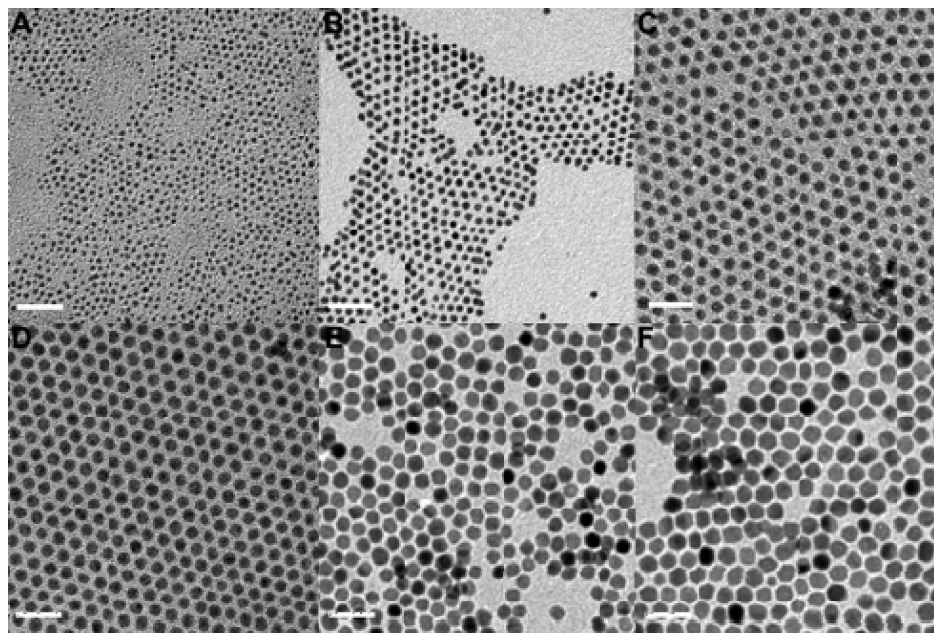
**Scheme 4.4. Tandem Methanolysis/Hydrogenolysis of a Benzylated Tertiary Amine–Borane<sup>79a</sup>**


not merely a tandem dehydrogenation of ammonia–borane/hydrogenation of olefin reaction but a true transfer hydrogenation, where the hydrogen does not dissociate from the metal center. It was observed that the reaction went to completion regardless of whether the system was open or closed. Similarly, vinyl epoxides could be reductively opened using Pd(PPh<sub>3</sub>)<sub>4</sub> as a catalyst in DCM with acetic acid as a stoichiometric additive.<sup>81</sup>

For reductions of this type, other applications are emerging: H<sub>3</sub>N·BH<sub>3</sub>, MeNH<sub>2</sub>·BH<sub>3</sub>, and Me<sub>2</sub>NH·BH<sub>3</sub> could be used to reduce water-soluble tetrazolium salts to insoluble formazan dyes which, in the presence of Ag(I), would form high density silver and dye photographic images.<sup>82</sup> The fact that metal centers react with amine–boranes in aqueous (or generally protic) media could also be utilized when the reduction of the metal itself was of interest.

The formation of <sup>118</sup>Re(H<sub>2</sub>O)<sub>3</sub>(CO)<sub>3</sub> was recently described as a potential therapeutic radiopharmaceutical.<sup>83</sup> The reduction of <sup>118</sup>ReO<sub>4</sub><sup>−</sup> with NH<sub>3</sub>·BH<sub>3</sub> in the presence of CO in aqueous solution to yield this precursor was recently described by Schibli and co-workers,<sup>84</sup> which improved on previous methods.<sup>83</sup>

If the substrate to be reduced is a metal salt itself, which is employed stoichiometrically, the reduction may be technically classed as a direct hydrogen transfer reaction, even though it may be related to the reduction processes known to occur in electroless plating applications (section 5.3). An interesting application for this process was the formation of monodisperse noble metal nanoparticles. The motive to develop such systems is that often, electronic and optical



**Figure 4.1.** TEM images of synthesized gold nanoparticles of different size, produced by varying reaction solvent (A, B) and temperature (C–F): (A)  $2.1 \pm 0.3$  nm; (B)  $3.5 \pm 0.3$  nm; (C)  $5.3 \pm 0.4$  nm; (D)  $6.2 \pm 0.3$  nm; (E)  $7.1 \pm 0.5$  nm; (F)  $8.3 \pm 0.5$  nm. All scale bars are 20 nm. Reprinted with permission from ref 87. Copyright 2006 American Chemical Society.

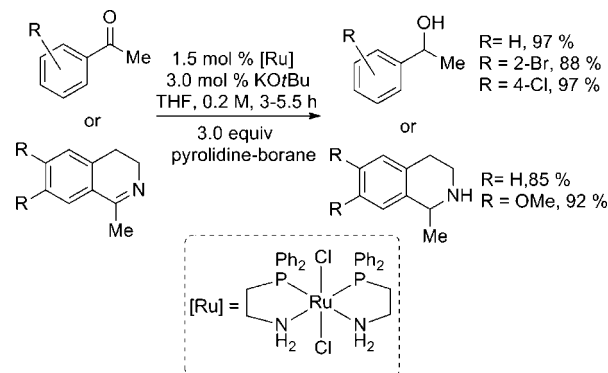
properties depend on the size and size distribution of metal nanoparticles.<sup>85</sup> Previous methods have generally employed biphasic systems and gave nanoparticles with a broad size dispersity.<sup>86</sup> The formation of nanoparticles with a small size distribution has recently been described by the reduction of Au, Ag, or Pd metal precursors by various amine–borane adducts in nonprotic organic solvents (Figure 4.1).<sup>87</sup> It was noted that slower reduction occurred with amine–borane adducts than the traditionally employed metal borohydrides, allowing for greater control of particle size. Varying reaction time and temperature resulted in control over nanoparticle size.

**4.1.1.2. Tandem and Transfer Dehydrogenation/Hydrogenation Reactions Facilitated by Metals.** Shortly after the catalytic dehydrocoupling of amine–boranes was reported (see section 5),<sup>88</sup> it was recognized that such compounds may serve as easy to handle dihydrogen sources for the reduction of organic substrates, where the catalyst may serve the dual role of dehydrocoupling the amine–borane and hydrogenating the organic substrate.<sup>89</sup> Substrates, such as cyclohexene or octene, were reduced in almost quantitative yield with *N,N*-dimethylamine–borane using  $\{\text{Rh}(1,5\text{-cod})(\mu\text{-Cl})\}_2$  in a sealed reaction vessel over 24 h. However, because the ligand was also reduced, it was found to be more practical to use rhodium on alumina as a catalyst, which gave purer products (by NMR).

$\text{Cp}_2\text{TiCl}_2$  in combination with *n*BuLi, which was also a catalytically active dehydrocoupling system for secondary amine–boranes (see section 5), showed a similar behavior with *N,N*-dimethylamine–borane as the reductant and cyclohexene as the organic substrate.<sup>90</sup> Those systems, however, had to be closed for the reaction to proceed to completion, which could be interpreted in terms of the presence of a fast dissociation/association process between  $\text{H}_2$  and the metal.

Ketones and imines were shown to be reduced in a similar tandem dehydrocoupling/hydrogenation reaction with a ruthenium catalyst (Scheme 4.5).<sup>91</sup> The system was closed, but it was not described whether an initial pressure built-up

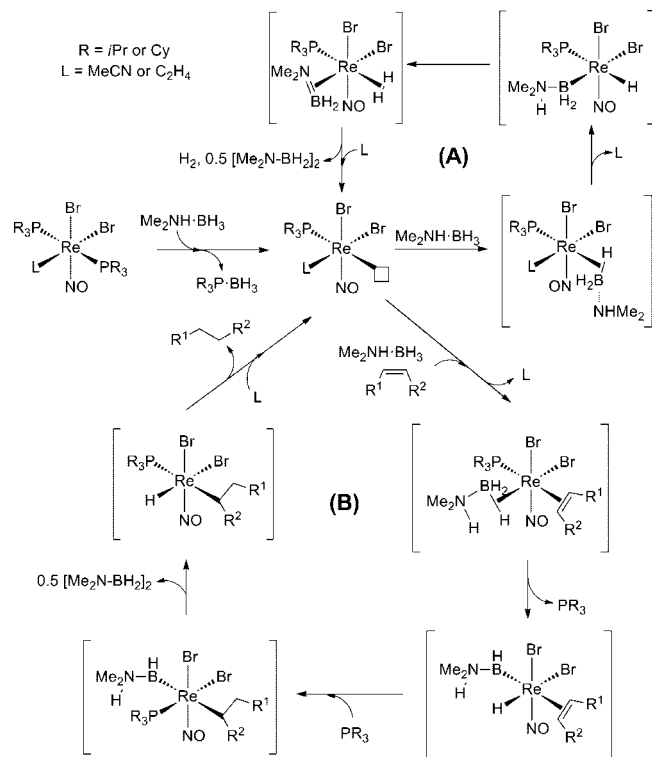
**Scheme 4.5. Hydrogenation Reactions of Imines and Ketones with Pyrrolidine–Borane as the Reductant**



was noted, (tandem dehydrogenation/hydrogenation) or whether pressure did not increase (true transfer hydrogenation).

The first verified true transfer dehydrogenation/hydrogenation process was achieved using a number of Re complexes ( $[\text{ReBr}_2(\text{NO})(\text{PR}_3)_2\text{-L}]$ ) with R = *i*Pr or Cy, L =  $\text{H}_2$ , MeCN, or ethene.<sup>92</sup> In combination with *N,N*-dimethylamine–borane, these catalysts were able to hydrogenate unactivated olefins such as 1-octene, indene, 4-methoxystyrene, and others with low catalyst loadings (1 mol %) at 85 °C in quantitative yield in an open system with the cyclic aminoborane as the byproduct. Because it was apparent that no hydrogen was lost into the gas phase, this reaction must have been a true transfer dehydrogenation/hydrogenation, for which a mechanism was postulated (Scheme 4.6). It was assumed that one phosphine ligand would dissociate, leaving a free coordination site, which could either be filled by the amine–borane (slow process, cycle A) or the olefin (fast process, cycle B). In the latter case, if a second coordination site, *cis* to the olefin was vacated and then occupied with an amine–borane, loss of a further phosphine ligand and B–H activation would lead to a Re–hydride species, which could transfer the hydride onto the olefin. Reassociation of the phosphine ligand and proton transfer from the amine–boryl

### Scheme 4.6. Postulated Mechanism for a Transfer Dehydrogenation/Hydrogenation Mechanism Using Re Catalysts



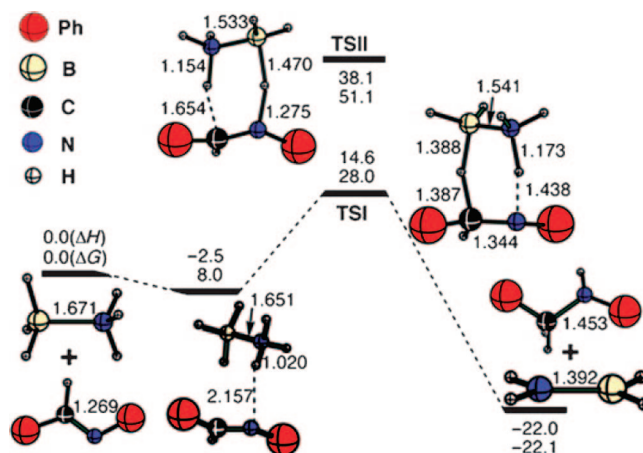
ligand would give the second R-H species, which would then be able to transfer the second H onto its now alkyl ligand and liberate the hydrogenated olefin.

Further work included extension of this chemistry to different Re catalysts (Table A1, Appendix), which were also able to perform this novel transformation.<sup>93</sup>

#### 4.1.1.3. Direct Transfer Hydrogenations without Metals.

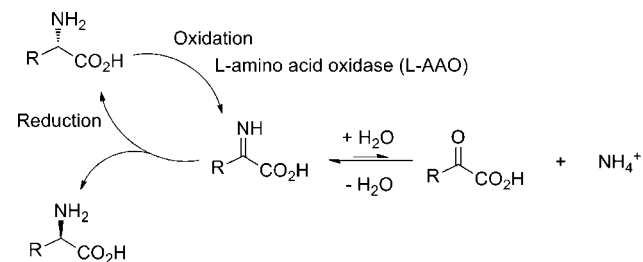
If the substrate for the reduction is sufficiently polar, such as a ketone or an imine, the hydride from the borane moiety of an amine–borane can be transferred without the activation of the substrate or the amine–borane by a metal. There is one account in the literature, where a detailed mechanistic investigation has been performed.<sup>94</sup> In this case, the hydrogenation of a range of imines with ammonia–borane as a reductant has been investigated by direct observation (<sup>11</sup>B NMR), kinetic studies including isotope studies and DFT calculations. It was found that the reaction was likely to proceed via a concerted double hydrogen transfer, where the protic hydrogen on nitrogen is transferred to the more electronegative nitrogen in the imine, with the hydridic hydrogen on boron attacking the more electrophilic carbon center (Figure 4.2). During this reaction, the amine–borane adduct was claimed to yield the aminoborane, [NH<sub>2</sub>=BH<sub>2</sub>], which then decomposed following routes which had already been described for ammonia–borane<sup>95</sup> and is discussed in detail in our other review.<sup>6</sup>

In many (but not all) cases, the direct hydrogen transfer reactions were performed in protic solvents with little regard to mechanistic questions. In such cases, the reaction may appear to somewhat resemble the metal-catalyzed solvolysis reactions discussed earlier, in terms of the oxidation products of the amine–borane adduct used. In an aqueous solution, the end product is most likely boric acid (or tetrahydroxyborate) and ammonia (or ammonium, depending on the pH), whereas in nonprotic solvents, aminoboranes and their



**Figure 4.2.** DFT calculations for the reaction of ammonia–borane, AB, with benzylidene aniline leading to aminoborane and *N*-benzylaniline. The bond lengths (Å) were obtained at the M05-2X/6-311++G\*\* level. The  $\Delta H$  and  $\Delta G$  values (kcal/mol) in THF at 298 K and 1 atm were corrected with the M05-2X/6-311++G\*\* gas-phase harmonic frequencies. Reprinted with permission from ref 94. Copyright 2010 Wiley VCH.

### Scheme 4.7. Deracemization of DL-Amino Acids Using L-Amino Acid Oxidase (L-AAO)

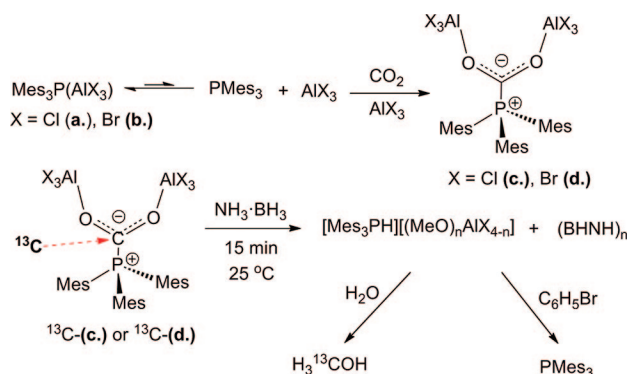


decomposition products may be expected. Because of the polar nature of the substrates discussed here and the fact that many amine–borane adducts are sufficiently hydrolytically stable, we assume that in most cases the reactions discussed are true transfer hydrogenations. For the purposes of this section, which has a primarily synthetic focus, we will discuss both systems together.

Recently, the reductive amination of a range of aldehydes and ketones with primary and secondary amine–boranes in methanol, water, and solventless conditions was reported.<sup>96</sup> A detailed mechanism is not known, but the fact that no metal was required and that the reaction also occurred in the absence of solvent allows us to speculate that this is likely to be a direct transfer hydrogenation. Here, the use of  $\alpha$ -picoline–borane (pic-BH<sub>3</sub>) as a reducing agent was superior to the more traditionally used reducing agents such as sodium cyanoborohydride (NaBH<sub>3</sub>CN) because of its high toxicity and formation of cyanide during the reaction.<sup>97</sup>

In a study describing the reduction of steroidal ketones with amine–borane adducts, it was observed that secondary amine–borane adducts (R<sub>2</sub>NH·BH<sub>3</sub> R = Me, Et, *cyclo*-C<sub>6</sub>H<sub>11</sub> or O(CH<sub>2</sub>CH<sub>2</sub>)<sub>2</sub>NH·BH<sub>3</sub>) were more versatile than commonly used sodium borohydride, allowing milder reaction conditions to be employed.<sup>98</sup>

A particularly interesting use of amine–borane adducts as reducing agents was in a deracemization protocol for amino acids.<sup>99</sup> For example, amine–borane adducts were shown to be efficient reducing agents in the deracemization of DL-amino acids in water (Scheme 4.7). Because the oxidation step required an enzyme, it was important to

**Scheme 4.8. Activation of Carbon Monoxide by Frustrated Lewis Pairs and Reduction with Ammonia–Borane**


perform the reduction at pH 7, at which sodium borohydride is unstable, rendering amine–boranes (NH<sub>3</sub>·BH<sub>3</sub>, pyr·BH<sub>3</sub>, *t*BuNH<sub>2</sub>·BH<sub>3</sub>) superior reductants. Furthermore, the use of the highly toxic alternative reagent, NaBH<sub>3</sub>CN, could be avoided. This system even allowed the realization of a one-pot system with ammonia–borane for the reduction step and living cells for the stereoselective oxidation of the imine in water. Similarly to the reaction described above, the reduction mechanism has not been determined aside from the observation that ammonia was released over time. Evolutionary screening of the enzyme for the oxidation allowed a further generalization of the system for the synthesis of a wider range of chiral amines.<sup>100</sup>

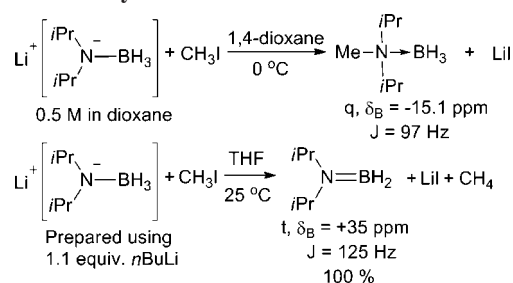
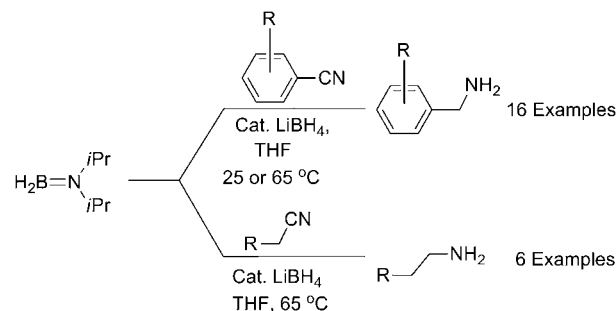
Further reductions of polar organic substrates include for example the reduction of α,β-unsaturated hydrazones by *N,N*-dimethylamine–borane/*p*-toluenesulfonic acid,<sup>101</sup> the reduction of aldehydes,<sup>102</sup> ketones,<sup>102a,103</sup> ketones stereoselectively,<sup>103b,104</sup> 1,2-diketones,<sup>105</sup> imines,<sup>106</sup> reductive coupling of aldoximes,<sup>107</sup> and in rare cases the reduction of esters.<sup>102e</sup>

A very unconventional direct transition metal-free transfer hydrogenation was achieved by using ammonia–borane as a stoichiometric reductant to reduce CO<sub>2</sub> to methanol (Scheme 4.8).<sup>108</sup> In this case, the briefly mentioned activation of small molecules using Lewis acid (AlCl<sub>3</sub> or AlBr<sub>3</sub>)/Lewis base (PMe<sub>3</sub>) pairs (section 3.3) was used to render carbon dioxide susceptible to reduction, although the exact mechanism has not been elucidated at the time of writing.

**4.1.2. Synthetic Applications of Amidoborane Adducts ([NR<sub>2</sub>·BR<sub>3</sub>]<sup>−</sup>)**

Lithium amidoborane adducts are increasingly used as alternative non-pyrophoric reductants instead of the highly reactive and pyrophoric LiAlH<sub>4</sub>. Their synthetic applications have been reviewed in 2005<sup>109</sup> and 2006<sup>75b</sup> so that we do not attempt to cover this vast field comprehensively and merely point out general reactivity patterns. Generally, these reagents have been used to reduce aromatic and aliphatic esters,<sup>110</sup> tertiary amides,<sup>110a,111</sup> α,β-unsaturated aldehydes and ketones<sup>110a</sup> (1,2-reduction) and azides.<sup>112</sup>

The reaction of lithium amidoboranes with methyl iodide as a representative alkyl halide<sup>113</sup> or alkyl methanesulfonate esters<sup>114</sup> was shown to either yield an aminoborane, [R<sub>2</sub>N=BH<sub>2</sub>], an *N*-alkylamine, or the amination product of the alkyl halide–borane, depending on the reaction conditions (Scheme 4.9).<sup>113</sup> Amination was found to be favored at lower temperatures in dioxane, whereas reduction of the alkyl halide by hydride transfer was observed predominantly in THF at ambient temperature. Mechanistically, it is believed

**Scheme 4.9. Lithium Amidoboranes for the Amination or Reduction of Alkyl Halides**

**Scheme 4.10. Selective Reduction of Nitriles with *N,N*-Diisopropylaminoborane and Catalytic Amounts of LiBH<sub>4</sub>**


that in the latter case the lithium on nitrogen in these reagents may coordinate with the halogen atom of the halide, while a hydride is transferred from the borane moiety,<sup>115</sup> whereas the amination reaction is formally an electrophilic substitution.

Lithium amidoboranes can thus serve as precursors to aminoboranes, which could be used as mild reducing agents themselves.<sup>116</sup> For this purpose, the lithium amidoborane was reacted with trimethylsilyl chloride, TMSCl, or alternatively, MeI to give the corresponding aminoborane. In the latter case, small amounts of LiBH<sub>4</sub> were produced as a byproduct of the reaction, and were found to have a catalytic effect on the reduction of aliphatic and aromatic nitriles to the corresponding primary amines by diisopropylaminoborane ([iPr<sub>2</sub>N=BH<sub>2</sub>]) (Scheme 4.10).

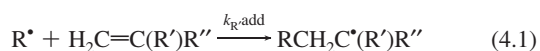
**4.1.3. Hydroboration with Amine–Borane Adducts**

Amine–borane adducts have been used extensively as hydroborating agents because of their distinct advantages over diborane itself, which is a highly pyrophoric, toxic gas,<sup>117</sup> or the two other commonly used borane carriers, BH<sub>3</sub>·THF<sup>118</sup> and BH<sub>3</sub>·SMe<sub>2</sub>.<sup>119</sup> Both are very active hydroboration agents but borane-THF suffers from instability over prolonged periods of time and is only available as a relatively low concentration solution in THF (~1 M, usually stabilized with *N*-isopropyl-*N*-methyl-*t*butylamine). Borane-dimethylsulfide can be obtained solvent-free (~10 M) but is also very flammable, volatile, and malodorous, while also releasing stoichiometric amounts of Me<sub>2</sub>S as a byproduct in the reaction. Amine–borane adducts on the other hand often are air- and moisture-stable complexes and can be dissolved readily in a variety of solvents. While the increased stability also has limited the scale of their use, requiring significantly higher reaction temperatures,<sup>1m</sup> in recent years, a range of more hydroboration-active amine–boranes have been synthesized and developed, enabling many processes to occur at 25 °C.<sup>1g,25a</sup> Moreover, their reactivity can be tuned by using different amine moieties. The documented examples of

hydroboration using phosphine–borane adducts are very limited because these generally require more forcing reaction conditions than amine–borane adducts and in their case the evidence also points toward a dissociative mechanism.<sup>120</sup> It should be noted, however, that the use of phosphite-boranes, (RO)<sub>3</sub>P•BH<sub>3</sub>, increased the hydroboration activity of these adducts.<sup>120c</sup>

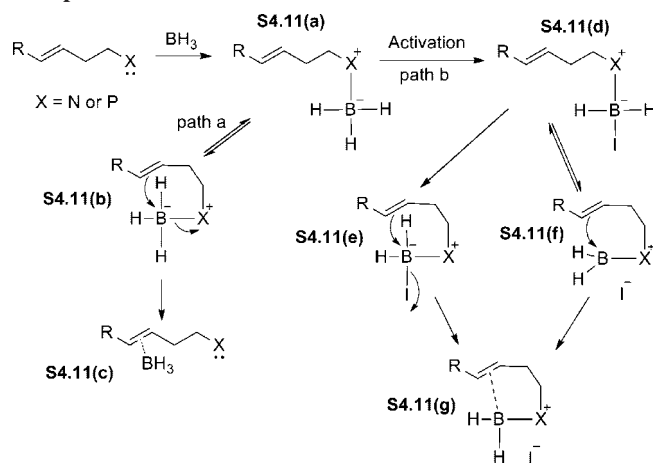
The vast majority of hydroboration reactions with amine–boranes rely on the dissociation of the adduct in solution.<sup>1g,k,121</sup> This type of reactivity will not be covered in this review as we focus on reactions and applications where these adducts react as a discrete unit rather than simply serving as a vehicle for delivering the borane, which has already been covered in numerous reviews.<sup>1g,k,121a</sup> However, there are notable exceptions to this general reactivity. For example, the hydroboration can be effected by a radical pathway or it may be achieved by adding catalytic oxidizing agents.

The radical pathway has been described by Ingold and Sheeller, where they used laser flash photolysis to generate amine–boryl radicals and measured absolute rate constants for their reaction with various substrates, among them olefins.<sup>122</sup> It was found that the strongly nucleophilic Et<sub>3</sub>N•BH<sub>2</sub><sup>•</sup> radical adds to olefins with an electron affinity EA ≥ −0.5 eV at the diffusion-controlled rate (eq 4.1). There were only a few exceptions to this general rule, α-methylstyrene, 1,1-diphenylethylene and pentafluorostyrene, which were attributed to the reduced overlap of the π-systems of the aromatic ring and the double bond in these species. For olefins with a lower electron affinity, the addition was correspondingly slower, but it could be demonstrated that the Et<sub>3</sub>N•BH<sub>2</sub><sup>•</sup> radical was much more nucleophilic than carbon-centered radicals such as benzyl, hydroxymethyl, *t*-butyl or 2-hydroxypropan-2-yl. However, since this was a purely spectroscopic study, the radical products were not trapped with a hydrogen radical donor or other radical scavengers to assess their synthetic usefulness, which would be a worthwhile study.

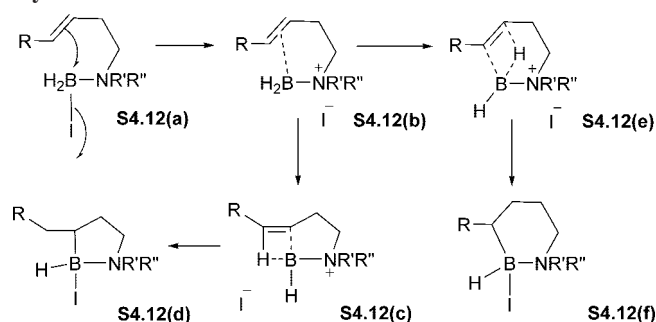


The first intramolecular [2 + 2] hydroboration by an allyl phosphine–borane was reported in 1994.<sup>123</sup> However, the first systematic studies of a metal-free, non-dissociative hydroboration employing amine–borane adducts were not reported until over a decade later by Vedejs and co-workers.<sup>124</sup> As substrates, homoallylic amine– and phosphine–boranes, **S4.11(a)**, were used. If there was no activator present, they argued that the only way the boron center could be attacked intramolecularly was by the double bond, **S4.11(b)**, with concomitant cleavage of the B–N dative bond to give **S4.11(c)** (Scheme 4.11, pathway a). Such a process should be inherently disfavored because the leaving group, in this case nitrogen, would be endocyclic with respect to the hypothetical cyclic transition state and therefore the affected orbitals would be unable to align. However, if the homoallylic amine–borane (or phosphine–borane) was treated with iodine, complex **S4.11(f)** should be generated, which has a labile B–I bond, which is either weakly covalent (**S4.11(e)**, S<sub>N</sub>2 pathway) or a borenium iodide (**S4.11(f)**, S<sub>N</sub>1 pathway) (Scheme 4.11, pathway b). In such a case, the leaving group upon attack of the olefin is now the iodide (*exocyclic* attack), rendering this reaction an intramolecular hydroboration with amines or phosphines functioning as directing groups. This

#### Scheme 4.11. Proposed Mechanisms for the Intramolecular Hydroboration in Homoallylic Amine– or Phosphine–Boranes



#### Scheme 4.12. Potential Mechanism Accounting for the Observed Regioselectivity in Oxidation-Triggered Hydroboration Reactions with Amine–Boranes



mechanistic hypothesis was further supported as catalytic amounts of iodine (10 mol %) were sufficient as the iodide is being regenerated in every turnover step.

An important aspect of this reaction was the regioselectivity. From intermediate **S4.11(g)** (or **S4.12(b)**) two possible [2 + 2] addition intermediates are possible (**S4.12(c)** and **S4.12(e)**, respectively), one of which leading to a five-membered, the other to a six-membered ring (Scheme 4.12), which upon oxidation will give rise to a 1,3-amino alcohol or a 1,4-amino alcohol. In an intramolecular *syn* addition an *endocyclic* TS would be predicted to be less stable than an *exocyclic* one, leading to the observed product distributions, underlining the conclusion that this is a genuine intramolecular process. In general, regioselectivity was higher for the hydroboration of *Z*-alkenes compared to the *E*-isomers. Likewise, terminal alkenes produced poorer regioselectivities, presumably because of the increased flexibility of the molecule.

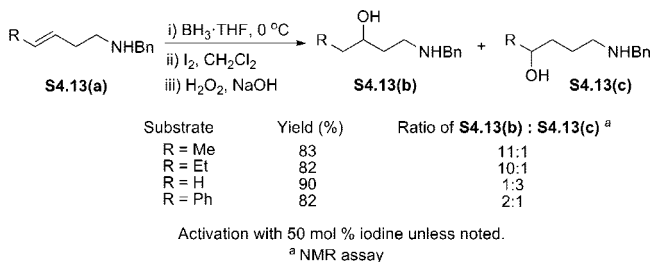
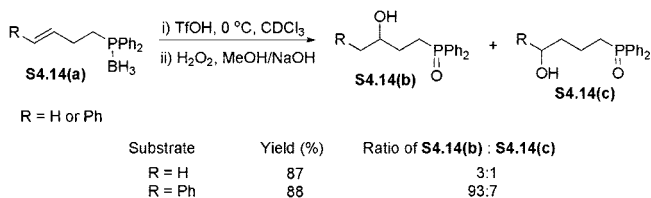
There was also evidence that the reaction proceeded intramolecularly (Table 4.2), as the product ratio was unaffected by concentration. If BH<sub>3</sub>•THF was added, then a conventional hydroboration competed, and the product ratio changed resulting in poorer selectivity. Finally, when an external trap for the hydroboration was added, only the intramolecular process was observed. The intramolecular mechanism was further underlined by crossover experiments with deuterium-labeled substrates.

In contrast to the homoallylic or bishomoallylic amine–boranes, allylic amine–boranes showed a different reactivity pattern. These reactions were much more sensitive to air and

**Table 4.2. Evidence for an Intramolecular Mechanism**

entry	conditions	ratio (b/c)
1	0.1 M	18/1
2	10 M	18/1
3	additional BH <sub>3</sub> ·THF (2 equiv)	2.4/1
4	β-methylstyrene (2 equiv)	18/1 <sup>a</sup>

<sup>a</sup> All β-methylstyrene was recovered.

**Scheme 4.13. Iodine-Promoted Hydroboration of Acyclic Homoallylic Amines<sup>124</sup>****Scheme 4.14. TfOH-Promoted Internal Hydroboration of Homoallylic Phosphines<sup>124</sup>**

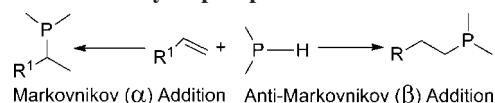
moisture and in this case, an intermolecular pathway seemed likely. Addition of iodine did not improve the regioselectivity and addition of β-methylstyrene also gave hydroboration products of this substrate. This difference in reactivity was attributed to the much more strained TS, which would have to be invoked for an intramolecular process.

Using the iodine-activation methodology, a number of amino-alcohols could be prepared (Scheme 4.13). In the case of phosphine-boranes, the best activator proved to be 1.1 equivalents of trifluoromethanesulfonic acid, but under the oxidizing conditions used to convert the borane to the alcohol, oxidation of the phosphine occurred (Scheme 4.14).

The regioselectivity in the case of the phosphine-boranes also favored the five-membered intermediate (leading to the 1,3-phosphinoalcohol) over the six-membered intermediate leading to the 1,4-phosphinoalcohol, which led to the conclusion that the mechanism is also intramolecular. This was confirmed by further experiments including variation of substrate concentration, competition with BH<sub>3</sub>·THF, and deuteration experiments.

#### 4.1.4. Hydrophosphination

The synthesis of functionalized phosphines is hampered by their toxicity, ease of oxidation, and pyrophoric nature, not to mention the odor in many cases. By comparison, the phosphine-boranes (R<sub>3</sub>P·BH<sub>3</sub>) are generally air stable and nonvolatile compounds. Their utilization as sources of P-H bonds for hydrophosphination reactions has recently received much attention, with several reviews published in the area.<sup>2c,125</sup>

**Scheme 4.15. Products of Markovnikov and Anti-Markovnikov Hydrophosphination**

The addition of a P-H bond across an unsymmetrical unsaturated carbon-carbon bond can give rise to two different isomers via Markovnikov (α-addition) or anti-Markovnikov (β-addition) addition (Scheme 4.15) with regioselectivity often determined by the reaction conditions. Nevertheless, challenges still exist in controlling regioselectivity and the number of P-H additions when more than one P-H bond is present in the molecule.

The use of phosphine-borane adducts for hydrophosphination was first described by Imamoto and co-workers, whereby tetradentate and bidentate phosphines were synthesized by the reaction of activated *P*-vinylphosphine-borane adducts with diarylphosphine-borane adducts in the presence of catalytic amounts of potassium hydroxide. They also described the AIBN-catalyzed hydrophosphination of cyclohexene and oct-1-ene by diphenylphosphine-borane.<sup>126</sup>

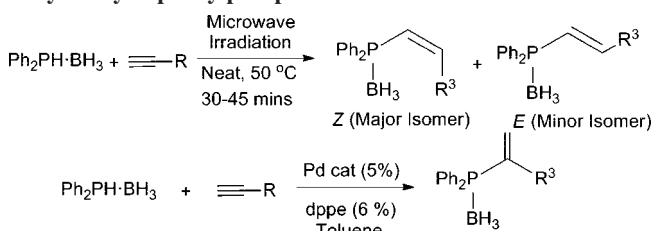
Since then, hydrophosphination reactions involving a range of metal catalysts have been reported. For example, the synthesis of *P*-stereogenic vinylphosphine-borane adducts via the Pd catalyzed hydrophosphination of 1-ethynylcyclohexene with racemic methylphenylphosphine-borane resulted in high enantiomeric excess (>42%) and good yields (>70%).<sup>127</sup>

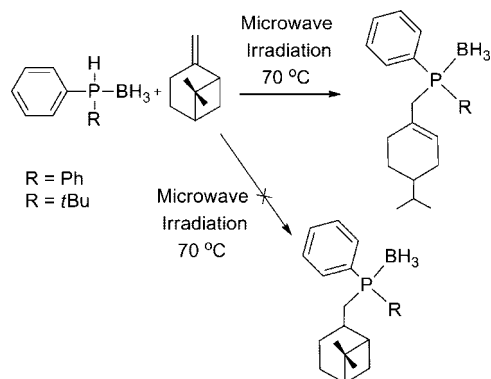
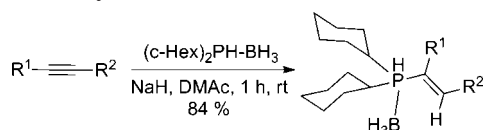
In an attempt to improve yields and develop a more general route to vinylphosphines, the regio- and stereoselective hydrophosphination of alkynes with various phosphine-borane adducts was highlighted.<sup>128</sup> It was observed that under thermal conditions, a mixture of alkyne and phosphine-borane adduct yielded only the anti-Markovnikov β-adduct, while addition of a Pd(0) catalyst resulted in the formation of solely the Markovnikov α-adduct (Scheme 4.16).

Subsequently, the hydrophosphination of unactivated alkenes with secondary phosphine-borane adducts was reported. On heating diphenyl- or methylphenylphosphine-borane with a range of alkenes (pent-1-ene, oct-1-ene, 2,3,3-trimethylbutene, (-)-β-pinene) under microwave irradiation (50–80 °C) or in an oil bath (20–60 °C), clean formation of the hydrophosphination product was observed in good yield (68% for oct-1-ene compared to 35% previously reported by the radical process<sup>126</sup>) (Scheme 4.17).<sup>129</sup>

This methodology has since also been applied to the synthesis of ketophosphine-boranes, vinyl ethers,<sup>130</sup> and thioethers.<sup>131</sup>

It has also been shown that hydrophosphinations may proceed catalytically using basic conditions, with a variety of unactivated internal alkynes and allenyl phosphine-oxides (Scheme 4.18).<sup>132</sup> These substrates could be reacted with a secondary

**Scheme 4.16. Thermal and Catalytic Hydrophosphination of Alkynes by Diphenylphosphine-Borane**

**Scheme 4.17. Uncatalyzed Hydrophosphination of (–)-β-Pinene under Microwave Irradiation with Isomerization**

**Scheme 4.18. Hydrophosphination Using Internal Unactivated Alkynes**


phosphine–borane adduct,  $\text{C}_2\text{PH}\cdot\text{BH}_3$ , and NaH as a base to give the hydrophosphinated products in good yields.

Glueck and co-workers reported synthesis of arylphosphine–borane adducts as starting materials for intramolecular phosphination reactions.<sup>133</sup>

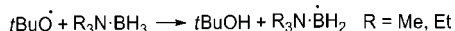
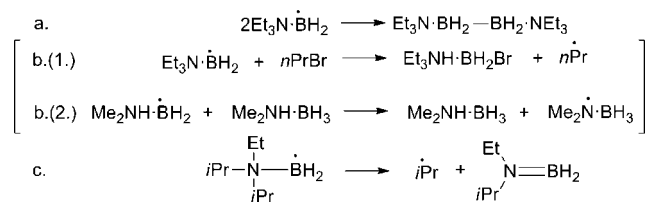
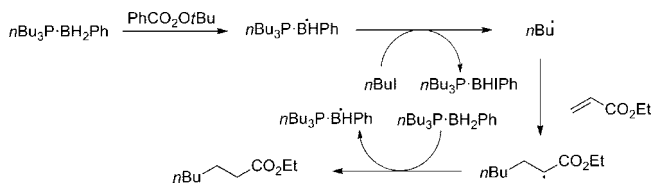
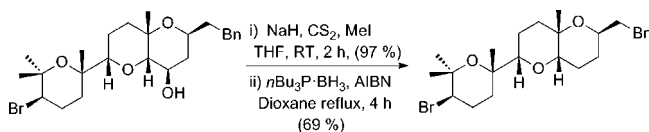
#### 4.1.5. Radical Reactions

##### 4.1.5.1. General Reactivity of Amine–Borane Complexes.

Amine–borane adducts have been shown to react rapidly with radical species, which abstract a hydrogen atom from boron to produce transient amine–boryl radicals (Scheme 4.19).

The seminal research in this area was initiated in the mid 1980s by Roberts and co-workers, who performed a large number of electron spin resonance (ESR) based studies on radical species resulting from hydrogen abstraction from *N,N,N*-trialkyl–<sup>134,135</sup> and *N,N*-dialkylamine–boranes,<sup>136</sup> and subsequently ammonia–borane.<sup>137</sup> Various reactivities of these amine–boryl radicals were demonstrated, all resulting in the quenching of the boryl radical (Scheme 4.20). The reactivity is fundamentally similar to that of carbon centered radicals, with consecutive reactions occurring via (a) self-reaction, (b) abstraction of halide radicals from alkyl halides or  $\text{H}\cdot$  radicals from other amine–boranes, and (c)  $\beta$ -scission. The reactivity was strongly dependent on the nature and substitution of the amine, and reaction conditions.

Of particular interest was reaction b.(2.) shown in Scheme 4.20, wherein a *N,N*-dimethylamine–boryl radical reacted

**Scheme 4.19. Hydrogen Abstraction from Trialkylamine–Boranes by *t*-Butoxylradicals<sup>134</sup>**

**Scheme 4.20. Reactions of Amine–Boryl Radicals**

**Scheme 4.21. Mechanism of the Phosphine–Borane Olefin Reduction Reaction**

**Scheme 4.22. Synthetic Use of the Barton–McCombie Reaction**


with a molecule of its precursor *N,N*-dimethylamine–borane to form *N,N*-dimethylaminyl–borane, a nitrogen centered radical. This reaction was a simple conversion between the kinetic product, where the radical was located at boron, and the thermodynamic product, where the radical was located at nitrogen.<sup>136</sup> Attack at boron of the alkoxy radical to produce the *N,N*-dimethylamine–boryl radical was initially favored because of polar effects operating in the transition state of hydrogen abstraction: the electrophilic alkoxy radical preferred to attack at the electron-rich borane moiety rather than the electron-poor amine component.

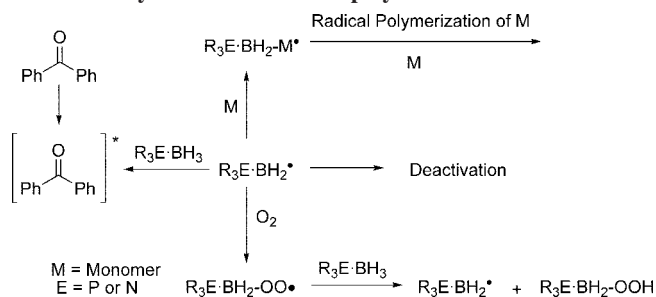
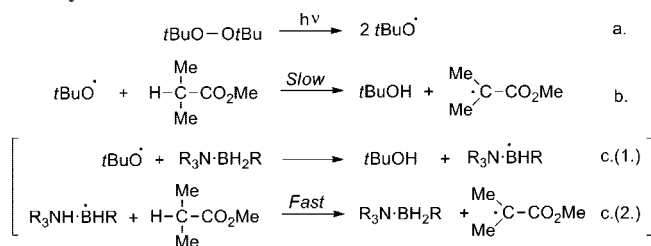
**4.1.5.2. Phosphine–Borane Complexes in Radical Chemistry.** *In situ* generated phosphine–boryl radicals have been introduced by Barton as deoxygenating reagents for xanthates prepared from sterically hindered secondary alcohols. Roberts and co-workers had shown earlier that phosphine–boryl radicals react with butyl iodide to abstract an  $\text{I}\cdot$  radical. The resulting *n*butyl radical could then add to an olefin and abstract a further hydrogen atom to give the alkane (Scheme 4.21).<sup>138,139</sup>

It was demonstrated that such phosphine–boranes could be employed in a Barton–McCombie reaction in place of the more toxic trialkyltinhydrides as hydrogen donors.<sup>140</sup> Since then, this reaction has found application in organic synthesis, for example in the synthesis of a natural product analogue of tyrsiferol (Scheme 4.22)<sup>141</sup> and others.<sup>142</sup>

It is beyond the scope of this article to discuss all of the examples where this type of reaction has been used, but a variety of comprehensive reviews exist.<sup>143</sup>

**4.1.5.3. Boryl Radicals as Photoinitiating Species.** Radical photopolymerizations are generally initiated by type I or type II initiation systems. In type I systems the radical is generated directly under the influence of light, whereas in type II initiators, this is followed by a hydrogen transfer from the solvent or a co-initiator to generate a secondary radical, which is the actual initiator for the polymerization reaction. On the basis of the ease of which boryl radicals can be produced in amine– and phosphine–boranes and their tendency to add to double bonds, the use of *t*BuNH<sub>2</sub>·BH<sub>3</sub>, morpholine·BH<sub>3</sub> and Ph<sub>3</sub>P·BH<sub>3</sub> as co-initiators has been investigated for the film polymerization of epoxyacrylate/tripropylenglycoldiacrylate (Ebecryl 605) using benzophenone as the primary photoinitiator.<sup>144</sup> The progress of the reaction under different conditions (i.e., in air and laminated (exclusion of air)) was followed by the disappearance of the IR signal of the double bond by real-time FT-IR. Compared to a standard amine co-initiator (ethyl 4-(dimethylamino)benzoate) the reactions with morpholine·BH<sub>3</sub> and PPh<sub>3</sub>·BH<sub>3</sub>



**Scheme 4.23. Mechanism of the Benzophenone/Amine–Boryl Co-induced Photopolymerization**

**Scheme 4.24. Action of  $R_3N\cdot BH_2R$  as a Polarity Reversal Catalyst**


were somewhat faster and showed reduced air sensitivity, whereas the reaction with  $t\text{BuNH}_2\cdot\text{BH}_3$  was the slowest and most sensitive to air. The latter was explained by the fragmentation of the amine–boryl radical (Scheme 4.23), which could be demonstrated by ESR and had also been observed before.<sup>134</sup>

Initially, benzophenone was excited to its triplet state and could be either quenched by monomer or oxygen or react with the amine– or phosphine–borane complex to give a boryl radical. The quantum yield for the photoreaction was high and the formation of the secondary radical  $B^*$  was very efficient, which has been shown by laser flash photolysis experiments. The boryl radical itself may then react with oxygen and then another amine or phosphine complex ( $t\text{BuNH}_2\cdot\text{BH}_3$  and  $\text{PPh}_3\cdot\text{BH}_3$  are more susceptible to this pathway than morpholine $\cdot\text{BH}_3$ ), be deactivated, or add to the double bond of the monomer. This was considered the chain propagating species, which itself can be quenched by oxygen.

A prominent use developed for amine–boryl radicals is in the field of polarity reversal catalysts in radical reactions (Scheme 4.24). In this role, the amine–boranes act as an inverter of radical polarity. For example, the easily formed alkoxy radicals such as  $t\text{BuO}\cdot$  favored for many radical reactions are electrophilic in character. This prevented rapid hydrogen abstraction from the  $\alpha$ -C-H groups in esters, the hydrogen in this case being too electron deficient for abstraction by alkoxy radicals which is therefore disfavored by polar effects in the transition state.<sup>145</sup>

Addition of an amine–alkylborane adduct can significantly increase the rate of abstraction. Mechanistically, an initial interaction of the alkoxy radical with the amine–alkylborane to produce an amine–alkylboryl radical is followed by abstraction of the  $\alpha$ -C-H hydrogen, the boryl species reacting significantly faster than the alkoxy radical because of favorable charge–charge interactions in the transition state (Scheme 4.24).<sup>145</sup>

Most recently, amine–boryl radicals carrying optically active alkyl functionality at boron have been demonstrated to be capable of enantioselective hydrogen abstraction from

various substrates.<sup>146</sup> This feature has been demonstrated in the kinetic resolution of various esters and camphor.<sup>145</sup> Within this application, the direction of enantiomeric hydrogen abstraction is defined by the stereochemistry of the alkyl group at the boron center.

**4.1.6. Applications of Amine–Boranes Based on the Polarity of the Bond**

A theoretical study investigated how the BN/CC isosteric analogy in amine–boranes could be exploited for liquid crystal or other applications where the longitudinal dipole and hence the positive dielectric anisotropy  $\Delta\epsilon$  plays a central role.<sup>147</sup> The argument was that the potential advantage of replacing a C–C bond with a B–N bond to achieve high dipole moments as opposed to more conventional push–pull systems could be that the absorption in the UV region is not increased and that such systems may provide insight into geometry independent, solely dipole induced mesogenic behavior. To achieve this, amine complexes with bicyclic boranes were computationally assessed, where the boron has increased Lewis acidity because of its position as the bridgehead. It was shown that such compounds may be stable enough and have an increased dipole moment, which should make them attractive targets as liquid crystal lead structures.

**4.1.7. The Borane Moiety as a Protecting Group for Amines**

The borane functional group is frequently used as a protecting group for phosphines to prevent facile oxidation, which is a less significant problem for amines. However, if the masking of an amine’s nucleophilic properties is required, borane can serve as a protecting group. The introduction of this group needs no further description and follows the amine–borane synthetic procedures described earlier. For its removal, a variety of conditions have been used, such as amine exchange,<sup>148</sup> refluxing in EtOH,<sup>149</sup> treatment with methanolic sodium carbonate,<sup>150</sup> TFA<sup>151</sup> or ammonium chloride<sup>152</sup> or reductive solvolysis in a protic solvent.<sup>79c</sup>

Furthermore, complexation of an amine with a borane may lead to a change in selectivity for further reactions with the amine. This fascinating aspect of amine–borane chemistry has recently been included in a review and will not be discussed here.<sup>11</sup>

**4.1.8. The Borane Moiety as a Protecting Group of Phosphines**

Although not a direct application of phosphine–boranes themselves, the formation of a borane adduct of an existing phosphine can be used to protect the phosphine and often enables alternative chemistry to be performed. Due to the relative ease of oxidation of phosphorus on interaction with oxidizing agents, a major use of borane as a protecting group occurs in systems containing a naked phosphorus center where selective oxidation is required elsewhere and several reviews on this aspect have appeared.<sup>1f,i,2a–c,g,153</sup> We therefore only cover this aspect briefly and highlight some basic concepts of this protection group.

The synthesis of phosphine–boranes and thereby the introduction of the borane protection group has been discussed in section 2. Deprotection can be achieved by various methods, including the use of secondary amines,<sup>153,154</sup> which remove the borane by formation of the stronger

amine–borane adduct, or the use of acids such as methanesulfonic acid or trifluoromethanesulfonic acid,<sup>154d,155</sup> HBF<sub>4</sub>,<sup>156</sup> or zeolites in combination with alcoholysis.<sup>157</sup> Mechanistically, the deprotection with acids is more complex.<sup>158</sup> For the deprotection with HBF<sub>4</sub>, it could be shown that the fluoride of the reagent exchanges with the hydride on the borane moiety of the phosphine–borane, thus rendering it more easily attacked by water, leading to hydrolysis.<sup>158</sup>

However, beyond its use as a mere protection group, the borane can activate the phosphorus atom toward reactions such as stereoselective  $\alpha$ -metalation,<sup>159</sup> which has made it instrumental for the synthesis of chiral phosphines.<sup>159b–d</sup> This aspect has recently been discussed in another review<sup>2d</sup> and will not be detailed here.

## 4.2. Functionalization of Amine– and Phosphine–Borane Adducts

The majority of functionalized amine– and phosphine–borane adducts are readily available by conventional Lewis acid–Lewis base reactions, which explains why the direct functionalization of existing adducts is only necessary in special cases.

### 4.2.1. Functionalization at Nitrogen and Phosphorus

**4.2.1.1. Functionalization by Deprotonation/Addition of an Electrophile.** The most common route to adduct functionalization of this type involves lithiation of the group 15 element, wherein primary or secondary adducts react directly with an alkyl lithium base to provide the monolithiated amine– or phosphine–borane (Scheme 4.25), although the reaction conditions need to be monitored (see section 4.1.2).<sup>116a</sup>

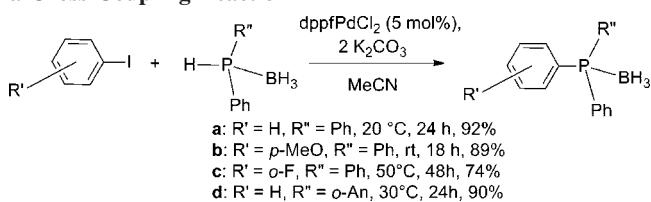
These species can then be functionalized with an appropriate electrophile, such as alkyl and aryl halides, to produce new bonds via salt elimination.<sup>113,160</sup> The use of these adducts in the preparation of new phosphines was first reported by Imamoto and co-workers,<sup>126,161</sup> whereby the reaction of secondary phosphine–borane adduct with an alkylhalide in the presence of KOH or NaH resulted in the formation of functionalized phosphine–borane adducts. The deprotonation of a phosphine–borane and subsequent reaction with an electrophile is now a well established route.<sup>38a,162</sup>

**4.2.1.2. Functionalization of Phosphine–Boranes by Cross-Coupling Routes.** Phosphine–borane modification could also be achieved by transition metal-catalyzed cross coupling. Pd-catalyzed coupling of aryl-iodides with secondary phosphine–borane adducts afforded the tertiary aryl phosphine–borane adducts (Scheme 4.26),<sup>163</sup> a process that is possibly similar to a Buchwald–Hartwig cross-coupling<sup>164</sup> known for amines and alcohols.

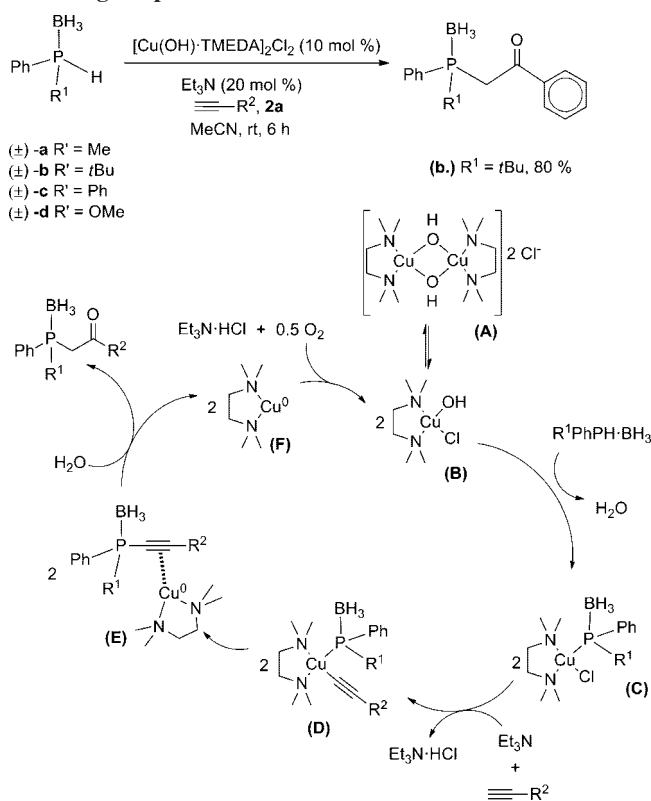
#### Scheme 4.25. Lithiation of *N,N*-Dimethylamine–Borane with *n*-Butyl Lithium



#### Scheme 4.26. Functionalization of Phosphine–Boranes Using a Cross-Coupling Reaction



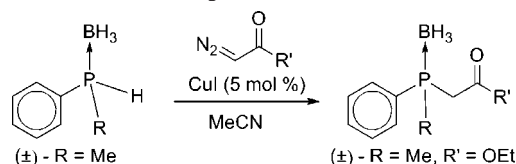
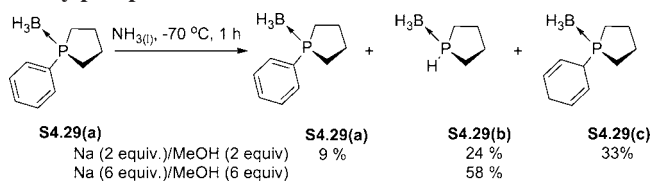
#### Scheme 4.27. Tandem Phosphorus–Carbon Bond Formation/Oxyfunctionalization of Phosphine–Boranes, Including Proposed Reaction Mechanism



The inclusion of electron withdrawing groups in the aryl substituent resulted in slower product elimination from the Pd center, which allowed for the isolation of the corresponding transition metal phosphine–borane complexes described in section 7.

Gaumont and co-workers have investigated the palladium-catalyzed cross-coupling of a range of aryl halides with secondary phosphine–borane adducts in ionic liquids.<sup>165</sup> They observed that catalyst recycling resulted in reduced turnover. Modification of the catalyst affinity for the ionic liquid by addition of a pyridinium salt resulted in significantly improved yields on recycling.<sup>166</sup> Subsequently, the Pd-catalyzed cross-coupling of vinyl-triflates and phosphine–boranes was reported. The methodology proved to be robust with a wide range of dialkyl-, alkyaryl-, and diarylvinyphosphines being synthesized. Also, the inclusion of a chiral vinyl-triflate allowed access to enantiopure vinylphosphines.<sup>167</sup> The Pd-catalyzed cross coupling of vinyltosylates and diphenylphosphine–borane has also been demonstrated, providing a new route to vinylphosphine–boranes.<sup>168</sup>

Copper(II) has also been reported as an efficient catalyst for a tandem phosphorus–carbon bond formation/oxidation reaction.<sup>169</sup> [Cu(OH)·TMEDA]<sub>2</sub>Cl<sub>2</sub> (TMEDA = tetramethylethylenediamine) was able to effect a cross-coupling between secondary phosphine–boranes and alkynes and subsequent hydrolysis of the triple bond to give the corresponding ketone (Scheme 4.27). The mechanism is not known, but it was speculated that the basic copper hydroxide **S4.27(B)** may attack the phosphidoborane to form a copper-phosphido species **S4.27(C)**. Alkynylation, reductive elimination, and attack of the alkynyl group by water may then furnish the product.

**Scheme 4.28. Stereocontrolled CuI-Catalyzed Functionalization of Phosphine–Borane Adducts****Scheme 4.29. Birch Reduction of a Phenylphosphine–Borane Adduct**

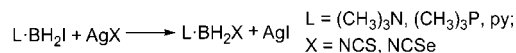
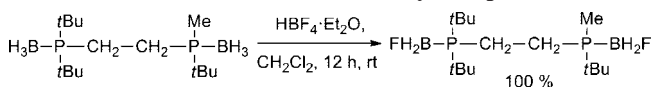
Secondary phosphine–borane adducts have been shown to react with copper carbenes, prepared in situ from a wide variety of diazo species and CuI (Scheme 4.28).<sup>170</sup> If chiral phosphine–boranes were used, the reaction proceeded with retention of the configuration and no loss in enantiomeric excess (*ee*).

**4.2.1.3. Functionalization of Phosphine–Boranes at the Periphery.** In cases where the phosphine–borane bears a phenyl group, it is possible to perform Birch reductions (Scheme 4.29), where the P–B bond remains unaffected, although mixtures of products are often obtained.<sup>171</sup> However, careful tuning of the reaction conditions allowed optimization such that **S4.29(c)** was the preferred product.

**4.2.2. Functionalization at Boron**

**4.2.2.1. Halogenation.** *B*-Halogenation of amine–boranes is a particularly useful reaction as the exchange of a hydrogen atom with a halogen atom usually renders the borane moiety a much improved electrophile. It is a well-known procedure, primarily by reaction with strong acids. Via this method, various boron-halogenated adducts of primary, secondary and tertiary amine–borane adducts can be produced via reaction with hydrofluoric, chloric and bromic acids respectively.<sup>172</sup> The iodinated species can also be synthesized via hydroiodic acid, but alternatively, it can be produced simply by direct reaction with an iodine solution in a variety of organic solvents.<sup>173,172a</sup> Depending on the reaction stoichiometry, mono- or disubstituted halogenated amine–boranes can be attained as required. Complexes of trihaloboranes can also be prepared conveniently via reaction of the required BX<sub>3</sub> (X = F, Cl, Br, I) species and free amine.

*B*-halogenated borane adducts can also be produced via the action of mercuric and silver salts on various adducts. Mercuric halides can be reacted directly with unfunctionalized adducts, producing monohalogenated species (Scheme 4.30).<sup>25a</sup> Silver halide and pseudohalide salts can also be used in conjunction with prehalogenated adducts to substitute halides, or introduce pseudohalide functionality (Scheme 4.31).<sup>174</sup> It must also be noted that in the case of the cyanide anion, many examples are known of similar reactions using sodium and potassium salts in conjunction with iodinated boranes.<sup>175</sup>

**Scheme 4.30. Halogenation of Trimethylamine–Borane with Mercuric Halides****Scheme 4.31. Reactions of Iodinated Borane Adducts with Silver Pseudohalides****Scheme 4.32. Fluorination of a Tertiary Phosphine–Borane**

Other less common routes to halogenated amine–borane adducts utilize halocarbon solvents, including CCl<sub>4</sub> and CBr<sub>4</sub>,<sup>176</sup> or *N*-halosuccinimides as the halide source.<sup>177</sup>

The halogenation of phosphine–borane adducts is much less well developed than that of the amine–borane adducts, despite being broadly similar to their amine analogs. Fluorination has been reported in the patent literature only, where HBF<sub>4</sub> etherate was used to *B*-fluorinate a tertiary phosphine–borane (Scheme 4.32).<sup>178</sup> It is possible that this lack of reports is due to the fact that such compounds are likely to be very labile, as this reagent can also be used to cleave off the borane moiety altogether (see section 4.1.8).<sup>156,158</sup>

Direct chlorination is similarly problematic and various reports indicate that the rate of reaction with hydrogen chloride is slow or that the reaction does not occur.<sup>172c,179</sup> However, there is one isolated report in the patent literature, where a reaction with aqueous HCl was claimed to produce a tertiary phosphine–*B*-chloroborane.<sup>180</sup> Another report claimed the direct chlorination using chlorine gas on *P,P,P*-triphenylphosphine–borane.<sup>181</sup> In general, if a *B*-chlorinated phosphine–borane adduct is required, it may be preferable to react the phosphine with a chlorinated borane directly.<sup>182</sup> *B*-Bromination of tertiary phosphine–boranes could be achieved using either bromine directly<sup>181,183</sup> or HBr,<sup>184</sup> although here, the reaction of a brominated borane with the respective phosphine is also used as an alternative.<sup>183b</sup> Iodination has been reported for secondary<sup>185</sup> and tertiary<sup>184</sup> phosphine–boranes and was typically performed directly with iodine. While in the halogenation reactions for phosphine–borane adducts cited above the borane moiety was always BH<sub>3</sub>, it has also been demonstrated that instead of a hydride, in iodinations with I<sub>2</sub>, TMS (trimethylsilyl) can serve as a leaving group, where the driving force is probably the formation of the strong Si–I bond.<sup>186</sup> However, vinyl lithium and ammonium fluoride did not react.

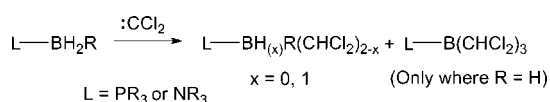
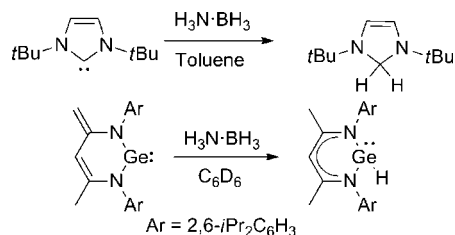
**4.2.2.2. Trifluoromethylsulfonation (Triflation).** Imamoto *et al.* developed a synthetic route to various boron-functionalized phosphine–borane adducts via reaction of tricyclohexylphosphine–borane with a single equivalent of triflic acid.<sup>172b</sup> This yielded a monotriflated species, Cy<sub>3</sub>P·BH<sub>2</sub>OTf, successfully characterized by single crystal X-ray studies. The trifluoromethylsulfonyl group in this adduct was then susceptible to attack by various nucleophilic reagents in THF at 25 °C, opening access to a wide range of *B*-functionalized phosphine–boranes (Table 4.3). Via reaction with a second equivalent of triflic acid, the ditriflated species can be produced and substituted similarly.<sup>172b</sup> The analogous chemistry for monotriflated tertiary amine–boranes was also briefly reported, and further functionalizations of these species were achieved using a similar range of nucleophiles.<sup>187,188</sup>

**4.2.2.3. Reactions with Carbenes and Related Group 14 Species.** In the early 1990s, tertiary phosphine–borane

**Table 4.3. B-Functionalization via Triflate/Nucleophile Exchange**

reagent	conditions <sup>a</sup>	product <sup>b</sup>	mp (°C)	yield <sup>c</sup> (%)
LiAlD <sub>4</sub>	0 °C, 0.5 h	Cy <sub>3</sub> P·BH <sub>2</sub> D	175–177	86
CeCl <sub>3</sub>	50 °C, 5 h	Cy <sub>3</sub> P·BH <sub>2</sub> Cl	163–164	89
LiBr	rt, 0.5 h	Cy <sub>3</sub> P·BH <sub>2</sub> Br	137–139	88
LiCN	rt, 1 h	Cy <sub>3</sub> P·BH <sub>2</sub> CN	174–176	45
PhSH/NaH	0 °C, 0.5 h	Cy <sub>3</sub> P·BH <sub>2</sub> SPh	101–103	82
Me <sub>3</sub> SiC≡CLi	rt, 6 h	Cy <sub>3</sub> P·BH <sub>2</sub> C≡CSiMe <sub>3</sub>	136–137	81
(CH <sub>3</sub> ) <sub>2</sub> Cu(CN)Li <sub>2</sub>	rt, 2 h <sup>d</sup>	Cy <sub>3</sub> P·BH <sub>2</sub> CH <sub>3</sub>	115–116	28 <sup>e</sup>
( <i>m</i> -C <sub>4</sub> H <sub>9</sub> ) <sub>2</sub> Cu(CN)Li <sub>2</sub>	–20 °C, 1 h, 0 °C, 0.5 h	Cy <sub>3</sub> P·BH <sub>2</sub> C <sub>4</sub> H <sub>9-<i>n</i></sub>	84–85	78
( <i>s</i> -C <sub>4</sub> H <sub>9</sub> ) <sub>2</sub> Cu(CN)Li <sub>2</sub>	–30 °C, 1 h, 0 °C, 0.5 h	Cy <sub>3</sub> P·BH <sub>2</sub> C <sub>4</sub> H <sub>9-<i>s</i></sub>	90–91	89

<sup>a</sup> All reactions carried out in THF using 1 mmol of Cy<sub>3</sub>P·BH<sub>2</sub>OTf and 2 mmol of nucleophile unless otherwise stated. <sup>b</sup> All compounds synthesized afforded satisfactory spectral data and elemental analysis (C, H, N). <sup>c</sup> Isolated yields. <sup>d</sup> In THF:Et<sub>2</sub>O, 2:1. <sup>e</sup> Cy<sub>3</sub>P·BH<sub>3</sub> produced in 25% yield.

**Scheme 4.33. Insertion Reactions of Dichlorocarbene with Tertiary Amine- and Tertiary Phosphine-Borane Adducts****Scheme 4.34. Reactions of Ammonia-Borane with a Selected Carbene and Germene**

adducts were shown to undergo insertion reactions of dichlorocarbene, CCl<sub>2</sub>, at the B–H bonds, producing dichloromethyl substitution at boron.<sup>189</sup> Analogous insertion compounds have since been demonstrated for amine-borane adducts.<sup>190</sup> However, literature documents only tertiary amine and phosphine adducts as substrates, with dichlorocarbene remaining the only species reported to perform this insertion chemistry (Scheme 4.33).<sup>190,191</sup>

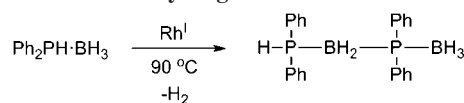
Reports are much sparser on the reactivity of primary amine-borane with carbenes, and none are reported for secondary amine-boranes. However, *N*-heterocyclic carbenes were shown to react with ammonia-borane to give the corresponding 1,1-dihydroimidazole (Scheme 4.34), whereas a similar germene also reacted but retained a germene-like character.<sup>192</sup>

## 5. Dehydrogenation Reactions

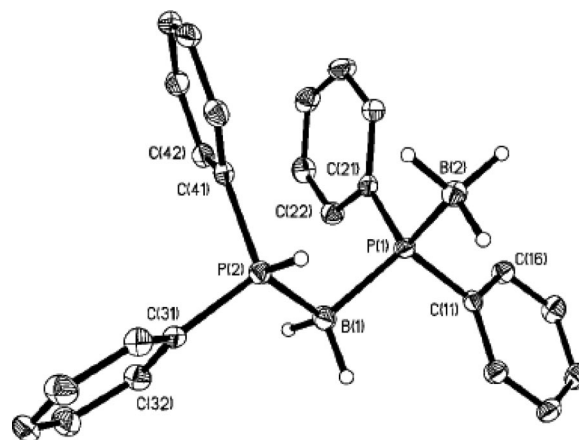
### 5.1. Catalytic Dehydrocoupling of Amine- and Phosphine-Boranes

#### 5.1.1. Experimental Studies

The first *catalytic* dehydrocoupling of amine-boranes was briefly mentioned in the patent literature in 1989 by Laine and Blum who claimed the dehydrogenation of several amine-boranes using Ru<sub>3</sub>(CO)<sub>12</sub> at 60 °C.<sup>193</sup> However, very little experimental or analytical data was presented. Another

**Scheme 5.1. First Example of a Catalytic Phosphine-Borane Dehydrogenation<sup>a</sup>**

<sup>a</sup> Catalysts: 0.3 mol % of {Rh(1,5-cod)(μ-Cl)}<sub>2</sub> or [Rh(1,5-cod)<sub>2</sub>][OTf], 14 h, Yield: 85%.

**Figure 5.1.** Molecular structure of Ph<sub>2</sub>PH-BH<sub>2</sub>-PPh<sub>2</sub>-BH<sub>3</sub> (thermal ellipsoids at the 30% probability level). Reprinted with permission from ref 195. Copyright 1999 Wiley VCH.

brief mention of such a reaction appeared in the same year by Roberts, where a heterogeneous Pd/C catalyst was used to convert Me(*t*Bu)NH·BH<sub>3</sub> to the corresponding dehydrogenated aminoborane Me(*t*Bu)N=BH<sub>2</sub> at 120 °C.<sup>194</sup> At this high temperature, a purely thermal dehydrocoupling reaction cannot be excluded and, as no blank reactions without a catalyst or reactions at lower temperatures with the catalyst were presented, catalysis was not proven.

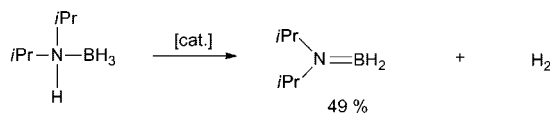
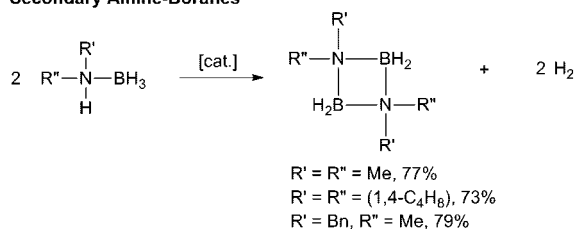
The first detailed report of a catalytic dehydrocoupling reaction of a group 13/15 adduct appeared in 1999.<sup>195</sup> Manners and co-workers reported that catalysts, such as [Rh(1,5-cod)<sub>2</sub>][OTf] or {Rh(1,5-cod)(μ-Cl)}<sub>2</sub> (1,5-cod = cycloocta-1,5-diene) with the catalyst loading of about 0.3 mol % were able to dehydrocouple a neat adduct diphenylphosphine-borane at 90 °C over 14 h to form a white, crystalline, air-stable product (Scheme 5.1). This dimeric phosphine-borane was characterized by single crystal X-ray crystallography (Figure 5.1) and multinuclear NMR spectroscopy. A similar result was reported for the dimerization of *t*BuPH<sub>2</sub>·BH<sub>3</sub> using NiCl<sub>2</sub> (10 mol %).<sup>162</sup> However, it was possible to extend the catalytic dehydrocoupling methodology to primary phosphine-borane adducts, which also allowed the successful synthesis of polyphosphinoboranes (see section 8).<sup>195</sup>

Since then, the majority of reports concerning the dehydrocoupling of group 13/15 adducts has centered mainly on amine-borane adducts, not least because the simplest example, ammonia-borane, has been discussed extensively as a hydrogen storage material with a high gravimetric hydrogen content of 19.6%, which is discussed in detail in our other review.<sup>6</sup>

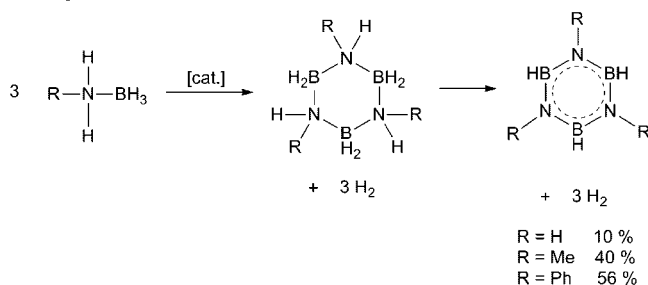
The first report in the open literature detailing a truly catalytic dehydrocoupling of amine-boranes focused on Rh(I) or Rh(III) based catalysts.<sup>88b</sup> Shortly after this, the reaction was further explored,<sup>88a</sup> where a range of amine-

### Scheme 5.2. First Rh-Catalyzed Dehydrogenation of Secondary and Primary Amine–Borane Adducts

#### Secondary Amine–Boranes



#### Primary Amine–Boranes

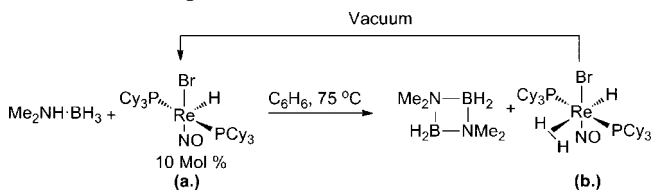


boranes and catalysts were studied. One of the most efficient catalysts discovered was {Rh(1,5-cod)(μ-Cl)}<sub>2</sub> in typical catalyst loadings of 0.5–5 mol %. Secondary amine–borane adducts were dehydrocoupled to give cyclic dimers [R'R''N-BH<sub>2</sub>]<sub>2</sub> in good yields or, in the case of bulky substituents on nitrogen, the corresponding aminoborane monomer. Primary amine–borane adducts on the other hand were reported to give cyclotriborazanes<sup>196</sup> initially, which converted into borazines upon prolonged heating, concurrent with the loss of another equivalent of dihydrogen (Scheme 5.2).

Since then, a significant amount of work has been devoted to the search for alternative catalysts for the dehydrocoupling of amine–boranes. Me<sub>2</sub>NH·BH<sub>3</sub> is often used as a test substrate because it is commercially available and easily purified by sublimation. Most importantly, in contrast to ammonia–borane, the product of the dehydrocoupling reaction is soluble in a large range of solvents, which simplifies analysis of the reaction products and facilitated much needed mechanistic studies. A summary of all catalysts used to date for the dehydrocoupling of Me<sub>2</sub>NH·BH<sub>3</sub> is presented in Table A.1 in the Appendix. In this section, we will discuss the catalysts which have been used for amine–borane dehydrocoupling reactions. The following sections will discuss the stepwise formation of the cyclic aminoborane [Me<sub>2</sub>N-BH<sub>2</sub>]<sub>2</sub> leading to a subsection describing the numerous mechanistic considerations.

After the initial success in particular with Rh(I) precatalysts, many alternative and in several cases more active catalysts were developed. In the following section we will describe the development of a rapidly increasing arsenal of (in most cases assumed rather than proven) homogeneous catalysts, with a particular focus on the most effective or best researched systems in the order from early to late transition metals. Using group 6 catalysts, a number of light-activated dehydrocoupling reactions were described, based on the removal of a CO ligand and generation of a vacant coordination site. However, as these complexes led to the

### Scheme 5.3. Generation of a Dihydrogen Complex from 16-Electron Re Species



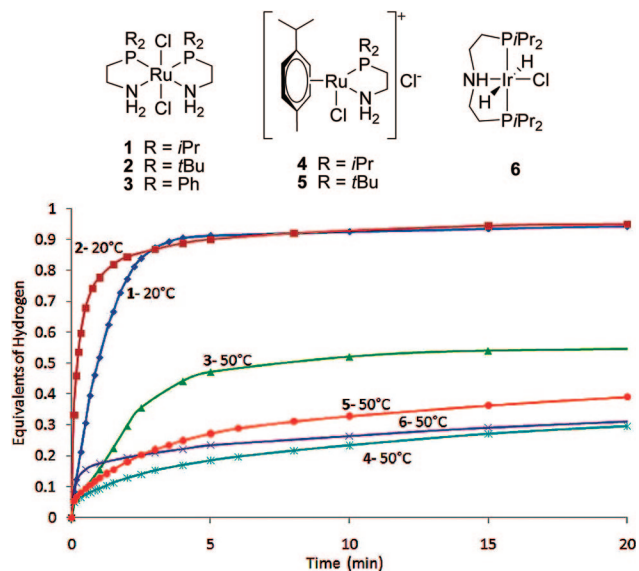
isolation of very interesting model complexes, we will discuss those in the section on transition metal complexes of group 13–group 15 adducts. Likewise, impressive advances have been achieved concerning the isolation of potential intermediates with Rh cationic complex catalysts, for which we refer the reader to section 7.

One of the first very effective homogeneous catalytic systems was titanocene, Cp<sub>2</sub>Ti, generated *in situ* from Cp<sub>2</sub>TiCl<sub>2</sub> with 2 equivalents of *n*BuLi (Table A.1, entry 2)<sup>91</sup> The secondary amine–borane adducts Me<sub>2</sub>NH·BH<sub>3</sub> and *i*Pr<sub>2</sub>NH·BH<sub>3</sub> were dehydrogenated to give the dimerized dehydrogenated amine–borane [Me<sub>2</sub>N-BH<sub>2</sub>]<sub>2</sub> or the monomeric *i*Pr<sub>2</sub>N=BH<sub>2</sub>, respectively, quantitatively at room temperature. However, this system was completely inactive with respect to ammonia–borane and dehydrogenation of primary amine–boranes proceeded only with negligible reaction rates. The reason for this selectivity is unknown at present. A very similar class of catalysts was subsequently reported in 2007 (Table A.1, entries 4 to 15).<sup>197</sup> In this contribution, a range of sandwich titanium and zirconium compounds were screened, the best of which was able to dehydrocouple *N,N*-dimethylamine–borane at 23 °C in benzene within minutes. These catalysts were highly active for secondary amine–boranes, but showed a slow kinetic profile for ammonia–borane, even at 65 °C. Again, the origin for the observed selectivity was unclear.

Another class of catalysts, based on rhenium, proved useful for dehydrocoupling of secondary amine–boranes.<sup>92</sup> However, the catalytic activity was relatively low and analogous experiments are yet to be carried out on primary amine–borane adducts. Nonetheless, this catalytic system can be used for hydrogen transfer reactions for the reduction of olefins and has been discussed in more detail in section 4.1.1.2.

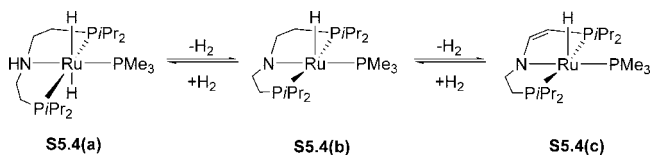
A more detailed study on these systems was published in 2009.<sup>93</sup> It was found that a number of the rhenium complexes synthesized were active catalysts for the dehydrocoupling of *N,N*-dimethylamine–borane. Here, the coordination of H<sub>2</sub> was directly observed, which allowed the conclusion that, at least for this system, the metal complex is more than merely a Lewis acid or a Lewis base. When the 16-electron species **S5.3(a)** was reacted with an excess of Me<sub>2</sub>NH·BH<sub>3</sub> at 75 °C, the dehydrocoupled product was observed and the dihydrogen complex **S5.3(b)**. The latter could be reconverted to **S5.3(a)** under vacuum (Scheme 5.3).

Some of the most active catalysts for the dehydrocoupling of Me<sub>2</sub>NH·BH<sub>3</sub> and ammonia–borane itself are ruthenium-based and were independently discovered by Fagnou and Schneider.<sup>91,198</sup> Although formally isoelectronic to ethane, the polarity and electronic structure of ammonia–borane are more closely related to methanol. Therefore Ru-catalysts which had already been successfully used for alcohol redox processes<sup>199</sup> were screened for their ability to dehydrogenate ammonia–borane.<sup>91</sup> Even very low catalyst loadings of 0.3 mol % allowed the release of up to 1 equivalent of hydrogen



**Figure 5.2.** Fagnou's results on  $\text{NH}_3 \cdot \text{BH}_3$  dehydrogenation with Ruthenium catalysts after activation with KOtBus. Reprinted with permission from ref 91. Copyright 2008 American Chemical Society.

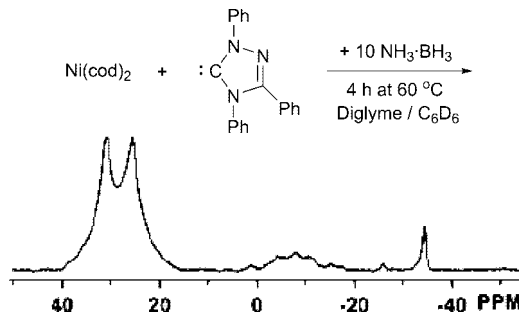
#### Scheme 5.4. Hydrogenation/Dehydrogenation Equilibria between Amino (a), Amido (b), and Enamido (c) Complexes



within 5 min at ambient temperature (Figure 5.2). However, to release 2 equivalents, it was necessary to dehydrogenate ammonia-borane together with *N*-methylamine-borane.

The advantage of the Ru(II) catalyst developed by Schneider,<sup>198</sup> bearing a PNP amido chelate ligand, is that it is a relatively stable isolable species and is not restricted to generation *in situ*. The latter situation hinders detailed mechanistic/kinetic studies as the exact concentration of the catalyst is unknown and varies during the time of formation. In solution, the catalyst  $[\text{Ru}(\text{H})(\text{PMe}_3)(\text{PNP})]$  showed interesting hydrogenation/dehydrogenation reactivity itself, which depended on the concentration of hydrogen (Scheme 5.4).<sup>198</sup> With this catalyst, loadings of 0.1 mol % were sufficient for the evolution of slightly more than 1 equivalent of hydrogen within 10 min, and indeed, even catalyst loadings as low as 0.01 mol % were effective.

Further investigations into Rh(I) salts as catalysts (or catalyst precursors) led to the discovery that a Wilkinson's catalyst analog, with strongly donating ligands,  $\text{RhCl}(\text{P}(\text{HCy}_2)_3)_3$ , was in fact a homogeneous catalyst (demonstrated by filtration and Hg poisoning experiments) for the dehydrocoupling of  $\text{Me}_2\text{NH} \cdot \text{BH}_3$ .<sup>200</sup> Already a more active catalyst than Wilkinson's catalyst for a range of amine-borane adducts, the rate of the reaction could be enhanced further by the addition of a strong Lewis acid,  $\text{B}(\text{C}_6\text{F}_5)_3$ . It was reasoned that this would shift the dissociation equilibrium for the dissociation of one phosphine ligand to liberate a coordination site by complexation to the phosphine. While this could not be spectroscopically observed with the employed low catalyst loading of 1 mol %, the control experiment, where one equivalent of phosphine was mixed with one equivalent for the Lewis acid, showed evidence for the corresponding phosphine-borane



**Figure 5.3.**  $^{11}\text{B}\{-^1\text{H}\}$  NMR spectrum in  $\text{C}_6\text{D}_6$ /diglyme from the reaction of 10 equiv of  $\text{NH}_3 \cdot \text{BH}_3$  with 1 and 2 equiv of  $\text{Ni}(\text{cod})_2$  and Enders' NHC, respectively, after 4 h at 60 °C. The signal at -36 ppm is attributable to the NHC-BH<sub>3</sub> adduct (~2% of total boron). Reprinted with permission from ref 205. Copyright 2007 American Chemical Society.

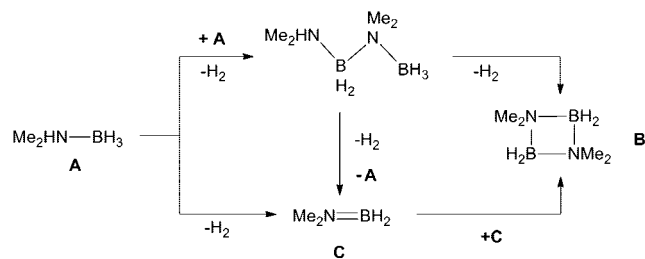
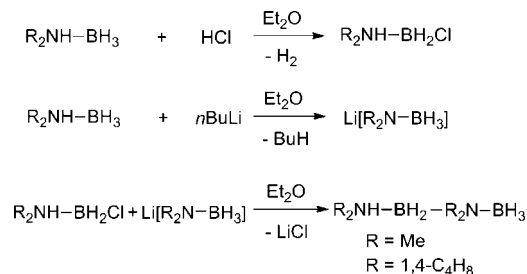
complex  $\text{C}_y\text{PH} \cdot \text{B}(\text{C}_6\text{F}_5)_3$ . The corresponding Ir catalyst,  $\text{IrCl}(\text{P}(\text{HCy}_2)_3)_3$ , was also active, but less so and was not able to dehydrogenate diphenylphosphine-borane,  $\text{Ph}_2\text{PH} \cdot \text{BH}_3$ , which was possible with  $\text{RhCl}(\text{P}(\text{HCy}_2)_3)_3$  at elevated temperatures (60–90 °C).

A very important breakthrough in terms of catalytic effectiveness for the removal of one equivalent of dihydrogen from primary amine-boranes was reported by Goldberg, Heinekey, and co-workers in 2006.<sup>201</sup> They demonstrated that Brookhart's iridium pincer complex,  $(\text{POCOP})\text{Ir}(\text{H})_2$  ( $\text{POCOP} = [\mu^3\text{-}1,3\text{-}(\text{OP}t\text{Bu}_2\text{C}_6\text{H}_3)]$ )<sup>202</sup> was able to dehydrogenate ammonia-borane in a dilute THF solution with a catalyst loading of 0.5 mol % within 14 min. Because of the poor solubility and the sole dependence on solid state analytical techniques (IR, WAXS, and  $^{11}\text{B}$  MAS NMR), the identity of the product was difficult to determine but was proposed to be cyclopentaborazane  $[\text{NH}_2\text{-BH}_2]_5$ .<sup>203</sup> The fact that only one equivalent of hydrogen was released and that secondary amine-boranes did not react may be the result of the sterically crowded catalytic center, which precludes the reaction of secondary amine-boranes. Interestingly, the catalyst was not stable over time, but converted into a resting state  $(\text{POCOP})\text{-IrH}_2(\text{BH}_3)$ ,<sup>204</sup> which could be reactivated by the addition of  $\text{H}_2$ .

In 2006, a very efficient class of group 10 transition metal catalysts (in terms of equivalents of hydrogen released) was presented, based on nickel, a relatively cheap metal.<sup>205</sup> In combination with various *N*-heterocyclic carbene ligands (NHCs), a  $\text{Ni}(\text{cod})_2$  solution in  $\text{C}_6\text{D}_6$ /diglyme was able to release up to 2.8 equivalents of hydrogen in approximately 4 h at 60 °C with a catalyst loading of 10 mol % (Figure 5.3). The major products showed peaks from 40 to 18 ppm in the  $^{11}\text{B}$  NMR spectrum and were suggested to be cross-linked borazine-type species. In this study kinetic isotope effects for  $\text{NH}_3 \cdot \text{BD}_3$  (1.7),  $\text{ND}_3 \cdot \text{BH}_3$  (2.3), and  $\text{ND}_3 \cdot \text{BD}_3$  (3.0), were also reported, which later were of great value in investigation of mechanism for this system (see section 5.1.3).

#### 5.1.2. Mechanistic Proposals Concerned with Product Formation

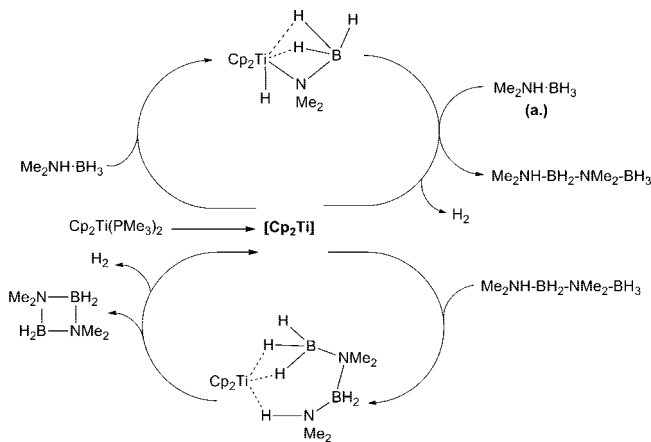
Most mechanistic proposals are based on the assumption that the initial product of the reaction is the aminoborane,  $\text{R}_2\text{N}=\text{BH}_2$ , which then dimerizes to give the cyclic dimer  $[\text{R}_2\text{N}=\text{BH}_2]_2$ . This dimerization is assumed to be facile, which is the reason most computational work only described the mechanism up to this step. As far as the formation of

**Scheme 5.5. Possible Pathways for the Formation of the Cyclic Aminoborane [Me<sub>2</sub>N-BH<sub>2</sub>]<sub>2</sub>**

**Scheme 5.6. Preparation of the Linear Dimers of *N,N*-Dimethylamine-Borane and Pyrrolidine-Borane**


the cyclic dimer from Me<sub>2</sub>NH·BH<sub>3</sub> is concerned, two B-N bonds and two H-H bonds need to be formed, while two N-H and B-H bonds, respectively, need to be broken, which implies a stepwise process. The dehydrogenation of Me<sub>2</sub>NH·BH<sub>3</sub> to the monomeric aminoborane Me<sub>2</sub>N=BH<sub>2</sub>, followed by dimerization to [Me<sub>2</sub>N-BH<sub>2</sub>]<sub>2</sub> is only one mechanistic possibility. Another possibility would be the initial formation of a linear dimer followed either by direct cyclization or, alternatively, disintegration to the aminoborane and again, subsequent dimerization (Scheme 5.5.)

The first attempt to shed light on the possible involvement of a linear dimer appeared in 2003, albeit with a view to investigate why no higher oligomers or polymers were observed in the reaction. The linear dimer of *N,N*-dimethylamine-borane, Me<sub>2</sub>NH-BH<sub>2</sub>-NMe<sub>2</sub>-BH<sub>3</sub> was prepared by reaction of a B-chlorinated *N,N*-dimethylamine-borane with *N,N*-dimethyl-*N*-lithioamidoborane (Scheme 5.6). The catalytic dehydrocoupling of the Me<sub>2</sub>NH·BH<sub>2</sub>-NMe<sub>2</sub>·BH<sub>3</sub> in toluene with a catalyst loading of 1.5 mol % {Rh(1,5-cod)(μ-Cl)}<sub>2</sub> took 2 days at ambient temperature, which was considerably slower than the formation of the cyclic dimer, [Me<sub>2</sub>N-BH<sub>2</sub>]<sub>2</sub>, from *N,N*-dimethylamine-borane. These results were interpreted as a preferred intramolecular reaction of the ends with each other over an intermolecular reaction to form oligomers. Therefore, the steric strain present in the isoelectronic cyclobutane is clearly not present in these N<sub>2</sub>B<sub>2</sub> cyclic dimers. The slower reaction kinetics when compared with the dehydrocoupling of Me<sub>2</sub>NH·BH<sub>3</sub> seems to point toward a mechanism where the linear dimer plays a minor role and Me<sub>2</sub>N=BH<sub>2</sub> is the main product, followed by dimerization.

That this, however, need not necessarily be the case was demonstrated for the catalytic dehydrocoupling of Me<sub>2</sub>NH·BH<sub>3</sub> with ruthenium pincer complexes [Ru(H)-(PMe<sub>3</sub>)(PNP)] with PNP = N(CH<sub>2</sub>CH<sub>2</sub>PiPr<sub>2</sub>)<sub>2</sub> and *trans*-[Ru(H)<sub>2</sub>(PMe<sub>3</sub>)(PNP)<sup>H</sup>] with PNP<sup>H</sup> = HN(CH<sub>2</sub>CH<sub>2</sub>PiPr<sub>2</sub>)<sub>2</sub>.<sup>206</sup> While by <sup>11</sup>B NMR, a signal for Me<sub>2</sub>N=BH<sub>2</sub> was observed, which quickly disappeared, presumably because of dimerization, an intermediate at δ = 1.2 ppm with *J* = 109 Hz was detected. Previously, this signal had been tentatively

**Scheme 5.7. Catalytic Cycle for the Transformation of Me<sub>2</sub>NH·BH<sub>3</sub> to the Cyclic Dimer [Me<sub>2</sub>N-BH<sub>2</sub>]<sub>2</sub> with Proposed Intermediates**


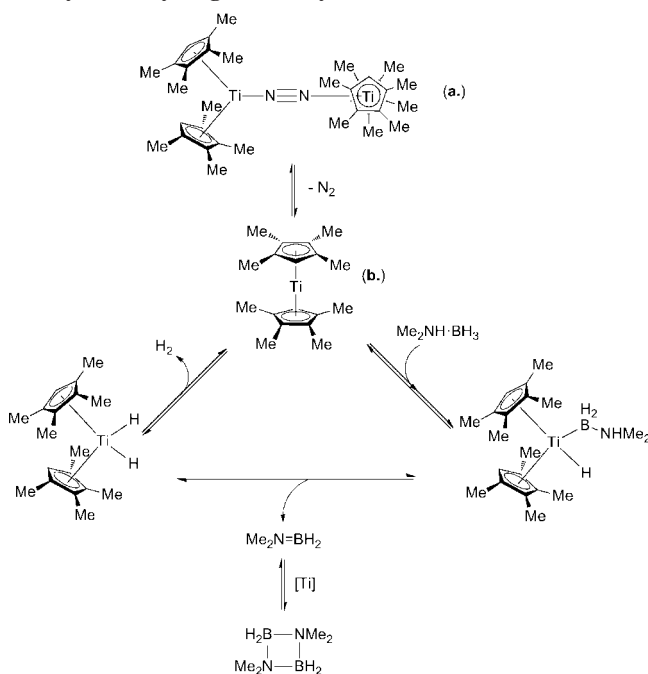
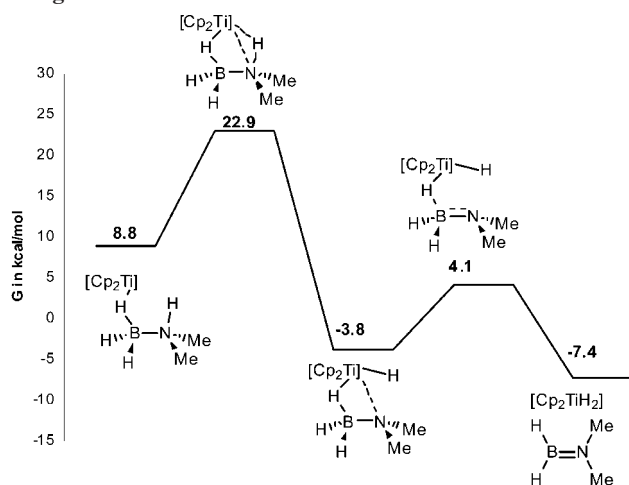
assigned<sup>90,205,207</sup> to the cyclic trimer, [R<sub>2</sub>N=BH<sub>2</sub>]<sub>3</sub>,<sup>208</sup> but was now conclusively assigned to the linear dimer Me<sub>2</sub>NH-BH<sub>2</sub>-NMe<sub>2</sub>-BH<sub>3</sub>. This species had been known and characterized since 1999,<sup>209</sup> but the coupling constant had been erroneous, which hindered the correct identification in reaction mixtures. At the time of writing the mechanism for this reaction has not been fully studied. Kinetic isotope effects (KIE) suggest a concerted mechanism, with KIEs of 2.1 (D<sub>3</sub>B·NH<sub>3</sub>), 5.2 (H<sub>3</sub>B·ND<sub>3</sub>), and 8.1 (D<sub>3</sub>B·ND<sub>3</sub>) found relative to H<sub>3</sub>B·NH<sub>3</sub> dehydrogenation.<sup>198</sup>

For the titanocene system with Cp<sub>2</sub>Ti(PMe<sub>3</sub>)<sub>2</sub> as a pre-catalyst, the involvement of this linear dimer species has also been demonstrated.<sup>210</sup> A detailed examination of this system showed that a two stage mechanism operated. Within this mechanism, the initial dehydrocoupling step produced the linear dimer, which then underwent cyclization to the product [Me<sub>2</sub>N-BH<sub>2</sub>]<sub>2</sub> (Scheme 5.7).<sup>210</sup> In addition to detailed kinetic evidence based on isotope effects and variation of the reaction conditions combined with kinetic modeling, the observation that the isolated linear dimer could undergo the transformation to the cyclic dimer was evidence that the computational model proposed by Ohno and Luo<sup>211</sup> (see section 5.1.3, Scheme 5.9), where the involvement of a linear dimer was dismissed, does not present the complete story.

For the cationic rhodium complex [Rh(PiBu<sub>3</sub>)<sub>2</sub>][BAR<sup>F</sup><sub>4</sub>], which is also active for the dehydrogenation of Me<sub>2</sub>NH·BH<sub>3</sub>, the involvement of the linear dimer was also demonstrated.<sup>212</sup> These catalytic results should also be viewed in the context of the thermal dehydrocoupling of this substrate where detailed isotope scrambling studies,<sup>213</sup> and gas phase pyrolysis studies suggested an involvement of a linear dimer, which then presumably disintegrates into the monomeric aminoborane prior to dimerization.

**5.1.3. Mechanistic Proposals Concerned with the Role of the Metal Center**

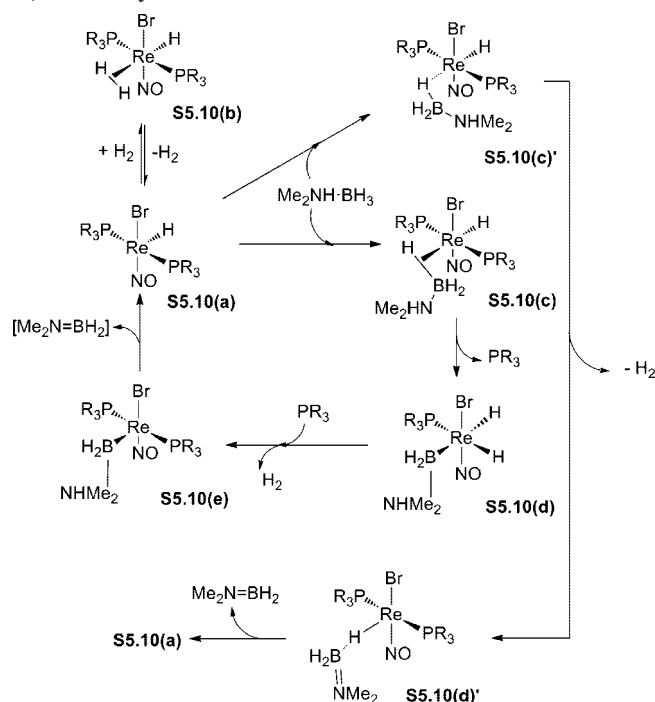
Group 4 metallocene catalysts have also been examined mechanistically with the aim of determining the nature of the transformations at the metal center. The well-defined catalyst (S5.8(a)), provided the first experimental mechanistic insights. For this species, the reaction was monitored by NMR, and a new paramagnetic species was observed, which was speculated to be the corresponding sandwich complex (S5.8(b)). Interestingly, when the reaction was performed under D<sub>2</sub> gas, the formation of HD and an incorporation of

**Scheme 5.8. Proposed Mechanism of the Titanocene Catalyzed Dehydrogenation by Chirik and Co-worker.**<sup>197</sup>**Scheme 5.9. DFT-Based Proposal for a Titanocene-Catalyzed Dehydrogenation Reaction with Gibbs Free Energies Corrected for Toluene**<sup>211</sup>

deuterium in the product in the hydridic B–H positions were detected. Whether there was deuterium incorporation in the protic N–H positions could not be ascertained because of NMR peak overlap.

Ohno and Luo<sup>211</sup> analyzed the closely related  $\text{Cp}_2\text{TiCl}_2/2 n\text{BuLi}$  system described in 2006 based on the assumption that titanocene is the catalytically active species.<sup>90</sup> They studied both bimolecular (catalyst and  $N,N$ -dimethylamine–borane) and trimolecular (catalyst and two molecules of  $N,N$ -dimethylamine–borane) pathways and found that the rate determining step for the former is much more favorable (Scheme 5.9).

Based on the assumption that a naked titanocene had been formed in situ, this species was then stabilized by coordinating the amine–borane via a B–H bond in an  $\eta^1$ -fashion, which was endoergic by 8.8 kcal/mol (entry point in Scheme 5.9). The following rate determining step was through a cyclic five-membered transition state (TS) (Ti–H–B–N–H–), representing an N–H activation step. The following TS trans-

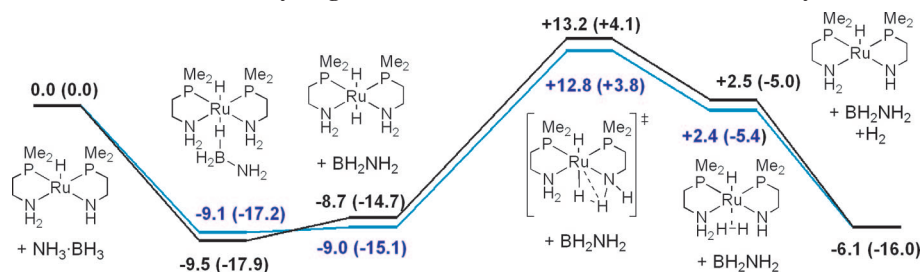
**Scheme 5.10. Mechanistic Proposal for the Rhenium-Catalyzed Dehydrocoupling of  $N,N$ -Dimethylamine–Borane**

ferred the hydrogen from nitrogen onto the metal, the Ti–N bond was cleaved and the dative  $\pi$ -bond from nitrogen to boron formed. This TS was subsequent to the release of the product, which subsequently dimerized, and  $\text{Cp}_2\text{TiH}_2$ . The loss of hydrogen from this species was possibly concomitant with a renewed binding of another molecule of dimethylamine–borane, but a TS for this was not presented. It is noteworthy that Ohno's mechanism did not describe a B–H activation/oxidative addition process as proposed by Chirik (Scheme 5.8) for a very similar catalyst.

For the Re-systems described by Berke,<sup>93</sup> all mechanistic evidence was experimental and no computational study has been presented to date. The current mechanistic proposal was based on the observation that the catalyst  $[\text{ReBrH}(\text{PCy}_3)_2(\text{NO})]$  was able to produce the cyclic dimer  $[\text{Me}_2\text{N–BH}_2]_2$  from  $\text{Me}_2\text{NH}\cdot\text{BH}_3$ . The catalyst was transformed to  $[\text{Re}(\text{H}_2)\text{BrH}(\text{PCy}_3)_2(\text{NO})]$ , which could lose  $\text{H}_2$  under vacuum to regenerate the original catalyst (Scheme 5.10). Following the formation of a vacant coordination site on the metal center in the catalyst, the amine–borane is proposed to form a  $\sigma$ -complex between its B–H bond and the metal. This step is presumably followed by oxidative addition to give a Re(III) species **5.10(d)** with concomitant phosphine dissociation. Formation of the dihydrogen  $\sigma$ -complex and subsequent dissociation of the dihydrogen, followed by phosphine association would then lead to **S5.10(e)** giving back the rhenium hydride catalyst species after a  $\beta$ -hydride shift which leads to the extrusion of  $\text{Me}_2\text{N=BH}_2$ . An alternative mechanism could involve an electrostatic interaction between the B–H bond and the metal center of the catalyst, followed by dihydrogen formation and would lead to an aminoborane–rhenium complex **S5.10(d)'**, which could expel the aminoborane and regenerate the catalyst.

Fagnou and co-workers also briefly investigated a possible mechanism for the Ru catalysts, which they introduced for the catalytic dehydrocoupling of ammonia–borane (Scheme 5.11).<sup>91</sup> They suggested a Ru-dihydride as the catalytically



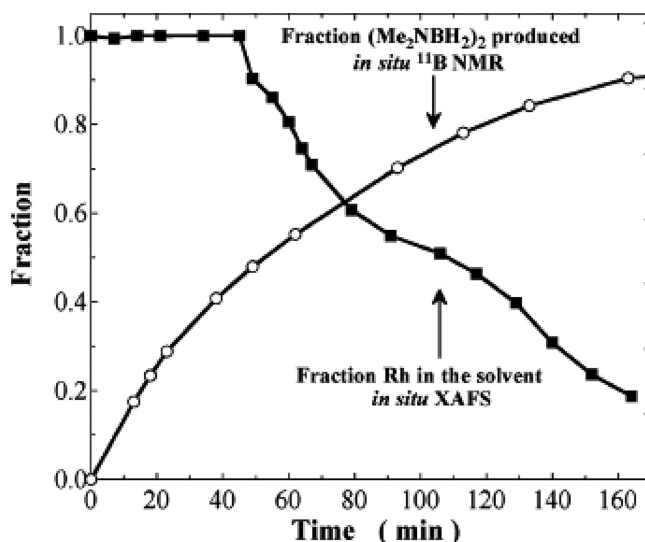
Scheme 5.11. Possible Mechanism for the Dehydrogenation of Ammonia-Borane with Ru Catalysts<sup>a</sup>

<sup>a</sup> Black and blue lines indicate different conformers of the P,N ligands of the Ru species. reported values are in kcal/mol.

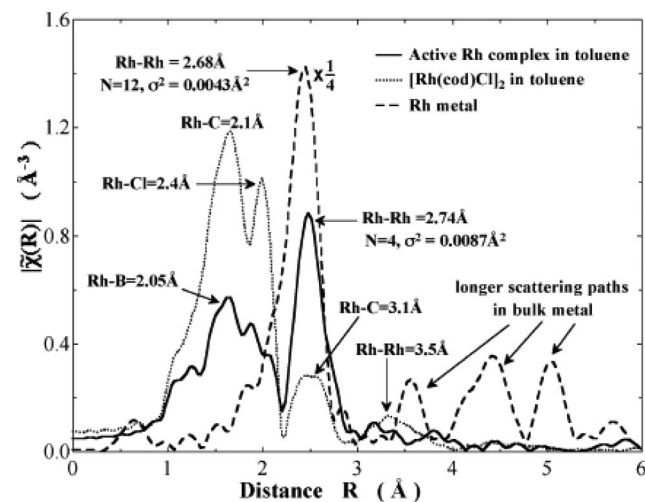
active species, which would be formed *in situ*. This could then be protonated at the amido group of the ligand by the protic hydrogens of ammonia-borane, which would then lead to the dehydrogenated ammonia-borane intermediate and a trans-Ru-dihydride. The latter could then be protonated by the ligand to give a dihydrogen complex, which would then be able to evolve dihydrogen and release the active catalytic species.

The nature of the catalytic Rh(I) systems with amine-boranes and phosphine-boranes sparked a debate on whether the process was homogeneous or heterogeneous in nature.<sup>179,215</sup> A systematic protocol first developed by Finke was followed, where a series of tests are performed.<sup>216</sup> These include (i) TEM analysis, (ii) UV-vis spectroscopy, (iii) analysis of the reaction kinetics, (iv) mercury poisoning experiments, (v) fractional poisoning experiments, and (vi) filtration experiments. The reaction of  $\text{Ph}_2\text{PH}\cdot\text{BH}_3$  with  $\{\text{Rh}(\text{1},5\text{-cod})(\mu\text{-Cl})_2\}$  at 90 °C in a 10 mol % catalytic loading displayed all indicators of a homogeneous process; there was no visible precipitate, only a color change from orange to red, no induction period, and attempted mercury and phosphine poisoning showed no marked effect on the rate of the dehydrocoupling reaction. In contrast to this, for amine-boranes, the orange solution, after an induction period, darkens to brown/black, which led to the hypothesis that Rh(I) was merely the catalytic precursor, which is then reduced to colloidal Rh(0), the actual catalytically active species. Analysis by transmission electron microscopy, TEM, showed Rh-nanoparticles of about 2 nm diameter. As there is a risk that these could simply be formed under the influence of the beam and therefore represent an artifact, their presence alone is insufficient evidence for the role of Rh-nanoparticles. Poisoning with mercury or phosphine halted the reaction as did nanofiltration. Taken together, these results strongly suggested a heterogeneous mechanism for the Rh-catalyzed dehydrogenation of amine-boranes.<sup>179</sup> However, this was disputed by Autrey, Fulton and Linehan, who analyzed the same reaction and various other amine-borane adducts using *in situ* XAFS (X-ray absorption fine structure spectroscopy) (Figure 5.4).<sup>217</sup> This technique utilizes amplitudes and phase shifts from the strong backscattering from heavy atoms such as transition metals to distinguish them from lighter elements, such as boron, carbon, or nitrogen.

From these data, bond distances and the atoms in the coordination spheres could be determined (Figure 5.5). Combined with results from *in situ* <sup>11</sup>B NMR spectroscopy they suggested that the catalytically active species is not colloidal Rh(0), but in fact, a Rh<sub>4-6</sub> cluster, which is in equilibrium with a polymeric aminoborane bridged Rh<sub>4-6</sub> cluster, where the edges of the cluster are connected by amine-borane molecules (Scheme 5.12).

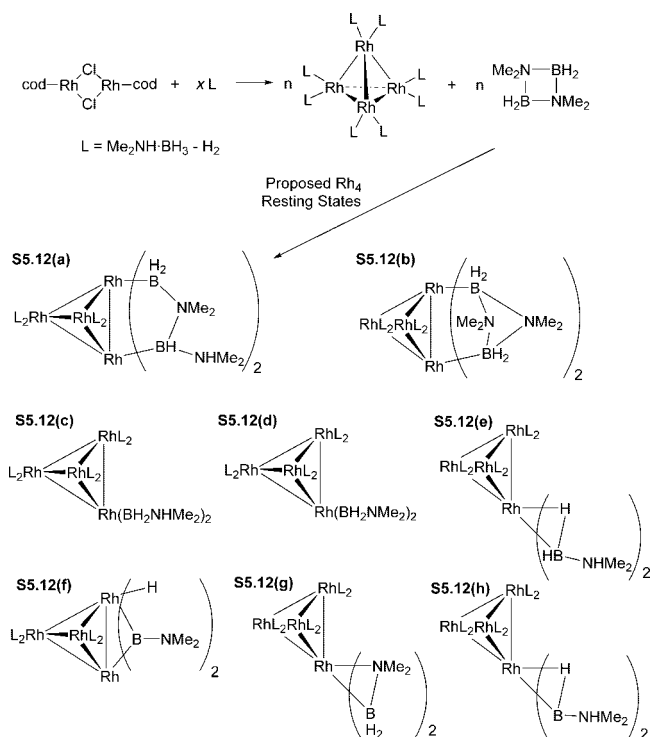


**Figure 5.4.** Time-evolving formation of  $[\text{Me}_2\text{N}-\text{BH}_2]_2$  measured *in situ* by <sup>11</sup>B NMR (O) and the soluble Rh complex in toluene measured from the *in situ* XAFS edge height (■). Reprinted with permission from ref 217a. Copyright 2005 American Chemical Society.

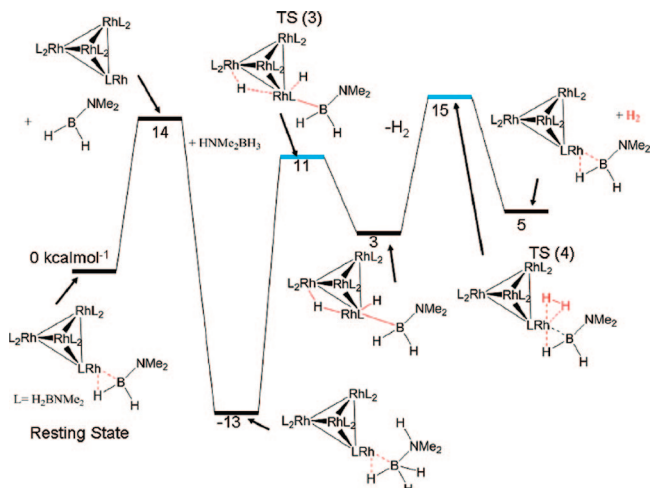


**Figure 5.5.** Radial structure plots for the active Rh complex in toluene at  $t = 34$  min (solid), the fresh Rh(cod) precatalyst in toluene (dotted) and Rh metal (dashed) without phase corrections. The phase-corrected Rh-Rh distances, coordination numbers, and Debye-Waller factors from a fit to the theoretical standard (FEFF8) are given. The Rh metal spectrum is multiplied by 1/4 to fit the graph. Reprinted with permission from ref 217a. Copyright 2005 American Chemical Society.

The experimental XAFS data were further supported by *ab initio* molecular dynamics calculations, which showed that the identified Rh structures were highly fluxional.<sup>218</sup> The

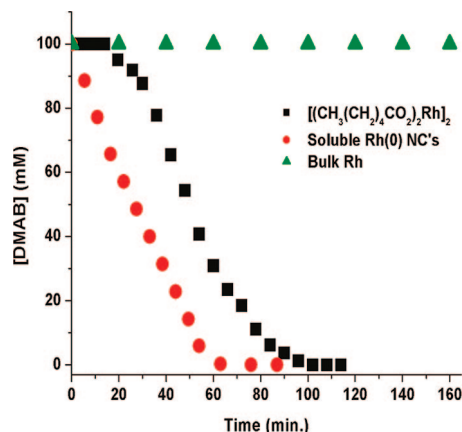
Scheme 5.12. Postulated Formation of a Rh<sub>4</sub> Cluster<sup>a</sup>

<sup>a</sup> Only a single ligand L is shown explicitly for clarity. The stick structures, which normally denote bonds between the rhodium and boron atoms, are in these structures used to denote the close proximity of the rhodium and the boron atoms as determined by XAFS. These atoms may indeed be held together by a direct Rh–B bond, by bridging hydrogens, or by both.



**Figure 5.6.** Postulated mechanism for the dehydrocoupling of *N,N*-dimethylamine–borane with Rh clusters. Black (blue) lines represent relative energies of intermediates (transition states). Insets show schematic structure of relevant intermediates and transition states. All energies are quoted in kcal/mol. Reprinted with permission from ref 218. Copyright 2009 American Chemical Society.

resting state Rh<sub>4</sub>(H<sub>2</sub>BNMe<sub>2</sub>)<sub>8</sub> proved to be compatible with operando XAFS measurements. Rousseau and co-workers further proposed a mechanism for catalytic *N,N*-dimethylamino–borane dehydrogenation with an energy barrier for the rate limiting step of approximately 28 kcal/mol (Figure 5.6).<sup>218</sup> The dehydrogenated Me<sub>2</sub>N=BH<sub>2</sub> ligand is proposed to dissociate from the cluster and a new amine–borane adduct adds to the vacated site. Both the hydridic and the protic hydrogens are then transferred to the



**Figure 5.7.** Catalytic performances of bulk rhodium, rhodium(0) nanoclusters (NCs) and a reaction with [(pentCO<sub>2</sub>)<sub>2</sub>Rh] (pent = pentyl) as a catalytic precursor. Reprinted with permission from ref 220. Copyright 2009 American Chemical Society.

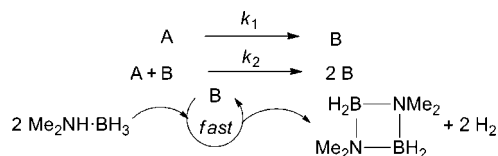
cluster and a dihydrogen complex forms in the rate limiting step. Release of dihydrogen releases the resting state again.

In reflection, it must be considered that both heterogeneous and homogeneous mechanisms could operate and also that the dominant component of the reaction mixture need not necessarily include the active catalytic species as these may be present in very low concentrations. It has subsequently been shown that the reaction is faster *in air*, proceeding with very short induction periods (1 min as opposed to >45 min).<sup>219</sup> In a further important contribution in 2009, it was conclusively demonstrated that dimethylammonium hexanoate stabilized rhodium(0) nanoclusters of about 1.9 ± 0.6 nm in size consisting of about 190 Rh(0) atoms could act as heterogeneous catalysts for the dehydrogenation of *N,N*-dimethylamine–borane in toluene at 25 °C with a very high turnover number (average TON = 40 h<sup>-1</sup>).<sup>220</sup> When rhodium(II)hexanoate in toluene was mixed with a solution of *N,N*-dimethylamine–borane, the reaction changed color from green to pink, then orange before it turned dark brown. Poisoning studies with mercury and CS<sub>2</sub> suggested a heterogeneous reaction as these reagents completely halted the reaction. In addition, filtration experiments showed that for reactions where the dark brown filtrate of a completed reaction was used for a further catalysis, the reaction proceeded without the induction period normally seen when the Rh(II) precursor was used. On the other hand, the black filter residue (interpreted as bulk Rh) had no catalytic activity (Figure 5.7), which was interpreted as evidence for soluble Rh(0) nanoclusters as the heterogeneous catalytically active species.

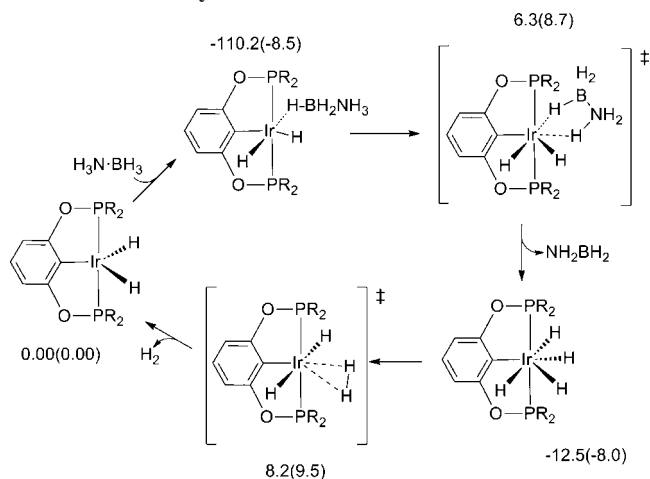
Further characterization of the postulated Rh(0) nanoclusters was provided using a combination of FTIR, XRD, XPS, UV, and NMR studies. The latter provided evidence for the salt [Me<sub>2</sub>NH<sub>2</sub>][pentCO<sub>2</sub>], which showed the participation of *N,N*-dimethylamine–borane in the formation of the stabilizing ligand for the Rh nanoclusters. Further compelling evidence for this role was provided by trapping the resulting released diborane as B(OMe)<sub>3</sub>. The kinetic analysis for this system was performed very thoroughly and was consistent with an autocatalytic nanocluster formation (Scheme 5.13).

Because of its outstanding efficiency for the dehydrocoupling of ammonia–borane, Brookhart's catalyst was also investigated by DFT methods, using a slightly simplified model.<sup>214</sup> Two different pathways were analyzed, one via a 14-electron iridium species, which they concluded could not

**Scheme 5.13. Autocatalytic Formation of the Rh Nanoclusters and Dehydrogenation of *N,N*-Dimethylamine–Borane**



**Scheme 5.14. Postulated Dehydrogenation Mechanism for Brookhart's Catalyst<sup>a</sup>**



<sup>a</sup> Total energies in kcal/mol in THF. Relative energies are calculated using B3LYP(CPCM)/B2//B3LYP/B1 with zero-point correction. Relative energies calculated with B3LYP(CPCM)/B1//B3LYP/B1 are shown in parentheses.

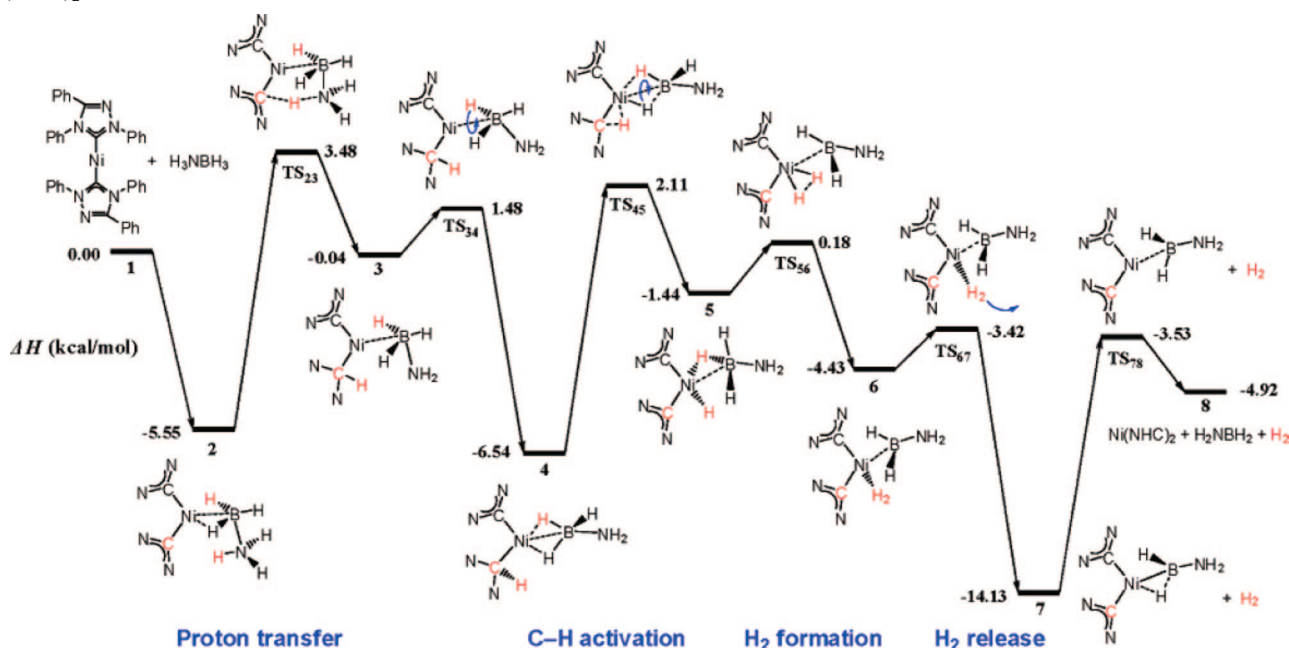
take place at room temperature, and another Ir(III)/Ir(V) process via a 16-electron species (Scheme 5.14), energies given are zero point corrected potential energies). Here, the catalyst is initially electrostatically stabilized by binding the substrate via the hydridic B–H hydrogen. In a concerted

TS, the protic N–H hydrogen was transferred to the iridium, followed by dissociation of the dehydrogenated amine–borane. In the second TS the dihydrogen is formed and leaves the complex. Both barriers for the TSs are very similar, so it is possible that there are two rate limiting steps in this reaction. Experimentally, the tetrahydride appeared as the major detectable intermediate, which is in accordance with the mechanism presented.

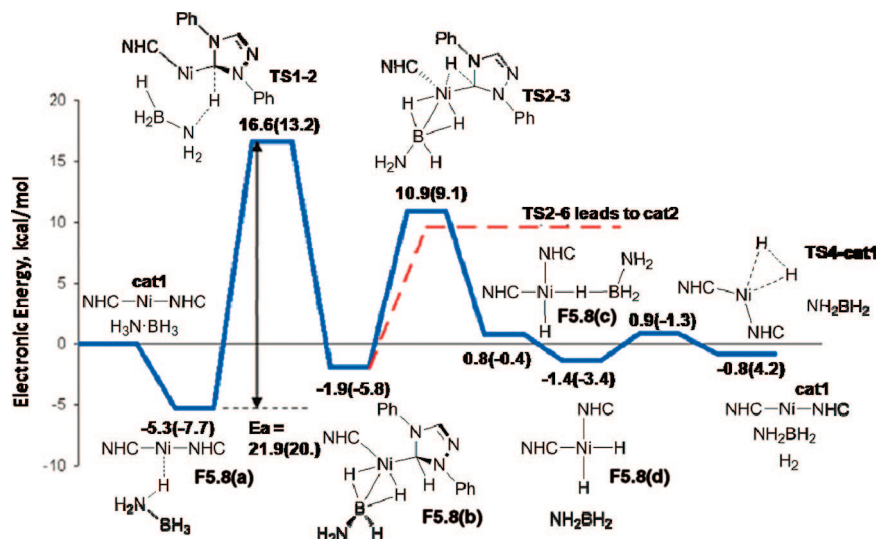
A cationic Ir complex, [Ir(dppm)<sub>2</sub>OTf], was also briefly studied for the catalytic dehydrocoupling of ammonia–borane.<sup>221</sup> While the corresponding dihydride, [Ir(dppm)<sub>2</sub>H<sub>2</sub>]-OTf could be isolated and the absence of a signal by <sup>11</sup>B NMR spectroscopy indicated the formation of insoluble product, no detailed studies were performed. However, a DFT calculation implied that B–H activation for this complex was feasible, which is in accordance with the more detailed studies on the similar cationic Rh complexes (see section 7).

The most complex mechanism so far was found for the nickel carbene complexes, which were computationally analyzed by Hall and co-worker (Scheme 5.15)<sup>222</sup> and later by Musgrave and Paul and co-workers.<sup>223</sup> Again, the catalyst complex was postulated to be initially stabilized by binding a substrate ammonia–borane molecule via a B–H–metal interaction, in a  $\sigma$ -complex. In the following unusual step, the carbene ligand on nickel participated in a proton transfer from nitrogen, which led, after rotation into a more stable conformer, to a NiH–H<sub>2</sub>BH–NH<sub>2</sub> complex. The proton, which intermittently resided on the carbon of the ligand, underwent migration to nickel and eventually a nickel-dihydrogen complex was formed with dehydrogenated amine–borane, H<sub>2</sub>N=NH, still bound to it. Both products are then released. The mechanism proposed here differs markedly from the initially proposed trimolecular process. Although it does explain the observed first order kinetics, provided that such a kinetic fit of the data is appropriate in the first place, it doesn't explain the kinetic isotope effects,

**Scheme 5.15. Predicted Reaction Mechanism and Relative Enthalpies of Ammonia–Borane Dehydrogenation Catalyzed by Ni(NHC)<sub>2</sub><sup>a</sup>**



<sup>a</sup> Four main steps are involved: transfer of H<sup>+</sup> from N to C(Carbene), transfer of H from C to Ni, transfer of H from B to Ni, and release of H<sub>2</sub> and H<sub>2</sub>B–NH<sub>2</sub>. Reproduced with permission from ref 222. Copyright 2008 American Chemical Society.



**Figure 5.8.** Reinvestigation of Hall's NHC Ni carbene mechanism by Zimmerman and co-workers. Reprinted with permission from ref 224. Copyright 2009 American Chemical Society.

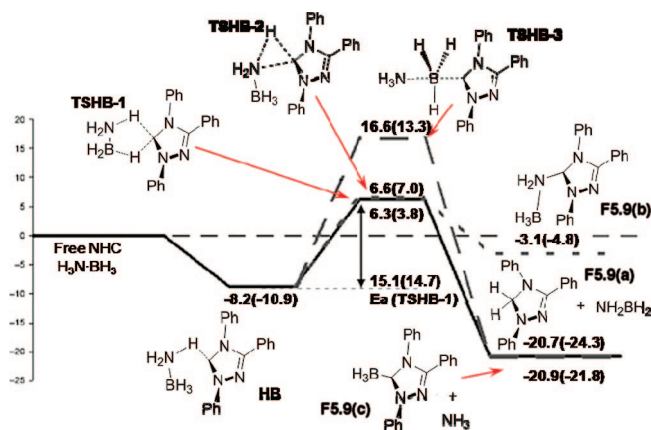
which were reported by Baker and co-workers:  $\text{ND}_3 \cdot \text{BH}_3$ , 2.3;  $\text{NH}_3 \cdot \text{BD}_3$ , 1.7;  $\text{ND}_3 \cdot \text{BD}_3$ , 3.0.<sup>205</sup>

Shortly after the communication by Hall and Yang, Paul and co-workers published another computational analysis of the same reaction, in which they reached slightly different conclusions.<sup>223a,224</sup> They discuss the mechanism proposed by Hall and Yang (Scheme 5.15), but suggest that the initially formed B–H  $\sigma$ -complex proposed by Hall was higher in energy than a N–H complex **F5.8(a)**, which therefore would be the species present in the reaction mixture (Figure 5.8). Therefore, the overall energy barriers that Zimmerman and Paul predicted were substantially different to those of Hall and co-workers. Another difference was that they found that **F5.8(c)** can dissociate into  $\text{NH}_2=\text{BH}_2$  and **F5.8(d)** without barrier, which would simplify Hall's mechanism in that the elimination steps that form  $\text{H}_2$  and  $\text{NH}_2=\text{BH}_2$  would not be necessary.

These authors found that the catalyst precursor (**1** in Scheme 5.15) decomposes in the presence of ammonia–borane to give  $[\text{Ni}(\text{NHC})-(\text{NH}_2\text{BH}_2)]$  with concomitant loss of a free carbene ligand. This free carbene ligand played a pivotal role in the mechanism (Figure 5.9) because it was capable of dehydrogenating ammonia–borane in a concerted mechanism to give  $\text{H}_2\text{N}=\text{BH}_2$  and the reduced NHC (with a barrier of 6.3 kcal/mol zero point corrected energy in the gas phase and with free NHC and ammonia–borane as the reference point). While this species on its own could not release  $\text{H}_2$  to reform the free NHC (barrier for reductive elimination is 50.5 kcal/mol zero point corrected energy in the gas phase), the initially formed catalyst  $[\text{Ni}(\text{NHC})-(\text{NH}_2\text{BH}_2)]$  (**cat3**) could perform a C–H insertion on the reduced NHC with a barrier of 22.1 kcal/mol (zero point corrected energy in the gas phase) to give species **F5.10(b)** (Figure 5.10). A second C–H activation then transferred the second hydrogen onto the metal center to give species **F5.10(c)**, which lost an NHC ligand, followed by loss of hydrogen to close the secondary catalytic cycle to give  $[\text{Ni}(\text{NHC})-(\text{NH}_2\text{BH}_2)]$  (**cat3**).

The overall catalytic mechanism as proposed by Zimmerman and co-workers is therefore a combination of catalytic processes that may all occur simultaneously (Scheme 5.16).<sup>224</sup>

There are clearly discrepancies in these accounts of the same mechanism, and a direct comparison is not possible

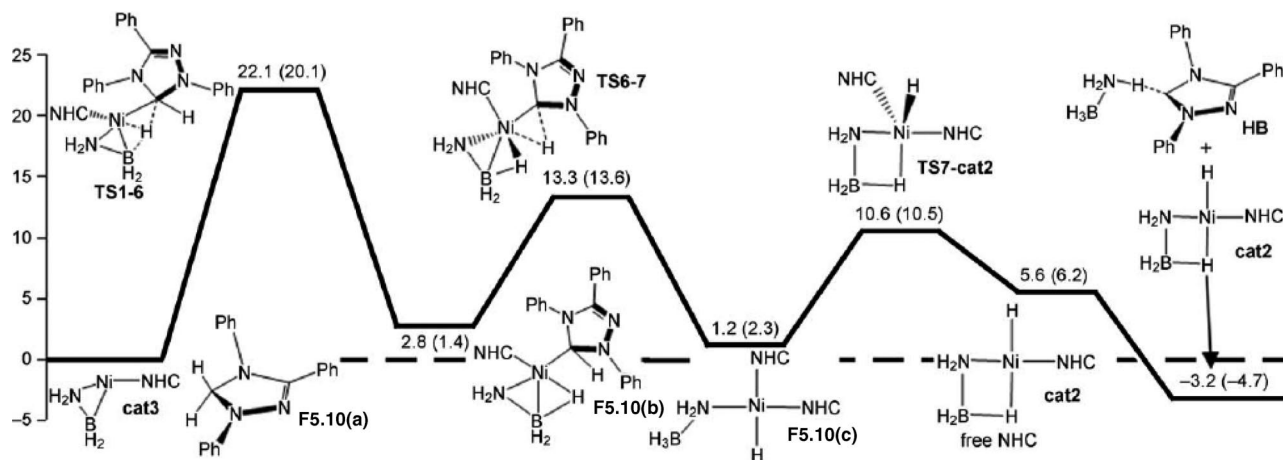


**Figure 5.9.** Energetic profile for three low-energy pathways for NHC reaction with ammonia–borane (upper loop of Scheme 5.16). Shown are N–H activation (**TSHB-2**),  $\text{S}_\text{N}2$  attack (**TSHB-3**), and concerted addition of hydrogen to free NHC (**TSHB-1**). B–H activation involves a barrier of 53.5 kcal/mol above **HB** and is not shown. **TSHB-2** has a similar energy barrier as **TSHB-1**, but the reaction is easily reversible because its product (**2**) is thermodynamically uphill from **HB**. Energies are reported as zero-point corrected, zero-Kelvin B3LYP CPCM solvation energies in THF with energies in benzene shown in parentheses. Energy scale in kcal/mol. Reprinted with permission from ref 223a. Copyright 2009 Wiley VCH.

because different functionals and basis sets were used.<sup>225</sup> The turnover limiting step in Hall's mechanism was only 9 kcal/mol, whereas in Zimmerman's mechanism it was 22.1 kcal/mol. However, Zimmerman's mechanism suggested calculated KIEs of  $\text{ND}_3 \cdot \text{BH}_3$  1.7,  $\text{NH}_3 \cdot \text{BD}_3$  1.4, and  $\text{ND}_3 \cdot \text{BD}_3$  2.4, which correspond well with the experimental observations, whereas Hall's mechanism could only account for a N–H KIE. Moreover, we would like to point out that if the mechanism is as complex as both Hall and Zimmerman suggest, a simple first-order fit of the experimental data upon which the KIEs were based is almost certainly not applicable.

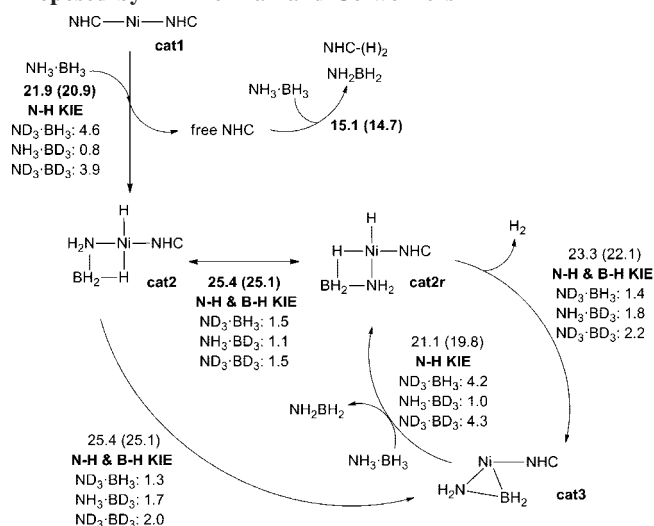
## 5.2. Solvolysis of Amine–Borane Adducts

A chemically different approach from catalytic dehydrocoupling reactions for utilizing B–N materials for hydrogen production/storage is metal-assisted solvolysis. In organic chemistry, amine-stabilized boranes have a long history as reducing agents (see section 4). In many cases, it appears



**Figure 5.10.** Full energetic profile for C–H activation of **F5.10(a)** (equals **F5.9(a)**) at **cat3** to regenerate free NHC. **Cat2** can release  $\text{H}_2$  to reform **cat3** and complete the catalytic cycle with a barrier of (25.4 kcal/mol). Reprinted with permission from ref 223a. Copyright 2009 Wiley VCH.

### Scheme 5.16. Overview of the Intertwined Mechanisms as Proposed by Zimmerman and Co-workers



that the borane moiety of the complex is the active species and the amine moiety simply a bystander, and it has been shown that transition metals catalyze the solvolysis of amine–boranes in solvents such as alcohols or water to give the corresponding ammonium salts of the boronic acid or ester, with concomitant release of hydrogen. Thus, the actual reducing agent is probably dihydrogen for many reactions (discussed in detail in section 4.1.1). The major difference of such systems compared to the dehydrogenation processes discussed in section 5.1, is that the amine–borane complex dissociates, and while one hydrogen atom originates from the borane, the other may come from the solvent or the amine. This dissociation was demonstrated by Couturier et al. who employed tertiary amine–boranes as hydrogen sources, to effect a palladium-catalyzed amine–borane methanolysis with concomitant reduction of nitrobenzenes to anilines.<sup>79b</sup> Since then, many more catalysts have been published for this transformation, but the emphasis for the optimization of these processes turned toward more efficient and cheap ways of releasing hydrogen, particularly for fuel cell applications. As these aspects concern mainly potential hydrogen storage applications, we refer the interested reader to our other review, where the literature concerning metal catalyzed solvolysis is cited comprehensively.<sup>6</sup>

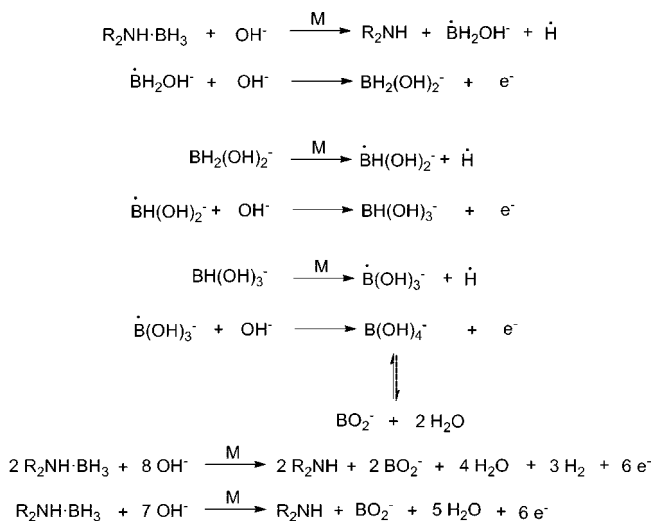
### 5.3. Electroless Plating

Long before the generation of hydrogen from amine–boranes became the focus of active research because of hydrogen storage applications, the ability of amine–boranes to act as reductants for metal ion-containing aqueous solutions was intensely investigated for electroless plating applications. This variant of the plating process is a chemical, autocatalytic process that does not depend on external electrical power. The use of amine–boranes as reductants has been discussed extensively in the patent and the open literature. Articles on this topic are too numerous to be dealt with in detail in this review and we therefore selected papers dealing with mechanistic aspects of this process.

The first attempt to understand how vacuum deposited metal films react with dimethylamine–borane were undertaken by Lelental and Malory.<sup>226,227</sup> Lelental previously proposed a mechanism where the palladium catalyst forms a complex with the aminoborane, which then decomposed to give the highly Lewis acidic palladium borane, which can either hydrolyze to give boric acid and dihydrogen or form elemental boron and dihydrogen, which can reduce other metals to be deposited.

A summary of the potential electrochemical mechanisms was presented by van den Meerakker (Scheme 5.17).<sup>228</sup> The

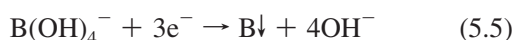
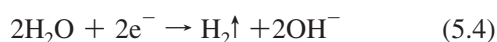
### Scheme 5.17. Potential Electrochemical Mechanisms for Reaction of $\text{Me}_2\text{NH}\cdot\text{BH}_3$ with Vacuum Deposited Metal Films (van den Meerakker)



crucial step appears to be the dehydrogenation, as all metals upon which electroless plating is possible were good hydrogenation/dehydrogenation catalysts. The reaction with amine–boranes is thought to initiate with the dissociation of the amine and the borane, facilitated by the metal catalyst.<sup>229</sup> The anodic oxidation process was described as a series of reactions that lead to hydrogen evolution and contribute electrons for the reduction of the plating metal. In combination, these processes led to the formation of H<sub>2</sub> along with water.



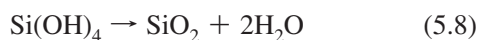
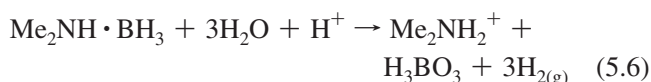
The overall reaction could then be described as follows:



The potential mechanisms for these type of reactions were computationally (*ab initio*) investigated by Homma and Nakai,<sup>230–232</sup> but at the time of writing there were no further experimental results in this area to confirm their findings.

#### 5.4. Anti-Reflection Films

The catalyzed hydrolysis of *N,N*-dimethylamine borane could also be utilized for the controlled increase of the pH (eq 5.6). Chigane and co-workers used this feature to deposit silica thin films onto poly(ethylene terephthalate) (PET) with ammonium hexafluorosilicate, where an increase in pH led to formation and esterification of silicon hydroxide (eqs 5.7 and 5.8).<sup>233</sup>



The applications of such films on transparent substrates range from anti-reflection films with high transmittance for liquid crystal displays to gas barriers or scratch resistant surfaces because of their chemical stability. The substrates were prepared for the reaction by “sensitizing” them with a SnCl<sub>2</sub> solution followed by an “activation” step using a PdCl<sub>2</sub> solution, which presumably generates some Pd(0) particles as active catalysts for the *N,N*-dimethylamine–borane dehydrogenation/hydrolysis reaction. The reflectance and transmittance were measured and AFM and TEM imaging were used for the analysis of samples prepared from various concentrations of *N,N*-dimethylamine–borane. Higher loadings gave less reflectance and better transmission, particularly when two silica films were deposited on top of each other. The silica particles under those conditions grew to a larger size, which was attributed to the higher pH generated on the surface by the decomposition of *N,N*-dimethylamine–borane.

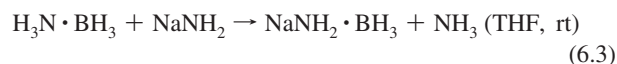
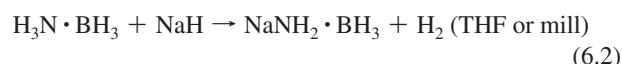
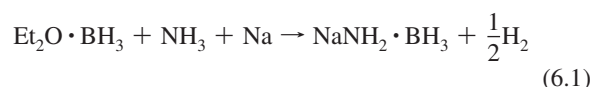
## 6. Synthesis of Main-Group Metal–Amidoboranes, Phosphidoboranes, and Related Species

### 6.1. Main-Group Metal Amidoboranes

Main-group metal amidoboranes can be regarded as a subclass of amine–boranes, where one substituent on nitrogen is an alkaline or alkaline earth metal. Because their properties resemble in many ways light metal hydrides, the main-group metal amidoboranes derived from ammonia–borane are receiving substantial research attention as potential hydrogen storage materials. We cover this aspect in detail in our other review,<sup>6</sup> and will only briefly summarize the major findings in this area. The focus here is on species which address mechanistic questions regarding the catalytic dehydrocoupling of amine–boranes.

One of the reasons hydrogen storage research has turned to metal amidoboranes is that, while many processes to obtain hydrogen from ammonia–borane are relatively high yielding in hydrogen gas, the purity of hydrogen is insufficient for fuel cells. In addition, when these processes were analyzed by TGA, the char yields were often low, which suggests mass loss due to molecules other than hydrogen and implies that the loss of material for such a fuel would be substantial. The use of main-group metal amido–boranes has led to substantial improvements in that regard.

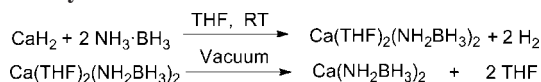
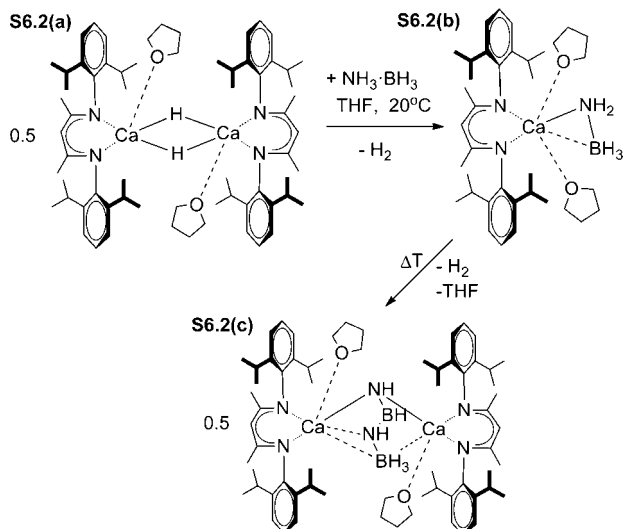
Syntheses for NaNH<sub>2</sub>·BH<sub>3</sub> include the reaction of ammonia and sodium (eq 6.1)<sup>234</sup> or the reaction of ammonia–borane in THF (or neat with ball milling) with sodium hydride at low temperatures (eq 6.2).<sup>235</sup> A similar reaction with LiH has been reported.<sup>235,236</sup> Additionally, the reaction of sodium amide<sup>237</sup> with ammonia–borane in THF also yields sodium amidoborane (eq 6.3).<sup>238</sup>



Initial reports on the performance of these materials as hydrogen carriers are encouraging in terms of hydrogen purity and lower release temperatures,<sup>235</sup> although there is some controversy over the reproducibility of these results.<sup>239</sup>

Yao and Lu combined the approach of kinetically facilitating the dehydrogenation of ammonia–borane through nanoconfinement in an ordered mesoporous carbon framework with the destabilizing effect of LiH on ammonia–borane.<sup>240</sup> However, impurities in the gas stream could not be completely avoided.

Alkaline earth metal amidoboranes have also been examined (Ca,<sup>241</sup> Sr<sup>242</sup>), but since the ball-milling technique did not result in the desired amidoborane for magnesium, it was evaluated how mechanically milled magnesium hydride with ammonia–borane would influence the thermal decomposition processes.<sup>243</sup> The latter reaction was less exothermic than that of neat ammonia–borane or LiNH<sub>2</sub>·BH<sub>3</sub><sup>240</sup> and NaNH<sub>2</sub>·BH<sub>3</sub>,<sup>235</sup> which is important with respect to a potential regeneration of the fuel, although this has been unsuccessful to date, even with pressures of up to 10 MPa. The hydrogen release reaction was also slower than from lithium or sodium

**Scheme 6.1. Synthesis of Calcium Amidoborane from Calcium Hydride and Ammonia-Borane**

**Scheme 6.2. Formation and Dehydrogenation of Amidoborane Complexes of Ammonia-Borane at a Calcium Center: (a) [(DIPP-nacnac)CaH(THF)]<sub>2</sub>, (b) [(DIPP-nacnac)CaNH<sub>2</sub>BH<sub>3</sub>(THF)<sub>2</sub>], (c) [(DIPP-nacnac)Ca(THF)<sub>2</sub>][HN-BH-NH-BH<sub>3</sub>]**


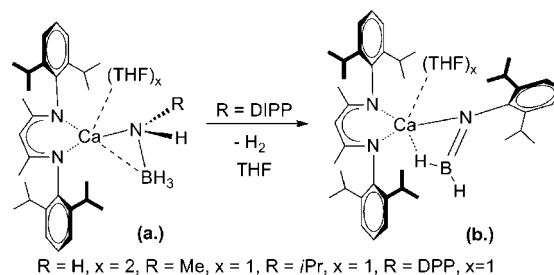
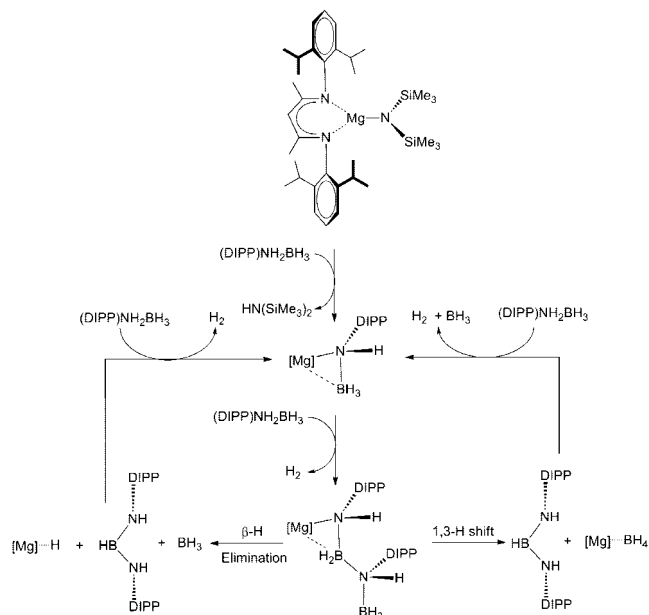
amidoborane, which raised hopes that this material might be a potentially reversible hydrogen storage material, but so far this has not been realized. Mechanistic investigations into these processes have also been reported, both experimentally<sup>236,244</sup> and computationally.<sup>243–245</sup>

The synthesis of the parent calcium amidoborane,  $\text{Ca}(\text{NH}_2 \cdot \text{BH}_3)_2$ , was achieved by mixing stoichiometric amounts of  $\text{CaH}_2$  and ammonia-borane at ambient temperature in THF as a solvent and then removing most of the remaining THF ligands from the initial product,  $\text{Ca}(\text{THF})_2(\text{NH}_2 \cdot \text{BH}_3)_2$ , under vacuum (Scheme 6.1).<sup>241</sup>

In 2008, well-defined calcium amidoborane complexes were prepared, which were soluble in aprotic organic solvents and could be fully characterized by single crystal X-ray crystallography, NMR spectroscopy, and elemental analysis (Scheme 6.2).<sup>246</sup> The soluble calcium hydride complex **S6.2(a)** reacted with ammonia-borane in THF at 20 °C but was otherwise stable, even at elevated temperatures. However, when the non-coordinating solvent benzene was used, the complex dehydrogenated and gave complex **S6.2(c)** with a linear dimeric amidoboranes at its core. The <sup>11</sup>B NMR chemical shifts for complex **S6.2(b)** and **S6.2(c)** were similar,  $\delta = -19.6$  ppm and  $\delta = -22.8$  ppm, respectively, which is common for amidoboranes.

In a further communication, the same methodology was used to access *N*-substituted calcium amidoborane complexes (Scheme 6.3).<sup>247</sup> Interestingly, it was found that if the substituent, R, was sterically encumbered, the dimeric calcium amidoboranes could not be formed, but dehydrogenation could still be achieved to give complex **S6.3(b)**.

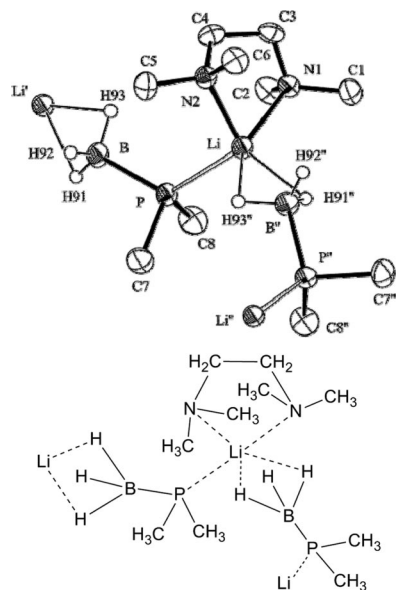
While  $\text{Mg}(\text{NH}_2 \cdot \text{BH}_3)_2$  has yet to be reported, a related soluble amidoborane has been described.<sup>248</sup> When 1 equivalent of  $(\text{DIPP})\text{NH}_2 \cdot \text{BH}_3$  was added to a solution of  $(\text{DIPP-nacnac})\text{MgN}(\text{SiMe}_3)_2$  in benzene at 20 °C, hydrogen was rapidly evolved, giving  $\text{HB}[\text{NH}(\text{DIPP})]_2$  as a clean product.

**Scheme 6.3. Dehydrogenation of Calcium Amidoborane Complexes**

**Scheme 6.4. Postulated Mechanistic Role for a Soluble Magnesium Amidoborane Complex for the Release of Dihydrogen from  $(\text{DIPP})\text{NH}_2 \cdot \text{BH}_3$** <sup>248</sup>


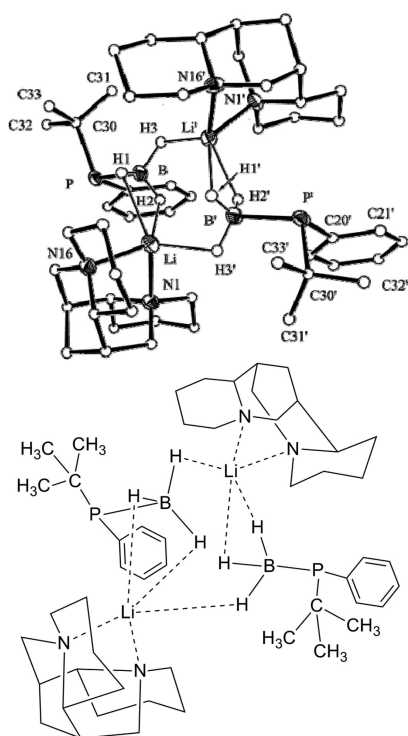
Surprisingly, the magnesium amide was not consumed and was found to act as a catalyst. It was postulated that in the initial step, the magnesium amidoborane was indeed formed (Scheme 6.4). The hydridic hydrogen atoms on boron in this compound may then react with further  $\text{HB}[\text{NH}(\text{DIPP})]_2$ , which may then react via a magnesium hydride or magnesium borohydride and consume a further equivalent of  $(\text{DIPP})\text{NH}_2 \cdot \text{BH}_3$  to restore the magnesium amidoborane.

**6.2. Main-Group Metal-Phosphidoboranes and Related Species**

Main-group metal-phosphido-boranes are less well-understood and few reports exist. The syntheses and isolation of a series of mono(borane)phosphide complexes of lithium and aluminum were reported.<sup>249</sup> Deprotonation of secondary phosphine-borane adducts,  $\text{Me}_2\text{PH} \cdot \text{BH}_3$  and  $t\text{BuPhPH} \cdot \text{BH}_3$ , by  $n\text{BuLi}$  in the presence of TMEDA or (–)-sparteine resulted in the isolation of the compounds depicted in Figures 6.1 and 6.2, respectively. In the case of reaction of  $\text{Me}_2\text{PH} \cdot \text{BH}_3$  with  $n\text{BuLi}$  in the presence of TMEDA (Figure 6.1), the sterically small Me groups allowed for direct P–Li coordination in the product as well as a B–H–Li interaction, forming an indefinite chain in the solid state. By comparison, the product of reaction of  $t\text{BuPhPH} \cdot \text{BH}_3$  with  $n\text{BuLi}$  in the presence of (–)-sparteine produced only dimeric complexes, with no Li–P interaction (Figure 6.2). The corresponding



**Figure 6.1.** X-ray crystal structure of TMEDA stabilized  $\text{Li}[\text{Me}_2\text{P}\cdot\text{BH}_3]$  and representative schematic. Reprinted with permission from ref 249. Copyright 2003 American Chemical Society.

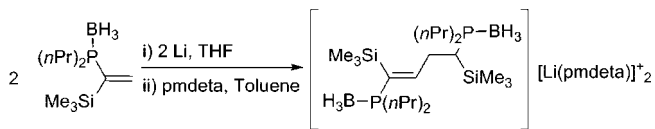


**Figure 6.2.** X-ray crystal structure of (-)-sparteine stabilized  $\text{Li}[\textit{n}\text{BuPhP}\cdot\text{BH}_3]$  and representative schematic. Reprinted with permission from ref 249. Copyright 2003 American Chemical Society.

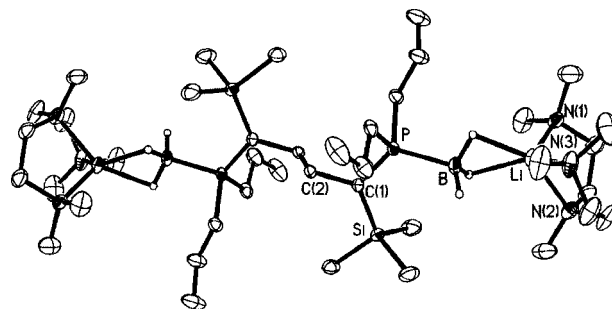
lithium aluminates were isolated by the reaction of  $\text{AlCl}_3$  with 4 equivalents of  $\text{Li}[\text{Me}_2\text{P}\cdot\text{BH}_3]$ .

$\alpha$ -Metalated phosphine-boranes are useful for the chiral resolution of phosphines and in reactions similar to Horner-Wittig olefination reactions.<sup>250</sup> A crystal structure of a bisdicarbanion stabilized with phosphine-boranes, which was prepared by the addition of elemental Li to a *P*-vinyl-phosphine-borane adduct revealed that contrary to expectation, the lithium cations were not associated with the carbanions, but instead complexed to the hydrides of the borane moieties (Scheme 6.5 and Figure 6.3).<sup>251</sup>

### Scheme 6.5. Preparation of a Phosphine-Borane-Stabilized Carbanion<sup>a</sup>

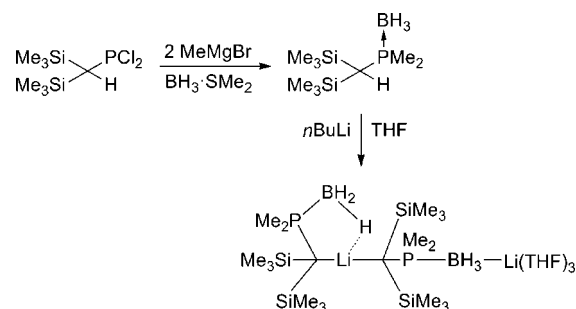


<sup>a</sup> pmdeta = pentamethyldiethylene-triamine.



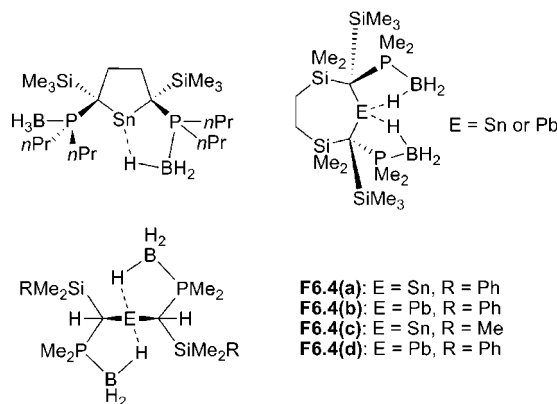
**Figure 6.3.** Single-Crystal X-ray Structure of a Phosphine-Borane-Stabilized Carbanion. Reprinted with permission from ref 251. Copyright 2004 RSC Publications.

### Scheme 6.6. Preparation of a Phosphine-Borane-Stabilized Carbanion with the C-Li Interaction Still Present<sup>252</sup>



However, this observation did not prove to be a general rule. When phosphine-borane adducts such as  $\text{RPMe}_2\cdot\text{BH}_3$  ( $\text{R} = \text{CH}(\text{SiMe}_3)_2$ ) were treated with *n*BuLi (Scheme 6.6), the cation remained associated with the carbanion but also complexed the hydrides of the borane moiety as evidenced by the crystal structure.<sup>252</sup>

Subsequently, it could be shown that this unusual bonding motif was not limited to a B-H-Li stabilization interaction, (see also ref 253) but could also be extended to the stabilization of a dialkylstannylene by a B-H $\cdots$ Sn- $\gamma$ -agostic-type interaction (Figure 6.4),<sup>253d,254</sup> and plumblylenes,<sup>253d,254b</sup> heavier alkali<sup>255</sup> and alkaline earth metals.<sup>256</sup>



**Figure 6.4.** Main-group metal complexes with the borane moiety of phosphine-boranes.



When treated with alkyl halides, **F6.4(c)** was shown to undergo oxidative addition at the Sn center without loss of the phosphine-borane moiety.<sup>257</sup>

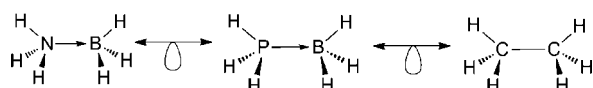
## 7. Coordination Chemistry of Amine- and Phosphine-Borane Adducts with Transition Metals

Novel coordination modes for amine- and phosphine-borane adducts are of fundamental interest for the understanding of catalytic dehydrogenation, dehydrocoupling, or cross-coupling reactions, thereby enhancing the potential for improved system design. A substantial effort has been exerted in terms of calculating mechanisms by DFT and *ab initio* methods, but much is also to be gained from testing theoretical results in the laboratory or at least probing analogous systems. Thus a general increase in the interest in phosphine- and amine-boranes has proceeded hand in hand with the exploration of metal complexes of these species.

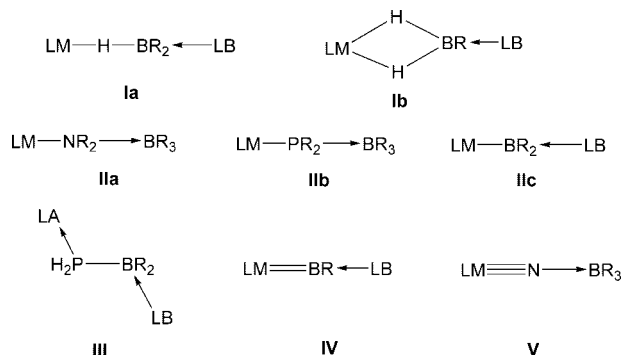
Phosphine-borane ( $R_3P \cdot BH_3$ ) and amine-borane ( $R_3N \cdot BH_3$ ) adducts are considered to be isoelectronic with carbon-based compounds (Figure 7.1; see also section 3).

As a result, parallels are often drawn between transition metal complexes of phosphine- or amine-borane adducts, and intermediates involved in transition metal catalyzed transformations in carbon based chemistry.<sup>258</sup> Accordingly,  $\eta^1$ - and  $\eta^2$ -borane complexes are sometimes viewed as good model systems for the initial complexation step before the oxidative addition of C-H bonds,<sup>259</sup> while metal-boryl species can be viewed as the analogous oxidative-addition products of C-H activation. The potential to gain further insight into the bonding in main-group complexes provides further motivation for the investigation of this interesting class of compounds.

The chemistry of transition metal complexes containing either amine- or phosphine-borane adducts is a rapidly expanding area of research. Since the first reports of well-characterized transition metal complexes containing directly bound  $BR_2$  ligands<sup>260</sup> there have been many reports of Lewis-base-stabilized metal borane ( $\eta^1$ -**Ia** and  $\eta^2$ -**Ib**), metal amidoborane (**IIa**), Lewis-acid-stabilized phosphido-borane (**IIb**), metal boryl (**IIc**), Lewis-acid/base-stabilized phosphanyl-borane (**IIIa**), metal borylene (**IV**) and Lewis acid stabilized metal nitrido complexes (**V**) (Figure 7.2). There have been several



**Figure 7.1.** Isolobal analogy of main-group compounds with carbon compounds.



**Figure 7.2.** Structural motifs for the interaction of group 13/group 15 Lewis acid (LA)-Lewis base (LB) adducts with metals.

reviews published concerning this work;<sup>261</sup> therefore, only the most recent reports, specifically from 2007 to 2010, will be discussed in this section or those of direct significance to the mechanism of dehydrocoupling of Group 13/15 Lewis acid/base adducts and of general fundamental relevance. We will restrict this section to complexes of type **Ia**, **Ib**, **IIa**, **IIb**, **IIc**, and **III** because complexes of type **IV** and **V** are not closely related to amine- and phosphine-boranes.

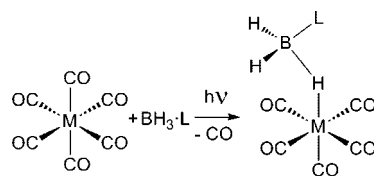
### 7.1. Metal Complexes of Phosphine- and Amine-Borane Adducts of Type Ia and Ib

#### 7.1.1. Monodentate Complexes

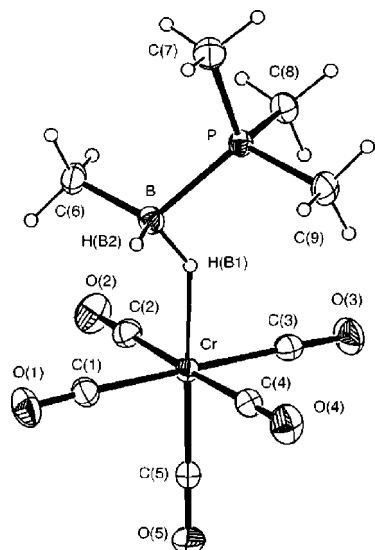
The first step of an oxidative addition of a C-H bond is potentially the coordination of the C-H fragment to the metal via the hydrogen.<sup>258b</sup> Accordingly, with electronic similarities between C-C, N-B and P-B fragments,  $\eta^1$ - and  $\eta^2$ -borane complexes are sometimes viewed as good model systems for the initial complexation step before the oxidative addition of C-H bonds.<sup>262</sup>

Shimoi and co-workers reported the formation of a series of phosphine-borane and amine-borane complexes of some group 6 transition metal carbonyl fragments,  $[M(CO)_5(\eta^1-BH_2R \cdot L)]$  ( $M = Cr, W$ ;  $L = PMe_3, PPh_3, NMe_3$ ;  $R = Et, Me, H, Ph, m-C_6H_4F$ ) and  $[CpMn(CO)_2(\eta^1-BH_2R \cdot L)]$  ( $L = PMe_3, NMe_3$ ;  $R = Et, Me, H, Ph, m-C_6H_4F$ ).<sup>259,263</sup> These were prepared by photolysis of the corresponding metal carbonyl complex ( $[M(CO)_6]$  or  $[CpMn(CO)_3]$ ) in the presence of a Lewis acid-Lewis base adduct, which resulted in the formation of a B-H-M three-center two-electron bond (Scheme 7.1). Complexes with Cr and W were isolated and well characterized, however the analogous Mo complexes were thermally unstable and were only characterized by NMR spectroscopy. The Cr, W, and Mo complexes exhibited broad <sup>1</sup>H NMR signals in the range  $\delta = -3.8$  to  $-1.0$  ppm, corresponding to bridging and terminal hydrogens, with the more basic  $PMe_3$  ligand resulting in increased shielding of those protons, leading to an upfield shift when compared to less basic  $PPh_3$  and  $NMe_3$ . The exchange process between bridging and terminal hydrides at boron was found to be rapid and could not be arrested at low temperature. The bonding situation could also clearly be appreciated in the X-ray crystal structure, which was concluded to represent incomplete oxidative-addition of the B-H bond (see for example, Figure 7.3). The study of model systems,  $[Cr(CO)_5(\eta^1-BH_3 \cdot PH_3)]$  and  $[CpMn(CO)_2(\eta^1-BH_3 \cdot PH_3)]$ , by computational methods had previously predicted that the M-H-B interaction would consist mainly of  $\sigma$ -donation, with minimal  $\pi$ -back-donation, because of the high energy of the BH  $\sigma^*$  orbitals.<sup>264</sup> In agreement with the computational study, it was noted that an increase in the electron-donating nature of the Lewis base bound to boron led to increased stability of the M-H-B interaction, by increasing the electron density available for B-H  $\sigma$  donation, with electron-

**Scheme 7.1.** Synthesis of Lewis-Base-Stabilized  $\sigma$ -Borane Complexes of Group 6 Metals<sup>a</sup>



<sup>a</sup> L =  $PMe_3, NMe_3$ .

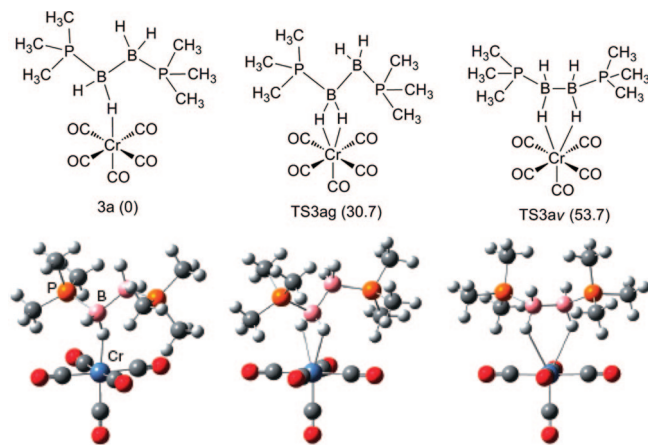


**Figure 7.3.** ORTEP of an X-ray single crystal structure of  $[\text{Cr}(\text{CO})_5(\eta^1\text{-BH}_3\cdot\text{PMe}_3)]$ . Hydrogen atoms bound to boron were determined by the difference Fourier syntheses and were refined isotropically. Reprinted with permission from ref 259. Copyright 2007 Wiley VCH.

withdrawing iodide and chloride substituents on boron precluding complex formation.<sup>259</sup> These results strongly contrast with the stability of analogous silane complexes  $[(\text{MeCp})\text{Mn}(\text{CO})_2(\eta^2\text{-HSiR}_3)]$ , where electron withdrawing R groups facilitate metal back-donation, thereby stabilizing the M–H–Si interaction.<sup>265</sup>

A computational study was used to investigate the structure and bonding in the series  $[\text{M}(\text{CO})_5(\text{BH}_3\cdot\text{PH}_3)]$  (M = Cr, Mo, W) and  $[\text{W}(\text{CO})_5(\text{BH}_3\cdot\text{EH}_3)]$  (E = N, P, As, Sb).<sup>264</sup> The study indicated that the energetic minimum for all complexes is monodentate,  $\eta^1$ -, and has  $C_1$  symmetry, with the transition state for hydrogen exchange involving a  $\eta^2$ -isomer. It was also noted that the charge transfer between metal and boron increases along the series  $\text{Sb} < \text{As} < \text{P} < \text{N}$ . The interaction between the metal center and B was found to decrease in the order  $\text{N} > \text{P} > \text{As}$ , with total interaction energies for coordination of  $\text{BH}_3\cdot\text{NH}_3$  and  $\text{BH}_3\cdot\text{PH}_3$  to the fragment  $\text{W}(\text{CO})_5$  calculated as 27.5 and 21.3 kcal/mol, respectively. In the presence of free CO, the tungsten complexes,  $[\text{W}(\text{CO})_5(\text{BH}_3\cdot\text{EH}_3)]$  (E = N or P), yield  $\text{W}(\text{CO})_6$  and free  $\text{BH}_3\cdot\text{EH}_3$ .<sup>263a</sup> This is in good agreement with the computational study, which calculated the energy for CO coordination to  $\text{W}(\text{CO})_5$  to be 46.2 kcal/mol, higher than that for adduct coordination.<sup>264</sup> The energy barriers for B–H exchange were calculated to increase in the order  $\text{Sb} < \text{As} < \text{P} < \text{N}$  and are in good agreement with experimental data from the series  $[\text{CpMn}(\text{CO})_2(\eta^1\text{-BH}_3\cdot\text{L})]$  (L =  $\text{NMe}_3$  or  $\text{PMe}_3$ ), where the energy barrier for B–H exchange is significantly higher when L =  $\text{NMe}_3$  compared to L =  $\text{PMe}_3$ ,<sup>266</sup> and was mainly attributed to the strength of interaction between  $\text{W}(\text{CO})_5$  and  $\text{BH}_3\cdot\text{EH}_3$ . Indeed, the fluxional exchange of bridging and terminal B–H bonds could be frozen out at low temperature when L =  $\text{NMe}_3$ , with the  $^1\text{H}$  NMR resonance at  $\delta = -6.1$  ppm collapsing at  $-22$  °C and a new resonance corresponding to M–H–B at  $\delta = -22.21$  ppm appearing at  $-60$  °C (terminal hydrogens showed overlapping signals with  $\text{NMe}_3$  resonance), while when L =  $\text{PMe}_3$ , the decoupled signal could not be observed.

The complexes  $[\text{M}(\text{CO})_5(\eta^1\text{-B}_2\text{H}_4\cdot 2\text{PMe}_3)]$  (M = Cr or W) were found to undergo two fluxional processes. Exchange of



**Figure 7.4.** Transition states calculated for vicinal hydrogen exchange in  $[\text{M}(\text{CO})_5(\eta^1\text{-B}_2\text{H}_4\cdot 2\text{PMe}_3)]$  (M = Cr or W). Energies in kJ/mol. Reprinted with permission from ref 268. Copyright 2006 Chemical Society of Japan.

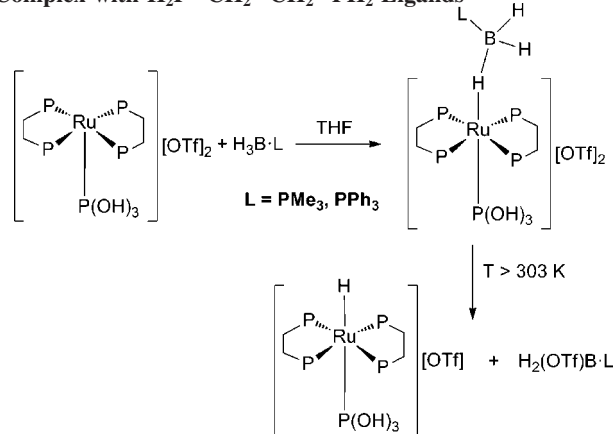
the coordinated B–H with a geminal H was found to occur very rapidly in solution, while a slower exchange was observed for vicinal hydrogens.<sup>267</sup> A computational investigation of this system suggested that vicinal hydrogen exchange occurred via a transition state involving bidentate coordination of the metal center by the  $\text{B}_2\text{H}_4\cdot 2\text{PMe}_3$  ligand (Figure 7.4).<sup>268</sup>

In addition to the liberation of a coordination site using the photolysis of M–CO bonds, it is also possible to achieve the same goal by the use of halide abstracting reagents with metal–halide complexes. Using this method, the synthesis of a range of cationic Ru complexes was synthesized by the reaction of  $[(\eta^5\text{-C}_5\text{R}_5)\text{Ru}(\text{PMe}_3)_2\text{Cl}]$  with  $\text{Na}[\text{BAR}^{\text{F}}_4]$  in the presence of  $\text{BH}_3\cdot\text{EMe}_3$  (E = P or N).<sup>269</sup> In this manner, a range of cationic Ru base stabilized  $\eta^1$ -borane complexes,  $[(\eta^5\text{-C}_5\text{R}_5)\text{Ru}(\text{PMe}_3)_2(\eta^1\text{-BH}_3\cdot\text{EMe}_3)][\text{BAR}^{\text{F}}_4]$  ((a) R = H,  $\text{EMe}_3 = \text{PMe}_3$ ; (b) R = Me,  $\text{EMe}_3 = \text{PMe}_3$ ; (c) R = H,  $\text{EMe}_3 = \text{NMe}_3$ ;  $[\text{BAR}^{\text{F}}_4] = [\text{B}\{3,5\text{-C}_6\text{H}_3(\text{CF}_3)_2\}_4]$ ) could be prepared. The complexes were remarkably stable; however they were rapidly hydrolyzed by trace amounts of water to afford the cationic dihydride,  $\text{trans-}[\text{CpRuH}_2(\text{PMe}_3)_2]^+$ . Furthermore, they were highly fluxional with rapid exchange of bridging and geminal hydrogen atoms and the  $\text{BH}_3\cdot\text{EMe}_3$  moiety could be displaced with a range of donors such as CO and MeCN.

The electrophilic, 16-electron Ru species  $[\text{RuP}(\text{OH})_3\text{-}(\text{dppe})_2][\text{OTf}]_2$  has previously been shown to cleave  $\text{H}_2$  in a heterolytic manner.<sup>270</sup> A combined experimental and theoretical report investigated B–H activation of  $\text{BH}_3\cdot\text{L}$  (L =  $\text{PMe}_3$  or  $\text{PPh}_3$ ) by this superelectrophilic Ru complex.<sup>271</sup> On warming a mixture of the two components to 30 °C the formation of a signal corresponding to Ru–H was noted in the  $^1\text{H}$  NMR spectrum at  $\delta = -8.90$  ppm. Analysis by  $^{11}\text{B}$  and  $^{31}\text{P}$  NMR spectroscopy identified  $\text{BH}_2(\text{OTf})\cdot\text{L}$ , indicating heterolytic cleavage of the B–H bond. Analysis of the reaction mechanism by DFT suggested that a  $\eta^1\text{-HBH}_2\cdot\text{L}$  interaction was involved as a reaction intermediate (Scheme 7.2).

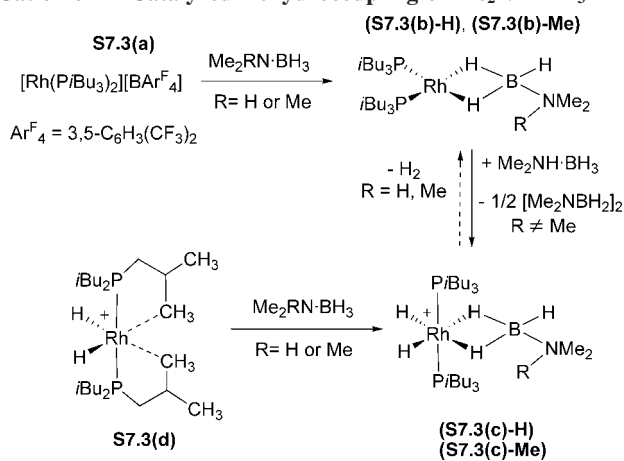
Weller and co-workers reported the catalytic dehydrocoupling of  $\text{Me}_2\text{NH}\cdot\text{BH}_3$  using a cationic Rh complex and subsequent isolation of some  $\eta^2$ -amine–borane complexes (Scheme 7.3).<sup>207</sup> Analysis of the reaction by NMR spectroscopy indicated the  $\eta^2$ -borane Rh(I) complex **S7.3(b)-H**, which was short-lived ( $t_{1/2} \approx 1$  min) and could not be isolated in pure form, because it converted to the octahedral Rh(III) species **S7.3(c)-H** by elimination of  $1/2[\text{Me}_2\text{N}-\text{BH}_2]_2$ . Low-temperature  $^1\text{H}$  NMR spectroscopy arrested the fluxional behavior of the  $\eta^2$ -borane moiety, with a new signal

**Scheme 7.2. Computational Investigation of B–H Activation by a Coordinatively Unsaturated, 16-Electron Ru(I) Complex with H<sub>2</sub>P–CH<sub>2</sub>–CH<sub>2</sub>–PH<sub>2</sub> Ligands<sup>a</sup>**



<sup>a</sup> H on P was not drawn for clarity.

**Scheme 7.3. Formation of Possible Intermediates in the Cationic Rh-Catalyzed Dehydrocoupling of Me<sub>2</sub>NH·BH<sub>3</sub><sup>207</sup>**



appearing at <sup>1</sup>H NMR  $\delta = -3.15$  ppm ( $\eta^2\text{-BH}_2$ ), while the terminal B–H resonance was not observed, possibly because of its broad nature or overlap with the aliphatic region. The isolated complex **S7.3(c)-H** proved to be an active catalyst for the dehydrocoupling of Me<sub>2</sub>NH·BH<sub>3</sub>, and was speculated to be involved in the catalytic cycle for the dehydrocoupling of amine–borane adducts (Scheme 7.3).

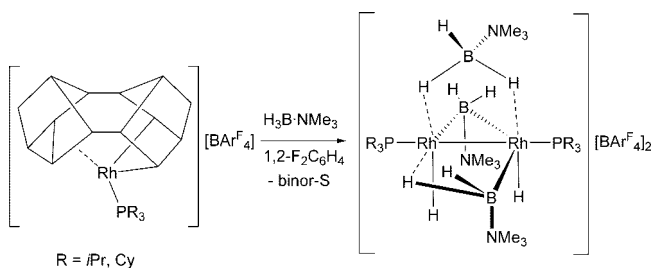
Subsequently, a range of complexes coordinating a variety of products from the Rh-catalyzed dehydrocoupling of Me<sub>2</sub>NH·BH<sub>3</sub> have been isolated, including the coordination of a possible reaction intermediate in [Rh(*i*Bu<sub>3</sub>P)<sub>2</sub>-( $\eta^2\text{-BH}_3\text{-NMe}_2\text{-BH}_2\text{-NHMe}_2$ )].<sup>212,272</sup>

Of particular interest was a bimetallic Rh complex with *N,N,N*-trimethylamine–borane, prepared by a reaction between the *N,N,N*-trimethylamine–borane adduct and a cationic Rh precursor (Scheme 7.4, Figure 7.5).<sup>272a</sup> The amine–borane is bound with two of the hydridic hydrogens on boron to both Rh centers. As this complex was also active for the dehydrogenation of *N,N*-dimethylamine–borane, it represented the first mimic for a Rh cluster or even heterogeneous Rh catalyst for this transformation.

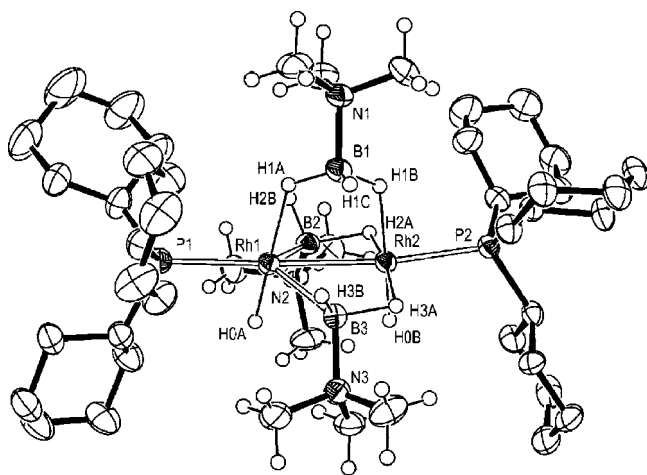
**7.1.2. Chelating Phosphine–Borane Ligands of Type Ia and Ib**

There are only few reports of compounds involving the bidentate coordination of a neutral group 15-borane adduct

**Scheme 7.4. Formation of a Bimetallic Rh Complex with an Amine–Borane<sup>a</sup>**



<sup>a</sup> binor-S = heptacyclo[8.4.0.0.2.12.0.3.8.0.4.6.0.5.9.0.11.13]tetradecane.



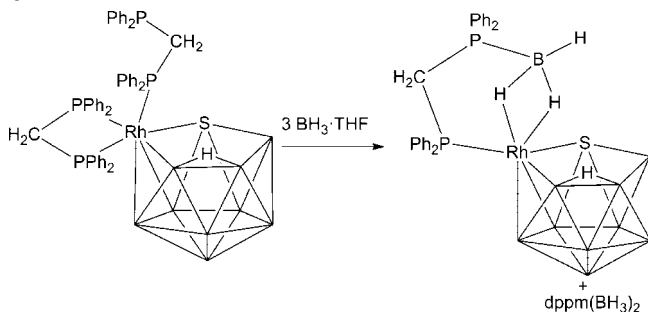
**Figure 7.5.** Solid-state structure of the product described in Scheme 7.4. Thermal ellipsoids set at 50% probability; phosphine H-atoms omitted for clarity. Reprinted with permission from ref 272a. Copyright 2010 Wiley VCH.

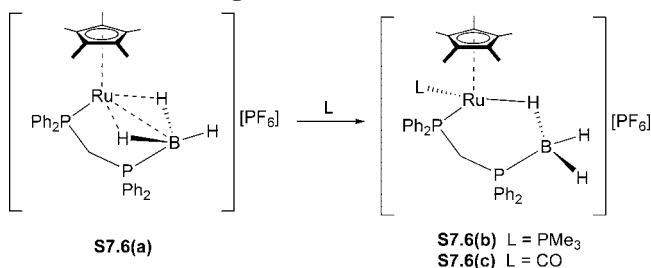
to a metal center, with examples of 1,2(PMe<sub>3</sub>)<sub>2</sub>·B<sub>2</sub>H<sub>4</sub> coordination of ZnCl<sub>2</sub>,<sup>273</sup> Ni(CO)<sub>2</sub>,<sup>274</sup> CuI,<sup>273</sup> Cu<sup>+</sup>,<sup>275</sup> and M(CO)<sub>4</sub> (M = Cr, Mo, W).<sup>267,268,276</sup>

A particularly interesting reaction was the addition of BH<sub>3</sub>·THF to two Rh containing boron clusters, [8,8-( $\eta^2\text{-dppm}$ )-8-( $\eta^1\text{-dppm}$ )-*nido*-8,7-RhSB<sub>9</sub>H<sub>10</sub>] and [9,9-( $\eta^2\text{-dppm}$ )-9-( $\eta^1\text{-dppm}$ )-*nido*-9,7,8-RhC<sub>2</sub>B<sub>3</sub>H<sub>11</sub>] (dppm = 1,2-bis(diphenylphosphino)methane), which led to displacement of one dppm ligand and coordination of the BH<sub>3</sub> moiety by the pendant phosphine (Scheme 7.5). The borane moiety was then bound to the Rh center by two 3-center-2-electron bonds, to give the first polyhedral borane derivatives with BH<sub>3</sub> adducts coordinated to the metal center in a bidentate manner.<sup>277</sup>

The use of bidentate phosphine–monoborane adducts, that is, BH<sub>3</sub>·dppm, as chelating ligands was extended by Weller

**Scheme 7.5. Displacement of a dppm Ligand from Rh by BH<sub>3</sub>·THF to Form Rh-Containing Cluster to Generate a  $\eta^2\text{-BH}_3\text{·dppm}$  Complex**



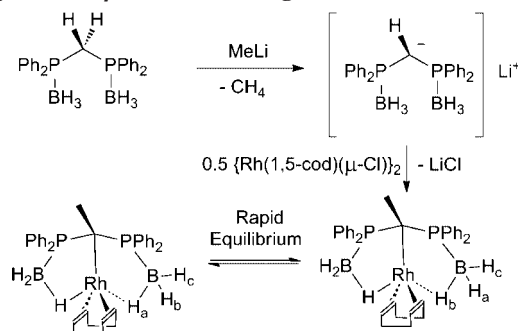
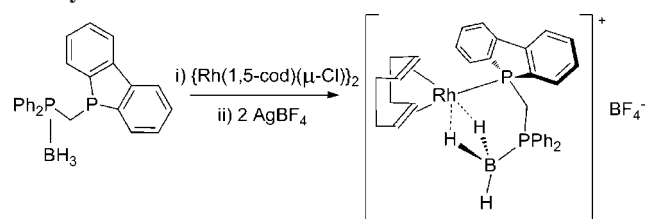
**Scheme 7.6. Displacement of One M–H–B Interaction by Addition of Donor Ligand**


and co-workers. In an initial report, they investigated a high yielding synthetic route to [(1,5-cod)Rh{( $\eta^2$ -BH<sub>3</sub>)Ph<sub>2</sub>PCH<sub>2</sub>PPh<sub>2</sub>}] [BF<sub>4</sub>].<sup>278</sup> Analysis by X-ray crystallography indicated a  $\eta^2$ -bound BH<sub>3</sub> fragment (all hydrogen atoms at borane were located); however, this motif was not retained in solution at room temperature. The BH<sub>3</sub> moiety was highly fluxional, undergoing rapid exchange with all three B–H bonds at room temperature, with low-temperature NMR spectroscopy revealing the presence of two different B–H environments corresponding to bridging and terminal hydrogens. Subsequently, the coordination of the chromium and ruthenium transition metal fragments Cr(CO)<sub>4</sub> and [CpRu(PR<sub>3</sub>)(NCMe)<sub>2</sub>]<sup>+</sup> by BH<sub>3</sub>·dppm to give [Cr(CO)<sub>4</sub>( $\eta^1$ -BH<sub>3</sub>·dppm)] and [CpRu(PR<sub>3</sub>)( $\eta^1$ -BH<sub>3</sub>·dppm)][PF<sub>6</sub>] (with R = Me, and R = OMe), respectively, has also been reported.<sup>279</sup> Both complexes were highly fluxional at room temperature on the NMR time scale. Generation of a coordinatively unsaturated species could be achieved by reaction of [Cp\*Ru(NCMe)<sub>3</sub>]<sup>+</sup> with BH<sub>3</sub>·dppm to yield [Cp\*Ru( $\eta^2$ -BH<sub>3</sub>·dppm)][PF<sub>6</sub>]. Here, the BH<sub>3</sub> moiety was found to be static on the NMR time scale, with both resonances observed in the <sup>1</sup>H NMR spectrum even at elevated temperatures (–53 to 67 °C). It has previously been shown that related 16-electron complexes, such as [Cp\*Ru(PMeiPr<sub>2</sub>)<sub>2</sub>]<sup>+</sup>, react readily with donor ligands to form the corresponding 18-electron species.<sup>280</sup> Addition of PMe<sub>3</sub> or CO to [Cp\*Ru( $\eta^2$ -BH<sub>3</sub>·dppm)][PF<sub>6</sub>] led to the displacement of one B–H moiety and the formation of [Cp\*Ru(PMe<sub>3</sub>)( $\eta^1$ -BH<sub>3</sub>·dppm)][PF<sub>6</sub>] (**S7.6(b)**) and [Cp\*Ru(CO)( $\eta^1$ -BH<sub>3</sub>·dppm)][PF<sub>6</sub>] (**S7.6(c)**), respectively (Scheme 7.6).<sup>279</sup>

The addition of weaker nucleophiles, such as MeCN, resulted in a slow exchange process and the gradual formation of [Cp\*Ru(NCMe)( $\eta^1$ -BH<sub>3</sub>·dppm)][PF<sub>6</sub>]. Similar behavior was observed with the Mn complexes [Mn(CO)<sub>3</sub>( $\eta^2$ -BH<sub>3</sub>·dppm)][BAr<sup>F</sup><sub>4</sub>], [Mn(CO)<sub>4</sub>( $\eta^1$ -BH<sub>3</sub>·dppm)][BAr<sup>F</sup><sub>4</sub>],<sup>281</sup> and the Ru(II) complex [Cp\*Ru( $\eta^2$ -H<sub>2</sub>ClB·dppm)][BAr<sup>F</sup><sub>4</sub>].<sup>182</sup>

A further example of a bidentate ligand exhibiting a type **Ia** behavior was prepared by treating a bis-phosphine–borane (H<sub>3</sub>B·PPh<sub>2</sub>–CH<sub>2</sub>–PPh<sub>3</sub>·BH<sub>3</sub>) with a strong base and complexing the resulting anion with a Rh(I) precursor (Scheme 7.7).<sup>282</sup> The resulting complex was analyzed using a combination of multinuclear NMR spectroscopy, single crystal X-ray and DFT methods. The hydrides on the borane moiety showed only one signal by NMR, which could be attributed to their highly fluxional behavior. The Rh–H–B interaction was described as agostic, which indicates that such a complex may represent a stage just before B–H activation.

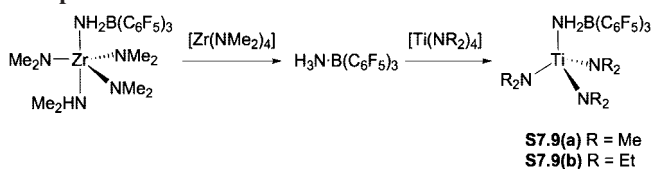
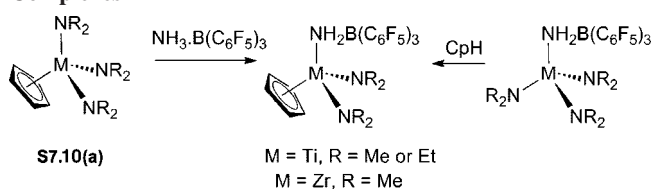
However, in a very similar example, a related cationic Rh complex showed  $\eta^2$ -bonding of the borane moiety to the metal (Scheme 7.8).<sup>283</sup>

**Scheme 7.7. Formation of a Bidentate Phosphine–Borane Complex with  $\eta^1$ -Borane Binding Motifs**

**Scheme 7.8. Chelating Phosphine–Borane Ligand Coordinated to a Rh Cation with  $\eta^2$ -Bonding of the Borane Moiety**

**7.2. Transition Metal Amidoborane Complexes of Type IIa**

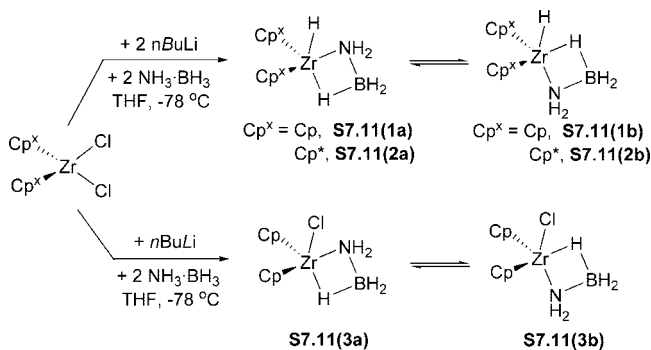
Synthesis of group 4 metal amidoborane complexes has been achieved by treatment of the homoleptic titanium amides, [Ti(NR<sub>2</sub>)<sub>4</sub>] (R = Me or Et), with the amine–borane adduct NH<sub>3</sub>·B(C<sub>6</sub>F<sub>5</sub>)<sub>3</sub>, which led to the loss of one amine ligand and subsequent formation of the tetracoordinate amidoborane complex [Ti(NR<sub>2</sub>)<sub>2</sub>(NH<sub>2</sub>·B(C<sub>6</sub>F<sub>5</sub>)<sub>3</sub>)] (Scheme 7.9).<sup>284</sup>

Contrasting reactivity was observed when using [Zr(NMe<sub>2</sub>)<sub>4</sub>], with the generation of trigonal-bipyramidal [Zr(NMe<sub>2</sub>)<sub>3</sub>(NH<sub>2</sub>·B(C<sub>6</sub>F<sub>5</sub>)<sub>3</sub>)(NMe<sub>2</sub>H)]. Addition of NH<sub>3</sub>·B(C<sub>6</sub>F<sub>5</sub>)<sub>3</sub> amine–borane adduct to the cyclopentadienyl complexes, [CpM(NR<sub>2</sub>)<sub>3</sub>] (M = Ti, R = Me or Et; M = Zr, R = Me) (**S7.10(a)**), led to the formation of the relevant cyclopentadienyl amidoborane complex, which could also be accessed by addition of cyclopentadiene to precursors (Scheme 7.10).

In 2009, the isolation of a series of  $\beta$ -B-agostic isomers of zirconocene amidoborane complexes was reported.<sup>285</sup> It was observed that the reaction of Cp<sup>x</sup>ZrCl<sub>2</sub> (Cp<sup>x</sup> = Cp or

**Scheme 7.9. Synthesis of Ti and Zr Amidoborane Complexes**

**Scheme 7.10. Synthesis of Functionalized Ti Amidoborane Complexes**


## Scheme 7.11. Synthesis of Zr Amidoborane Complex



Cp\*) with one or two equivalents of  $n\text{BuLi}$ , in the presence of  $\text{NH}_3 \cdot \text{BH}_3$  resulted in the formation of the first transition metal amidoborane complexes in which different stereoisomers could be identified (Scheme 7.11). Complexes of this type may be able to aid the mechanistic understanding of catalytic dehydrocoupling processes of amine–borane adducts by early transition metals, which possibly differs substantially for late transition metals.

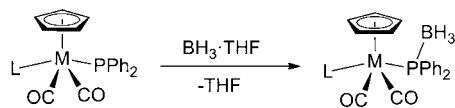
## 7.3. Lewis-Acid-Stabilized Metal Phosphidoborane Complexes of Type IIb

The simplest route for the preparation of complexes of type **IIb** was demonstrated in 1985, where metal–phosphides were simply reacted with  $\text{BH}_3 \cdot \text{THF}$  to yield the corresponding complexes in excellent yields (Scheme 7.12).<sup>286</sup>

In 2007, the formation of the bidentate phosphine borane, *rac/meso*-[HP(BH<sub>3</sub>)(Ph)CH<sub>2</sub>]<sub>2</sub> was reported, which upon deprotonation with KH and addition of  $\text{CpFe}(\text{CO})_2\text{I}$ , underwent a salt elimination reaction to afford the dinuclear iron complex, [(Cp<sub>2</sub>Fe(CO)<sub>2</sub>)-μ-(P(BH<sub>3</sub>)(Ph)CH<sub>2</sub>)<sub>2</sub>] (Scheme 7.13).<sup>287</sup> This synthetic process is completely analogous to the formation of main-group metal phosphidoboranes described in section 6.2.

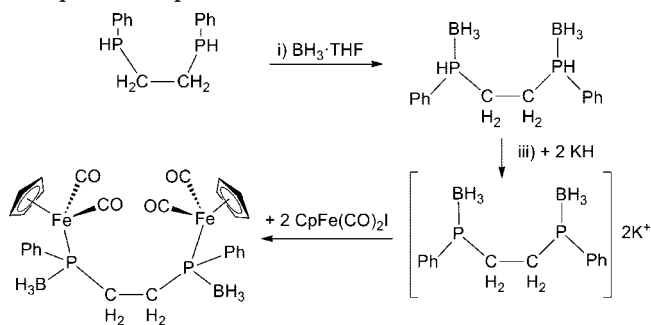
Some effort has been invested into improving our understanding of such complexes. A recent study used X-ray crystallography, NMR [ $\delta(^{13}\text{C})$ ] spectroscopy, IR [ $\nu(\text{CO})$ ]

## Scheme 7.12. Simple Formation of a Transition Metal Phosphido–Borane Complex

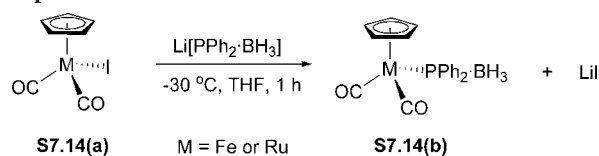


- S7.12(a) M = W, L = CO  
 S7.12(b) M = Mo, L = PMe<sub>3</sub>  
 S7.12(c) M = W, L = PMe<sub>3</sub>

## Scheme 7.13. Synthesis of Lewis-Acid-Stabilized Dinuclear Phosphido Complex



## Scheme 7.14. Synthesis of Metal Phosphido–borane Complexes of Fe and Ru via Salt Elimination



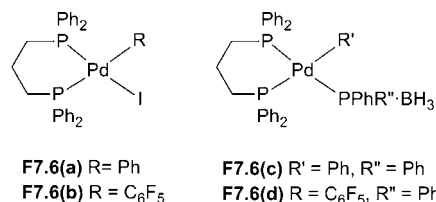
spectroscopy and quantum chemical calculations to compare a range of complexes  $[\text{CpFe}(\text{CO})_2(\text{EPh}_2 \cdot \text{XH}_3)]^{n+}$  (E = Si, X = C; E = P, X = C, B; n = 0, 1). The conclusion was that the electron donating nature of the series of ligands decreased in the order silyl > phosphidoborane > phosphine. The same trend was observed with the chalcogenide series,  $[\text{CpFe}(\text{CO})_2(\text{SEtBu}_2\text{XH}_3)]^{n+}$  (E = Si, X = C; E = P, X = C, B; n = 0, 1), with the sulfur-containing phosphidoborane ligand acting as the intermediate electron donor.<sup>288</sup>

It was hoped that transition metal phosphidoborane complexes may shed some light on catalytic dehydrocoupling processes. Synthesis of  $\text{CpM}(\text{CO})_2\text{PPh}_2 \cdot \text{BH}_3$  (M = Fe or Ru) was achieved via salt elimination (Scheme 7.14).<sup>160d</sup>

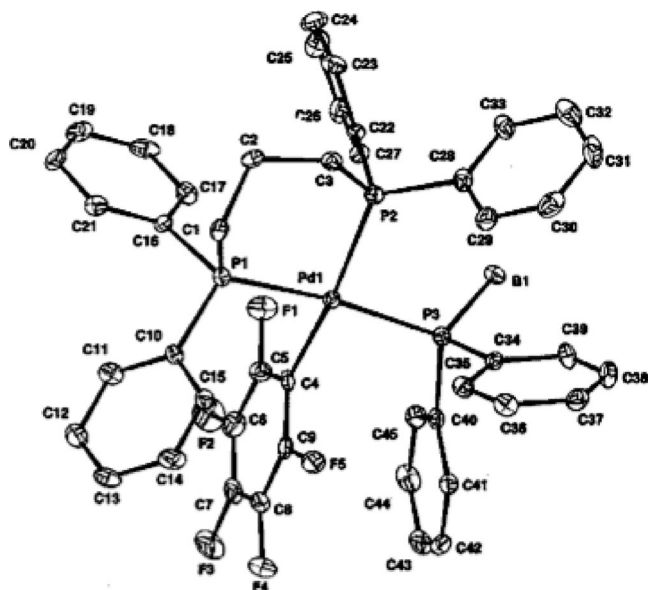
Both **S7.14(a)** and **S7.14(b)** were indeed found to be catalysts for the dehydrocoupling  $\text{Ph}_2\text{PH} \cdot \text{BH}_3$ , but catalytic activity was relatively poor, giving 60% conversion to linear dimer  $\text{Ph}_2\text{PH}-\text{BH}_2-\text{PPh}_2-\text{BH}_3$  in the melt at 120 °C. Therefore, the mechanistic details of phosphine–borane catalytic dehydrocoupling reactions are still unknown and require further work.

That such transition metal phosphidoborane complexes may be of pivotal importance for understanding the catalytic process was demonstrated during a study of the functionalization of phosphine–boranes at phosphorus by palladium-catalyzed cross coupling with aryl iodides.<sup>163</sup> Here, it was possible to isolate the reactive intermediate for the reaction of Pd-precursors **F7.6(a)** and **F7.6(b)** with secondary phosphine–boranes (Figures 7.6 and 7.7; for a description of the synthetic relevance see section 4). It was found that if the Pd center had electron poor aryl substituents, the product elimination to give the corresponding phosphine–borane from the Pd center was relatively slow so that in the case of phosphine–borane adduct **F7.6(b)**, complex **F7.6(d)** could be isolated and fully characterized. Re-solution of **F7.6(d)** and prolonged standing resulted in decomposition to yield the associated phosphine–borane adduct (Figures 7.6 and 7.7).

The aforementioned complexes illustrate that catalytic dehydrocoupling of phosphine–borane adducts can conceivably occur with an initial B–H activation, P–H activation, or concerted B–H and P–H activation. To model P–H activation, a series of Pt(0) compounds were investigated.<sup>385–387</sup> Addition of either the primary or secondary phosphine–borane adduct,  $\text{PhRPH} \cdot \text{BH}_3$  (R = H or Ph), to a Pt(0) precursor led to oxidative addition of a P–H bond to the Pt(0) center of  $\text{Pt}(\text{PEt}_3)_3$  and loss of one  $\text{PEt}_3$  ligand to form *trans*-[PtH(PRPh·BH<sub>2</sub>)(PEt<sub>3</sub>)<sub>2</sub>] (Scheme 7.15).<sup>289</sup>

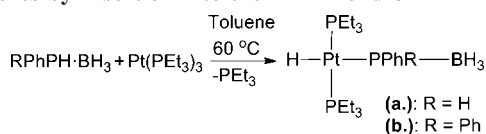


**Figure 7.6.** Palladium iodide precursor and palladium phosphido-borane complexes.

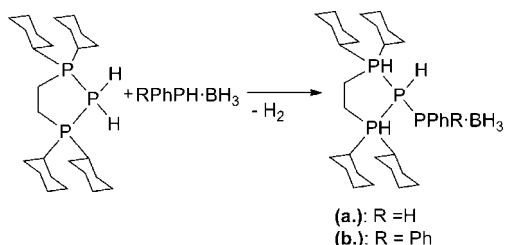


**Figure 7.7.** Single-crystal X-ray structure of palladium phosphido borane, F7.6(d). Reprinted with permission from ref 163. Copyright 1999 RSC Publishing.

**Scheme 7.15. Synthesis of Metal Phosphido Borane Complexes by Insertion into the H–P Bond of RPHPH·BH<sub>3</sub>**



**Scheme 7.16. Addition of PhRPH·BH<sub>3</sub> to *cis*-[PtH<sub>2</sub>(dcype)]**



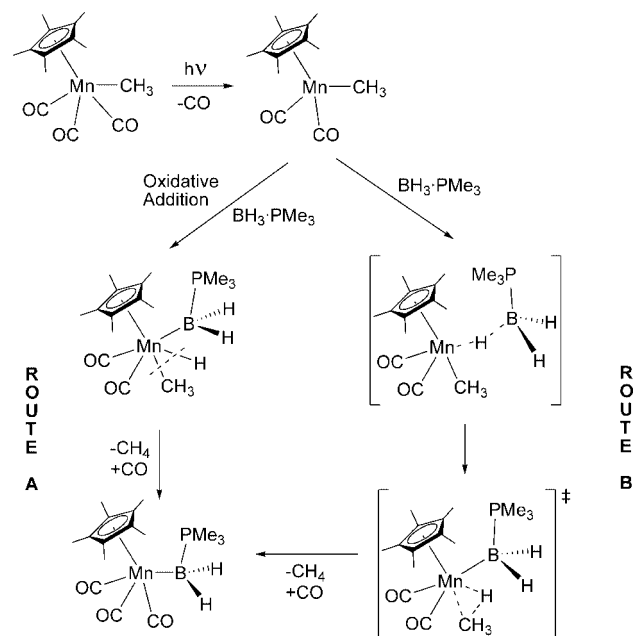
Treatment of **S7.15(a)** with Ph<sub>2</sub>PH·BH<sub>3</sub> or PhPH<sub>2</sub>·BH<sub>3</sub> resulted in no further reaction. Similar reactivity was noted with the bidentate ligand dcype (bis-(1,2-dicyclohexylphosphino)ethane), where addition of Ph<sub>2</sub>PH·BH<sub>3</sub> to *cis*-[PtH<sub>2</sub>(dcype)] resulted in the evolution of one equivalent of H<sub>2</sub> and the formation of a Pt–P bond. Addition of further equivalents of phosphine–borane resulted in no catalytic dehydrocoupling (Scheme 7.16).<sup>290</sup>

## 7.4. Metal Boryl Complexes of Type IIc

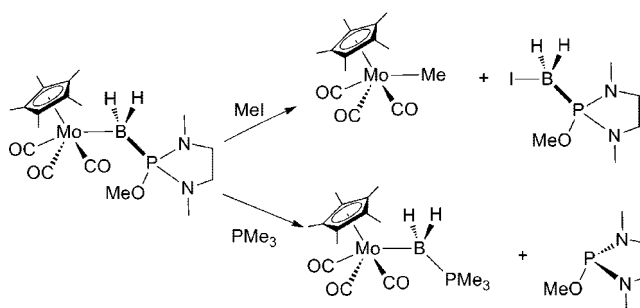
A very early example of this type of coordination was found by Puddephatt and co-workers, when they reacted CoCl<sub>2</sub> or CoBr<sub>2</sub> with sodium borohydride in the presence of CO and dppm.<sup>291</sup> They could isolate a complex, [(CO)<sub>2</sub>(η<sup>1</sup>-dppm)Co(μ-dppm)BH<sub>2</sub>], where the boryl moiety was stabilized by the phosphine, which gave a much more stable complex than a similar example found earlier, where the stabilizing Lewis base was merely THF.<sup>292</sup>

To access an oxidative-addition product from σ-borane-phosphine complexes by B–H insertion, transition metal species with the strongly electron donating ligand, Cp\* (pentamethylcyclopentadienyl), were investigated. Photolysis of Cp\*M(CO)<sub>3</sub>Me (M = Mo and W) in the presence of the

**Scheme 7.17. Mechanism Proposed for M–B Bond Formation on Irradiation of Cp\*M(CO)<sub>3</sub>Me in the Presence of Me<sub>3</sub>P·BH<sub>3</sub>**



**Scheme 7.18. M–B Cleavage of Phosphine–Boranyl Metal Complexes with an Alkyl Halide or Phosphine Exchange with PMe<sub>3</sub>**



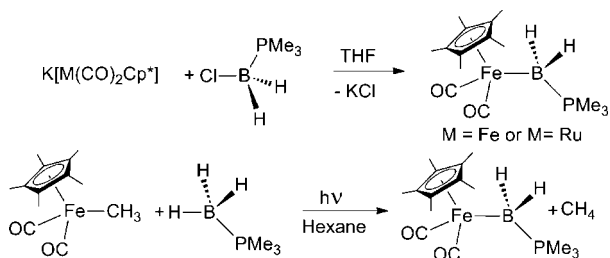
tertiary phosphine–borane adducts, Me<sub>3</sub>P·BH<sub>3</sub>, resulted in oxidative addition of the B–H bond and evolution of CH<sub>4</sub>, yielding a M–B-bound base-stabilized metal boryl complex (Scheme 7.17). Initial irradiation resulted in the elimination of CO, giving a coordinatively unsaturated 16-electron metal species, Cp\*M(CO)<sub>2</sub>Me. It was proposed that M–B bond formation could occur via two routes; oxidative addition of a B–H bond, followed by reductive elimination of CH<sub>4</sub> (route A) or concerted rearrangement (route B), followed by reassociation of CO to form a stable 18-electron species.<sup>293</sup>

In 2006 and 2007, examples of group 6 base stabilized boryl complexes, [(η<sup>5</sup>-C<sub>5</sub>Me<sub>5</sub>)Mo(CO)<sub>3</sub>(BH<sub>2</sub>·L)] (L = P(OMe)-(NMeCH<sub>2</sub>)<sub>2</sub>, P(OMe)(NEt<sub>2</sub>)<sub>2</sub>, P(OMe)(Ph)<sub>2</sub> or P(OMe)<sub>3</sub>) were reported.<sup>294</sup> It was observed that the phosphite could be displaced by a more basic phosphine such as PMe<sub>3</sub>, and that the Mo–B bond was cleaved by MeI (Scheme 7.18).

Synthesis of the group 8 analogs of Lewis-base-stabilized transition metal boryl complexes could be achieved via salt elimination from the parent haloborane–Lewis base adduct and transition metal fragment salt or via photolysis of the Lewis acid–base adduct in the presence of the methylated metal fragment (Scheme 7.19).<sup>295</sup>

In an analogous manner, complexes of the type [Mn(CO)<sub>4</sub>(PR<sub>2</sub>R')(BH<sub>2</sub>·PMe<sub>3</sub>)] (R = Me, R' = Ph; R = R' = Me) were synthesized by photolysis of Mn(CO)<sub>4</sub>-

### Scheme 7.19. Synthesis of Base-Stabilized Metal Boryl Complexes via Salt Elimination or Photolysis



( $PR_2R'$ )( $CH_3$ ) in the presence of  $BH_3 \cdot PMe_3$ .<sup>296</sup> Treatment of the base-stabilized metal boryl complex with the Brønsted acid  $[H(OEt_2)_2]B_{Ar}^F$  ( $B_{Ar}^F = [B\{3,5-C_6H_3(CF_3)_2\}_2]$ ) gave access to the  $\eta^1$ -borane complex. Mechanistically, this may have occurred via protonation of the  $BH_2$  moiety, and subsequent rearrangement to form the  $\eta^1$ -complex  $[Mn(CO)_4-(PR_2R)(\eta^1-BH_3 \cdot PMe_3)]$ . The reverse reaction was not achieved, even with strong bases such as NaH. However, the  $\eta$ -borane complex decomposed in solution to yield  $[MnH(CO)_4(PR_2R')]$  and  $[BH_2 \cdot 2PMe_3]^+$ , suggesting heterolytic B–H bond cleavage occurs.

### 7.5. Lewis-Acid/Base-Stabilized Phosphinoborane, Complexes of Type III

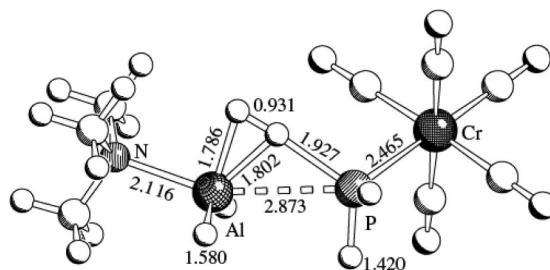
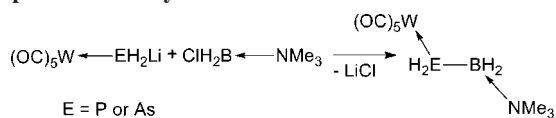
The chemistry of phosphinoboranes,  $R_2P-BR'_2$ , is a diverse area, with many studies reported in the literature.<sup>297</sup> However the parent compound,  $PH_2BH_2$ , has never been experimentally identified. The stabilization of the heavier group 13 analogs,  $H_2AlPH_2$  and  $H_2GaPH_2$ , via the coordination of a Lewis acid and base to give  $[(CO)_5W(H_2PEH_2 \cdot NMe_3)]$  ( $E = Al$  or  $Ga$ ) has been demonstrated.<sup>298</sup> In 2006, the isolation of phosphinoborane,  $H_2PBH_2$ , stabilized by the Lewis acid  $W(CO)_5$  and Lewis base  $NMe_3$  and the corresponding As congener were reported (Scheme 7.20).<sup>299</sup> Contrary to the case of the heavier group 13 analogs, which were synthesized via  $H_2$  elimination from the parent  $[W(CO)_5PH_3]$  and  $H_3E \cdot NMe_3$  ( $E = Al$  or  $Ga$ ), the phosphinoborane complexes had to be synthesized via salt elimination (Scheme 7.20).

A computational investigation of this system indicated that a 5- or 6-coordinate transition state was required, which is not readily accessible for boron, which prefers a tri- or tetracoordinate geometry, but is not uncommon for aluminum and gallium (Figure 7.8).<sup>300</sup>

This work has since expanded to yield a broad range of complexes. Reaction of  $[(CO)_5W(H_2P-EH_2 \cdot NMe_3)]$  ( $E = P$  or  $As$ ) with the Pt(0) complex  $Pt(PPh_3)_2(CH_2CH_2)$  resulted in oxidative addition of the P–H bond to the Pt center, yielding *cis*- $[(Ph_3P)_2Pt(H)(\mu-PHBH_2 \cdot NMe_3)W(CO)_5]$ , which on heating reversibly lost CO to form  $[(Ph_3P)_2Pt(H)(\mu-PHBH_2 \cdot NMe_3)W(CO)_4]$  (Scheme 7.21).<sup>301</sup>

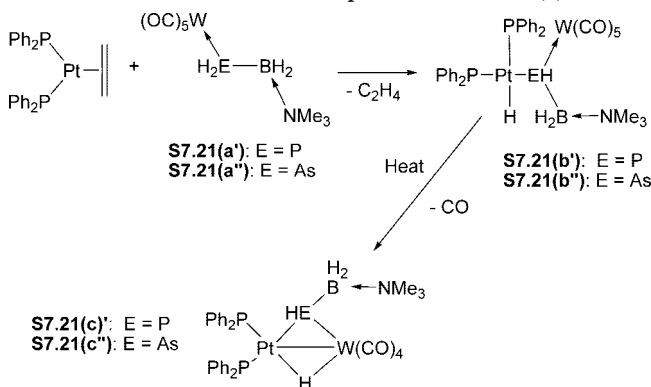
Subsequently, the first Lewis-base-stabilized phosphinoborane,  $H_2PBH_2 \cdot NMe_3$ , was prepared by abstraction of the stabilizing Lewis acid with  $P(OMe)_3$ . Subsequent addition of another Lewis acid,  $Fe(CO)_4$  or  $BH_3$ , resulted in recom-

### Scheme 7.20. Synthesis of Lewis-Acid/Base-Stabilized Phosphinoborane by Salt Elimination

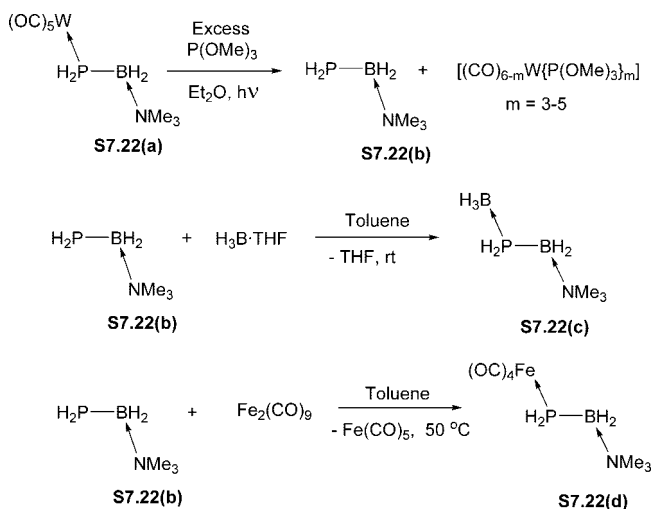


**Figure 7.8.** Proposed hexa-coordinate transition state for  $H_2$  elimination for the reaction of  $[(Cr(CO)_5PH_3)]$  and  $Me_3N \cdot AlH_3$ . Reprinted with permission from ref 301. Copyright 2005 Wiley VCH.

### Scheme 7.21. Oxidative Addition of P–H Bond in Lewis-Acid/Base-Stabilized Phosphinoborane to Pt(0) Center



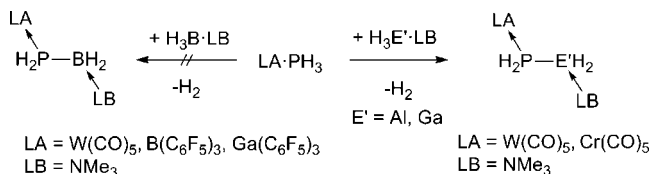
### Scheme 7.22. Removal of $W(CO)_5$ from Lewis-Acid/Base-Stabilized Phosphinoborane and Subsequent Coordination of Other Lewis Acids



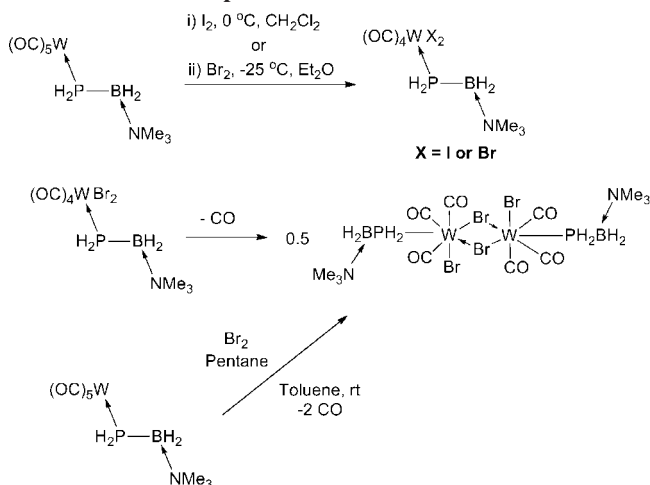
plexation (Scheme 7.22). Complex **S7.22(b)** was stable in solution and the solid state structure indicated an antiperiplanar orientation of the lone pair at phosphorus and the  $NMe_3$  group on boron.<sup>302</sup>

A series of compounds with varying Lewis acids and bases, as well as functionalization on phosphorus have since been prepared,  $[(LA)(PHRBH_2 \cdot LA)]$  ( $LA =$  Lewis acid,  $LB =$  Lewis base;  $LA = Cr(CO)_5$ ,  $R = H$ ,  $LB = NMe_3$ ;<sup>300</sup>  $LA = (C_6F_5)_3B$ ,  $R = H$  or  $Ph$ ,  $LB = NMe_3$ ;<sup>303</sup>  $LA = (C_6F_5)_3Ga$ ,  $R = Ph$ ,  $LB = NMe_3$ ;<sup>303</sup>  $LA = (C_6F_5)_3B$ ,  $R = Ph$ ,  $LB = NHC^{Me}$ ;<sup>304</sup>  $LA = (C_6F_5)_3Ga$ ,  $R = Cp^*$ ,  $Ph$ ,  $LB = NHC^{Me}$ ;<sup>304</sup>  $NHC^{Me} = 1,3,4,5$ -tetramethylimidazoline). It is of significance that the first example of B–P bond formation, which

### Scheme 7.23. Lewis-Acid-Stabilized Phosphinoborane Reacting with Amine–Gallanes and Amine–Alanes but Not Boranes



### Scheme 7.24. Halogenation and Dimerization of Lewis-Acid/Base-Stabilized Phosphinoborane



produced [(C<sub>6</sub>F<sub>5</sub>)<sub>3</sub>Ga(PHRBH<sub>2</sub>·NHC<sup>Me</sup>)] (R = Ph or Cp\*), via H<sub>2</sub> loss in these compounds was observed with these compounds (Scheme 7.23).<sup>304</sup>

Further reactivity of the W(CO)<sub>5</sub>-stabilized phosphinoborane complex [(CO)<sub>5</sub>W(PH<sub>2</sub>BH<sub>2</sub>·NMe<sub>3</sub>)] with various halide sources was investigated. The use of tetrahalomethanes, CX<sub>4</sub> (X = Cl or Br), was found to selectively halogenate at phosphorus, giving [(CO)<sub>5</sub>W(PX<sub>2</sub>BH<sub>2</sub>·NMe<sub>3</sub>)] (X = Cl or Br), which represent the first group of Lewis-acid/base-stabilized dihalophosphinoboranes.<sup>305</sup> By comparison, reaction of [(CO)<sub>5</sub>W(PH<sub>2</sub>BH<sub>2</sub>·NMe<sub>3</sub>)] with Br<sub>2</sub> or I<sub>2</sub> resulted in halogenation at the tungsten center, giving [(CO)<sub>4</sub>WX<sub>2</sub>(PH<sub>2</sub>BH<sub>2</sub>·NMe<sub>3</sub>)], whereas the brominated compound is unstable toward dimerization by loss of a CO ligand (Scheme 7.24).<sup>306</sup>

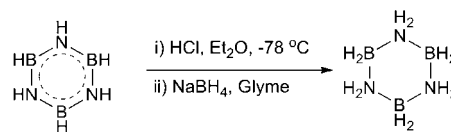
## 8. Polyaminoboranes and Polyphosphinoboranes<sup>307</sup>

### 8.1. Polyaminoboranes

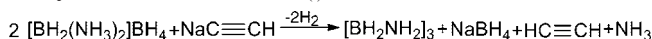
#### 8.1.1. Cyclic Oligomers

The unsubstituted cyclic oligomers of the general formula [NH<sub>2</sub>–BH<sub>2</sub>]<sub>x</sub> are of intrinsic interest as analogs of cycloalkanes and also as potential products in the thermal and catalytic decomposition processes of ammonia–borane and generally amine–boranes with their relevance for hydrogen storage applications. Cyclotriborazane (CTB, also known as hexahydroborazole) was synthesized by Dahl and Schaeffer for the first time by hydrochlorination of borazine and reduction with sodium borohydride (Scheme 8.1).<sup>308</sup> The air-stable product was characterized by elemental analysis, IR spectroscopy, <sup>11</sup>B NMR spectroscopy (reported as a 1:2:1 triplet, but no coupling constant or chemical shift were

### Scheme 8.1. First Synthesis of Cyclotriborazane



### Scheme 8.2. Synthesis of CTB via Reaction of Sodium Acetylide and DADB in NH<sub>3</sub>(l)



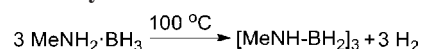
presented), powder XRD, and later by a single-crystal X-ray structure,<sup>309</sup> dipole moment measurements,<sup>310</sup> and a chemical shift by <sup>11</sup>B NMR spectroscopy of –11.1 ppm.<sup>311</sup>

Subsequently, CTB was isolated by a reaction of sodium acetylide with the diammoniate of diborane (DADB) in liquid ammonia (Scheme 8.2), but this reaction was lower yielding (about 15%) and also gave polymeric products, which were not analyzed.<sup>312</sup>

A more systematic study into the synthesis of cycloborazanes was described by Shore and co-workers.<sup>203</sup> The cycloborazanes were prepared by reaction of diborane, ammonia, and sodium amide in liquid ammonia. The cycloborazanes with ring sizes 4, 6, and 8 were extracted in ether and purified by fractional sublimations, whereas the 10-membered ring, pentacycloborazane, remained insoluble and was freed from impurities by extraction with ice–water. The molecular weight of these cyclic compounds was analyzed by cryoscopy and their chemical composition by elemental analysis. Cyclodiborazane was found to slowly isomerize into cyclotriborazane upon standing. Cyclotetrazaborazane could not be analyzed satisfactorily because of its facile decomposition. Cyclopentaborazane was characterized by IR, powder XRD and cryoscopy and proved very stable under hydrolytic conditions. Under pyrolytic conditions, it gave cyclodiborazane and ammonia–borane alongside another species, B<sub>2</sub>NH<sub>7</sub>, which was trapped at lower temperatures. Cyclopentaborazane is of some importance, since it has been cited in the more modern literature as a suggested reaction product of an Ir catalyzed ammonia–borane dehydrocoupling reaction, based on powder XRD.<sup>201</sup> However, it has to be borne in mind that Shore's paper of 1966 neither presented <sup>11</sup>B NMR nor any MS data, which would unequivocally identify this product.

The *N*-methylated congeners are of relevance for catalytic dehydrocoupling research and also because they are oligomeric models of soluble polyaminoboranes (see section 8.1.2). *N,N',N''*-Trimethylcycloborazane could be synthesized via thermal dehydrogenation of *N*-methylamine–borane, MeNH<sub>2</sub>·BH<sub>3</sub>, at 100 °C in 88% yield (Scheme 8.3),<sup>313,314</sup> where the identity of the product was assigned on the basis of elemental analysis and cryoscopy.

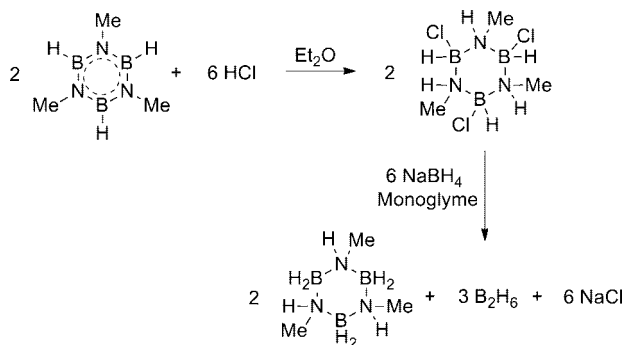
### Scheme 8.3. Thermal Dehydrogenation of Methylamine–Borane to Produce *N,N',N''*-Trimethylborazane



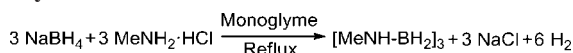
Since this first report, various other syntheses of this compound have been described, such as hydrochloration of *N,N',N''*-trimethylborazine with subsequent reduction in 70% yield (Scheme 8.4)<sup>315</sup> or by reaction of *N*-methylamine hydrochloride with sodium borohydride in about 50% yield (Scheme 8.5).<sup>315</sup>



**Scheme 8.4. Synthesis of *N',N'',N'''*-Trimethylborazane via Hydrochlorination of the Corresponding Borazine with Subsequent Reduction with Sodium Borohydride**



**Scheme 8.5. Synthesis of *N',N'',N'''*-Trimethylborazane via Reaction of Methylamine Hydrochloride and Sodium Borohydride**



For a sample of *N',N'',N'''*-trimethylcycloborazane (prepared by a thermolysis of the amine-borane adduct,  $\text{MeNH}_2 \cdot \text{BH}_3$  at  $100^\circ\text{C}$ ), it could be shown for the first time that it was possible to separate two different isomers, 1(e),3(e),5(e)-trimethylcycloborazane and 1(e),3(e),5(a)-trimethylcycloborazane from the reaction mixture by fractional crystallization (with a = axial, e = equatorial).<sup>196</sup> The heterocycles were characterized by IR spectroscopy, MS,  $^{11}\text{B}$ ,  $^1\text{H}$ , and  $^{13}\text{C}$  NMR spectroscopy and single X-ray crystallographic data for both isomers was presented. By  $^{11}\text{B}$  NMR, both isomers displayed the same chemical shift,  $-5.4$  ppm,  $J_{\text{BH}} = 107$  Hz, whereas differences were noted in the proton and  $^{13}\text{C}$  NMR spectra. In the latter, the all equatorial species showed a single shift at 34.5 ppm, whereas the isomer with one axial group displayed two peaks at 38.3 and 38.5 ppm in a 1: 2 ratio.

### 8.1.2. Synthesis of Polyaminoboranes

The nomenclature for boron-nitrogen containing isosteres to the corresponding hydrocarbons was first introduced by Wiberg.<sup>203,316</sup> In this system, compounds of the principal composition  $\text{R}_3\text{N} \cdot \text{BR}_3$  were referred to as amine-boranes,  $\text{R}_2\text{N}=\text{BR}_2$  as aminoboranes or, if they were cyclized oligomers, cycloborazanes  $[\text{R}_2\text{N}-\text{BR}_2]_x$ , and compounds of formula  $[\text{RB}-\text{NR}]_3$  as borazines.

The first implicit reference to a polymeric material of the empirical formula  $[\text{NH}_2-\text{BH}_2]_n$  was reported by Schlesinger and Burg in 1938 as a decomposition product of  $\text{B}_2\text{H}_7\text{N}$ , for which compound they suggested the molecular formula  $\text{H}_2\text{B}-\text{NH}_2-\text{BH}_3$ .<sup>317</sup> In 1948, detailed studies on the thermal formation and chemistry of borazines and cycloborazanes were reported.<sup>116,117</sup> It was claimed that during the pyrolysis of ammonia-borane at temperatures between  $150$  and  $180^\circ\text{C}$ ,  $\text{NH}_2=\text{BH}_2$  was produced as an intermediate, which then polymerized to give  $[\text{NH}_2-\text{BH}_2]_n$ . Such a product was also reported to form upon reaction of diborane and lithium amide<sup>318</sup> and as a decomposition product of alkali metal amidoboranes upon removal of the solvent ( $\text{NH}_3$ ) used to prepare the compound.<sup>319</sup> The salt  $\text{K}[\text{Me}_2\text{N} \cdot \text{BMe}_3]$  and diborane in ether was also reported to give a polymeric product of the composition  $[\text{BH}_2\text{NH}_2]_n$ .<sup>320</sup> However, in none of the above cases was the postulated polymeric product characterized.

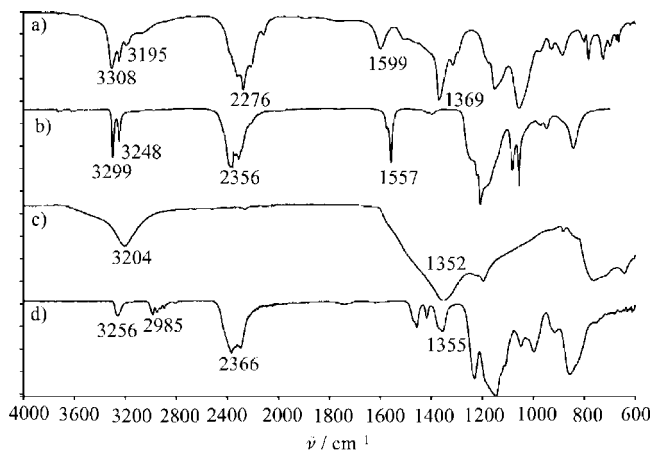
In an attempt to better characterize the proposed polymeric products, Shore and co-workers<sup>321</sup> repeated the synthesis of Schaeffer and co-workers, reacting diborane and lithium amide.<sup>318</sup> They found by cryoscopic molecular weight determination that the degree of polymerization was very low (between 3 and 5), which indicated that the material was oligomeric rather than polymeric.

In the 1980s, oligomers and polymers with B-N skeletons elicited a considerable interest as preceramic materials which could be processed into a desired shape and then pyrolyzed to give hexagonal boron nitride (h-BN), which has a similar structure to graphite and has a similar range of applications, for example, as an industrial lubricant.

The unsubstituted polyaminoborane (PAB),  $[\text{NH}_2\text{BH}_2]_n$ , is unarguably the most investigated polymer in this class of materials. It has been claimed as a likely thermal decomposition product of ammonia-borane,<sup>6</sup> but characterization has been hampered by its insolubility in all organic solvents. Moreover, there is a growing body of evidence that the chemical composition of this polymer (for example linear vs. branched vs. cyclic) is largely dependent on the exact conditions used for its synthesis.

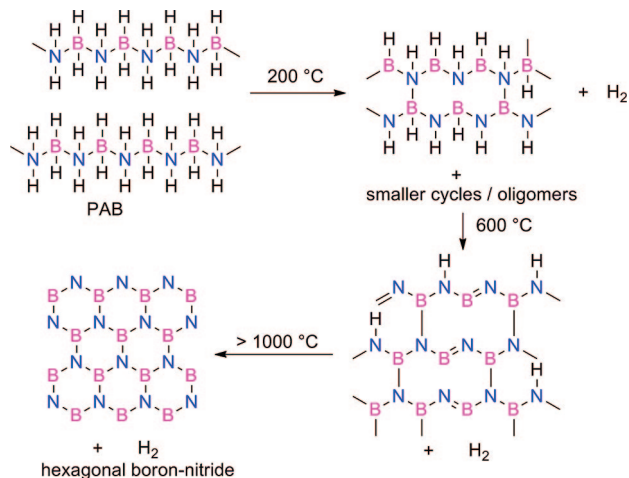
There have been several attempts to synthesize the unsubstituted PAB by pyrolysis of ammonia-borane or borazine.<sup>322-324</sup> Kim and co-workers prepared a material, which they assigned to be PAB, in low yield by a thermal reaction between  $\text{NaBH}_4$  and  $(\text{NH}_4)_2\text{SO}_4$ .<sup>325</sup> Another, unusual method reported to yield PAB,  $[\text{NH}_2\text{BH}_2]_n$ , was the exposure of borazine to a radio frequency discharge.<sup>326</sup>

Solid-state  $^{11}\text{B}$  NMR spectroscopy of a sample obtained by thermal decomposition of ammonia-borane at  $90^\circ\text{C}$  revealed signals for both tri- and tetracoordinated boron, indicative of a nonunitary structure.<sup>324,327</sup> Powder XRD of the sample showed no sharp peaks, indicating that the material was an amorphous solid.<sup>324</sup> FTIR spectra of this sample and samples generated by similar methods all showed broad bands in the area of  $3300-3500\text{ cm}^{-1}$  for the N-H bonds and  $2300-2400\text{ cm}^{-1}$  for the B-H bonds. Kim and co-workers found a similar lack of sharp peaks by powder XRD and reported a similar IR spectrum.<sup>325</sup> In 2006, Goldberg and Heinekey showed that ammonia-borane could be very efficiently dehydrocoupled using Brookhart's  $\text{IrH}_2\text{POCOP}$  catalyst (see section 5).<sup>201</sup> They obtained an insoluble product, which they suggested to be a cyclic pentamer  $[\text{NH}_2-\text{BH}_2]_5$  on the basis of WAXS in comparison to similar values reported for this species by Shore.<sup>203</sup> The same reaction was later examined by Manners and co-workers under more concentrated reaction conditions.<sup>328</sup> Their data for the product was not consistent with cyclic pentamer but suggested a different material was obtained, and a polymer structure was assigned. This material gave much sharper bands in the IR spectrum than the thermally produced samples, but the spectrum also differed from that obtained for the pentamer<sup>203</sup> (Figure 8.1). There were two peaks at  $3299$  and  $3248\text{ cm}^{-1}$ , assigned as the symmetric and asymmetric N-H stretches and two bands for B-H, indicating a more uniform sample. The notion that this material was indeed different to thermally produced samples was further reinforced by the WAXS pattern. Thermogravimetric experiments on the various thermally produced materials gave fairly comparable results, with polyaminoborane from the thermal reaction of  $\text{NaBH}_4$  and  $(\text{NH}_4)_2\text{SO}_4$ ,<sup>325</sup> polyaminoborane from the thermal decomposition of borazine,<sup>324</sup> and a sample from the thermal decomposition of



**Figure 8.1.** IR spectra of (a) ammonia-borane ( $\text{NH}_3 \cdot \text{BH}_3$ ), (b) polyaminoborane prepared by catalytic dehydrocoupling of *N*-methylamine-borane with  $\text{IrH}_2\text{POCOP}$ , (c) pyrolyzed ( $900^\circ\text{C}$ ), and (d) poly(*N*-methylaminoborane). Reprinted with permission from ref 328. Copyright 2008 Wiley VCH.

### Scheme 8.6. Postulated Mechanism for the Thermal Decomposition of Polyaminoborane



ammonia-borane,<sup>329</sup> all producing ceramic yields of around 75% at  $1000^\circ\text{C}$ . The products of the thermolysis were all interpreted as boron nitride. However, the sample of PAB prepared using the Brookhart Ir catalyst gave only a ceramic yield of 36% at  $900^\circ\text{C}$  (all at a heating rate of  $10^\circ\text{C}/\text{min}$ ).

On the basis of these results, it was postulated that thermal reactions to give PAB may produce materials of the composition  $\text{NBH}_x$ , which are cross-linked or branched. This would render these materials more stable toward thermal decomposition and loss of small oligomeric volatile species than a linear polymer. In the case of the material from the  $\text{IrH}_2\text{POCOP}$ -catalyzed reaction, however, branching or cross-linking probably did not occur, giving rise to an essentially linear polymer, which could lose more volatile oligomers during the heating process. The final ceramic product was boron nitride, but in all cases, the IR spectrum still showed weak N-H bands which is indicative of an incomplete pyrolysis process (Scheme 8.6).

Polyaminoboranes and other ceramic precursors for boron nitride were studied by high resolution solid state NMR spectroscopy.<sup>327</sup> The sample of PAB, which was prepared via a procedure published by Sneddon and Wideman<sup>330</sup> and Kim and co-workers,<sup>325</sup> was found to contain mainly four

coordinate N sites ( $\delta = -330$  to  $-380$  ppm) with traces of trigonal planar N (broad peak at about  $\delta = 355$  ppm) by cross-polarization  $^{15}\text{N}$  NMR spectroscopy. The  $^{11}\text{B}$  NMR spectrum revealed again a variety of peaks, a low intensity, two broad peaks in the boron three coordinate area ( $\delta = 30$  to  $10$  ppm), a major broad peak at about  $\delta = -25$  ppm with a small side peak at  $\delta = -36$  ppm), both in the boron tetracoordinate area. These spectra not only showed that the material obtained was not a well-defined linear PAB of the formulation  $[\text{NH}_2\text{BH}_2]_n$  but also that it contained other bonding motifs. This was confirmed by the study of thermally produced PAB, which was similarly ill-defined.<sup>324</sup>

The first reported soluble polyaminoborane was poly(aminodifluoroborane),  $[\text{NH}_2\text{BF}_2]_n$ , which was prepared by initial pyrolysis of ammonia-trifluoroborane at  $185^\circ\text{C}$ , condensing the monomeric product,  $\text{NH}_2=\text{BF}_2$  at low temperature ( $-196^\circ\text{C}$ ) and subsequently warming to room temperature.<sup>329</sup> The molecular weight was measured using static light scattering and determined to be 23 kDa, with an error of 19%. However, since no structural characterization was described (for example NMR, elemental analyses or mass spectrometry), it is not clear if this sample was in fact the purported polymer.

Poly(*N*-methylaminoborane) was claimed to be a component in an equilibrium between *N*-methylaminodiborane on the one hand, and poly(*N*-methylaminoborane) and diborane on the other (eq 8.1).<sup>15b</sup> However, there were no efforts at the time to characterize the polymer if indeed it existed.



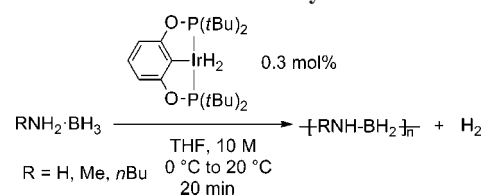
In 2008, it was found that concentrated solutions of *N*-monoalkylamine-borane adducts can be dehydrocoupled using Brookhart's  $\text{IrH}_2\text{POCOP}$  catalyst to yield soluble linear polyaminoboranes, which were characterized by a variety of solution state analytical techniques including multinuclear NMR spectroscopy and IR spectroscopy to provide structural characterization and GPC and DLS to determine the molecular weight (Scheme 8.7).<sup>328</sup>

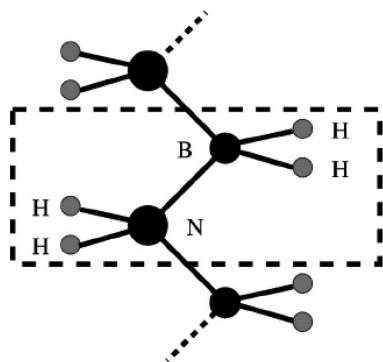
Goldberg and Heinekey subsequently analyzed the system and reported that low concentrations (0.5 M) led to the formation of oligomers, analyzed by electrospray ionization mass spectrometry (ESI-MS).<sup>331</sup>

### 8.1.3. Computational Analysis of Polyaminoboranes

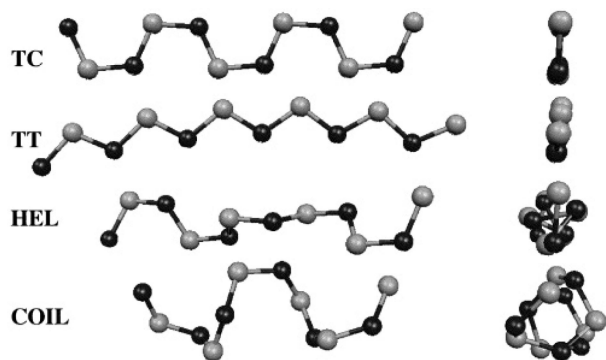
Polyaminoboranes may be significant in aiding a deeper understanding of the isoelectronic relationship between C-C and N-B bonds. Unsurprisingly, there have been a number of computational studies of these polymers. The first were reported by Perkins,<sup>332</sup> which were superseded by more modern calculations, notably by Dolg and co-workers, who used Wannier orbital-based Hartree-Fock and other correlated ab initio calculations for the calculation of polyaminoborane and polyiminoborane.<sup>333</sup> Using an extrapolation of an

### Scheme 8.7. Catalytic Dehydrocoupling of Primary Amine-Boranes to Give Soluble Polyaminoboranes





**Figure 8.2.** Unit cell used for the calculation of polyaminoborane. Reprinted with permission from ref 333. Copyright 1999 American Institute of Physics.

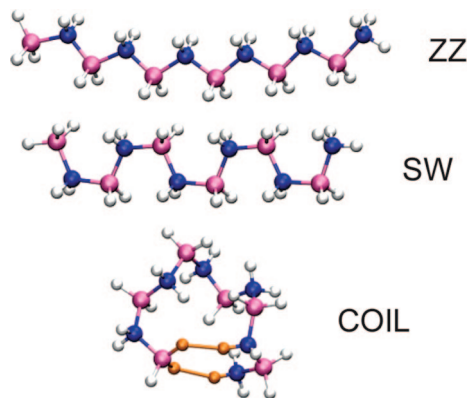


**Figure 8.3.** Conformations accessible to polyaminoborane. Reprinted with permission from ref 334. Copyright 2004 American Chemical Society.

optimized unit cell (Figure 8.2), no bond-alternation in the backbone of polyaminoborane was found.

While the approach based on an extrapolation involving a unit cell will represent the structure of the polymer in the solid state much better than gas phase approaches, an issue could be that other possible conformations of the polymer have not been taken into account. There may be more than one modification, as with the possibly electronically similar poly(vinylidenedifluoride) (PVdF), which is experimentally known to exist in an amorphous  $\alpha$ -phase or a metastable  $\beta$ -phase, which exhibits the same *trans* structure as the that assumed for polyaminoborane by Dolg and co-workers.

A related study by Jacquemin and co-workers, who analyzed polyaminoborane in the gas phase is therefore of interest.<sup>334</sup> A set of four different conformations, *trans-cisoid* (TC), *trans-transoid* (TT), helical (HEL), and coiled (COIL) (which was similar to the helical structure and consisted merely of an end group effect), were analyzed (Figure 8.3). Among the two planar conformations, the *trans-cisoid* was found to be more stable than the *trans-transoid*, but vibrational analysis showed that in fact this *trans-cisoid* conformation was a transition-state-like form, connecting the left-handed and right-handed helical structures. The *trans-transoid* was the only conformation that did not show any bond length alteration<sup>335</sup> and had a larger dipole moment than the other conformers. For the polymer, the relative energies of the different conformations were extrapolated to 0.0 (TC), +4.0 (TT), -0.6 (COIL), and -1.3 (HEL) (kcal/



**Figure 8.4.** Possible conformations for polyaminoborane. Reprinted with permission from ref 359. Copyright 2007 American Chemical Society.

mol per cell). With such small differences and a rotational barrier of only about 7 kcal/mol rotational energy per B–N bond, all conformers should coexist at room temperature. The corresponding vibrational spectra were also calculated for each conformation. Both the HEL and COIL conformations, which were found to be similar with respect to stability, dipole moments, partial atomic charges (Merz–Kollmann) and excitation energies, corresponded to some extent to the experimentally recorded PAB (as synthesized thermally before the introduction of Brookhart’s catalyst). However, there were discrepancies between the calculated and measured IR spectra for polymers prepared by both thermal and catalytic routes, and the possibility that inter- or intramolecular dihydrogen bonds play a substantial role in the structure of polyaminoborane was not analyzed at the time. Such additional bonds seem very likely, given that they were found to occur in ammonia–borane, as well as the mono- and dimethylamine–boranes, and also because polyaminoborane is completely insoluble, even when prepared by the catalytic method.

A very similar study described oligoaminoboranes in terms of their conformation in the gas phase.<sup>359</sup> To localize the global minima, a simulated annealing search was used, with a simple cubic lattice, but it is not clear how the authors decided on the dimensions of the cell, which would have an impact on the results of the calculations. The conformations they analyzed were zigzag (ZZ, corresponding to Jacquemin’s TT conformation), square-wave (SW, corresponding to Jacquemin’s TC conformation), and coiled structures (corresponding to Jacquemin’s COIL conformation) (Figure 8.4). The SW conformation proved to be much more stable than ZZ, which was attributed to shorter and stronger B–N-bonds and smaller dipole moments. The most stable conformation was found to be the coiled structure with a staggered conformation along the backbone. The coiled conformation was also found to be stabilized by dihydrogen bonds. This latter finding raises the suspicion that such dihydrogen bonds may also stabilize the other conformations, but in an intermolecular fashion, which is why they were not found computationally. Branched structures and diradical structures were also considered all of which were substantially higher in energy than the previously described structures, in any conformation.

A further computational analysis of PAB used analogous structures for polyethylene (both orthorhombic and monoclinic) and ammonia–borane for the calculation of the

structure in the solid state.<sup>336</sup> The most stable conformer was a coiled structure as in the studies described above.

In addition to their fundamental interest, polyaminoboranes constitute a group of new materials, which may be exploited as ceramic precursors for boron nitride and other applications. Furthermore, there is potential that these polymers may also function as piezoelectric materials. This has been suggested by Bernholc and co-workers who used *ab initio* calculations to predict the piezoelectric response of polyaminoboranes such as poly(aminodifluoroborane).<sup>337</sup>

Because of the highly polar nature of the monomeric unit of polyaminoboranes (and polyiminoborane, [RB-NR']<sub>n</sub>, PIB) these polymers have been discussed as potential nonlinear optical materials, which were analyzed computationally.<sup>338</sup> All calculations were performed on the TC structure, which, despite being *transition-state-like*, is the most stable *planar* conformer. The electronically relevant parameters were the dipole moments, which depend on geometry, charges and the polarizability  $\alpha$ , and first hyperpolarizability  $\beta$ . The bond length alteration at the polymeric limit was estimated to be 0.016 Å for PAB and -0.003 Å for *trans*-polyiminoborane. The dipole moment was calculated to be 3.18 D for PAB and 0.94 D for PIB. Both, PAB and polyiminoborane were found to exhibit a very low polarizability and first hyperpolarizabilities (see Table 8.2 below). It was therefore concluded that neither PAB nor PIB would be suitable as nonlinear optical materials.

## 8.2. Polyphosphinoboranes

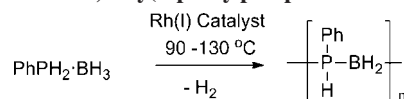
### 8.2.1. Synthesis of Polyphosphinoboranes

The first reports of polyphosphinoboranes and polymers with P–B bonds in the backbone, interlinked with organic spacers can be found in patents by Hofmann,<sup>339</sup> Burg and Wagner,<sup>340</sup> but there was no characterization of the proposed polymers. Korshak and co-workers re-examined this chemistry in the 1960s.<sup>341</sup> Thermolysis experiments with PhPH<sub>2</sub>·BH<sub>3</sub> at temperatures between 100 and 150 °C for 13 h led to an oligomer, which was soluble in benzene and had a molecular weight of  $M_n = 2150$ , as determined by ebullioscopy. Additionally, a variety of diphosphines of the general formula PhPH–R–PPh were heated with a slight excess of *N,N,N*-triethylamine–borane to 300 °C to obtain glassy insoluble compounds of indeterminable molecular weight.<sup>341b</sup> IR spectra showed a strong absorption band at 2440–2380 cm<sup>-1</sup> consistent with B–H stretching in the BH-group, but apart from thermogravimetry, these materials were not analyzed further.

The first soluble, high molecular weight polyphosphinoborane was reported in 1999.<sup>195</sup> It was demonstrated that the phosphine–borane adduct Ph<sub>2</sub>PH·BH<sub>3</sub> could be successfully dehydrocoupled catalytically to yield a linear dimer (see section 5). This reaction was then attempted with a primary and therefore less sterically hindered phosphine–borane adduct PhPH<sub>2</sub>·BH<sub>3</sub>, which was thought to facilitate polymer formation. Indeed, when this precursor was reacted in the absence of solvent with a Rh(I) catalyst (90 °C, 3 h, then 130 °C 3 h, ~0.3 mol % [Rh(1,5-cod)<sub>2</sub>][OTf]), poly(*P*-phenylphosphineborane) was cleanly formed (Scheme 8.8), which could be purified by precipitation into hexanes as a non-solvent.

In the <sup>31</sup>P{<sup>1</sup>H} NMR spectrum of the polymer a broad singlet at  $\delta = -48.9$  ppm was visible, which split into a doublet ( $J_{\text{PH}} = 360$  Hz) in the <sup>1</sup>H-coupled spectrum and

### Scheme 8.8. First Synthesis of a Soluble High Molecular Weight Polyphosphinoborane, Poly(*P*-phenylphosphinoborane)



is characteristic of a single hydrogen atom at phosphorus (and in close proximity to the PhPH<sub>2</sub>·BH<sub>3</sub> signal ( $\delta = -47$  ppm). The <sup>1</sup>H NMR spectrum clearly showed the BH<sub>2</sub> protons ( $\delta = 0.65$ – $2.20$  ppm) and a broad doublet ( $\delta = 4.25$  ppm;  $J_{\text{PH}} = 360$  Hz) for the PH group. In the <sup>11</sup>B NMR spectrum a single broad resonance at  $\delta = -34.7$  ppm was observed. The IR spectrum exhibited strong absorptions at 2421 and 2381 cm<sup>-1</sup>, which is the region typical for both the P–H and B–H stretching vibrations, respectively,<sup>342</sup> and suggests that Korshak and co-workers may indeed have synthesized related materials. The absolute weight average molecular weight ( $M_w$ ) of 31 000 was confirmed by static light scattering (SLS), which corresponds to a degree of polymerization, DP<sub>w</sub>, of 254. It should be noted that the reaction also proceeded in an uncatalyzed manner under the reaction conditions used. However, the obtained molecular weight was considerably lower<sup>195</sup> and the reaction less clean.<sup>342</sup> It was found that the polymer was poorly soluble in THF at 22 °C and is close to precipitating ( $\theta$ -conditions).<sup>343</sup> This hampered characterization attempts by GPC and the polymers instead had to be analyzed by DLS.

It is important to note that polyphosphinoboranes obtained from primary phosphine–boranes still contain P–H and B–H bonds, which still can potentially take part in a second dehydrocoupling reaction. This seems to be the case when the heating time at 130 °C was prolonged to 5 h, with the product insoluble in DCM or THF, and instead a swellable gel. The <sup>31</sup>P and <sup>11</sup>B NMR spectra were similar to those of the high molecular weight polymers so that it seems likely that the polymers became lightly cross-linked under those conditions. This behavior was also reported for [*p*-*n*BuC<sub>6</sub>H<sub>4</sub>PH·BH<sub>2</sub>]<sub>n</sub><sup>343</sup> and is likely to be a general effect.

Chemically, these polymers seem to be stable toward exposure to diethylamine and tri*n*butylphosphine in solution and reasonably stable toward air and moisture in the solid state. The effect of further structural variation of the monomer on the polymerization was also investigated. Electron-withdrawing groups on phosphorus in the phosphine–borane as in *p*CF<sub>3</sub>–C<sub>6</sub>H<sub>4</sub>–PH<sub>2</sub>·BH<sub>3</sub> accelerated the reaction. With this monomer, the reaction could be performed at temperatures as low as 60 °C to give high molecular weight polymers (For a comparison of the characteristics of polyphosphinoboranes prepared to date, see Table 8.1).

### 8.2.2. Toward Applications for Polyphosphinoboranes and Alternative Synthetic Approaches

A potentially interesting application for these materials is their use as ceramic precursors for shaped boron phosphide monoliths and fibers. The ability of the polymer to be easily processed into shapes and fibers, and the intimate atomic scale mixing can allow milder conditions for thermal conversion to boron phosphide than is possible with conventional ceramic synthesis and powder processing techniques. Boron phosphide is a useful material because of its semiconducting properties<sup>344</sup> and it has been suggested computationally that its nonlinear optic response might be

Table 8.1. Selected Analytical Data for Polyphosphinoboranes

	[PhPH–BH <sub>2</sub> ] <sub>n</sub>	[iBuPH–BH <sub>2</sub> ] <sub>n</sub>	[dodecyl C <sub>6</sub> H <sub>4</sub> PH–BH <sub>2</sub> ] <sub>n</sub>	[p-nBuC <sub>6</sub> H <sub>4</sub> PH–BH <sub>2</sub> ] <sub>n</sub>	[p-CF <sub>3</sub> -C <sub>6</sub> H <sub>4</sub> PH–BH <sub>2</sub> ] <sub>n</sub>
catalysis	[[Rh(μ-Cl)(1,5-cod)] <sub>2</sub> ], [Rh(1,5-cod) <sub>2</sub> ][OTf] (0.3 mol %), anhydrous RhCl <sub>3</sub> , RhCl <sub>3</sub> hydrate 1 mol % rhodium, 3 h at 90 °C and 3 h at 130 °C	[[Rh(μ-Cl)(1,5-cod)] <sub>2</sub> ], 13 h at 120 °C	[[Rh(μ-Cl)(1,5-cod)] <sub>2</sub> ], 1 mol %, 9.5 h at 120 °C	[[Rh(μ-Cl)(1,5-cod)] <sub>2</sub> ], 1.5 mol %, 5 h at 100 °C	[[Rh(μ-Cl)(1,5-cod)] <sub>2</sub> ], 2.5 mol %, neat, 2 h, 60 °C
<sup>31</sup> P NMR	-48.9 ppm (ν <sub>1/2</sub> , 135 Hz)	-69 ppm (ν <sub>1/2</sub> ca. 300 Hz)	CDCl <sub>3</sub> : -49.4 (d, J <sub>PH</sub> = 332.4 Hz)	CDCl <sub>3</sub> : -49.7 (br d, J <sub>PH</sub> = 356 Hz)	CDCl <sub>3</sub> : -46.9 (t); CDCl <sub>3</sub> : 7.20–6.40 (br, 4H, Ar-H), 4.21 (br d, J <sub>PH</sub> = 356 Hz, 1H, PH), 2.45 (br, 2H, CH <sub>2</sub> CH <sub>2</sub> CH <sub>2</sub> CH <sub>3</sub> ), 1.48 (br, 2H, CH <sub>2</sub> CH <sub>2</sub> CH <sub>2</sub> CH <sub>3</sub> ), 1.29 (br, 2H, CH <sub>2</sub> CH <sub>2</sub> CH <sub>2</sub> CH <sub>3</sub> ), 0.88 (br, 3H, CH <sub>2</sub> CH <sub>2</sub> CH <sub>2</sub> CH <sub>3</sub> ), BH <sub>2</sub> not observed.
<sup>1</sup> H NMR	CDCl <sub>3</sub> : δ = 6.65 ± 7.90 ppm (PH); δ = 4.25 ppm (J <sub>PH</sub> = 360 Hz) (PH); δ = 0.65 ± 2.20 ppm (BH <sub>2</sub> )	CDCl <sub>3</sub> : 3.86 ppm (J <sub>HP</sub> = 335 Hz, 1H, br d), C <sub>6</sub> H <sub>4</sub> CH <sub>2</sub> (C <sub>11</sub> H <sub>23</sub> ), 1.8–1.2 (br, 20H, C <sub>6</sub> H <sub>4</sub> CH <sub>2</sub> (CH <sub>2</sub> ) <sub>10</sub> CH <sub>3</sub> ), 0.94 (br, 3H, (CH <sub>2</sub> ) <sub>11</sub> CH <sub>3</sub> ), BH <sub>2</sub> not observed	CDCl <sub>3</sub> : 8.2–6.4 (br, 4H, Ar-H), 4.21 (br d, J <sub>PH</sub> = 350 Hz, PH), 2.53 (br, 2H, C <sub>6</sub> H <sub>4</sub> CH <sub>2</sub> (C <sub>11</sub> H <sub>23</sub> )), 1.8–1.2 (br, 20H, C <sub>6</sub> H <sub>4</sub> CH <sub>2</sub> (CH <sub>2</sub> ) <sub>10</sub> CH <sub>3</sub> ), 0.94 (br, 3H, (CH <sub>2</sub> ) <sub>11</sub> CH <sub>3</sub> ), BH <sub>2</sub> not observed	CDCl <sub>3</sub> : 7.20–6.40 (br, 4H, Ar-H), 4.21 (br d, J <sub>PH</sub> = 356 Hz, 1H, PH), 2.45 (br, 2H, CH <sub>2</sub> CH <sub>2</sub> CH <sub>2</sub> CH <sub>3</sub> ), 1.48 (br, 2H, CH <sub>2</sub> CH <sub>2</sub> CH <sub>2</sub> CH <sub>3</sub> ), 1.29 (br, 2H, CH <sub>2</sub> CH <sub>2</sub> CH <sub>2</sub> CH <sub>3</sub> ), 0.88 (br, 3H, CH <sub>2</sub> CH <sub>2</sub> CH <sub>2</sub> CH <sub>3</sub> ), BH <sub>2</sub> not observed.	CDCl <sub>3</sub> : 7.9–6.5 (br, Ar-H), 4.42 (br d, J <sub>PH</sub> = 354 Hz, PH), 2.2–0.8 (br, BH <sub>2</sub> )
<sup>11</sup> B NMR	δ = -34.7	-36 ppm	-37.5	-35.7 (br)	CDCl <sub>3</sub> : -34.3 (br, BH <sub>2</sub> ) -62.5 (s, CF <sub>3</sub> )
<sup>19</sup> F NMR	n/a	n/a	n/a	n/a	n/a
IR	2421 and 2381 cm <sup>-1</sup>	2421 cm <sup>-1</sup>	D <sub>h</sub> = 14 nm. (CHCl <sub>3</sub> )	M <sub>w</sub> = 20 800, PDI = 7.35 (THF)	M <sub>w</sub> = 56 170, PDI = 1.67 (THF, 0.1% [Bu <sub>4</sub> N]Br) THF
DLS	D <sub>h</sub> values ~10 (dissolved polymer) and 30 nm (aggregates) (THF)	D <sub>h</sub> values ~7 (dissolved polymer) and 25 nm (aggregates) (THF)			
SLS	31 000				
GPC					
soluble in	THF, chlorinated hydrocarbons; moderately soluble in toluene and benzene	THF, chlorinated solvents, toluene, hexanes	CHCl <sub>3</sub>	THF	THF
insoluble in	water, methanol	water, methanol	iPrOH	iPrOH	pentane
DSC			T <sub>g</sub> = -1 °C	T <sub>g</sub> = 8 °C	

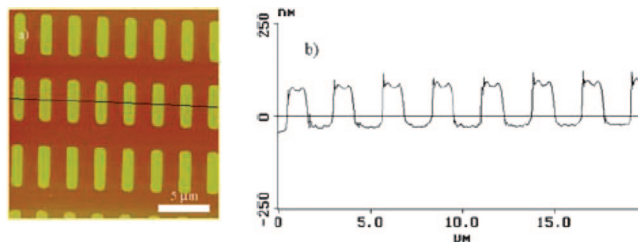
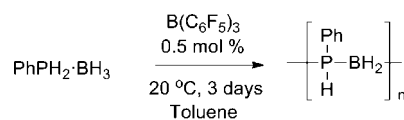


Figure 8.5. Left: Tapping mode AFM image of lithographically patterned bars of [(p-CF<sub>3</sub>C<sub>6</sub>H<sub>4</sub>)PH-BH<sub>2</sub>]<sub>n</sub>. Right: Cross-sectional analysis. Reprinted with permission from ref 346. Copyright 2005 Wiley InterScience.

### Scheme 8.9. Lewis-Acid-Catalyzed Formation of Polyphosphinoboranes



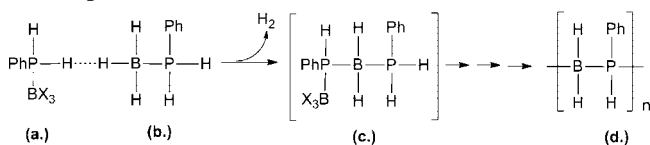
high due to its large electronic first hyperpolarizability.<sup>345</sup> As a result of their synthetic accessibility, polyphosphinoboranes may have advantages over existing materials in this regard. The ceramic yields after heating to 1000 °C, defined in terms of the remaining percentage of the original weight, were in the range of 75–80% for [PhPH–BH<sub>2</sub>]<sub>n</sub>, 40–45% for [iBuPH–BH<sub>2</sub>]<sub>n</sub>, and 35–40% for [(p-nBuC<sub>6</sub>H<sub>4</sub>)PH-BH<sub>2</sub>]<sub>n</sub>.

Polymer films based on [(p-CF<sub>3</sub>C<sub>6</sub>H<sub>4</sub>)PH–BH<sub>2</sub>]<sub>n</sub> were tested for a potential application in electron beam lithography (EBL).<sup>346</sup> To this end, a solution of the polymer in toluene was spin-coated onto a silicon wafer and EBL was carried out using a scanning electron microscope (SEM). After sonication in THF, the material that had not been exposed to the beam had been washed away, but the exposed material was firmly attached to the surface, its insolubility presumably due to cross-linking by radical dimerization induced by the electron beam. Tapping mode atomic force microscopy (AFM) was used to visualize the resulting lithographic pattern (Figure 8.5)

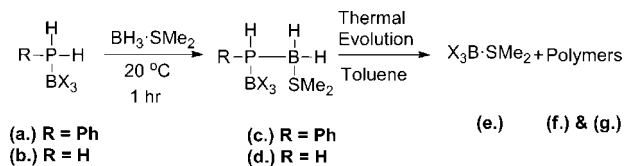
Following the initial reports of polyphosphinoboranes, Denis, Gaumont and co-workers found that the catalytic addition of a strong Lewis acid B(C<sub>6</sub>F<sub>5</sub>)<sub>3</sub> to a solution of the PhPH<sub>2</sub>·BH<sub>3</sub> monomer allowed the formation of polyphenylphosphinoborane at 20 °C over the course of three days (Scheme 8.9) or at 90 °C over the course 3 h.<sup>347</sup> In both cases, NMR signals were observed that were consistent with polyphenylphosphinoborane (<sup>31</sup>P NMR –48.9 ppm and <sup>11</sup>B NMR –35.8), but there were also poorly resolved peaks from δ = –52 to –56 (<sup>31</sup>P NMR), which had been observed in the thermal polymerization discussed above.

In a further experiment, the Lewis acid-catalyzed dehydrocoupling was explored for the synthesis of the unsubstituted parent polymer, [PH<sub>2</sub>–BH<sub>2</sub>]<sub>n</sub>. Because of the thermal instability of the monomer, PH<sub>3</sub>·BH<sub>3</sub>, this was generated *in situ* by bubbling PH<sub>3</sub> and diborane through a solution of B(C<sub>6</sub>F<sub>5</sub>)<sub>3</sub> in DCM at –50 °C and later warming it to 20 °C, at which temperature oligomerization started. Further warming to 70 or 90 °C allowed the reaction to complete. NMR analysis revealed broad peaks by <sup>31</sup>P NMR (δ = –107 ppm) and <sup>11</sup>B NMR (–32 ppm), but the material proved to be too air sensitive for further analysis by high resolution mass spectrometry, HRMS, or elemental analysis. In a mechanistic hypothesis, it was suggested that the Lewis acid formed a complex with the phosphine, thus rendering the hydrogen

### Scheme 8.10. Proposed Mechanism for the Polymerization of Phosphine–Boranes with a Lewis Acid



### Scheme 8.11. Polycondensation Route to Polyphosphinoboranes



on the phosphorus atom more acidic (Scheme 8.10). This complex would then react with monomer in an acid–base reaction to release dihydrogen. Species **S8.10(c)** would then exchange  $B(C_6F_5)_3$  with  $BH_3$ , thus generating a new initiator and a reactive dimer.

Another pathway for the formation of polyphosphinoboranes (Scheme 8.11) proved to be the treatment of the isolable complexes **S8.11(a)** and **S8.11(b)**, respectively, with  $BH_3 \cdot SMe_2$  at 20 °C, which initially gave the dehydrocoupled products **S8.11(c)** and **S8.11(d)**, which polymerized thermally.<sup>347</sup> However, in this case the polymerization reaction was not a dehydrocoupling route but rather a polycondensation, where  $B(C_6F_5)_3 \cdot SMe_2$  was liberated.

### 8.2.3. Computational Structure Analysis and Predictions of Polyphosphinoboranes

Polymers with a high longitudinal dipolar first hyperpolarizability  $\beta$  have elicited considerable interest as potential materials for applications based on nonlinear optical (NLO) properties. As polyphosphinoboranes have a polar monomer unit, and their dehydrogenated congeners, poly(*B,P*-dehydrophosphinoborane) have conjugated (formally)  $\pi$ -bonds which may allow delocalization of electrons, the structural and electronic properties of these two polymers are of interest in order to elucidate their value for possible applications. A computational study, using *ab initio* methods showed that the most stable planar conformation for PPB was *trans-cisoid* (Figure 8.6),<sup>348,349</sup> which was also found for the dehydrogenated polymer DHPPB (Figure 8.7). This conformation was only slightly higher in energy than the helical coiled structures. Although the helical coiled structure represented the global minimum, the *trans-cisoid* conformations with their simpler geometry were used to enable comparisons between the hydrogenated and dehydrogenated

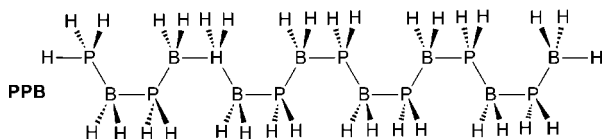


Figure 8.6. Planar *trans-cisoid* structure for polyphosphinoborane.

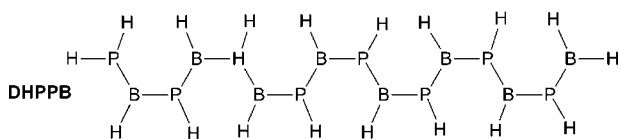


Figure 8.7. *Trans-cisoid* conformation for dehydrogenated polyphosphinoborane.

Table 8.2. Static First Hyperpolarizabilities

entry	polymer	$\beta_L/W$ ( $cm^5 esu^{-1} g^{-1} mol$ )	ref
1	PPB	$0.02 \times 10^{-30}$	349
2	DHPPB	$0.95 \times 10^{-30}$	349
3	3-methyl-4-nitroaniline (MNA) monomer	$0.10 \times 10^{-30}$	351
4	<i>N</i> -(4-nitrophenyl)-(L)-prolinol (NPP)	$0.06 \times 10^{-30}$	352
5	$\alpha,\omega$ -nitro,amino- <i>trans</i> -hexatriene	$0.66 \times 10^{-30}$	353
6	polymethineimine	$4.2 \times 10^{-30}$	354
7	polyaminoborane	$0.01 \times 10^{-30}$	338
8	polyiminoborane	$0.03 \times 10^{-30}$	338

species. The IR spectra were also calculated for all possible extreme conformations, which, if this parent system was to be synthesized, could be useful in determining the polymers' actual preferred conformation in the solid state and in solution.

In the detailed structural and electronic analysis of the *trans-cisoid* PPB and DHPPB, it was found that the bond alternation converged quickly when going from oligomers to the polymeric limit.<sup>349</sup> For PPB,  $\Delta_r$  was small but non zero, whereas for DHPPB almost equal bond lengths were found. The charge alternation in the backbone was more difficult to estimate, with different calculation techniques (Mulliken, ESP = Merz–Kollman charges) giving different results. If one is to believe the generally more reliable ESP charges, then the charge alteration  $\Delta_q$  is rather small for both PPB and DHPPB, whereas the longitudinal dipole moment  $\mu_L$  is small for DHPPB and somewhat larger for PPB, as would be expected. The static polarizability  $\alpha_L$ , which is a parameter that depends on electron delocalization, not geometry, was predicted to be twice as high for DHPPB as for PPB, which attests to the easy delocalization of electrons in the former polymer. The first hyperpolarizability  $\beta_L$  also depends on the delocalization, it was therefore unsurprising that this parameter was relatively small in PPB but much larger in DHPPB. This difference became even more pronounced when the dynamic parameters were calculated, which take into account frequency dispersion. A comparison with other organic materials with NLO properties was also provided and this clearly showed that while PPB has little potential for NLO properties, the synthesis and evaluation of DHPPB may be worthwhile (Table 8.2). A later report summarized a comparison of PPB and DHPPB with other inorganic and organic polymers.<sup>350</sup>

Prompted by the experimental finding that polyphosphinoboranes with some alkyl and phenyl substituents on phosphorus are accessible, it was also explored how these substituents would affect the relative stabilities of the conformations and thereby the electronic properties of these polymers by *ab initio* methods.<sup>355</sup> With the introduction of one substituent on phosphorus, this atom becomes a chiral center and both the isotactic and syndiotactic configurations had to be taken into account. If polymers of the same conformation are compared, the dipole moments and the structures, except for the dihedral angles, vary very little. However, the charge separation was larger for the *i*Bu substituent than it was for Ph, whereas the flexibility was greater for the latter polymer, which should in theory be reflected in the glass transition temperature  $T_g$ . The tacticity determined which was the most stabilized conformation, which was no longer always (for a planar constraint) the *trans-cisoid* or (without constraint) the helical conformation like in the unsubstituted polymer. For example, in the isotactic poly(*P*-phenylphosphinoborane), the *trans-transoid*

conformation was the most stable, whereas for the syndio-tactic conformation a helical conformation was predicted, which was more stable than the isotactic polymer. To date, the tacticity of polyphosphinoboranes has not been investigated experimentally.

### 8.3. Polyphosphinoborane/Polyaminoborane Copolymers (PPB/PAB)

#### 8.3.1. Linear Oligomers

Linear mixed amine–borane–phosphine–borane adducts were reported for the first time by Keller and co-workers, who reacted amine hydrochlorides with the salt  $\text{Li}[\text{BH}_3\text{—PMe}_2\text{—BH}_3]$  (Scheme 8.12).<sup>356</sup> When these mixed group 15–boranes were thermolyzed at 150–240 °C, skeletal bond cleavage occurred yielding the dehydrogenated products of the corresponding amine– and phosphine–boranes, but no mixed NBPB products were found.<sup>160a</sup>

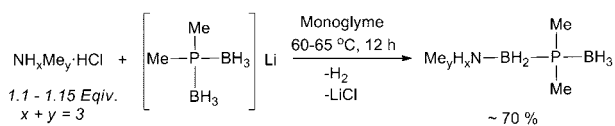
On the basis of the successful formation of polyphosphinoboranes by means of catalytic dehydrocoupling, the use of mixed amine–borane–phosphine–borane adducts as monomers for a similar reaction was attempted.<sup>160a</sup> In this case, the mixed adducts were prepared by reacting a lithiated phosphine–borane with a *B*-chlorinated amine–borane (Scheme 8.12). These adducts were characterized by NMR spectroscopy, single crystal X-ray analysis (Figure 8.8), mass spectrometry, infrared spectroscopy and elemental analysis. An association between the chains where the hydridic hydrogen on the terminal  $\text{BH}_3$  groups associate with the protic hydrogen groups on the  $\text{Me}_2\text{NH}$  terminus in hydrogen bonds was evident. Thermolysis of  $\text{Me}_2\text{NH—BH}_2\text{—PPh}_2\text{—BH}_3$  at 130 °C resulted in a complex mixture of compounds, whereas thermolysis of  $\text{Me}_2\text{NH—BH}_2\text{—PPhH—BH}_3$  gave  $[\text{Me}_2\text{N—BH}_2]_2$  and the polymer  $[\text{PhPH—BH}_2]_n$  which is similar to Keller's results, although Keller did not report or analyze polymeric products. When the dehydrocoupling reaction of  $\text{Me}_2\text{NH—BH}_2\text{—PPh}_2\text{—BH}_3$  was explored using 1.5 mol % of  $\{\text{Rh}(1,5\text{-cod})(\mu\text{-Cl})_2\}_2$  at 50 °C, chain cleavage products  $\text{Me}_2\text{NH}\cdot\text{BH}_3$  (approximately 5%),  $[\text{Me}_2\text{N—BH}_2]_2$  (approximately 45%), and  $\text{Ph}_2\text{PH}\cdot\text{BH}_3$  (approximately 50%) were observed as well as unreacted starting material by  $^{11}\text{B}$  and  $^{31}\text{P}$  NMR spectroscopy. Similar results were found for  $\text{Me}_2\text{NH—BH}_2\text{—PPhH—BH}_3$ . Thus, polymers with a NBPB backbone have still not been realized and are a worthy subject for future investigations.

#### 8.3.2. Computational Analysis of PBNB Polymers

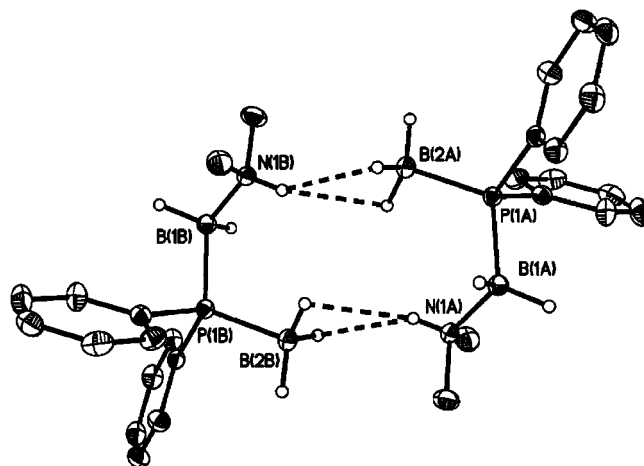
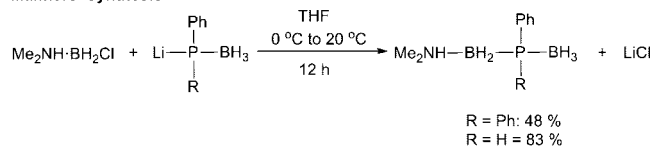
Despite the fact that at the time of writing, there are no known polyphosphinoborane-aminoborane copolymers, these

#### Scheme 8.12. Syntheses of Amine–Borane–Phosphine–Boranes

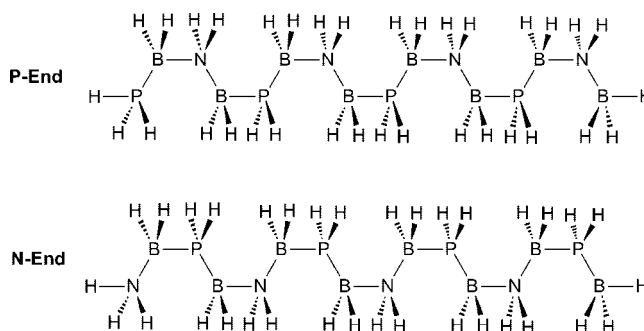
##### Keller's Synthesis



##### Manners' Synthesis



**Figure 8.8.** Crystal structure of a  $\text{Me}_2\text{NH}\cdot\text{BH}_2\text{—PPh}_2\cdot\text{BH}_3$  dimer. Reprinted with permission from ref 160a. Copyright 2004 American Chemical Society.



**Figure 8.9.** Structures of polyphosphinoborane–aminoborane copolymers.

materials and the corresponding dehydropolyphosphinoborane/polyiminoborane ( $[\text{PH}=\text{BH—NH}=\text{BH}]_n$ ) have been analyzed computationally. The relationship between the chain length and geometry parameters, partial atomic charges, electric dipole moments, polarizabilities, and first hyperpolarizabilities of both phosphorus- and nitrogen-terminated chains was emphasized.<sup>357</sup> Such properties are dependent on the conformation of the polymer chain. The most stable planar conformer for both PAB and PPB was the planar *trans-cisoid* (TC) conformation, which was used throughout the study.

Nonlinear optical properties of a conjugated polymer are to a large extent dependent on its geometry. Encouragingly, there is a bond length alteration throughout the polymer: at 16 polymer units, the BN bond length parallel to the chain averages to 1.597 (N-end) or 1.595 Å (P-end), perpendicular to the chain to 1.578 Å (both N-end and P-end), for the PB bond parallel to the chain to 1.979 (N-end) or 1.978 Å (P-end) and for the PB bond perpendicular to the chain 1.966 Å for N-end and 1.965 Å (P-end).

The evolution of the partial charges on the atoms of the central unit with chain length was also estimated. For longer oligomers  $n > 6$ , the charges are almost independent of the chain length and whether it is an N-end or P-end polymer (Figure 8.9). Typical values (for  $n = 12$ , N-end) were  $q^{\text{N}} = 0.37$ ,  $q^{\text{B}^2} = -0.21$ ,  $q^{\text{P}} = 0.44$  and  $q^{\text{B}^1} = -0.40$ . For comparison, the charge alternations for the PAB component was 0.6 |e|, for the PPB component 0.8 |e|, which is slightly less than in the corresponding homopolymers with 0.8 |e| for PAB and 0.9 |e| for PPB. Consistent with the small changes in bond length and partial charges when one compares the homopolymers to the copolymer is the fact

that the dipole moment of the unit cell of the copolymer ( $-4.37$  D) is close to the average of the values for PAB ( $-3.18$  D) and PPB ( $-5.29$  D) homopolymers ( $-4.24$  D). This dipole moment is largely unaffected by the end groups of the polymer, which is also true for the hyperpolarizability  $\alpha_L$  (51 au), which approximately equals the average value obtained from the homopolymers (PAB 33 au, PPB 71 au). However, this is no longer true for the first hyperpolarizability  $\beta_L$ , which is more strongly affected by the end groups and converges only for larger polymers ( $n > 8$ ) toward a small but positive polymeric  $\beta_L$  ( $\infty$ ) limit ( $16 \pm 9$  au). PAB/PPB copolymers are therefore expected to have negligible NLO responses because of the cancellation of the unit cell contributions of the PPB and PAB components.

## 9. Outlook

Amine–boranes and phosphine–boranes have served as readily available and versatile reagents in organic synthesis for many years and their use as reductants in the former case, and as protected phosphine synthons in the latter, is likely to expand still further. As new applications are emerging, it is likely that additional methods for the functionalization of these species will be developed. Synthetically, new methods for P–C bond formation are highly desirable, as this fundamental transformation is often difficult to achieve but indispensable, for example, in ligand synthesis for transition metal catalysis.

Surprisingly, even now, after many years of research and debate, there are still new and important additions to our understanding of the bonding in, and chemistry of, these adducts and increasingly emphasis is being placed on the structure in the solid state (as opposed to gas-phase calculations) and on dihydrogen bonding. Discoveries of unusual reactivity patterns where an amine or phosphine and a borane are too sterically encumbered to permit a stable dative bond to be formed, for example, underscore the continued importance of fundamental exploratory research in areas of the periodic table long regarded as fully developed. The coordination chemistry of amine– and phosphine–boranes with transition metals and main-group metals is only just emerging at this point in time, and this area offers exciting future opportunities.

Catalytic dehydrogenation/dehydrocoupling reactions for amine–boranes have advanced rapidly since the turn of the 21st century, and this area has been given additional impetus by the realization that ammonia–borane is a potential hydrogen storage material for the transport sector. However, the developments for phosphine–boranes are lagging behind, and it is highly desirable to find more efficient catalysts for these transformations as well. Polyaminoboranes and polyphosphinoboranes represent intriguing and novel inorganic polymers derived from cheap and readily available substrates, whose properties are only now starting to be investigated. With the correct design and the ability to control the side group variety, a range of applications are conceivable.

## 10. Abbreviations and Definitions

a	axial
AFM	atomic force microscopy
AIBN	azo-bis-(isobutyronitrile)
$\text{BAr}_4^{\text{F}}$	$[\text{B}\{3,5\text{-C}_6\text{H}_3(\text{CF}_3)_2\}_4]$
binor-S	heptacyclo[8.4.0.0 <sup>2,12</sup> .0 <sup>3,8</sup> .0 <sup>4,6</sup> .0 <sup>5,9</sup> .0 <sup>11,13</sup> ]tetradecane
Bn	benzyl

Bz	benzoyl
cod	cyclooctadiene
COIL	coiled conformation
Cp	cyclopentadienyl
Cp*	pentamethylcyclopentadienyl
Cy	cyclohexyl
D	Debye
DCM	dichloromethane
DFT	density functional theory
DHPPB	dehydrogenated polyphosphinoborane
DIPP	2,6- <i>i</i> Pr <sub>2</sub> C <sub>6</sub> H <sub>3</sub>
DLS	dynamic light scattering
DMAB	<i>N,N</i> -dimethylamine–borane
dmpe	1,2-bis(dimethylphosphino)ethane
dppe	1,2-bis(diphenylphosphino)ethane
dppf	1,1'-bis(diphenylphosphino)ferrocene
e	equatorial
EBL	electron beam lithography
<i>ee</i>	enantiomeric excess
ESP	Merz–Kollman charges
ESR	electron spin resonance
FLP	frustrated Lewis pair
FTIR	Fourier transform infrared spectroscopy
HEL	helical conformation
HRMS	high resolution mass spectrometry
KIE	kinetic isotope effect
<i>m</i> CPBA	<i>meta</i> -chloroperoxybenzoic acid
Mes	mesityl
NBO	natural bond orbital
NHC	<i>N</i> -heterocyclic carbene
NLO	nonlinear optical
PAB	polyaminoborane
pent	pentyl
PIB	polyiminoborane
pM	picomolar
POCOP	1,3-( <i>t</i> Bu <sub>2</sub> PO) <sub>2</sub> C <sub>6</sub> H <sub>4</sub>
PPB	polyphosphinoborane
Pyr	pyridine
rt	room temperature
SEM	scanning electron microscopy
SLS	static light scattering
TC	<i>trans-cisoid</i> conformation
TEM	transmission electron microscopy
TMEDA	tetramethylethylenediamine
TMS	trimethylsilyl
TS	transition state
Tf	trifluoromethylsulfonyl
TFA	trifluoroacetic acid
$T_g$	glass transition temperature
TON	turnover number
TT	<i>trans-transoid</i> conformation
WAXS	wide-angle X-ray scattering
wt	weight
XAFS	X-ray absorption fine structure spectroscopy
XRD	X-ray diffraction
$\alpha_L$	static polarizability
$\beta_L$	first hyperpolarizability
$\Delta_r$	bond length alternation
$\Delta_q$	charge alternation

## 11. Acknowledgments

With respect to contributions from our research program we thank the ACS-PRF, NSERC, and EPSRC for funding catalytic dehydrocoupling research on group 13–group 15 Lewis acid–Lewis base adducts in the IM research groups at the University of Toronto, Canada (1990–2006) and the University of Bristol, England, (2006–present). I.M. also thanks the EU for a Marie Curie Chair and the Royal Society for a Wolfson Research Merit Award.



## 12. Appendix

Table A.1. Active Catalysts for the Dehydrocoupling of  $\text{Me}_2\text{NH}\cdot\text{BH}_3$ 

Entry	Catalyst	Solvent	Temp. (°C)	Loading (mol %)	Time	Yield (%) <sup>a)</sup>	Ref.
1	None	toluene	45	-	168 h	0	<sup>88a</sup>
2	$\text{Cp}_2\text{TiCl}_2 / 2 n\text{BuLi}$	toluene	20	2.0	4 h	100 <sup>b)</sup>	<sup>91</sup>
3	$\text{Cp}_2\text{Ti}(\text{PMe}_3)_2$	toluene	20	2.0	7 h	100	<sup>210</sup>
4	$\text{Me}_2\text{Si}(\text{C}_5\text{H}_4)_2\text{TiCl}_2 / n\text{BuLi}$	toluene	20	2.0	20 h	50	<sup>197</sup>
5		$\text{C}_6\text{D}_6$	65	2.0	1000	80 <sup>c)</sup>	<sup>197</sup>
6		$\text{C}_6\text{D}_6$	65	2.0	0.5	80 <sup>c)</sup>	<sup>197</sup>
7		$\text{C}_6\text{D}_6$	23	2.0	1.4 h	80 <sup>c)</sup>	<sup>197</sup>
8		$\text{C}_6\text{D}_6$	23	2.0	6 min	80 <sup>c)</sup>	<sup>197</sup>
9		$\text{C}_6\text{D}_6$	23	2.0	0.5 h	80 <sup>c)</sup>	<sup>197</sup>
10		$\text{C}_6\text{D}_6$	65	2.0	250 h	80 <sup>c)</sup>	<sup>197</sup>
11		$\text{C}_6\text{D}_6$	65	2.0	1250 h	80 <sup>c)</sup>	<sup>197</sup>
12		$\text{C}_6\text{D}_6$	65	2.0	147 h	80 <sup>c)</sup>	<sup>197</sup>
13		$\text{C}_6\text{D}_6$	65	2.0	625 h	80 <sup>c)</sup>	<sup>197</sup>

Table A.1. Continued

Entry	Catalyst	Solvent	Temp. (°C)	Loading (mol %)	Time	Yield (%) <sup>a)</sup>	Ref.
14		C <sub>6</sub> D <sub>6</sub>	65	2.0	294 h	80 <sup>c)</sup>	197
15		C <sub>6</sub> D <sub>6</sub>	65	2.0	2500	80 <sup>c)</sup>	197
16	[Cr(CO) <sub>6</sub> ]	THF	8	5.0	1 h <sup>d)</sup>	90	358
17	[Cr(CO) <sub>6</sub> ]	THF	8	5.0	5 min <sup>d)</sup> then 1 h 20 °C	95	358
18	[Cr(CO) <sub>5</sub> (THF)]	THF	20	5.0	1.5 h	94	358
19	[Cr(CO) <sub>5</sub> (η <sup>1</sup> -BH <sub>3</sub> -NMe <sub>3</sub> )]	THF	20	5.0	1 h	93	358
20	[Mo(CO) <sub>6</sub> ]	THF	8	5.0	1 h <sup>d)</sup>	94	358
21	[W(CO) <sub>6</sub> ]	THF	8	5.0	1 h <sup>d)</sup>	95	358
22	[ReBr <sub>2</sub> (NO)(P <i>i</i> Pr <sub>3</sub> ) <sub>2</sub> -(η <sup>2</sup> -H <sub>2</sub> )]	dioxane	85	1.0	4 h	92 <sup>b)</sup>	92
23	[ReBr <sub>2</sub> (NO)(PCy <sub>3</sub> ) <sub>2</sub> -(η <sup>2</sup> -H <sub>2</sub> )]	dioxane	85	1.0	4 h	96 <sup>b)</sup>	92
24	[ReBr <sub>2</sub> (NO)(P <i>i</i> Pr <sub>3</sub> ) <sub>2</sub> -(MeCN)]	dioxane	85	1.0	4 h	99 <sup>b)</sup>	92
25	[ReBr <sub>2</sub> (NO)(PCy <sub>3</sub> ) <sub>2</sub> -(MeCN)]	dioxane	85	1.0	4 h	91 <sup>b)</sup>	92
26	[ReBr <sub>2</sub> (NO)(P <i>i</i> Pr <sub>3</sub> ) <sub>2</sub> -(η <sup>2</sup> -CH <sub>2</sub> =CH <sub>2</sub> )]	dioxane	85	1.0	4 h	88 <sup>b)</sup>	92
27	[ReBr <sub>2</sub> (NO)(PCy <sub>3</sub> ) <sub>2</sub> -(η <sup>2</sup> -CH <sub>2</sub> =CH <sub>2</sub> )]	dioxane	85	1.0	4 h	91 <sup>b)</sup>	92
28		benzene	75	1.0	1.3 h	100 <sup>b)</sup>	93
29		benzene	75	1.0	1.5 h	83 <sup>b)</sup>	93
30		benzene	75	1.0	1.0 h	100 <sup>b)</sup>	93
31		benzene	75	1.0	1.0 h	92 <sup>b)</sup>	93
32		benzene	75	1.0	3.0 h	99 <sup>b)</sup>	93
33		benzene	75	1.0	2.0 h	88 <sup>b)</sup>	93
34	<i>trans</i> -RuMe <sub>2</sub> (PMe <sub>3</sub> ) <sub>4</sub>	toluene	25	0.5	16 h	100	88a
35	[Ru(H)(PMe <sub>3</sub> )(PNP)]; PNP = N(CH <sub>2</sub> CH <sub>2</sub> P <i>i</i> Pr <sub>2</sub> ) <sub>2</sub>	THF	20	2.0	1.2 min	70	206
36	[Ru(H) <sub>2</sub> (PMe <sub>3</sub> )(PNP) <sup>H</sup> ]; PNP <sup>H</sup> = HN(CH <sub>2</sub> CH <sub>2</sub> P <i>i</i> Pr <sub>2</sub> ) <sub>2</sub>	THF	20	0.2	2 min	50	206
37	{Rh(1,5-cod)(μ-Cl)} <sub>2</sub>	toluene	25	0.5	8 h	100	88a
38	{Rh(1,5-cod)(μ-Cl)} <sub>2</sub>	toluene	45	0.5	2 h	90	88a
39	{Rh(1,5-cod)(μ-Cl)} <sub>2</sub>	toluene	25	5.0	<2 h	100	88a
40	{Rh(1,5-cod)(μ-Cl)} <sub>2</sub>	toluene	45	5.0	<2 h	100	88a
41	RhCl <sub>3</sub>	toluene	25	0.5	22.5 h	90	88a
42	RhCl <sub>3</sub> ·2H <sub>2</sub> O	toluene	25	0.5	64 h	90	88a
43	RhCl(PPh <sub>3</sub> ) <sub>3</sub>	toluene	25	0.5	44 h	95	88a
44	{Cp*Rh(μ-Cl)Cl} <sub>2</sub>	toluene	25	0.5	112 h	100	88a
45	{Rh(1,5-cod) <sub>2</sub> OTf}	toluene	25	0.5	7.5 h	95	88a

Table A.1. Continued

Entry	Catalyst	Solvent	Temp. (°C)	Loading (mol %)	Time	Yield (%) <sup>a)</sup>	Ref.
46	{Rh(1,5-cod)(dmpe)}PF <sub>6</sub>	toluene	25	0.5	112 h	95	88a
47	HRh(CO)(PPh <sub>3</sub> ) <sub>3</sub>	toluene	25	0.5	160 h	5	88a
48	Rh/Al <sub>2</sub> O <sub>3</sub> (5%)	toluene	25	2.0	5 h	ca. 100	179
49	RhCl(PHCy <sub>2</sub> ) <sub>3</sub>	toluene	20	1.0	20 h	100 <sup>b)</sup>	200
50	RhCl(PHCy <sub>2</sub> ) <sub>3</sub>	toluene	20	1	20 h	100	200
51	[Rh(PtBu <sub>3</sub> ) <sub>2</sub> ][BAR <sup>F</sup> ]	1,2-F <sub>2</sub> C <sub>6</sub> H <sub>4</sub>	25	5	10 h	100	212
52	C <sub>3</sub> H <sub>11</sub> CO <sub>2</sub> <sup>+</sup> Me <sub>2</sub> NH <sub>2</sub> <sup>+</sup> stabilized Rh(0) nanocluster	toluene	25	0.25 (Rh)	3.0 h	100	220
53	IrCl <sub>3</sub>	toluene	25	0.5	160 h	25	88a
54	{Ir(1,5-cod)(μ-Cl)} <sub>2</sub>	toluene	25	0.5	136 h	95	88a
55	Trans-PdCl <sub>2</sub> (P( <i>o</i> -tolyl) <sub>3</sub> ) <sub>2</sub>	toluene	25	0.5	160 h	20	88a
56	Pd/C (10%)	toluene	25	0.5	68 h	95	88a
57	CuCl(I-dipp)	C <sub>6</sub> D <sub>6</sub>	20	20	24 h	ca. 90	205

<sup>a</sup> Calculated via integration of <sup>11</sup>B NMR spectra. <sup>b</sup> The authors indicate that cyclotriborazane was a product. This may be based on a paper by Manners and co-workers, who observed an intermediate by <sup>11</sup>B NMR in the titanocene catalyzed dehydrocoupling of secondary amine–boranes.<sup>90</sup> They tentatively speculated that this could be the cyclotriborazane, but it later emerged that in fact, the <sup>11</sup>B NMR peak was the BH<sub>2</sub>-signal of the linear dimer Me<sub>2</sub>N–BH<sub>2</sub>–NMe<sub>2</sub>–BH<sub>3</sub>, with the other boron signal for BH<sub>3</sub> overlapping with the starting material.<sup>206,210,212</sup> In this case, some adjustment of the yields reported is necessary. <sup>c</sup> The reactions were monitored to 80% conversion and TOFs (turn over frequencies) provided, from which the time for this table was calculated. <sup>d</sup> Irradiation with a 450 W Hg lamp.

### 13. References

- (1) (a) Belen'kii, L. I. *Compr. Org. Funct. Group Transform. II* **2005**, 2, 343. (b) Matos, K.; Pichlmair, S.; Burkhardt, E. R. *Chim. Oggi* **2007**, 25, 17. (c) Jabbour, A.; Smoum, R.; Takroui, K.; Shalom, E.; Zaks, B.; Steinberg, D.; Rubinstein, A.; Goldberg, I.; Katzhendler, J.; Srebnik, M. *Pure Appl. Chem.* **2006**, 78, 1425. (d) Takroui, K.; Dembitsky, V. M.; Srebnik, M. *Stud. Inorg. Chem.* **2005**, 22, 495. (e) Burnham, B. S. *Curr. Med. Chem.* **2005**, 12, 1995. (f) Carboni, B.; Carreaux, F. *Sci. Synth.* **2004**, 6, 455. (g) Kanth, J. V. B. *Aldrichimica Acta* **2002**, 35, 57. (h) Baxter, E. W.; Reitz, A. B. *Org. React.* **2002**, 59, 1. (i) Carboni, B.; Monnier, L. *Tetrahedron* **1999**, 55, 1197. (j) Pawelke, G.; Bürger, H. *Appl. Organomet. Chem.* **1996**, 10, 147. (k) Hutchins, R. O.; Learn, K.; Nazer, B.; Pytlewski, D.; Pelter, A. *Org. Prep. Proced. Int.* **1984**, 16, 335. (l) Büchner, W.; Niederprüm, H. *Pure Appl. Chem.* **1977**, 49, 733. (m) Lane, C. F. *Aldrichim. Acta* **1973**, 6, 51.
- (2) (a) Pietrusiewicz, K. M.; Stankevič, M. *Curr. Org. Chem.* **2005**, 9, 1883. (b) Gaumont, A.-C.; Carboni, B. *Sci. Synth.* **2004**, 6, 485. (c) Brunel, J. M.; Faure, B.; Maffei, M. *Coord. Chem. Rev.* **1998**, 178–180, 665. (d) Ohff, M.; Holz, J.; Quirnbach, M.; Börner, A. M. *Synthesis* **1998**, 1391. (e) Keglevich, G.; Toke, L. *Trends Org. Chem.* **1995**, 5, 151. (f) Keglevich, G.; Töke, L.; Újszászy, K.; Szöllosy, A. *Phosphorus, Sulfur Silicon Relat. Elem.* **1996**, 109–110, 457. (g) Andrushko, N.; Börner, A. *Phosphorus Ligands in Asymmetric Catal.* **2008**, 3, 1275. (h) Barton, L.; Volkov, O.; Hata, M.; McQuade, P.; Rath, N. P. *Pure Appl. Chem.* **2003**, 75, 1165. (i) Kodama, G. *Mol. Struct. Energy* **1988**, 5, 105. (j) Schmidbaur, H. *J. Organomet. Chem.* **1980**, 200, 287.
- (3) Roesky, H. W.; Atwood, D. A. *Group 13 Chemistry I: Fundamental New Developments*; Springer: New York, 2002.
- (4) (a) The terms dehydrogenation and dehydrocoupling are interchanged freely. However, dehydrogenations of group 13–15 Lewis acid–base adducts can generate monomeric products (e.g., R<sub>2</sub>N=BR'<sub>2</sub>), in which case the term dehydrocoupling is not strictly accurate. (b) Clark, T. J.; Lee, K.; Manners, I. *Chem.–Eur. J.* **2006**, 12, 8634.
- (5) (a) Peng, B.; Chen, J. *Energy Environ. Sci.* **2008**, 1, 479. (b) Smythe, N. C.; Gordon, J. C. *Eur. J. Inorg. Chem.* **2010**, 4, 509. (c) Marder, T. B. *Angew. Chem., Int. Ed.* **2007**, 46, 8116. (d) Hamilton, C. W.; Baker, R. T.; Staubitz, A.; Manners, I. *Chem. Soc. Rev.* **2009**, 38, 279. (e) Stephens, F. H.; Pons, V.; Baker, R. T. *Dalton Trans.* **2007**, 2613.
- (6) Staubitz, A.; Robertson, A. P. M.; Manners, I. *Chem. Rev.* **2010**, 110, DOI: 10.1021/cr100088b.
- (7) Gay-Lussac, J. L. *Mem. Phys. Chim. Soc. D'Arcueil* **1809**, 2, 211.
- (8) Davy, J. *Phil. Trans* **1812**, 30, 365.
- (9) Muetterties, E. L. *Boron Hydride Chemistry*; Academic Press: New York, 1975.
- (10) Burg, A. B.; Schlesinger, H. I. *J. Am. Chem. Soc.* **1937**, 59, 780.
- (11) (a) Welch, G. C.; San Juan, R. R.; Masuda, J. D.; Stephan, D. W. *Science* **2006**, 314, 1124. (b) Stephan, D. W.; Erker, G. *Angew. Chem., Int. Ed.* **2010**, 49, 46. (c) Power, P. P. *Nature* **2010**, 463, 171.
- (12) (a) Stock, A. *The Hydrides of Boron and Silicon*; Cornell University Press: New York, 1933; (b) Lane, C. F. *Chem. Rev.* **1976**, 76, 773. (c) Lane, C. F. *Synth. Reagents* **1977**, 3, 1.
- (13) Burkhardt, E. R.; Coleridge, B. M. *Tetrahedron Lett.* **2008**, 49, 5152.
- (14) Kuhn, N.; Schulten, M.; Zauder, E.; Augart, N.; Boese, R. *Chem. Ber.* **1989**, 122, 1891.
- (15) (a) Paz-Sandoval, M. A.; Camacho, C.; Contreras, R.; Wrackmeyer, B. *Spectrochim. Acta, Part A* **1987**, 43A, 1331. (b) Burg, A. B.; Randolph, C. L., Jr. *J. Am. Chem. Soc.* **1949**, 71, 3451.
- (16) (a) Swain, C. J.; Kneen, C.; Baker, R. *Tetrahedron Lett.* **1990**, 31, 2445. (b) Narayana, C.; Periasamy, M. *J. Chem. Soc., Chem. Commun.* **1987**, 1857.
- (17) (a) Mayer, E. *Inorg. Chem.* **1972**, 11, 866. (b) Parry, R. W.; Edwards, L. J. *J. Am. Chem. Soc.* **1959**, 81, 3554.
- (18) Potyén, M.; Josyula, K. V. B.; Schuck, M.; Lu, S.; Gao, P.; Hewitt, C. *Org. Process Res. Dev.* **2007**, 11, 210.
- (19) Negishi, E.; Brown, H. C. *Synthesis* **1974**, 77.
- (20) Brown, H. C.; Negishi, E.; Katz, J.-J. *J. Am. Chem. Soc.* **1975**, 97, 2791.
- (21) (a) Egan, B. Z.; Shore, S. G.; Bonnell, J. E. *Inorg. Chem.* **1964**, 3, 1024. (b) Mikhailov, B. M.; Shchegoleva, T. A.; Sheludiyakov, V. D. *Izv. Akad. Nauk SSSR, Ser. Khim.* **1963**, 816. (c) Mikhailov, B. M.; Sheludiyakov, V. D.; Shchegoleva, T. A. *Izv. Akad. Nauk SSSR, Ser. Khim.* **1962**, 1559. (d) Burg, A. B.; Wagner, R. I. *J. Am. Chem. Soc.* **1954**, 76, 3307. (e) Thaisrivongs, S.; Wuest, J. D. *J. Org. Chem.* **1977**, 42, 3243. (f) Young, D. E.; McAchran, G. E.; Shore, S. G. *J. Am. Chem. Soc.* **1966**, 88, 4390.
- (22) (a) Steinberg, H. *Boron–Oxygen and Boron–Sulfur Compounds*; Interscience Publishers: New York, 1964. (b) Mikhailov, B. M. *Isvest. Akad. Nauk USSR Otdel. Khim. Nauk.* **1959**, 10, 1868.
- (23) Hawthorne, M. F. *J. Am. Chem. Soc.* **1961**, 83, 1345.
- (24) (a) Davis, B. L.; Dixon, D. A.; Garner, E. B.; Gordon, J. C.; Matus, M. H.; Scott, B.; Stephens, F. H. *Angew. Chem., Int. Ed.* **2009**, 48, 6812. (b) Sutton, A. D.; Davis, B. L.; Bhattacharyya, K. X.; Ellis, B. D.; Gordon, J. C.; Power, P. P. *Chem. Commun.* **2010**, 46, 148.
- (25) (a) Beachley, O. T., Jr.; Washburn, B. *Inorg. Chem.* **1975**, 14, 120. (b) Schaeffer, G. W.; Anderson, E. R. *J. Am. Chem. Soc.* **1949**, 71, 2143. (c) Heldebrand, D. J.; Karkamkar, A.; Linehan, J. C.; Autrey, T. *Energy Environ. Sci.* **2008**, 1, 156.
- (26) Uppal, S. S.; Kelly, H. C. *J. Chem. Soc., Chem. Commun.* **1970**, 23, 1619.
- (27) (a) Singaram, B.; Cole, T. E.; Brown, H. C. *Organometallics* **1984**, 3, 774. (b) Brown, H. C.; Cole, T. E.; Srebnik, M.; Kim, K.-W. *J. Org. Chem.* **1986**, 51, 4925. (c) Brown, H. C.; Cole, T. E. *Organometallics* **1983**, 2, 1316.
- (28) Vidal, J. L.; Ryschkeiwitsch, G. E. *Inorg. Chem.* **1977**, 16, 1673.
- (29) (a) Brown, H. C.; Schlesinger, H. I.; Cardon, S. Z. *J. Am. Chem. Soc.* **1942**, 64, 325. (b) Baldwin, R. A.; Washburn, R. M. *J. Org. Chem.* **1961**, 26, 3549.
- (30) Izutsu, K.; Nakamura, T.; Takizawa, K.; Takeda, A. *Bull. Chem. Soc. Jpn.* **1985**, 58, 455.
- (31) Besson, A. *Comptes Rendus* **1890**, 110, 516.
- (32) Gamble, E. L.; Gilmont, P. J. *J. Am. Chem. Soc.* **1940**, 62, 717.
- (33) Stock, A. *Ber.* **1923**, 56B, 789.
- (34) Rudolph, R. W.; Parry, R. W.; Farran, C. F. *Inorg. Chem.* **1966**, 5, 723.
- (35) Burg, A. B.; Wagner, R. I. *J. Am. Chem. Soc.* **1953**, 75, 3872.

- (36) (a) Khater, B.; Guillemin, J.-C.; Benidar, A.; Begue, D.; Pouchan, C. *J. Chem. Phys.* **2008**, *129*, 224308/1. (b) Németh, B.; Khater, B.; Veszprémi, T.; Guillemin, J.-C. *Dalton Trans.* **2009**, 3526.
- (37) Laneman, S. C. *Spec. Chem. Mag.* **2008**, 28.
- (38) (a) Hurtado, M.; Yáñez, M.; Herrero, R.; Guerrero, A.; Dávalos, J. Z.; Abboud, J.-L. M.; Khater, B.; Guillemin, J.-C. *Chem.—Eur. J.* **2009**, *15*, 4622. (b) Chan, V. S.; Chiu, M.; Bergman, R. G.; Toste, F. D. *J. Am. Chem. Soc.* **2009**, *131*, 6021. (c) Carreira, M.; Charemsnuk, M.; Eberhard, M.; Fey, N.; van Ginkel, R.; Hamilton, A.; Mul, W. P.; Orpen, A. G.; Phetmung, H.; Pringle, P. G. *J. Am. Chem. Soc.* **2009**, *131*, 3078. (d) Seitz, T.; Muth, A.; Huttner, G. *Chem. Ber.* **1994**, *127*, 1837.
- (39) (a) Imamoto, T.; Hirakawa, E.; Yamanoi, Y.; Inoue, T.; Yamaguchi, K.; Seki, H. *J. Org. Chem.* **1995**, *60*, 7697. (b) Hirakawa, E.; Takeda, N.; Imamoto, T. *Heterocycles* **2000**, *52*, 667.
- (40) Oshiki, T.; Imamoto, T. *Bull. Chem. Soc. Jpn.* **1990**, *63*, 2846.
- (41) McNulty, J.; Zhou, Y. *Tetrahedron Lett.* **2004**, *45*, 407.
- (42) Imamoto, T.; Kusumoto, T.; Suzuki, N.; Sato, K. *J. Am. Chem. Soc.* **1985**, *107*, 5301.
- (43) Burg, A. B.; Slota, P. J. *J. Am. Chem. Soc.* **1960**, *82*, 2145.
- (44) (a) Parry, R. W.; Bissot, T. C. *J. Am. Chem. Soc.* **1956**, *78*, 1524. (b) Graham, W. A. G.; Stone, F. G. A. *J. Inorg. Nucl. Chem.* **1956**, *3*, 164.
- (45) Suenram, R. D.; Thorne, L. R. *Chem. Phys. Lett.* **1981**, *78*, 157.
- (46) Haaland, A. *Angew. Chem., Int. Ed.* **1989**, *28*, 992.
- (47) (a) Bessac, F.; Frenking, G. *Inorg. Chem.* **2006**, *45*, 6956. (b) Plumley, J. A.; Evanseck, J. D. *J. Phys. Chem. A* **2009**, *113*, 5985.
- (48) (a) Pearson, R. G. *J. Chem. Educ.* **1968**, *45*, 643. (b) Pearson, R. G. *J. Chem. Educ.* **1968**, *45*, 581. (c) Pearson, R. G. *J. Am. Chem. Soc.* **1963**, *85*, 3533. (d) Mayer, U.; Gutmann, V.; Gerger, W. *Monatsh. Chem.* **1975**, *106*, 1235. (e) Gutmann, V. *Coord. Chem. Rev.* **1975**, *15*, 207. (f) Gutmann, V.; Steininger, A.; Wychera, E. *Monatsh. Chem.* **1966**, *97*, 460. (g) Drago, R. S. *Struct. Bonding (Berlin)* **1973**, *15*, 73. (h) Drago, R. S.; Wayland, B. B. *J. Am. Chem. Soc.* **1965**, *87*, 3571.
- (49) (a) Rowsell, B. D.; Gillespie, R. J.; Heard, G. L. *Inorg. Chem.* **1999**, *38*, 4659. (b) Khaliliulin, R. Z.; Cobar, E. A.; Lochan, R. C.; Bell, A. T.; Head-Gordon, M. *J. Phys. Chem. A* **2007**, *111*, 8753.
- (50) Coyle, T. D.; Kaesz, H. D.; Stone, F. G. A. *J. Am. Chem. Soc.* **1959**, *81*, 2989.
- (51) (a) Rothe, E. W.; Mathur, B. P.; Reck, G. P. *Inorg. Chem.* **1980**, *19*, 829. (b) Mente, D. C.; Mills, J. L.; Mitchell, R. E. *Inorg. Chem.* **1975**, *14*, 123. (c) Miller, J. M.; Onyszczuk, M. *Can. J. Chem.* **1964**, *42*, 1518. (d) Brinck, T.; Murray, J. S.; Politzer, P. *Inorg. Chem.* **1993**, *32*, 2622.
- (52) (a) Hirao, H.; Omoto, K.; Fujimoto, H. *J. Phys. Chem. A* **1999**, *103*, 5807. (b) Branchadell, V.; Oliva, A. *THEOCHEM* **1991**, *82*, 75. (c) Cotton, F. A.; Leto, J. R. *J. Chem. Phys.* **1959**, *30*, 993. (d) Liebman, J. F. *Struct. Chem.* **1990**, *1*, 395. (e) Lanthier, G. F.; Miller, J. M. *J. Chem. Soc. A* **1971**, 346. (f) Brown, H. C.; Holmes, R. R. *J. Am. Chem. Soc.* **1956**, *78*, 2173. (g) Shriver, D. F.; Swanson, B. *Inorg. Chem.* **1971**, *10*, 1354.
- (53) Tri-coordinate borane moieties are formally electron deficient, with only 6 valence electrons. To complete the valence shell, two further electrons are required. In the context of estimating Lewis acidity, it is possible to use quantification of the ability to accept an electron pair as a measure of Lewis acidity in such systems.
- (54) Bessac, F.; Frenking, G. *Inorg. Chem.* **2003**, *42*, 7990.
- (55) Kuczowski, R. L.; Lide, D. R. *J. Chem. Phys.* **1967**, *46*, 357.
- (56) Umeyama, H.; Kudo, T.; Nakagawa, S. *Chem. Pharm. Bull.* **1981**, *29*, 287.
- (57) Staubitz, A.; Besora, M.; Harvey, J. N.; Manners, I. *Inorg. Chem.* **2008**, *47*, 5910.
- (58) McCoy, R. E.; Bauer, S. H. *J. Am. Chem. Soc.* **1956**, *78*, 2061.
- (59) Burg, A. B.; Fu, Y.-C. *J. Am. Chem. Soc.* **1966**, *88*, 1147.
- (60) Fenwick, J. T. F.; Wilson, J. W. *J. Chem. Soc., Dalton Trans.* **1972**, 1324.
- (61) (a) Jeffers, P. M.; Bauer, S. H. *Inorg. Chem.* **1982**, *21*, 2516. (b) Carpenter, J. D.; Ault, B. S. *J. Phys. Chem. A* **1992**, *96*, 4288.
- (62) Flores-Segura, H.; Torres, L. *Struct. Chem.* **1997**, *8*, 227.
- (63) (a) Gilbert, T. M. *J. Phys. Chem. A* **2004**, *108*, 2550. (b) Gille, A. L.; Gilbert, T. M. *J. Chem. Theory Comput.* **2008**, *4*, 1681.
- (64) Earnshaw, A.; Greenwood, N. *Chemistry of The Elements*, 2nd ed.; Butterworth-Heinemann, 1997.
- (65) Liu, Z.; Marder, T. B. *Angew. Chem., Int. Ed.* **2008**, *47*, 242.
- (66) Grant, D. J.; Dixon, D. A. *J. Phys. Chem. A* **2006**, *110*, 12955.
- (67) Lide, D. R. *CRC Handbook of Chemistry and Physics*, 69th ed.; CRC Press: Boca Raton, FL, 2008.
- (68) Hu, M. G.; van Paasschen, J. M.; Geanangel, R. A. *J. Inorg. Nucl. Chem.* **1977**, *39*, 2147.
- (69) (a) Stephan, D. W. *Org. Biomol. Chem.* **2008**, *6*, 1535. (b) Stephan, D. W. *Dalton Trans.* **2009**, 3129. (c) Kenward, A. L.; Piers, W. E. *Angew. Chem., Int. Ed.* **2008**, *47*, 38.
- (70) Geier, S. J.; Stephan, D. W. *J. Am. Chem. Soc.* **2009**, *131*, 3476.
- (71) Rokob, T. A.; Hamza, A.; Stirling, A.; Pápai, I. *J. Am. Chem. Soc.* **2009**, *131*, 2029.
- (72) Grimme, S.; Kruse, H.; Goerigk, L.; Erker, G. *Angew. Chem., Int. Ed.* **2010**, *49*, 1402.
- (73) Hetzer, R. H.; Gais, H.-J.; Raabe, G. *Synthesis* **2008**, 1126.
- (74) Schlieve, C. R.; Tam, A.; Nilsson, B. L.; Lieven, C. J.; Raines, R. T.; Levin, L. A. *Exp. Eye Res.* **2006**, *83*, 1252.
- (75) (a) Bartoli, G.; Bartolacci, M.; Giuliani, A.; Marcantoni, E.; Masciaci, M. *Eur. J. Org. Chem.* **2005**, 2867. (b) Pasumansky, L.; Goralski, C. T.; Singaram, B. *Org. Process Res. Dev.* **2006**, *10*, 959.
- (76) (a) Das, M. K.; Bandyopadhyay, S. N.; Bhattacharyya, S.; Banerjee, R. *J. Chem. Soc., Dalton Trans.* **1991**, *11*, 2929. (b) Wechsler, D.; Cui, Y.; Dean, D.; Davis, B.; Jessop, P. G. *J. Am. Chem. Soc.* **2008**, *130*, 17195. (c) Clark, T. J.; Whittell, G. R.; Manners, I. *Inorg. Chem.* **2007**, *46*, 7522.
- (77) Lane, C. F. *Aldrichimica Acta* **1973**, *6*, 51.
- (78) Kelly, H. C.; Giusto, M. B.; Marchelli, F. R. *J. Am. Chem. Soc.* **1964**, *86*, 3882.
- (79) (a) Couturier, M.; Andresen, B. M.; Tucker, J. L.; Dubé, P.; Brenek, S. J.; Negri, J. T. *Tetrahedron Lett.* **2001**, *42*, 2763. (b) Couturier, M.; Tucker, J. L.; Andresen, B. M.; Dubé, P.; Brenek, S. J.; Negri, J. T. *Tetrahedron Lett.* **2001**, *42*, 2285. (c) Couturier, M.; Tucker, J. L.; Andresen, B. M.; Dubé, P.; Negri, J. T. *Org. Lett.* **2001**, *3*, 465.
- (80) Cordero, F. M.; Bonanno, P.; Neudeck, S.; Vurchio, C.; Brandi, A. *Adv. Synth. Catal.* **2009**, *351*, 1155.
- (81) David, H.; Dupuis, L.; Guillerez, M.-G.; Guibé, F. *Tetrahedron Lett.* **2000**, *41*, 3335.
- (82) Lelental, M.; Axup, A. W. *J. Photogr. Sci.* **1984**, *32*, 1.
- (83) Satpati, D.; Korde, A.; Kothari, K.; Sarma, H. D.; Venkatesh, M.; Banerjee, S. *Cancer Biother. Radiopharm.* **2008**, *23*, 741.
- (84) Schibli, R.; Schwarzbach, R.; Alberto, R.; Ortner, K.; Schmallo, H.; Dumas, C.; Egli, A.; Schubiger, P. A. *Bioconjugate Chem.* **2002**, *13*, 750.
- (85) (a) Daniel, M. C.; Astruc, D. *Chem. Rev.* **2004**, *104*, 293. (b) Astruc, D.; Lu, F.; Aranzaes, J. R. *Angew. Chem., Int. Ed.* **2005**, *44*, 7852.
- (86) (a) Templeton, A. C.; Wuelfing, M. P.; Murray, R. W. *Acc. Chem. Res.* **2000**, *33*, 27. (b) Wuelfing, W. P.; Gross, S. M.; Miles, D. T.; Murray, R. W. *J. Am. Chem. Soc.* **1998**, *120*, 12696. (c) Brust, M.; Walker, M.; Bethell, D.; Schiffrin, D. J.; Whyman, R. *J. Chem. Soc., Chem. Commun.* **1994**, 801.
- (87) Zheng, N.; Fan, J.; Stucky, G. D. *J. Am. Chem. Soc.* **2006**, *128*, 6550.
- (88) (a) Jaska, C. A.; Temple, K.; Lough, A. J.; Manners, I. *J. Am. Chem. Soc.* **2003**, *125*, 9424. (b) Jaska, C. A.; Temple, K.; Lough, A. J.; Manners, I. *Chem. Commun.* **2001**, 962.
- (89) Jaska, C. A.; Manners, I. *J. Am. Chem. Soc.* **2004**, *126*, 2698.
- (90) Clark, T. J.; Russell, C. A.; Manners, I. *J. Am. Chem. Soc.* **2006**, *128*, 9582.
- (91) Blaquiere, N.; Diallo-Garcia, S.; Gorelsky, S. I.; Black, D. A.; Fagnou, K. *J. Am. Chem. Soc.* **2008**, *130*, 14034.
- (92) Jiang, Y.; Berke, H. *Chem. Commun.* **2007**, 3571.
- (93) Jiang, Y.; Blacque, O.; Fox, T.; Frech, C. M.; Berke, H. *Organometallics* **2009**, *28*, 5493.
- (94) Yang, X.; Zhao, L.; Fox, T.; Wang, Z.-X.; Berke, H. *Angew. Chem., Int. Ed.* **2010**, *49*, 2058.
- (95) (a) Hu, M. G.; Geanangel, R. A.; Wendlandt, W. W. *Thermochim. Acta* **1978**, *23*, 249. (b) Shaw, W. J.; Linehan, J. C.; Szymczak, N. K.; Heldebrand, D. J.; Yonker, C.; Camaioni, D. M.; Baker, R. T.; Autrey, T. *Angew. Chem., Int. Ed.* **2008**, *47*, 7493. (c) Pons, V.; Baker, R. T.; Szymczak, N. K.; Heldebrand, D. J.; Linehan, J. C.; Matus, M. H.; Grant, D. J.; Dixon, D. A. *Chem. Commun.* **2008**, 6597.
- (96) Sato, S.; Sakamoto, T.; Miyazawa, E.; Kikugawa, Y. *Tetrahedron* **2004**, *60*, 7899.
- (97) Borch, R. F.; Bernstein, M. D.; Durst, H. D. *J. Am. Chem. Soc.* **1971**, *93*, 2897.
- (98) Leontjeva, A. E.; Vasiljeva, L. L.; Pivnitsky, K. K. *Russ. Chem. Bull.* **2004**, *53*, 703.
- (99) Alexandre, F. R.; Pantaleone, D. P.; Taylor, P. P.; Fotheringham, I. G.; Ager, D. J.; Turner, N. J. *Tetrahedron Lett.* **2002**, *43*, 707.
- (100) Alexeeva, M.; Enright, A.; Dawson, M. J.; Mahmoudian, M.; Turner, N. J. *Angew. Chem., Int. Ed.* **2002**, *41*, 3177.
- (101) (a) Kikugawa, Y.; Kawase, M. *Synth. Commun.* **1979**, *9*, 49. (b) Burk, M. J.; Martinez, J. P.; Feaster, J. E.; Cosford, N. *Tetrahedron* **1994**, *50*, 4399. (c) Casarini, M. E.; Ghelfi, F.; Libertini, E.; Pagnoni, U. M.; Parsons, A. F. *Tetrahedron* **2002**, *58*, 7925.
- (102) (a) Kelly, H. C.; Edwards, J. O. *J. Am. Chem. Soc.* **1960**, *82*, 4842. (b) Lau, C. K.; Tardif, S.; Dufresne, C.; Scheigetz, J. *J. Org. Chem.* **1989**, *54*, 491. (c) Huber, V.; Sengupta, S.; Würthner, F. *Chem.—Eur. J.* **2008**, *14*, 7791. (d) Wiegand, M.; Lindhorst, T. K. *Eur. J. Org. Chem.* **2006**, 2006, 4841. (e) Goddard-Borger, E. D.; Ghisalberti, E. L.; Stick, R. V. *Eur. J. Org. Chem.* **2007**, 2007, 3925.

- (103) (a) Messinger, P.; Von Vietinghoff-Scheel, R. *Arch. Pharm.* **1985**, *318*, 445. (b) Dolle, R. E.; Schmidt, S. J.; Erhard, K. F.; Kruse, L. I. *J. Am. Chem. Soc.* **1989**, *111*, 278.
- (104) (a) Eleveld, M. B.; Hogeveen, H. *Tetrahedron Lett.* **1986**, *27*, 635. (b) Iida, T.; Shinohara, T.; Momose, T.; Tamura, T.; Matsumoto, T.; Nambara, T.; Chang, F. C. *Synthesis* **1986**, 998. (c) Toda, F.; Mori, K. *J. Chem. Soc., Chem. Commun.* **1989**, 1245.
- (105) Hashimoto, S.; Sakata, S.; Sonogawa, M.; Ikegami, S. *J. Am. Chem. Soc.* **1988**, *110*, 3670.
- (106) (a) Billman, J. H.; McDowell, J. W. *J. Org. Chem.* **1961**, *26*, 1437. (b) Hynes, J. B.; Kumar, A.; Tomazic, A.; Washtien, W. L. *J. Med. Chem.* **1987**, *30*, 1515. (c) Seo, J. H.; Adachi, K.; Lee, B. K.; Kang, D. G.; Kim, Y. K.; Kim, K. R.; Lee, H. Y.; Kawai, T.; Cha, H. J. *Bioconj. Chem.* **2007**, *18*, 2197. (d) Löser, R.; Frizler, M.; Schilling, K.; Gütschow, M. *Angew. Chem., Int. Ed.* **2008**, *47*, 4331. (e) Yang, Y.; Coward, J. K. *J. Org. Chem.* **2007**, *72*, 5748.
- (107) Andersson, H.; Wang, X.; Björklund, M.; Olsson, R.; Almqvist, F. *Tetrahedron Lett.* **2007**, *48*, 6941.
- (108) Ménard, G.; Stephan, D. W. *J. Am. Chem. Soc.* **2010**, *132*, 1796.
- (109) Pasumansky, L.; Singaram, B. *Aldrichimica Acta* **2005**, *38*, 61.
- (110) (a) Fisher, G. B.; Fuller, J. C.; Harrison, J.; Alvarez, S. G.; Burkhardt, E. R.; Goralski, C. T.; Singaram, B. *J. Org. Chem.* **1994**, *59*, 6378. (b) Dubois, L.; Fiaud, J.-C.; Kagan, H. B. *Tetrahedron* **1995**, *51*, 3803.
- (111) Fisher, G. B.; Fuller, J. C.; Harrison, J.; Goralski, C. T.; Singaram, B. *Tetrahedron Lett.* **1993**, *34*, 1091.
- (112) Alvarez, S. G.; Fisher, G. B.; Singaram, B. *Tetrahedron Lett.* **1995**, *36*, 2567.
- (113) Pasumansky, L.; Collins, C. J.; Pratt, L. M.; Nguÿên, N. V.; Ramachandran, B.; Singaram, B. *J. Org. Chem.* **2007**, *72*, 971.
- (114) Thomas, S.; Huynh, T.; Enriquez-Rios, V.; Singaram, B. *Org. Lett.* **2001**, *3*, 3915.
- (115) Pratt, L. M.; Nguÿên, N. V. *J. Org. Chem.* **2005**, *70*, 10561.
- (116) (a) Pasumansky, L.; Haddenham, D.; Clary, J. W.; Fisher, G. B.; Goralski, C. T.; Singaram, B. *J. Org. Chem.* **2008**, *73*, 1898. (b) Haddenham, D.; Pasumansky, L.; DeSoto, J.; Eagon, S.; Singaram, B. *J. Org. Chem.* **2009**, *74*, 1964.
- (117) Barendt, J. M.; Dryden, B. W. *e-EROS Encycl. Reagents Org. Synth.* **2001**.
- (118) Zaidlewicz, M.; Brown, H. C. *e-EROS Encycl. Reagents Org. Synth.* **2001**.
- (119) Zaidlewicz, M. *e-EROS Encycl. Reagents Org. Synth.* **2001**.
- (120) (a) Bestmann, H. J.; Röder, T.; Sühs, K. *Chem. Ber.* **1988**, *121*, 1509. (b) Bestmann, H. J.; Sühs, K.; Röder, T. *Angew. Chem.* **1981**, *93*, 1098. (c) Pelter, A.; Rosser, R.; Mills, S. *J. Chem. Soc., Chem. Commun.* **1981**, 1014.
- (121) (a) Zaidlewicz, M.; Brown, H. C. *Spec. Publ.—R. Soc. Chem.* **1997**, *201*, 171. (b) Brown, H. C.; Chandrasekharan, J. *J. Am. Chem. Soc.* **1984**, *106*, 1863.
- (122) Sheeller, B.; Ingold, K. U. *J. Chem. Soc., Perkin Trans. 2* **2001**, 480.
- (123) Gaumont, A.-C.; Bourumeau, K.; Denis, J. M.; Guenet, P. *J. Organomet. Chem.* **1994**, *484*, 9.
- (124) Scheideman, M.; Shapland, P.; Vedejs, E. *J. Am. Chem. Soc.* **2003**, *125*, 10502.
- (125) (a) Gaumont, A.-C.; Gulea, M.; Levillain, J. *Chem. Rev.* **2009**, *109*, 1371. (b) Mimeau, D.; Delacroix, O.; Join, B.; Gaumont, A.-C. *C. R. Chim.* **2004**, *7*, 845. (c) Delacroix, O.; Gaumont, A.-C. *Curr. Org. Chem.* **2005**, *9*, 1851. (d) Glueck, D. S. *Chem.—Eur. J.* **2008**, *14*, 7108. (e) Kolodiazhnyi, O. I. *Tetrahedron Asymmetry* **1998**, *9*, 1279. (f) Enders, D.; Saint-Dizier, A.; Lannou, M.-I.; Lenzen, A. *Eur. J. Org. Chem.* **2006**, *2006*, 29.
- (126) Imamoto, T.; Oshiki, T.; Onozawa, T.; Kusumoto, T.; Sato, K. *J. Am. Chem. Soc.* **1990**, *112*, 5244.
- (127) Join, B.; Mimeau, D.; Delacroix, O.; Gaumont, A.-C. *Chem. Commun.* **2006**, 3249.
- (128) Mimeau, D.; Gaumont, A.-C. *J. Org. Chem.* **2003**, *68*, 7016.
- (129) Mimeau, D.; Delacroix, O.; Gaumont, A.-C. *Chem. Commun.* **2003**, 2928.
- (130) Join, B.; Delacroix, O.; Gaumont, A.-C. *Synlett* **2005**, 1881.
- (131) Join, B.; Lohier, J. F.; Delacroix, O.; Gaumont, A.-C. *Synthesis* **2008**, 3121.
- (132) Busacca, C. A.; Farber, E.; DeYoung, J.; Campbell, S.; Gonnella, N. C.; Grinberg, N.; Haddad, N.; Lee, H.; Ma, S.; Reeves, D.; Shen, S.; Senanayake, C. H. *Org. Lett.* **2009**, *11*, 5594.
- (133) Bruncker, T. J.; Anderson, B. J.; Blank, N. F.; Glueck, D. S.; Rheingold, A. L. *Org. Lett.* **2007**, *9*, 1109.
- (134) Baban, J. A.; Marti, V. P. J.; Roberts, B. P. *J. Chem. Soc., Perkin Trans. 2* **1985**, 1723.
- (135) Baban, J. A.; Roberts, B. P. *J. Chem. Soc., Chem. Commun.* **1983**, 1224.
- (136) Green, I. G.; Roberts, B. P. *J. Chem. Soc., Perkin Trans. 2* **1986**, 1597.
- (137) Baban, J. A.; Marti, V. P. J.; Roberts, B. P. *J. Chem. Res.* **1985**, 90.
- (138) Baban, J. A.; Roberts, B. P. *J. Chem. Soc., Perkin Trans. 2* **1988**, 1195.
- (139) Paul, V.; Roberts, B. P. *J. Chem. Soc., Perkin Trans. 2* **1988**, 1895.
- (140) Barton, D. H. R.; Jacob, M. *Tetrahedron Lett.* **1998**, *39*, 1331.
- (141) (a) Little, R. D.; Nishiguchi, G. A. *Stud. Nat. Prod. Chem.* **2008**, *35*, 3. (b) Nishiguchi, G. A.; Little, R. D. *J. Org. Chem.* **2005**, *70*, 5249.
- (142) Florent, J.-C.; Monneret, C. *Glycoscience* **2001**, 231.
- (143) (a) Studer, A.; Amrein, S. *Synthesis* **2002**, 835. (b) Gilbert, B. C.; Parsons, A. F. *J. Chem. Soc., Perkin Trans. 2* **2002**, 367.
- (144) Lalevée, J.; Tehfe, M. A.; Allonas, X.; Fouassier, J. P. *Macromolecules* **2008**, *41*, 9057.
- (145) Mok, P. L. H.; Roberts, B. P.; McKetty, P. T. *J. Chem. Soc., Perkin Trans. 2* **1993**, 665.
- (146) (a) Dang, H. S.; Diart, V.; Roberts, B. P. *J. Chem. Soc., Perkin Trans. 1* **1994**, 1033. (b) Dang, H. S.; Diart, V.; Roberts, B. P. *J. Chem. Soc., Perkin Trans. 1* **1994**, 2511. (c) Dang, H. S.; Diart, V.; Roberts, B. P.; Tocher, D. A. *J. Chem. Soc., Perkin Trans. 1* **1994**, 1039. (d) Mok, P. L. H.; Roberts, B. P. *J. Chem. Soc., Chem. Commun.* **1991**, 150. (e) Mok, P. L. H.; Roberts, B. P. *Tetrahedron Lett.* **1992**, *33*, 7249.
- (147) Kaszynski, P.; Pakhomov, S.; Gurskii, M. E.; Erdyakov, S. Y.; Starikova, Z. A.; Lyssenko, K. A.; Antipin, M. Y.; Young, V. G., Jr.; Bubnov, Y. N. *J. Org. Chem.* **2009**, *74*, 1709.
- (148) Steurer, M.; Wang, Y.; Mereiter, K.; Weissensteiner, W. *Organometallics* **2007**, *26*, 3850.
- (149) Picot, A.; Lusinchi, X. *Bull. Soc. Chim. Fr.* **1977**, 1227.
- (150) Schwartz, M. A.; Rose, B. F.; Vishnuvajjala, B. *J. Am. Chem. Soc.* **1973**, *95*, 612.
- (151) Choi, S.; Bruce, I.; Fairbanks, A. J.; Fleet, G. W. J.; Jones, A. H.; Nash, R. J.; Fellows, L. E. *Tetrahedron Lett.* **1991**, *32*, 5517.
- (152) Ferey, V.; Vedrenne, P.; Toupet, L.; Le Gall, T.; Mioskowski, C. *J. Org. Chem.* **1996**, *61*, 7244.
- (153) Pellon, P. *Tetrahedron Lett.* **1992**, *33*, 4451.
- (154) (a) Imamoto, T.; Oshiki, T.; Onozawa, T.; Kusumoto, T.; Sato, K. *J. Am. Chem. Soc.* **1990**, *112*, 5244. (b) Wolfe, B.; Livinghouse, T. *J. Am. Chem. Soc.* **1998**, *120*, 5116. (c) Brisset, H.; Gourdel, Y.; Pellon, P.; Le Corre, M. *Tetrahedron Lett.* **1993**, *34*, 4523. (d) Bradley, D.; Williams, G.; Lombard, H.; van Niekerk, M.; Coetzee, P. P.; Holzapfel, C. W. *Phosphorus, Sulfur Silicon Relat. Elem.* **2002**, *177*, 2799. (e) Desponds, O.; Huynh, C.; Schlosser, M. *Synthesis* **1998**, 983.
- (155) McKinstry, L.; Livinghouse, T. *Tetrahedron* **1995**, *51*, 7655.
- (156) McKinstry, L.; Livinghouse, T. *Tetrahedron Lett.* **1994**, *35*, 9319.
- (157) Van Overschelde, M.; Verweken, E.; Modha, S. G.; Cogen, S.; Van der Eycken, E.; Van der Eycken, J. *Tetrahedron* **2009**, *65*, 6410.
- (158) McKinstry, L.; Overberg, J. J.; Soubra-Ghaoui, C.; Walsh, D. S.; Robins, K. A.; Toto, T. T.; Toto, J. L. *J. Org. Chem.* **2000**, *65*, 2261.
- (159) (a) Mohr, B.; Lynn, D. M.; Grubbs, R. H. *Organometallics* **1996**, *15*, 4317. (b) Gammon, J. J.; Canipa, S. J.; O'Brien, P.; Kelly, B.; Taylor, S. *Chem. Commun.* **2008**, 3750. (c) Canipa, S. J.; O'Brien, P.; Taylor, S. *Tetrahedron: Asymmetry* **2009**, *20*, 2407. (d) Granander, J.; Secci, F.; O'Brien, P.; Kelly, B. *Tetrahedron: Asymmetry* **2009**, *20*, 2432. (e) Miura, T.; Yamada, H.; Kikuchi, S.; Imamoto, T. *J. Org. Chem.* **2000**, *65*, 1877. (f) Imamoto, T. *Pure Appl. Chem.* **1993**, *65*, 655.
- (160) (a) Jaska, C. A.; Lough, A. J.; Manners, I. *Inorg. Chem.* **2004**, *43*, 1090. (b) Collins, C. J.; Lanz, M.; Goralski, C. T.; Singaram, B. *J. Org. Chem.* **1999**, *64*, 2574. (c) Fuller, A.-M.; Mountford, A. J.; Scott, M. L.; Coles, S. J.; Horton, P. N.; Hughes, D. L.; Hursthouse, M. B.; Lancaster, S. J. *Inorg. Chem.* **2009**, *48*, 11474. (d) Lee, K.; Clark, T. J.; Lough, A. J.; Manners, I. *Dalton Trans.* **2008**, 2732.
- (161) Imamoto, T.; Kusumoto, T.; Suzuki, N.; Sato, K. *J. Am. Chem. Soc.* **1985**, *107*, 5301.
- (162) Oohara, N.; Imamoto, T. *Bull. Chem. Soc. Jpn.* **2002**, *75*, 1359.
- (163) Gaumont, A.-C.; Hursthouse, M. B.; Coles, S. J.; Brown, J. M. *Chem. Commun.* **1999**, 63.
- (164) Schlummer, B.; Scholz, U. *Adv. Synth. Catal.* **2004**, *346*, 1599.
- (165) Vallette, H.; Pican, S.; Boudou, C.; Levillain, J.; Plaquevent, J. C.; Gaumont, A.-C. *Indian J. Chem., Sect. B: Org. Chem. Incl. Med. Chem.* **2006**, *45*, 2286.
- (166) Vallette, H.; Pican, S.; Boudou, C.; Levillain, J.; Plaquevent, J.-C.; Gaumont, A.-C. *Tetrahedron Lett.* **2006**, *47*, 5191.
- (167) Julienne, D.; Lohier, J.-F.; Delacroix, O.; Gaumont, A.-C. *J. Org. Chem.* **2007**, *72*, 2247.
- (168) Julienne, D.; Delacroix, O.; Gaumont, A.-C. *Phosphorus Sulfur Silicon Relat. Elem.* **2009**, *184*, 846.
- (169) Kumaraswamy, G.; Rao, G. V.; Murthy, A. N.; Sridhar, B. *Synlett* **2009**, 1180.
- (170) Kumaraswamy, G.; Rao, G. V.; RamaKrishna, G. *Synlett* **2006**, 1122.
- (171) Stankevič, M.; Pietrusiewicz, M. K. *Tetrahedron Lett.* **2009**, *50*, 7093.
- (172) (a) Myers, W. H.; Ryschewitsch, G. E.; Mathur, M. A.; King, R. W. *Inorg. Chem.* **1975**, *14*, 2874. (b) Imamoto, T.; Asakura, K.; Tsuruta, H.; Kishikawa, K.; Yamaguchi, K. *Tetrahedron Lett.* **1996**, *37*, 503.

- (c) Ketchum, D. R.; DeGraffenreid, A. L.; Niedenzu, P. M.; Shore, S. G. *J. Mater. Res.* **1999**, *14*, 1934. (d) Geanangel, R. A. *J. Inorg. Nucl. Chem.* **1972**, *34*, 1083. (e) Sisler, H. H.; Mathur, M. A. *J. Inorg. Nucl. Chem.* **1977**, *39*, 1745.
- (173) Lowe, J. R.; Uppal, S. S.; Weidig, C.; Kelly, H. C. *Inorg. Chem.* **1970**, *9*, 1423.
- (174) Denniston, M. L.; Chiusano, M. A.; Martin, D. R. *J. Inorg. Nucl. Chem.* **1976**, *38*, 979.
- (175) (a) Bratt, P. J.; Brown, M. P.; Seddon, K. R. *J. Chem. Soc., Dalton. Trans.* **1974**, 2161. (b) Vidal, J. L.; Ryschkewitsch, G. E. *Inorg. Chem.* **1977**, *16*, 1898.
- (176) Ryschkewitsch, G. E.; Miller, V. R. *J. Am. Chem. Soc.* **1973**, *95*, 2836.
- (177) Douglass, J. E. *J. Org. Chem.* **1966**, *31*, 962.
- (178) Hoge, G. s.; Goel, O. M. U.S. Pat. 2003073868, 2003.
- (179) Jaska, C. A.; Manners, I. *J. Am. Chem. Soc.* **2004**, *126*, 9776.
- (180) Bao, J.; Beylin, V. G.; Greene, D. J.; Hoge, G.; Kissel, W. S.; Marlatt, M. E.; Pflum, D. A.; Wu, H.-P. U.S. Patent, 2005; Vol. PCT Int. Appl.
- (181) Das, M. K.; Roy, S. *Synth. React. Inorg. Met.-Org. Chem.* **1985**, *15*, 53.
- (182) Merle, N.; Frost, C. G.; Kociok-Köhn, G.; Willis, M. C.; Weller, A. S. *J. Organomet. Chem.* **2005**, *690*, 2829.
- (183) (a) Imamoto, T.; Morishita, H. *J. Am. Chem. Soc.* **2000**, *122*, 6329. (b) Schmidbaur, H.; Wimmer, T.; Reber, G.; Müller, G. *Angew. Chem.* **1988**, *100*, 1135.
- (184) Schmidbaur, H.; Weiss, E.; Müller, G. *Synth. React. Inorg. Met.-Org. Chem.* **1985**, *15*, 401.
- (185) Yamamoto, T.; Koizumi, T.; Katagiri, K.; Furuya, Y.; Danjo, H.; Imamoto, T.; Yamaguchi, K. *Org. Lett.* **2006**, *8*, 6103.
- (186) Buynak, J. D.; Geng, B. *Organometallics* **1995**, *14*, 3112.
- (187) De Vries, T. S.; Vedejs, E. *Organometallics* **2007**, *26*, 3079.
- (188) Cibura, K.; Haas, A. *Rev. Roum. Chim.* **1986**, *31*, 927.
- (189) Bedel, C.; Foucaud, A. *Tetrahedron Lett.* **1993**, *34*, 311.
- (190) Monnier, L.; Delcros, J. G.; Carboni, B. *Tetrahedron* **2000**, *56*, 6039.
- (191) Keglevich, G.; Újszászy, K.; Szöllösy, Á.; Ludányi, K.; Töke, L. *J. Organomet. Chem.* **1996**, *516*, 139.
- (192) Jana, A.; Schulzke, C.; Roesky, H. W. *J. Am. Chem. Soc.* **2009**, *131*, 4600.
- (193) Blum, Y. D.; Laine, R. M. U.S. Pat. 4801439, 1989.
- (194) Green, I. G.; Johnson, K. M.; Roberts, B. P. *J. Chem. Soc., Perkin Trans. 2* **1989**, 1963.
- (195) Dorn, H.; Singh, R. A.; Massey, J. A.; Lough, A. J.; Manners, I. *Angew. Chem., Int. Ed.* **1999**, *38*, 3321.
- (196) Narula, C. K.; Janik, J. F.; Duesler, E. N.; Paine, R. T.; Schaeffer, R. *Inorg. Chem.* **1986**, *25*, 3346.
- (197) Pun, D.; Lobkovsky, E.; Chirik, P. J. *Chem. Commun.* **2007**, 3297.
- (198) Käss, M.; Friedrich, A.; Drees, M.; Schneider, S. *Angew. Chem., Int. Ed.* **2009**, *48*, 905.
- (199) (a) Clapham, S. E.; Hadzovic, A.; Morris, R. H. *Coord. Chem. Rev.* **2004**, *248*, 2201. (b) Li, T.; Churlaud, R.; Lough, A. J.; Abdur-Rashid, K.; Morris, R. H. *Organometallics* **2004**, *23*, 6239. (c) Abdur-Rashid, K.; Clapham, S. E.; Hadzovic, A.; Harvey, J. N.; Lough, A. J.; Morris, R. H. *J. Am. Chem. Soc.* **2002**, *124*, 15104.
- (200) Sloan, M. E.; Clark, T. J.; Manners, I. *Inorg. Chem.* **2009**, *48*, 2429.
- (201) Denney, M. C.; Pons, V.; Hebden, T. J.; Heinekey, D. M.; Goldberg, K. I. *J. Am. Chem. Soc.* **2006**, *128*, 12048.
- (202) Göttker-Schnetmann, I.; White, P.; Brookhart, M. *J. Am. Chem. Soc.* **2004**, *126*, 1804.
- (203) Bøddeker, K. W.; Shore, S. G.; Bunting, R. K. *J. Am. Chem. Soc.* **1966**, *88*, 4396.
- (204) Hebden, T. J.; Denney, M. C.; Pons, V.; Piccoli, P. M. B.; Koetzle, T. F.; Schultz, A. J.; Kaminsky, W.; Goldberg, K. I.; Heinekey, D. M. *J. Am. Chem. Soc.* **2008**, *130*, 10812.
- (205) Keaton, R. J.; Blacquiere, J. M.; Baker, R. T. *J. Am. Chem. Soc.* **2007**, *129*, 1844.
- (206) Friedrich, A.; Drees, M.; Schneider, S. *Chem.-Eur. J.* **2009**, *15*, 10339.
- (207) Douglas, T. M.; Chaplin, A. B.; Weller, A. S. *J. Am. Chem. Soc.* **2008**, *130*, 14432.
- (208) Campbell, G. W.; Johnson, L. *J. Am. Chem. Soc.* **1959**, *81*, 3800.
- (209) Nöth, H.; Thomas, S. *Eur. J. Inorg. Chem.* **1999**, 1373.
- (210) Sloan, M. E.; Staubitz, A.; Clark, T. J.; Russell, C. A.; Lloyd-Jones, G. C.; Manners, I. *J. Am. Chem. Soc.* **2010**, *132*, 3831.
- (211) Luo, Y.; Ohno, K. *Organometallics* **2007**, *26*, 3597.
- (212) Douglas, T. M.; Chaplin, A. B.; Weller, A. S.; Yang, X.; Hall, M. B. *J. Am. Chem. Soc.* **2009**, *131*, 15440.
- (213) Beachley, O. T., Jr. *Inorg. Chem.* **1967**, *6*, 870.
- (214) Paul, A.; Musgrave, C. B. *Angew. Chem., Int. Ed.* **2007**, *46*, 8153.
- (215) Jaska, C. A.; Manners, I. *J. Am. Chem. Soc.* **2004**, *126*, 1334.
- (216) Widegren, J. A.; Finke, R. G. *J. Mol. Cat. A: Chem.* **2003**, *198*, 317.
- (217) (a) Chen, Y.; Fulton, J. L.; Linehan, J. C.; Autrey, T. *J. Am. Chem. Soc.* **2005**, *127*, 3254. (b) Fulton, J. L.; Linehan, J. C.; Autrey, T.; Balasubramanian, M.; Chen, Y.; Szymczak, N. K. *J. Am. Chem. Soc.* **2007**, *129*, 11936.
- (218) Rousseau, R.; Schenter, G. K.; Fulton, J. L.; Linehan, J. C.; Engelhard, M. H.; Autrey, T. *J. Am. Chem. Soc.* **2009**, *131*, 10516.
- (219) Lee, K. PhD thesis, University of Bristol, 2009.
- (220) Zahmakiran, M.; Özkaz, S. *Inorg. Chem.* **2009**, *48*, 8955.
- (221) Rossin, A.; Caporali, M.; Gonsalvi, L.; Guerri, A.; Lledós, A.; Peruzzini, M.; Zanobini, F. *Eur. J. Inorg. Chem.* **2009**, 2009, 3055.
- (222) Yang, X.; Hall, M. B. *J. Am. Chem. Soc.* **2008**, *130*, 1798.
- (223) (a) Zimmerman, P. M.; Paul, A.; Zhang, Z.; Musgrave, C. B. *Angew. Chem., Int. Ed.* **2009**, *48*, 2201. (b) Zimmerman, P. M.; Paul, A.; Zhang, Z.; Musgrave, C. B. *Inorg. Chem.* **2009**, *48*, 1069.
- (224) Zimmerman, P. M.; Paul, A.; Musgrave, C. B. *Inorg. Chem.* **2009**, *48*, 5418.
- (225) Hall: theoretical level of ab initio Tao-Perdew-Staroverov-Scuseria (TPSS) meta-GGA density functional and the all-electron correlation-consistent polarized valence double-zeta (ccpVDZ) basis sets; Paul: hybrid-exchange B3LYP density functional. The 6-31G\* basis set is used on all carbene atoms and 6-31++G\*\* is applied to all ammonia-borane and Ni atoms.
- (226) Leleental, M. *J. Electrochem. Soc.* **1973**, *120*, 1650.
- (227) Malory, G. O. *Plating* **1971**, *58*, 319.
- (228) van den Meerakker, J. E. A. M. *J. Appl. Electrochem.* **1981**, *11*, 395.
- (229) Leleental, M. *J. Catal.* **1974**, *32*, 429.
- (230) Homma, T.; Tamaki, A.; Nakai, H.; Osaka, T. *J. Electroanal. Chem.* **2003**, *559*, 131.
- (231) Homma, T.; Nakai, H.; Onishi, M.; Osaka, T. *J. Phys. Chem. B* **1999**, *103*, 1774.
- (232) Nakai, H.; Homma, T.; Komatsu, I.; Osaka, T. *J. Phys. Chem. B* **2001**, *105*, 1701.
- (233) Chigane, M.; Izaki, M.; Hatanaka, Y.; Shinagawa, T.; Ishikawa, M. *Thin Solid Films* **2006**, *515*, 2513.
- (234) Schlesinger, H. I.; Burg, A. B. *J. Am. Chem. Soc.* **1938**, *60*, 290.
- (235) Xiong, Z.; Yong, C. K.; Wu, G.; Chen, P.; Shaw, W.; Karkamkar, A.; Autrey, T.; Jones, M. O.; Johnson, S. R.; Edwards, P. P.; David, W. I. F. *Nat. Mater.* **2008**, *7*, 138.
- (236) Xiong, Z.; Chua, Y. S.; Wu, G.; Xu, W.; Chen, P.; Shaw, W.; Karkamkar, A.; Linehan, J.; Smurthwaite, T.; Autrey, T. *Chem. Commun.* **2008**, 5595.
- (237) Addition of 10% LiNH<sub>2</sub> to ammonia-borane was observed to lower the dehydrogenation temperature and increase the hydrogen yield by Sneddon and co-workers which was published as a preliminary result in *New Methods for Promoting Amineborane Dehydrogenation/Regeneration Reactions*, Sneddon, L. G. DoE Hydrogen Program, FY2006 Annual Progress Report, Section IV.B.4g, p 418.
- (238) Xiong, Z.; Wu, G.; Chua, Y. S.; Hu, J.; He, T.; Xu, W.; Chen, P. *Energy Environ. Sci.* **2008**, *1*, 360.
- (239) Fijalkowski, K. J.; Grochala, W. *J. Mater. Chem.* **2009**, *19*, 2043.
- (240) Li, L.; Yao, X.; Sun, C.; Du, A.; Cheng, L.; Zhu, Z.; Yu, C.; Zou, J.; Smith, S. C.; Wang, P.; Cheng, H.-M.; Frost, R. L.; Lu, G. Q. *Adv. Funct. Mater.* **2009**, *19*, 265.
- (241) Diyabalanage, H. V. K.; Shrestha, R. P.; Semelsberger, T. A.; Scott, B. L.; Bowden, M. E.; Davis, B. L.; Burrell, A. K. *Angew. Chem., Int. Ed.* **2007**, *46*, 8995.
- (242) Zhang, Q.; Tang, C.; Fang, C.; Fang, F.; Sun, D.; Ouyang, L.; Zhu, M. *J. Phys. Chem. C* **2010**, *114*, 1709.
- (243) Kang, X.; Ma, L.; Fang, Z.; Gao, L.; Luo, J.; Wang, S.; Wang, P. *Phys. Chem. Chem. Phys.* **2009**, *11*, 2507.
- (244) Lee, T. B.; McKee, M. L. *Inorg. Chem.* **2009**, *48*, 7564.
- (245) (a) Wu, H.; Zhou, W.; Yildirim, T. *J. Am. Chem. Soc.* **2008**, *130*, 14834. (b) Kim, D. Y.; Singh, N. J.; Lee, H. M.; Kim, K. S. *Chem.-Eur. J.* **2009**, *15*, 5598. (c) Armstrong, D. R.; Perkins, P. G.; Walker, G. T. *THEOCHEM* **1985**, *122*, 189.
- (246) Spielmann, J.; Jansen, G.; Bandmann, H.; Harder, S. *Angew. Chem., Int. Ed.* **2008**, *47*, 6290.
- (247) Spielmann, J.; Harder, S. *J. Am. Chem. Soc.* **2009**, *131*, 5064.
- (248) Spielmann, J.; Bolte, M.; Harder, S. *Chem. Commun.* **2009**, 6934.
- (249) Müller, G.; Brand, J. *Organometallics* **2003**, *22*, 1463.
- (250) Gourdel, Y.; Ghanimi, A.; Pellon, P.; Le Corre, M. *Tetrahedron Lett.* **1993**, *34*, 1011.
- (251) Izod, K.; McFarlane, W.; Tyson, B. V.; Clegg, W.; Harrington, R. W. *Chem. Commun.* **2004**, 570-571.
- (252) Izod, K.; Wills, C.; Clegg, W.; Harrington, R. W. *Organometallics* **2006**, *25*, 38.
- (253) (a) Izod, K.; Wills, C.; Clegg, W.; Harrington, R. W. *Organometallics* **2007**, *26*, 2861. (b) Izod, K.; Wills, C.; Clegg, W.; Harrington, R. W. *Dalton Trans.* **2007**, 3669. (c) Izod, K.; Wills, C.; Clegg, W.; Harrington, R. W. *J. Organomet. Chem.* **2007**, *692*, 5060. (d) Izod, K.; Wills, C.; Clegg, W.; Harrington, R. W. *Organometallics* **2009**, *28*, 5661.

- (254) (a) Izod, K.; McFarlane, W.; Tyson, B. V.; Carr, I.; Clegg, W.; Harrington, R. W. *Organometallics* **2006**, *25*, 1135. (b) Izod, K.; Wills, C.; Clegg, W.; Harrington, R. W. *Organometallics* **2009**, *28*, 2211.
- (255) Izod, K.; Wills, C.; Clegg, W.; Harrington, R. W. *Organometallics* **2006**, *25*, 5326.
- (256) Izod, K.; Wills, C.; Clegg, W.; Harrington, R. W. *Inorg. Chem.* **2007**, *46*, 4320.
- (257) Wills, C.; Izod, K.; Clegg, W.; Harrington, R. W. *Dalton Trans.* **2010**, *39*, 2379.
- (258) (a) Zarić, S.; Hall, M. B. *J. Phys. Chem. A* **1997**, *101*, 4646. (b) Crabtree, R. H. *Chem. Rev.* **1985**, *85*, 245. (c) Hall, C.; Perutz, R. N. *Chem. Rev.* **1996**, *96*, 3125. (d) Shilov, A. E.; Shul'pin, G. B. *Chem. Rev.* **1997**, *97*, 2879. (e) Ritleng, V.; Sirlin, C.; Pfeffer, M. *Chem. Rev.* **2002**, *102*, 1731.
- (259) Kawano, Y.; Yamaguchi, K.; Miyake, S.-Y.; Kakizawa, T.; Shimoi, M. *Chem.—Eur. J.* **2007**, *13*, 6920.
- (260) (a) Knorr, J. R.; Merola, J. S. *Organometallics* **1990**, *9*, 3008. (b) Baker, R. T.; Ovenall, D. W.; Calabrese, J. C.; Westcott, S. A.; Taylor, N. J.; Williams, I. D.; Marder, T. B. *J. Am. Chem. Soc.* **1990**, *112*, 9399.
- (261) (a) Vidovic, D.; Pierce, G. A.; Aldridge, S. *Chem. Commun.* **2009**, 1157. (b) Aldridge, S.; Kays, D. L. *Main Group Chem.* **2006**, *5*, 223. (c) Braunschweig, H.; Kollann, C.; D. R. *Angew. Chem., Int. Ed.* **2006**, *45*, 5254. (d) Aldridge, S.; Coombs, D. L. *Coord. Chem. Rev.* **2004**, *248*, 535. (e) Irvine, G. J.; Lesley, M. J. G.; Marder, T. B.; Norman, N. C.; Rice, C. R.; Robins, E. G.; Roper, W. R.; Whittell, G. R.; Wright, L. *Chem. Rev.* **1998**, *98*, 2685.
- (262) Piers, W. E. *Angew. Chem., Int. Ed.* **2000**, *39*, 1923.
- (263) (a) Shimoi, M.; Nagai, S.-I.; Ichikawa, M.; Kawano, Y.; Katoh, K.; Urichi, M.; Ogino, H. *J. Am. Chem. Soc.* **1999**, *121*, 11704. (b) Kawano, Y.; Yasue, T.; Shimoi, M. *J. Am. Chem. Soc.* **1999**, *121*, 11704.
- (264) Ariafard, A.; Amini, M. M.; Azadmehr, A. *J. Organomet. Chem.* **2005**, *690*, 1147.
- (265) (a) Schubert, U.; Meyer, J. *J. Organomet. Chem.* **1986**, *303*, C5. (b) Schubert, U.; Ackermann, K.; Wörle, B. *J. Am. Chem. Soc.* **1982**, *104*, 7378. (c) Dong, D. F.; Hoyano, J. K.; Graham, W. A. G. *Can. J. Chem.* **1981**, *59*, 1455. (d) Colomer, E.; Corriu, R. J. P.; Marzin, C.; Vioux, A. *Inorg. Chem.* **1982**, *21*, 368. (e) Carré, F.; Colomer, E.; Corriu, R. J. P.; Vioux, A. *Organometallics* **1984**, *21*, 1272.
- (266) Kakizawa, T.; Kawano, Y.; Shimoi, M. *Organometallics* **2001**, *20*, 3211.
- (267) Shimoi, M.; Katoh, K.; Kawano, Y.; Kodama, G.; Ogino, H. *J. Organomet. Chem.* **2002**, *659*, 102.
- (268) Kawano, Y.; Kakizawa, T.; Yamaguchi, K.; Shimoi, M. *Chem. Lett.* **2006**, *35*, 568.
- (269) Kawano, Y.; Hashiva, M.; Shimoi, M. *Organometallics* **2006**, *25*, 4420.
- (270) Nagaraja, C. M.; Nethaji, M.; Jagirdar, B. R. *Inorg. Chem.* **2005**, *44*, 4145.
- (271) Nagaraja, C. M.; Parameswaran, P.; Jemmis, E. D.; Jagirdar, B. R. *J. Am. Chem. Soc.* **2007**, *129*, 5587.
- (272) (a) Chaplin, A. B.; Weller, A. S. *Angew. Chem., Int. Ed.* **2010**, *49*, 581. (b) Chaplin, A. B.; Weller, A. S. *Inorg. Chem.* **2010**, *49*, 1111. (c) Dallanegra, R.; Chaplin, A. B.; Weller, A. S. *Angew. Chem., Int. Ed.* **2009**, *48*, 6875.
- (273) Snow, S. A.; Shimoi, M.; Ostler, C. D.; Thompson, B. K.; Kodama, G.; Parry, R. W. *Inorg. Chem.* **1984**, *23*, 511.
- (274) Snow, S. A.; Kodama, G. *Inorg. Chem.* **1985**, *24*, 795.
- (275) Shimoi, M.; Katoh, K.; Tobita, H.; Ogino, H. *Inorg. Chem.* **1990**, *29*, 814.
- (276) (a) Katoh, K.; Shimoi, M.; Ogino, H. *Inorg. Chem.* **1992**, *31*, 670. (b) Shimoi, M.; Katoh, K.; Ogino, H. *J. Chem. Soc., Chem. Comm.* **1990**, 811. (c) Hata, M.; Kawano, Y.; Shimoi, M. *Inorg. Chem.* **1998**, *37*, 4482.
- (277) (a) Macias, R.; Rath, N. P.; Barton, L. *Angew. Chem., Int. Ed.* **1999**, *38*, 162. (b) Volkov, O.; Macias, R.; Rath, N. P.; Barton, L. *Inorg. Chem.* **2002**, *41*, 5837.
- (278) Ingleson, M.; Patmore, N. J.; Ruggiero, G. D.; Frost, C. G.; Mahon, M. F.; Willis, M. C.; Weller, A. S. *Organometallics* **2001**, *20*, 4434.
- (279) Merle, N.; Koicok-Köhn, G.; Mahon, M. F.; Frost, C. G.; Ruggiero, G. D.; Weller, A. S.; Willis, M. C. *Dalton Trans.* **2004**, 3883.
- (280) Jiménez-Tenorio, M.; Puerta, M. C.; Valerga, P. *Eur. J. Inorg. Chem.* **2004**, 17.
- (281) Merle, N.; Frost, C. G.; Kociok-Köhn, G.; Willis, M. C.; Weller, A. S. *Eur. J. Inorg. Chem.* **2006**, *2006*, 4068.
- (282) Blug, M.; Grünstein, D.; Alcaraz, G.; Sabo-Etienne, S.; Le Goff, X.-F.; Le Floch, P.; Mézailles, N. *Chem. Commun.* **2009**, 4432.
- (283) Nguyen, D. H.; Lauréano, H.; Jugé, S.; Kalck, P.; Daran, J.-C.; Coppel, Y.; Urrutigoity, M.; Gouygou, M. *Organometallics* **2009**, *28*, 6288.
- (284) Mountford, A. J.; Clegg, W.; Coles, S. J.; Harrington, R. W.; Horton, P. N.; Humphrey, S. M.; Hursthouse, M. B.; Wright, J. A.; Lancaster, S. J. *Chem.—Eur. J.* **2007**, *13*, 4535.
- (285) Forster, T. D.; Tuononen, H. M.; Parvez, M.; Roesler, R. *J. Am. Chem. Soc.* **2009**, *131*, 6689.
- (286) Maisch, R.; Ott, E.; Buchner, W.; Malisch, W.; Colquhoun, I. J.; McFarlane, W. *J. Organomet. Chem.* **1985**, *286*, C31.
- (287) Dornhaus, F.; Bolte, M.; Lerner, H.-W.; Wagner, M. *J. Organomet. Chem.* **2007**, *692*, 2949.
- (288) Ma, K.; Scheibitz, M.; Scholz, S.; Wagner, M. *J. Organomet. Chem.* **2002**, *652*, 11.
- (289) Jaska, C. A.; Dorn, H.; Lough, A. J.; Manners, I. *Chem.—Eur. J.* **2003**, *9*, 271.
- (290) Jaska, C. A.; Lough, A. J.; Manners, I. *Dalton Trans.* **2005**, 326.
- (291) Elliot, D. J.; Levy, C. J.; Puddephatt, R. J.; Holah, D. G.; Hughes, A. N.; Magnuson, V. R.; Moser, I. M. *Inorg. Chem.* **1990**, *29*, 5014.
- (292) Basil, J. D.; Aradi, A. A.; Bhattacharyya, N. K.; Rath, N. P.; Eigenbrot, C.; Fehlner, T. P. *Inorg. Chem.* **1990**, *29*, 1260.
- (293) Kawano, Y.; Yasue, T.; Shimoi, M. *J. Am. Chem. Soc.* **1999**, *121*, 11744.
- (294) (a) Nakazawa, H.; Itazaki, M.; Ohba, M. *J. Organomet. Chem.* **2007**, *692*, 201. (b) Nakazawa, H.; Ohba, M.; Itazaki, M. *Organometallics* **2006**, *25*, 2903.
- (295) Yasue, T.; Kawano, Y.; Shimoi, M. *Chem. Lett.* **2000**, 58.
- (296) Yasue, T.; Kawano, Y.; Shimoi, M. *Angew. Chem., Int. Ed.* **2003**, *42*, 1727.
- (297) Paine, R. T.; Nöth, H. *Chem. Rev.* **1995**, *95*, 343.
- (298) Vogel, U.; Timoshkin, A. Y.; Scheer, M. *Angew. Chem., Int. Ed.* **2001**, *40*, 4409.
- (299) Vogel, U.; Hoemensch, P.; Schwan, K.-C.; Timoshkin, A. Y.; Scheer, M. *Chem.—Eur. J.* **2003**, *9*, 515.
- (300) Vogel, U.; Timoshkin, A. Y.; Schwan, K.-C.; Bodensteiner, M.; Scheer, M. *J. Organomet. Chem.* **2006**, *691*, 4556.
- (301) Vogel, U.; Schwan, K.-C.; Hoemensch, P.; Scheer, M. *Eur. J. Inorg. Chem.* **2005**, *2005*, 1453.
- (302) Schwan, K.-C.; Timoshkin, A. Y.; Zabel, M.; Scheer, M. *Chem.—Eur. J.* **2006**, *12*, 4900.
- (303) Adolf, A.; Zabel, M.; Scheer, M. *Eur. J. Inorg. Chem.* **2007**, *2007*, 2136.
- (304) Adolf, A.; Vogel, U.; Zabel, M.; Timoshkin, A. Y.; Scheer, M. *Eur. J. Inorg. Chem.* **2008**, *2008*, 3482.
- (305) Schwan, K.-C.; Adolf, A.; Thoms, C.; Zabel, M.; Timoshkin, A. Y.; Scheer, M. *Dalton Trans.* **2008**, 5054.
- (306) Schwan, K.-C.; Vogel, U.; Adolf, A.; Zabel, M.; Scheer, M. *J. Organomet. Chem.* **2009**, *694*, 1189.
- (307) Although they are not discussed in this review, a range of other polymers with boron in the main chain or side group exist, including materials with 4-coordinate B, P—B bonds, or B<sub>2</sub>N<sub>2</sub> rings in the main chain. See: (a) Chujo, Y.; Tomita, I.; Murata, N.; Mauermann, H.; Saegusa, T. *Macromolecules* **1992**, *25*, 27–32. (b) Miyata, M.; Matsumi, N.; Chujo, Y. *Macromolecules* **2001**, *34*, 7331–7335. (c) Matsumoto, F.; Chujo, Y. *Pure Appl. Chem.* **2006**, *78*, 1407–1411. (d) Lorbach, A.; Bolte, M.; Li, H.; Lerner, H.-W.; Holthausen, M. C.; Jäkle, F.; Wagner, M. *Angew. Chem., Int. Ed.* **2009**, *48*, 4584–4588. (e) Malenfant, P. R. L.; Wan, J.; Taylor, S. T.; Manoharan, M. *Nat. Nanotechnol.* **2007**, *2*, 43–46. (f) Sundararaman, A.; Victor, M.; Varughese, R.; Jäkle, F. *J. Am. Chem. Soc.* **2005**, *127*, 13748–13749. (g) Parab, K.; Venkatasubbaiah, K.; Jäkle, F. *J. Am. Chem. Soc.* **2006**, *128*, 12879–12885. (h) Scheibitz, M.; Li, H.; Schnorr, J.; Sanchez Perucha, A.; Bolte, M.; Lerner, H.-W.; Jäkle, F.; Wagner, M. *J. Am. Chem. Soc.* **2009**, *131*, 16319–16329. (i) Grosche, M.; Herdtweck, E.; Peters, F.; Wagner, M. *Organometallics* **1999**, *18*, 4669.
- (308) Dahl, G. H.; Schaeffer, R. *J. Am. Chem. Soc.* **1961**, *83*, 3032.
- (309) Corfield, P. W. R.; Shore, S. G. *J. Am. Chem. Soc.* **1973**, *95*, 1480.
- (310) Leavers, D. R.; Taylor, W. J. *J. Phys. Chem.* **1977**, *81*, 2257.
- (311) Wang, J. S.; Geanangel, R. A. *Inorg. Chim. Acta* **1988**, *148*, 185.
- (312) Shore, S. G.; Hickam, C. W. *Inorg. Chem.* **1963**, *2*, 638.
- (313) Bissot, T. C.; Parry, R. W. *J. Am. Chem. Soc.* **1955**, *77*, 3481.
- (314) Brown, M. P.; Heseltine, R.; Sutcliffe, L. *J. Chem. Soc. A* **1968**, 612.
- (315) Gaines, D. F.; Schaeffer, R. *J. Am. Chem. Soc.* **1963**, *85*, 395.
- (316) Wiberg, E. Presented at the 16th IUPAC Conference, Paris, 1957.
- (317) Schlesinger, H. I.; Ritter, D. M.; Burg, A. B. *J. Am. Chem. Soc.* **1938**, *60*, 2297.
- (318) Schaeffer, G. W.; Basile, L. J. *J. Am. Chem. Soc.* **1955**, *77*, 331.
- (319) Schaeffer, G. W.; Adams, M. D.; Koenig, F. J. *J. Am. Chem. Soc.* **1956**, *78*, 725.
- (320) Holliday, A. K.; Thompson, N. R. *J. Chem. Soc.* **1960**, 2695.
- (321) Denton, D. L.; Johnson, A. D.; Hickam, C. W.; Bunting, R. K.; Shore, S. G. *J. Inorg. Nucl. Chem.* **1975**, *37*, 1037.
- (322) Komm, R.; Geanangel, R. A.; Liepins, R. *Inorg. Chem.* **1983**, *22*, 1684.
- (323) Geanangel, R. A.; Rabalais, J. W. *Inorg. Chim. Acta* **1985**, *97*, 59.

- (324) Baumann, J.; Baitalow, F.; Wolf, G. *Thermochim. Acta* **2005**, *430*, 9.
- (325) Kim, D.-P.; Moon, K.-T.; Kho, J.-G.; Economy, J.; Gervais, C.; Babonneau, F. *Polym. Adv. Technol.* **1999**, *10*, 702.
- (326) McGee, H. A., Jr.; Kwon, C. T. *Inorg. Chem.* **1970**, *9*, 2458.
- (327) Gervais, C.; Babonneau, F. *J. Organomet. Chem.* **2002**, *657*, 75.
- (328) Staubitz, A.; Soto, A. P.; Manners, I. *Angew. Chem., Int. Ed.* **2008**, *47*, 6212.
- (329) Pusatcioglu, S. Y.; McGee, H. A., Jr.; Fricke, A. L.; Hassler, J. C. *J. Appl. Polym. Sci.* **1977**, *21*, 1561.
- (330) Wideman, T.; Sneddon, L. G. *Inorg. Chem.* **1995**, *34*, 1002. Although this paper does not explicitly describe the synthesis of polyaminoborane, it was the foundation for the work by Kim and co-workers, ref 325.
- (331) Dietrich, B. L.; Goldberg, K. I.; Heinekey, D. M.; Autrey, T.; Linehan, J. C. *Inorg. Chem.* **2008**, *47*, 8583.
- (332) (a) Armstrong, D. R.; McAloon, B. J.; Perkins, P. G. *J. Chem. Soc., Faraday Trans. 2* **1973**, *69*, 968. (b) Armstrong, D. R.; Jamieson, J.; Perkins, P. G. *Theor. Chim. Acta* **1978**, *49*, 55.
- (333) Abdurahman, A.; Albrecht, M.; Shukla, A.; Dolg, M. *J. Chem. Phys.* **1999**, *110*, 8819.
- (334) Jacquemin, D.; Perpète, E. A.; Wathelet, V.; André, J.-M. *J. Phys. Chem. A* **2004**, *108*, 9616.
- (335) For a comparison of the bond length alteration of different conformers of a variety of polymers with a polar unit cell, see: Jacquemin, D.; Femenias, A.; Chermette, H.; André, J.-M.; Perpète, E. A. *J. Phys. Chem. A* **2005**, *109*, 5734.
- (336) Miranda, C. R.; Ceder, G. *J. Chem. Phys.* **2007**, *126*, 184703/1.
- (337) Nakhmanson, S. M.; Nardelli, M. B.; Bernholc, J. *Phys. Rev. Lett.* **2004**, *92*, 115504/1.
- (338) Jacquemin, D. *J. Phys. Chem. A* **2004**, *108*, 9260.
- (339) Hoffmann, E. U.K. Patents 941556; 941557, 1963.
- (340) Burg, A. B.; Wagner, R. I. U.S. 2948689, 1960.
- (341) (a) Korshak, V. V.; Zamyatina, V. A.; Solomatina, A. I. *Izv. Akad. Nauk SSSR, Ser. Khim.* **1964**, 1541. (b) Korshak, V. V.; Zamyatina, V. A.; Solomatina, A. I.; Fedin, E. I.; Petrovskii, P. V. *J. Organomet. Chem.* **1969**, *17*, 201.
- (342) Dorn, H.; Singh, R. A.; Massey, J. A.; Nelson, J. M.; Jaska, C. A.; Lough, A. J.; Manners, I. *J. Am. Chem. Soc.* **2000**, *122*, 6669.
- (343) Dorn, H.; Rodezno, J. M.; Brunnhöfer, B.; Rivard, E.; Massey, J. A.; Manners, I. *Macromolecules* **2003**, *36*, 291.
- (344) Kumashiro, Y. *J. Mater. Res.* **1990**, *5*, 2933.
- (345) Jacquemin, D.; Medved, M.; Perpète, E. A. *Int. J. Quantum Chem.* **2005**, *103*, 226.
- (346) Clark, T. J.; Rodezno, J. M.; Clendinning, S. B.; Aouba, S.; Brodersen, P. M.; Lough, A. J.; Ruda, H. E.; Manners, I. *Chem.—Eur. J.* **2005**, *11*, 4526.
- (347) Denis, J.-M.; Forintos, H.; Szelke, H.; Toupet, L.; Pham, T.-N.; Madec, P.-J.; Gaumont, A.-C. *Chem. Commun.* **2003**, 54.
- (348) Jacquemin, D.; Lambert, C.; Perpète, E. A. *Macromolecules* **2004**, *37*, 1009.
- (349) Jacquemin, D. *J. Phys. Chem. A* **2004**, *108*, 500.
- (350) Jacquemin, D.; Femenias, A.; Chermette, H.; André, J.-M.; Perpète, E. A. *J. Phys. Chem. A* **2005**, *109*, 5734.
- (351) Castet, F.; Champagne, B. *J. Phys. Chem. A* **2001**, *105*, 1366.
- (352) Champagne, B.; Perpète, E. A.; Legrand, T.; Jacquemin, D.; André, J.-M. *J. Chem. Soc., Faraday Trans* **1998**, *94*, 1547.
- (353) Jacquemin, D.; Champagne, B.; Hättig, C. *Chem. Phys. Lett.* **2000**, *319*, 327.
- (354) Jacquemin, D.; Champagne, B.; André, J.-M. *Chem. Phys. Lett.* **1998**, *284*, 24.
- (355) Jacquemin, D.; Wathelet, V.; Perpète, E. A. *Macromolecules* **2004**, *37*, 5040.
- (356) Schwartz, L. D.; Keller, P. C. *J. Am. Chem. Soc.* **1972**, *94*, 3015.
- (357) Jacquemin, D.; Perpète, E. A. *J. Phys. Chem. A* **2005**, *109*, 6380.
- (358) Kawano, Y.; Uruichi, M.; Shimoi, M.; Taki, S.; Kawaguchi, T.; Kakizawa, T.; Ogino, H. *J. Am. Chem. Soc.* **2009**, *131*, 14946.
- (359) Li, J.; Kathmann, S. M.; Schenter, G. K.; Gutowski, M. *J. Phys. Chem. C* **2007**, *111*, 3294.

CR100105A